NATURAL CYCLES OF BROMINATED METHANES: MACROALGAL PRODUCTION AND MARINE MICROBIAL DEGRADATION OF BROMOFORM AND DIBROMOMETHANE

Thesis by

Kelly D. Goodwin

In Partial Fulfillment of the Requirements
for the Degree of
Doctor of Philosophy

California Institute of Technology
Pasadena, California

1996

(Submitted September 15, 1995)

Acknowledgments

I gratefully acknowledge Amy Garner, Mike Mulqueen, and Penny Sherman – their efforts were vital to the completion of this project. I am grateful to my advisors Dr. Mary Lidstrom and Dr. Wheeler North for their input, support, and guidance. I also appreciate the unwavering encouragement of Dr. Steven Manley. I thank all Lidstrom lab members for fellowship. I thank Dr. Regina Dugan for her loving support and am grateful that she could be here for the celebration. I sincerely thank Edye Udell for her joyous friendship. I thank my mother for love, unconditional approval, and a cherished bond. Finally, I cannot possibly thank Dr. Robert Johnson enough — but I hope to have a lifetime trying.

I stand unshackled
at the rim of
possibility

Abstract

Two pieces of the bromine biogeochemical cycle were investigated – marine macroalgal production and microbial degradation of brominated methanes. Seawater concentrations of bromoform ($CHBr_3$) and dibromomethane (CH_2Br_2), as well as methyl iodide, were measured from a variety of southern California coastal sites. Elevated concentrations were associated with the Giant Kelp, *Macrocystis pyrifera*. A strong cross-shore gradient was observed with highest halomethane concentrations in and around the kelp bed relative to surface waters 5 km offshore. Water exiting a productive estuary was also enriched with CH_2Br_2. Seawater adjacent to decaying macroalgae on the bottom of a submarine canyon was not enriched in these halomethanes relative to surface water, indicating that bacterial degradation of drift kelp was not a significant source of halomethanes in this environment.

M. pyrifera produced $CHBr_3$ and CH_2Br_2 during incubations of tissue disks and whole blades. Median production rates measured from whole blade incubations were 171 ng $CHBr_3$/gfwt·day (0.68 nmoles $CHBr_3$/gfwt·day) and 48 ng CH_2Br_2/gfwt·day (0.27 nmoles CH_2Br_2/gfwt·day), based on a 12 hr photoperiod (n = 19; 190 blades). Comparable production rates were measured from preliminary incubations *in situ*, supporting the validity of laboratory measurements.

Light and algal photosynthetic activity affected $CHBr_3$ and CH_2Br_2 release by *M. pyrifera*. These results suggest that environmental factors that influence kelp physiology (e.g., health, light, season, climate, etc.) may ultimately affect release of halomethanes into the atmosphere.

M. pyrifera, the dominant macroalga in southern California, produces an estimated $3x10^6$ g Br/yr from $CHBr_3$, CH_2Br_2, and methyl bromide (MeBr) in Orange and San Diego Counties. Bromoform contributes 77% of that bromine. Anthropogenic bromine emissions appear to dominate macroalgal emissions in this region because MeBr fumigation alone releases an estimated 10^8 g Br/yr. California accounts for approximately 10% of global MeBr use, thus this pattern of dominant MeBr emission is not expected for all coastal regions, but it may represent other areas with dense urban and agricultural development.

Although both $CHBr_3$ and CH_2Br_2 are released by macroalgae, only CH_2Br_2 was degraded by kelp-associated microorganisms in seawater enrichments. Dibromomethane degradation rates in seawater enrichments ranged from 0.11 to 73 nmoles CH_2Br_2/day·L seawater, depending in part on the initial CH_2Br_2 concentration. Microbial degradation was observed only for dihalomethanes; CH_2Br_2 and dichloromethane (CH_2Cl_2) were degraded, but $CHBr_3$ and MeBr were not. Dibromomethane degradation was associated with particles >1.2 μm, supporting the hypothesis that CH_2Br_2-degrading bacteria may be attached to kelp surfaces in the environment. Inhibitor studies indicated that eukaryotic organisms and a number of microbial processes, including methanotrophy, did not contribute to CH_2Br_2 degradation.

Laboratory degradation rates were extrapolated to environmental conditions based on seawater CH_2Br_2 concentrations measured in a *M. pyrifera* canopy (0.018 nM). Microbial degradation at this CH_2Br_2 concentration was estimated as 0.023 ng CH_2Br_2/day·L, at maximum; approximately 136 days would be required to deplete 0.018

nM CH_2Br_2 at this degradation rate. This result indicates that the rate of microbial degradation is slower than volatilization of CH_2Br_2 from the ocean yet faster than hydrolysis or halide substitution. Macroalgal production was estimated as 19 ng CH_2Br_2/day·L seawater based on whole blade incubations and *M. pyrifera* biomass density, which was 0.4 kg/m^3 (averaged over the water column) estimated from field and laboratory measurements. Microbial CH_2Br_2 degradation thus represents only 0.1% of CH_2Br_2 production by *M. pyrifera*, well within the error of the production estimate itself. Although microbial degradation of CH_2Br_2 occurs, it appears to be an insignificant water column sink within the kelp bed. Microbes attached to kelp surfaces, however, could encounter elevated CH_2Br_2 concentrations, and significant degradation might occur at the kelp surface. Macroalgal production measurements would thus reflect net production from kelp and associated CH_2Br_2-degrading microbes, but production estimates themselves would remain unchanged.

Table of Contents

List of Tables

List of Figures

Preface

Chapter 2 is from the following publication with permission: Manley, S.L., Goodwin, K., and North W.J. (1992). The Production of Bromoform, Methylene Bromide, and Methyl Iodide by Macroalgae and Distribution on Nearshore Southern California Waters. *Limnol. Oceanogr.* **37**(8), 1652-1659.

The work presented here was accomplished through the efforts of many people. Dr. Steven Manley (Cal. State University, Long Beach) performed all laboratory macroalgal incubations presented in Chapter 2. All gas chromatography for that chapter was performed in Dr. Manley's laboratory. Dr. Wheeler North (Caltech Environmental Engineering Science) collected algal samples for laboratory incubations presented in Chapter 2, and he was central to completing field work presented in both Chapter 2 and Chapter 5.

Amy Garner and Mike Mulqueen were essential to accomplishing the work presented in Chapter 3, "Macroalgal Production of Bromoform and Dibromomethane," through their assistance with laboratory incubations and numerous injections into gas chromatographs (GC). Polyethylene films were analyzed for light transmission by Dr. George Rossman (Caltech Geology and Planetary Science). Nuclear magnetic resonance chemical shifts were assigned by Dr. Robert Johnson and Vidyasankar Sundaresan (Caltech Chemical Engineering). Dr. Johnson additionally assisted with figure preparation and proofreading of this manuscript.

Penny Sherman was key to completing the work presented in Chapter 4, "Marine Microbial Degradation of Dibromomethane," through her assistance with GC injections,

protein assays, and isolation studies. The efforts of A. Garner and P. Sherman sometimes overlapped; each assisted with both aspects of the project – microbial degradation and macroalgal production. Andria Costello assisted with GC injections and Becky Green assisted with protein assays during an early phase of the microbial degradation project. Dr. Andrei Chistoserdov provided advice regarding inhibition and induction studies, and Kelly Smith provided methanotroph isolates.

Monique Wong and Erika Brandenburg assisted with field work and laboratory biomass analyses detailed in Chapter 5, "*Macrocystis Pyrifera* Biomass and Production of Brominated Methanes *in Situ*." Rasheeda Abdush-Shaheed assisted with GC injections and construction of mylar bags used for *in situ* incubations.

Chapter One

Introduction: Brominated Methanes In The Environment

Bromine in the Atmosphere

Brominated methanes are investigated partly because of concerns over the roles brominated species play in atmospheric chemistry. Bromine involvement in catalytic destruction of ozone was first recognized in the 1970's (e.g., Wofsy *et al.* 1975), and it is now widely acknowledged. Ozone is a critical component of the atmosphere. Stratospheric ozone screens out almost all solar radiation with wavelengths between 240-290 nm (Wayne 1985, p. 113; Stamnes 1993). Radiative energy in the UV-B (280-320 nm) and UV-C (< 280 nm) regions can produce harmful biological effects (Setlow 1974; Stamnes 1993), including skin cancer (Wayne 1985, pp. 145-149). There is thus increasing concern over the biological consequences of the stratospheric "ozone hole" (Solomon 1990; World Meteorological Organization 1991).

Ozone absorbs both solar and infrared (IR) radiation, thus it is important to the energy balance of both the troposphere (surface to 10-15 km in height) and the stratosphere (troposphere to about 50 km in height) (Lacis *et al.* 1990). Changes in ozone concentrations may have complex climatic consequences, and even a relatively small redistribution of ozone in the troposphere and stratosphere may have significant impacts on climate (Ramanathan *et al.* 1985; Lacis *et al.* 1990). Model calculations indicate that decreased ozone concentrations above 30 km could produce surface warming and that decreased ozone concentrations below 30 km could produce surface cooling (Lacis *et al.*

1990). Furthermore, model calculations have suggested that between 1979-1990 surface cooling from ozone depletion below 30 km could have offset approximately 30% of surface warming due to greenhouse gases from that same period (Molnar *et al.* 1994). The complex interplay of atmospheric processes highlights the need to understand the biogeochemical cycles of compounds involved in ozone-depleting chemistry.

Bromine is estimated to cause 20-30% of the observed ozone loss in the Antarctic lower stratosphere during periods of polar stratospheric clouds and ClO concentrations >1 ppb (v/v) (U.N. Environment Programme 1992). Bromine chemistry and bromine biogeochemical cycles may impact ozone concentrations even in the troposphere (Li *et al.* 1994). In fact, bromine appears to be a key component in seasonal ozone losses observed in the Arctic troposphere. Concomitant with the Arctic spring ozone minimum, high concentrations of bromine have been collected on particulate filters in several Arctic locations such as Alert, Northwest Territories, Canada (e.g., Barrie *et al.* 1994) and Barrow, Alaska (e.g., Oltmans *et al.* 1989). Such findings suggest that bromine involvement in ozone depletion is an Arctic-wide phenomenon (Li *et al.* 1994).

Bromine is estimated to be about 40 times more effective than chlorine at destroying ozone on a per molecule basis (U.N. Environment Programme 1992). The balance of reactive bromine compounds (Br and BrO) and reservoir compounds (HBr, HOBr, BrCl and $BrONO_2$) depends on altitude, latitude, season, and the abundance of a variety of other reactive compounds (e.g., OH); thus bromine involvement in the catalytic destruction of ozone will vary with such factors (U.N. Environment Programme 1992). Bromine-catalyzed ozone depletion in the stratosphere mainly occurs through coupled

bromine and chlorine reactions as in the following sequence (U.N. Environment Programme 1992; Cicerone 1994) first proposed by Yung *et* al. 1980:

$$Br + O_3 \rightarrow BrO + O_2$$
$$Cl + O_3 \rightarrow ClO + O_2$$
$$\underline{ClO + BrO + (h\nu) \rightarrow Cl + Br + O_2}$$
$$Net: 2O_3 \rightarrow 2O_2$$

A dominant source of bromine to the atmosphere is marine aerosols (Wofsy *et al.* 1975); however, this particulate material is readily rained out and more volatile gases typically mix higher into the atmosphere (Moore and Tokarczyk 1993). Free bromine is released from brominated methanes primarily through photodissociation or reaction with hydroxyl radicals (OH or OH·).

Changes in brominated methane concentrations have the potential to affect OH concentrations, as well as ozone. Hydroxyl radicals are the major oxidant in the lower atmosphere, and most trace gases with carbon-hydrogen bonds react with them (Graedel and Crutzen 1993, pp. 117-118). Most hydrogen-containing gases involved in ozone and radiatively active ("greenhouse") gas chemistry are destroyed by OH (Prinn *et al.* 1995). Diminished concentrations of tropospheric OH could perturb the chemistry of the atmosphere by causing many trace gases to increase in concentration (Rasmussen and Khalil 1986; Crutzen and Andreae 1990), including greenhouse gases and gases involved in stratospheric ozone depletion. Therefore, understanding the balance of atmospheric gases is important if we are to accurately predict the consequences of changing that balance.

Selected Sources of Brominated Methanes

Investigation of brominated methanes is motivated by the need to formulate environmental policy based on a solid scientific framework, as well as scientific curiosity (Cicerone 1994). Atmospheric budgets help in understanding the atmospheric balance. A budget is formulated, in part, by assessing sources and sinks of atmospheric constituents and distinguishing natural from anthropogenic sources. Natural sources provide the background abundance to which anthropogenic sources are added.

The distinction between natural and anthropogenic sources is particularly relevant for the brominated methane, methyl bromide (MeBr). Methyl bromide has both natural and anthropogenic sources including biomass burning, which can be either natural or anthropogenic (Manö and Andreae 1994). Production of synthetic MeBr has grown 50% between 1984 and 1991, and in 1993 the EPA proposed to phase out MeBr production because of its involvement in ozone-depleting chemistry (Cicerone 1994). A final ruling has been on hold partly because the scientific basis for the ruling has been debated. More information regarding bromine biogeochemical cycles are needed to better assess the impact of MeBr anthropogenic emissions. In fact, understanding production of MeBr by marine organisms is listed by the U.N. Environmental Programme (1992) as a high priority research need.

Li *et al.* (1994) suggest that even though MeBr is often cited as the most important carrier of bromine to the atmosphere, other brominated methanes warrant investigation. They cite evidence that brominated methane species with relatively short atmospheric lifetimes can reach relatively high altitudes; therefore total organic bromine,

and not only MeBr, should be salient to ozone cycling in the stratosphere and the troposphere. Bromoform ($CHBr_3$) and dibromomethane (CH_2Br_2) are two other brominated methanes important to the bromine biogeochemical cycle (Reifenhäuser and Heumann 1992). Bromoform is prevalent in Antarctic (Heumann 1993) and Arctic (Li *et al.* 1994) atmospheres. Its concentrations are negatively correlated with ozone concentrations after polar sunrise in the Arctic (Oltmans *et al.* 1989; Leaitch *et al.* 1994), even on an hourly basis (Yokouchi *et al.* 1994). Bromoform has been suggested as the key supplier of reactive bromine causing photolytic destruction of tropospheric ozone in the Arctic spring (Sheridan *et al.* 1993). Heterogeneous reactions are implicated because gas phase photochemistry is apparently too slow to account for the temporal relationship of $CHBr_3$ to ozone (Sheridan *et al.* 1993). The surface snowpack or ice crystals in the air above the snowpack have been suggested as possible surfaces for heterogeneous reactions (Leaitch *et al.* 1994).

Marine biogenic sources of $CHBr_3$ and CH_2Br_2 have been indicated from concentration patterns in air (Class and Ballschmiter 1988; Atlas *et al.* 1993) and seawater (Class and Ballschmiter 1988; Reifenhäuser and Heumann 1992; Moore and Tokarczyk 1993). Furthermore, seawater from macroalgal stands are associated with elevated concentrations of these compounds (e.g., Manley *et al.* 1992; Klick 1992). Heumann (1993) stressed the need to investigate biogenic production of halogenated compounds because of halocarbon involvement in Arctic ozone cycling and the fact that halocarbons strongly absorb IR radiation. He suggested that the global warming potential of biogenic halocarbons be investigated in light of proposals to fertilize the Antarctic Ocean in order

to increase algal primary productivity and thus carbon dioxide (CO_2) uptake. A similar idea has been proposed to uptake atmospheric CO_2 using open-ocean farms consisting of macroalgae such as the California species, *Macrocystis pyrifera* (Ritschard 1992). The potential roles of biogenic halocarbons in atmospheric chemistry suggest a need to investigate halocarbon releases from temperate macroalgae. Production of $CHBr_3$ and CH_2Br_2 by the macroalga *M. pyrifera* were investigated in this study and results are presented in Chapters 2, 3, and 5.

Brominated Methane Sinks

Sinks, as well as sources, of brominated methanes are an important part of the bromine biogeochemical cycle. Sinks determine the residence time of the compound, and compounds that are longer-lived in the atmosphere are more likely to survive transport to the stratosphere, where they may there undergo reactions that deplete ozone. Important atmospheric sinks of brominated methanes include photolysis (Moortgat *et al.* 1993) and reaction with hydroxyl radicals (Mellouki *et al.* 1992). Brominated methane atmospheric lifetimes are usually estimated from laboratory experiments or model calculations of destruction rates from photolysis or OH.

Aquatic sinks such as hydrolysis, halide substitution, or photolysis may also be important, at least for MeBr. Aqueous MeBr is substantially more reactive than $CHBr_3$ or CH_2Br_2. For example, the half-life of MeBr due to hydrolysis is about three weeks in 25 °C freshwater compared to 183 years for CH_2Br_2 and 686 years for $CHBr_3$ (Mabey and Mill 1978). The half-life of MeBr due to chloride substitution is about three weeks for seawater at 17 °C (Elliott and Rowland 1993) while the half-life for $CHBr_3$ was found to

range from 1.3 - 18.5 years for seawater at 25 °C (Geen 1992). There apparently have been few relevant studies of aqueous phase halocarbon photoreactions (Zepp and Ritmiller 1995), and none were located in the literature for $CHBr_3$ or CH_2Br_2. Adsorption of polyhalogenated compounds to humic materials in estuarine and marine waters was concluded to be negligible by Helz and Hsu (1978).

Longshore currents dominate coastal currents in southern California. Current velocities through a well-developed kelp bed are on the order of 1 cm/s, about a third of velocities measured outside the bed. Residence time of water in a kelp bed (~1-7 km long) is thus on the order of a few days (Jackson and Winant 1983).

Volatilization appears to be the major water column sink for $CHBr_3$ and CH_2Br_2. Volatilization is an aquatic sink but an atmospheric source of brominated methanes. The half-lives of a number of volatile halocarbons, including $CHBr_3$, were calculated for relatively shallow, well-mixed coastal waters by Helz and Hsu (1978). They estimated halocarbon half-lives from volatilization on the order of less than one week (see Table 6.1). Half-lives for CH_2Br_2 and MeBr should be similar to $CHBr_3$ based on their similar diffusivities (equations of Hayduk and Laudie 1974).

Microbial sinks of brominated methanes in natural systems have been little studied even though microbial processes often influence the cycles of natural compounds. Microbial degradation of MeBr in soils (Oremland 1994) and $CHBr_3$ degradation in an anaerobic aquifer (Bouwer *et al.* 1981) have been reported. However, no studies were located in the literature describing microbial degradation of $CHBr_3$ or CH_2Br_2 in a marine environment. Degradation of $CHBr_3$ and CH_2Br_2 by microbes associated with the

macroalga *M. pyrifera* were investigated in this study and results are presented in Chapter 4.

References

Atlas, E., Pollock, W., Greenberg, J. & Heidt, L. (1993). Alkyl Nitrates, Nonmethane Hydrocarbons, and Halocarbon Gases Over the Equatorial Pacific Ocean During Saga 3. *J. Geophys. Res.* **98**, 16933-16947.

Barrie, L.A., Li, S.-M. & Toom, D.L. (1994). Lower Tropospheric Measurements of Halogens, Nitrates, and Sulphur Oxides During Polar Sunrise Experiment 1992. *J. Geophys. Res.* **99**, 25453-25467.

Bouwer, E.J., Rittmann, B.E. & McCarty, P.L. (1981). Anaerobic Degradation of Halogenated 1- and 2-Carbon Organic Compounds. *Environ. Sci. Technol.* **15**, 596-599.

Cicerone, R.J. (1987). Changes in Stratospheric Ozone. *Science* **237**, 35-42.

Cicerone, R.J. (1994). Fires, Atmospheric Chemistry, and the Ozone Layer. *Science* **263**, 1243-1244.

Class, TH. & Ballschmiter, K. (1988). Chemistry of Organic Traces in Air VIII: Sources and Distribution of Bromo- and Bromochloromethanes in Marine Air and Surfacewater of the Atlantic Ocean. *J. Atmos. Chem.* **6**, 35-46.

Crutzen, P.J. & Andreae, M.O. (1990). Biomass Burning in the Tropics: Impact on Atmospheric Chemistry and Biogeochemical Cycles. *Science* **250**, 1669-1678.

Elliott, S. & Rowland, S. (1993). Nucleophilic Substitution Rates and Solubilities for Methyl Halides in Seawater. *Geophys. Res. Lett.* **20**, 1043-1046.

Geen, C.E. (1992). Selected Marine Sources and Sinks of Bromoform and Other Low Molecular Weight Organobromines. M.Sc. Thesis, Dalhousie University, Halifax, Nova Scotia.

Graedel, T.C. & Crutzen, P.J. (1993). *Atmospheric Change An Earth System Perspective.* W.H. Freeman & Co., NY.

Hayduk, W. & Laudie, H. (1974). Prediction of Diffusion Coefficients for Nonelectrolytes in Dilute Aqueous Solutions. *AIChE Journal* **20**, 611-615.

Helz, G.R. & Hsu, R.Y. (1978). Volatile Chloro- and Bromocarbons in Coastal Waters. *Limnol. Oceanogr.* **23**, 858-869.

Heumann, K.G. (1993). Determination of Inorganic and Organic Traces in the Clean Room Compartment of Antarctica. *Analytica Chemica Acta* **283**, 230-245.

Jackson, G.A. & Winant, C.D. (1983). Effect of a Kelp Forest on Coastal Currents. *Cont. Shelf Res.* **2**, 75-80.

Klick, S. (1992). Seasonal Variations of Biogenic and Anthropogenic Halocarbons in Seawater from a Coastal Site. *Limnol. Oceanogr.* **37**, 1579-1585.

Lacis, A.A., Wuebbles, D.J. & Logan, J.A. (1990). Radiative Forcing of Climate by Changes in the Vertical Distribution of Ozone. *J. Geophys. Res.* **95**, 9971-9981.

Leaitch, W.R., Barrie, L.A., Bottenheim, J.W., Li, S.-M., Shepson, P.B., Muthuramu, K. & Yokouchi, Y. (1994). Airborne Observations Related to Ozone Depletion at Polar Sunrise. *J. Geophys. Res.* **99**, 25499-25517.

Li, S.-M., Yokouchi, Y., Barrie, L.A., Muthuramu, K., Shepson, P.B., Bottenheim, J.W., Sturges, W.T. & Landsberger, S. (1994). Organic and Inorganic Bromine Compounds and Their Composition in the Arctic Troposphere During Polar Sunrise. *J. Geophys. Res.* **99**, 25415-25428.

Mabey, W. & Mill, T. (1978). Critical Review of Hydrolysis of Organic Compounds in Water Under Environmental Conditions. *J. Phys. Chem. Ref. Data* **7**, 383-409.

Manley, S.L., Goodwin, K. & North, W.J. (1992). Laboratory Production of Bromoform, Methylene Bromide and Methyl Iodide by Macroalgae and Distribution in Nearshore Southern California Waters. *Limnol. Oceanogr.* **37**, 1652-1659.

Manö, S. & Andreae, M.O. (1994). Emission of Methyl Bromide from Biomass Burning. *Science* **263**, 1255-1257.

Mellouki, A., Talukdar, R.K., Schmoltner, A.-M., Gierczak, T., Mills, M.J., Solomon, S. & Ravishankara, A.R. (1994). Atmospheric Lifetimes and Ozone Depletion Potentials of Methyl Bromide (CH_3Br) and Dibromomethane (CH_2Br_2). *Geophys. Res. Lett.* **19**, 2059-2062.

Molnar, G.I., Ko, M.K.W., Zhou, S. & Sze, N.D. (1994). Climatic Consequences of Observed Ozone Loss in the 1980s: Relevance to the Greenhouse Problem. *J. Geophys. Res.* **99**, 25755-25760.

Moore, R.M. & Tokarczyk, R. (1993). Volatile Biogenic Halocarbons in the Northwest Atlantic. *Global Biogeochem. Cycles* **7**, 195-210.

Moortgat, G.K., Meller, R. & Schneider, W. (1993). Temperature Dependence (256-296K) of the Absorption Cross Sections of Bromoform in the Wavelength Range 285-360 nm. In *The Tropospheric Chemistry of Ozone in the Polar Regions* (Niki, H. and Becker, K.H. eds.), Springer-Verlag, NY, pp. 359-369.

Oltmans, S.J., Schnell, R.C., Sheridan, P.J., Peterson, R.E., Li, S.-M., Winchester, J.W., Tans, P.P., Sturges, W.T., Kahl, J.D. & Barrie, L.A. (1989). Seasonal Surface Ozone and Filterable Bromine Relationship in the High Arctic. *Atmos. Environ.* **23**, 2431-2441.

Oremland, R.S., Miller, L.G., Culbertson, C.W., Connell, T.L. & Jahnke, L.L. (1994). Degradation of Methyl Bromide by Methanotrophic Bacteria in Cell Suspensions and Soils. *Appl. Environ. Micro.* **60**, 3640-3646.

Prinn, R.G., Weiss, R.F., Miller, B.R., Huang, J., Alyea, F.N., Cunnold, D.M., Fraser, P.J., Hartley, D.E. & Simmonds, P.G. (1995). Atmospheric Trends and Lifetime of CH_3CCl_3 and Global OH Concentrations. *Science* **269**, 187-192.

Ramanathan, V., Cicerone, R.J., Singh, H.B. & Kiehl, J.T. (1985). Trace Gas Trends and Their Potential Role in Climate Change. *J. Geophys. Res.* **90**, 5547-5566.

Rasmussen, R.A. & Khalil, M.A.K. (1986). The Behavior of Trace Gases in the Troposphere. *Science Total Environ.* **48**, 169-186.

Reifenhäuser, W. & Heumann, K.G. (1992). Bromo- and Bromochloromethanes in the Antarctic Atmosphere and the South Polar Sea. *Chemosphere* **9**, 1293-1300.

Ritschard, R.L. (1992). Marine Algae as a CO_2 Sink. *Water Air Soil Pollut.* **64**, 289-303.

Setlow, R.B. (1994). The Wavelengths in Sunlight Effective in Producing Skin Cancer: A Theoretical Analysis. *Proc. Nat. Acad. Sci. USA* **71**, 3363-3366.

Sheridan, P.J., Schnell, R.C., Zoller, W.H., Carlson, N.D., Rasmussen, R.A., Harris, J.M. & Sievering, H. (1993). Composition of Br-containing Aerosols and Gases Related to Boundary Layer Ozone Destruction in the Arctic. *Atmos. Environ.* **27A**, 2839-2849.

Solomon, S. (1990). Antarctic Ozone: Progress Toward a Quantitative Understanding. *Nature* **347**, 347-354.

Stamnes, K. (1993). The Stratosphere as a Modulator of Ultraviolet Radiation into the Biosphere. *Surveys in Geophysics* **14**, 167-186.

U.N. Environment Programme. (1992). Montreal Protocol Assessment Supplement. Methyl Bromide: Its Atmospheric Science, Technology and Economics. Nairobi, Kenya.

Wayne, R.P. (1985). *Chemistry of Atmospheres*. Clarendon Press, Oxford.

Wofsy, S.C., McElroy, M.B. & Yung, Y.L. (1975). The Chemistry of Atmospheric Bromine. *Geophys. Res. Lett.* **2**, 215-218.

World Meteorological Organization. (1991). Scientific Assessment of Stratospheric Ozone: 1991. Global Ozone Research and Monitoring Project – Report No. 25, Geneva, Switzerland.

Yokouchi, Y., Akimoto, H., Barrie, L.A., Bottenheim, J.W., Anlauf, K. & Jobson, B.T. (1994). Serial Gas Chromatographic/Mass Spectrometric Measurements of Some Volatile Organic Compounds in the Arctic Atmosphere During the 1992 Polar Sunrise Experiment. *J. Geophys. Res.* **99**, 25379-25389.

Yung, Y.L., Pinto, J.P., Watson, R.T. & Sander, S.P. (1980). Atmospheric Bromine and Ozone Perturbations in the Lower Stratosphere. *J. Atmos. Sci.* **37**, 339-353.

Zepp, R.G. & Ritmiller, L.F. (1995). Photoreactions Providing Sinks and Sources of Halocarbons in Aquatic Environments. In *Aquatic Chemistry: Interfacial and Interspecies Processes, Adv. Chem. Ser. 244* (Huang, C.P., O'Melia, C.R. and Morgan, J.J. eds.), American Chemical Society, Washington, pp. 253-278.

Chapter Two

Laboratory Production of Bromoform, Methylene Bromide, and Methyl Iodide by Macroalgae and Distribution in Nearshore Southern California Waters[a]

Introduction

Bromoform ($CHBr_3$), methylene bromide (CH_2Br_2), and methyl iodide (CH_3I) are major natural vectors of gaseous bromine (Penkett *et al.* 1985) and iodine (Rasmussen *et al.* 1982) to the atmosphere. Productive coastal waters are enriched with $CHBr_3$ (Fogelqvist and Krysell 1991; Class and Ballschmiter 1988), CH_2Br_2 (Class and Ballschmiter 1988), and CH_3I (Lovelock 1975; Manley and Dastoor 1988) due in part to their production by marine macroalgae and possibly by marine microbes. Seaweeds appear to be the dominant natural oceanic source of $CHBr_3$ and CH_2Br_2 (Gschwend *et al.* 1985).

In addition to field observations, macroalgal production of these halomethanes has been measured in the laboratory. Gschwend *et al.* (1985) reported production rates for $CHBr_3$ [0.14-14 $\mu g\ d^{-1}\ (g\ DW)^{-1}$; g DW = g dry weight] and CH_2Br_2 [0.25-21 $\mu g\ d^{-1}\ (g\ DW)^{-1}$] for six algal species. Previous work (Manley and Dastoor 1988) on production rates of CH_3I [100-300 $ng\ d^{-1}\ (g\ DW)^{-1}$] was performed on five kelp species (order Laminariales). Several lines of evidence support the conclusion that algae, not associated microbes, are primarily responsible for the halomethane production observed (Gschwend

---

[a] originally published as Manley, S. L., K. Goodwin, and W. J. North, *Limnol. Oceanogr.*, 37(8), 1992, 1652-1659.

et al. 1985). Furthermore, axenic tissue cultures of *Macrocystis pyrifera* have produced CH_3I (Manley and Dastoor 1988).

The biosynthesis of halomethanes by marine macroalgae has been studied by several researchers (e.g., Theiler *et al.* 1978; Wuosmaa and Hager 1990; Wever *et al.* 1991). Enzymes involved in methyl halide (monohalomethane) production appear to be different from those involved in polyhalomethane production.

This study determined production rates of $CHBr_3$, CH_2Br_2, and CH_3I by estuarine and nonestuarine subtidal macroalgae. The focus was on ecologically abundant and previously unreported species. In addition, seawater halomethane concentrations were used to identify areas of high halomethane production among several coastal environments in southern California.

Materials and Methods

Seaweeds for production rate studies were obtained from outside a bed of *M. pyrifera* (Figure 2.1, site 1) except for *Ulva* sp. and *Enteromorpha intestinalis* which were obtained from upper Newport Bay (site 4). Algae free of visible epiphytes were used except for *Rhodymenia californica* and *Dictyota binghamiae*; these had an estimated 15% and 20% epiphytic cover consisting primarily of bryozoans. Seaweeds were stored in large outdoor flow-through tanks for 1-4 d before use.

Seawater samples were obtained from several locations (Figure 2.1) and analyzed for halomethanes. Samples were collected by SCUBA in glass syringes with no headspace as described previously (Manley and Dastoor 1987). Seawater samples were taken from the canopy (site 1) and bottom (site 2) of a *Macrocystis* bed, from 0.7 km offshore (site

3), from an estuary (site 4), and from 5 km offshore (site 7). There were no sewage outfalls near the kelp bed. All surface samples were taken in the first 0.6 m of the water column. Seawater samples from the estuary and floor of the kelp bed were taken just above the sediments (0.1 and 9.8 m depths, respectively). A submarine canyon was a site of decaying macroalgal debris. Seawater samples were taken from the surface water above the canyon (site 5) and from the canyon bottom (site 6) adjacent to debris (21-m depth).

Seaweed production of halomethanes was measured by the method of Manley and Dastoor (1987). Tissue samples were placed with no headspace in separate serum bottles containing filtered (0.45 μm) offshore, surface seawater. The seawater was previously purged with ultrapure air to lower background halomethane concentrations. Whole algal thalli from separate individuals were used when possible. Sections of mature fronds were used for *Egregia menziesii*. Three tissue disks cut from the middle of separate mature blades were used for species with thalli too large for serum bottles. Disks were cut from different fronds of *Macrocystis* and from different individuals of *Laminaria farlowii* and *Eisenia arborea*. Excised tissue was placed in seawater 1 h before use to minimize physiological effects of wounding (see Arnold and Manley 1985). Previous studies (Manley and Dastoor 1988) have not found blade wounding to significantly affect CH_3I production.

Tissue samples were incubated for 2 or 3 h at 18°C and 150 μEinst m^{-2} s^{-1} illumination. Controls consisted of filtered seawater only. At the conclusion of the incubation, the seawater was extracted into nitrogen and analyzed for halomethanes.

Halomethane production was normalized to fresh weight (FW), dry weight (DW), and ash-free dry weight (AFDW). Previous work (Manley and Dastoor 1987) showed no significant differences in monohalomethane production in light or dark. Algal production of polyhalomethanes in the dark was not determined. All production rates were extrapolated to 24 h assuming equal production in light or dark.

Halomethanes were measured by an electron capture detector (^{63}Ni, Valco Inst. 140 BN) gas chromatograph (Perkin-Elmer No. 3920; HP 3390A integrator). Seawater samples in glass syringes were brought into equilibrium with ultrapure N_2. The gas phase was concentrated onto a cooled sampling loop (Dry Ice, isopropanol slurry, -78°C). The halomethanes were injected onto the column by simultaneously flushing the loop with carrier gas and immersing it in hot oil (275°C) (Manley and Dastoor 1987). The stainless steel column (3.05 m long x 0.32 cm diam) was packed with Porasil B 80/100 mesh. Column temperature was kept at 75°C for 20 min and then increased 2°C min^{-1} to a final temperature of 120°C. The carrier gas was argon : methane (95% : 5%) with a flow rate of 25 ml min^{-1}.

Peak identification and quantification was achieved by comparison to known standards prepared from dilution of liquid $CHBr_3$, CH_2Br_2, and CH_3I (Aldrich Chem. Co.) in pentane (nanograde, Mallinckrodt). Recovery ranged from 76 to 94% for $CHBr_3$, 91 to 95% for CH_2Br_2, and 89 to 96% for CH_3I. Values are presented without recovery correction.

Equilibrium concentrations in seawater were determined from headspace analysis using dimensionless partition coefficients at the temperature of extraction (Hunter-Smith

et al. 1983). Partition coefficients for $CHBr_3$ (Nicholson *et al.* 1984) and CH_2Br_2 (Mackay and Shiu 1981) were multiplied by 1.2 to account for the effect of seawater (Singh *et al.* 1983). The formula of Singh *et al.* (1983) was used for CH_3I. Partition coefficients [of seawater][b] at 25°C are the following: 0.029[c] $CHBr_3$, 0.015[d] CH_2Br_2, and 0.29 CH_3I.

Results and Discussion

Laboratory Production

Observed production rates of $CHBr_3$ and CH_2Br_2 by kelps (Table 2.1) were in the range reported for nonkelp species by Gschwend *et al.* (1985); production rates for kelps were not found in the literature. Additionally, production rates given here for five genera of nonkelp macroalgae appear to be previously unreported. Production rates observed for Pacific species of *Ulva* sp. and *Enteromorpha intestinalis* (Table 2.1) were 4-64 times greater than those reported for Atlantic species of *E. linza* and *Ulva lacta* by Gschwend *et al.* (1985). Production rates observed for the brown alga *Cystoseira osmundacea* (Order Fucales) were comparable to that of two other fucalean species reported by Gschwend *et al.* (1985).

Algal CH_3I production rates available in the literature appear to be limited to kelps. CH_3I production rates for seven nonkelp species were measured in this study (Table 2.1).

---

[b] added for clarity.
[c] original publication stated the freshwater value (0.025); values are unaffected.
[d] Tse *et al.* (1992) has since published improved partition coefficient data for CH_2Br_2; interpolating to 25°C and multiplying by the salting-out coefficient (1.2) gives a value of 0.043. Using this partition coefficient reduces all CH_2Br_2 concentrations reported in the original publication by a factor of 3.0 to 3.2 depending on the temperature of extraction.

Observed CH_3I production rates were higher for the kelps than for other species except for a nonkelp brown alga, *Cystoseira*. Observed CH_3I production rates by kelps were lower than values reported previously (Manley and Dastoor 1988). The reasons for this variability have not been thoroughly investigated. Tissue age does not seem to be a factor (Manley and Dastoor 1988). However, inherent and environmentally induced physiological differences may have affected CH_3I production.

Dictyota binghamiae did not produce bromomethanes and CH_3I production was low relative to other species (Table 2.1). *Rhodymenia californica* produced moderate amounts of bromomethanes but little CH_3I. *Corallina officinalis* did not produce CH_3I and produced the lowest amounts of bromomethanes, even when normalized to AFDW to account for heavy calcification. For example, the production of $CHBr_3$ was 2.5×10^3 ng h^{-1} (g AFDW)$^{-1}$, whereas the next lowest production rate was observed from the noncalcified *Cystoseira* at 5.2×10^3 ng h^{-1} (g AFDW)$^{-1}$.

Seawater Concentrations

Halomethane concentrations were measured in seawater collected on three dates from seven locations (Table 2.2). $CHBr_3$ was significantly more concentrated in seawater samples from the kelp bed canopy (site 1) than in seawater from outside the bed (site 3, $P < 0.05$, 14 September; $P < 0.10$, 14 August), from the estuary (site 4, $P < 0.05$), above and in the submarine canyon (site 5 and site 6, $P < 0.05$), or from the outer coastal area (site 7, $P < 0.05$). The high [$CHBr_3$] in the canopy was a result of *Macrocystis* $CHBr_3$ production (Table 2.1) and was the probable cause of the high [$CHBr_3$] in peripheral surface waters (Table 2.2). No enhanced [$CHBr_3$] was seen in seawater from the

submarine canyon or estuary as compared to the outer coast (Table 2.2). Seawater from algal belts of unknown species distribution has yielded $CHBr_3$ concentrations as high as 300 ng liter^{-1}, while $CHBr_3$ concentrations in noncoastal waters have been reported in a range of 1-23 ng liter^{-1} (Fogelqvist and Krysell 1991).

CH_2Br_2 was significantly ($P < 0.05$; Table 2.2) more concentrated in seawater samples from the kelp bed canopy and bottom (sites 1 and 2) than in seawater from outside the bed (site 3), above and in the submarine canyon (sites 5 and 6), or from seawater offshore (site 7). The relatively high [CH_2Br_2] in the canopy was a result of *Macrocystis* CH_2Br_2 production (Table 2.1). Estuarine seawater had a greater [CH_2Br_2] than seawater from any of the other locations ($P < 0.05$), including the kelp bed canopy. CH_2Br_2 was the only halomethane measured in which the highest concentration was not seen in kelp canopy seawater. The two estuarine species *Enteromorpha* and *Ulva* produced CH_2Br_2 during incubations (Table 2.1); however, these species also produced $CHBr_3$ which was not more concentrated in estuarine water relative to the canopy. The estuarine environment remains an interesting area for further research.

CH_3I was significantly ($P < 0.05$; Table 2.2) more concentrated in seawater from the kelp canopy and bottom (sites 1 and 2) than in seawater from the estuary (site 4), submarine canyon (site 6), or offshore (site 7). CH_3I concentrations were significantly higher ($P < 0.10$) in kelp bed seawater than in surface seawater above the submarine canyon (site 5).

The *Macrocystis* canopy had a density of 12 ± 5 kg FW m^{-2} (mean ± 95% C.I.) determined by quadrat sampling (McFarland and Prescott 1959). CH_3I concentrations

measured at the floor of the kelp bed and in the canopy–the region of highest biomass–were equal (Table 2.2). These results might be explained by vertical mixing because no thermocline was observed on this day. However, concentrations in the canopy were higher relative to the bottom for $CHBr_3$ and CH_2Br_2. Previous data (Manley and Dastoor 1987) show a vertical [CH_3I] gradient on one instance (June 1985; canopy and bottom, 3.5 and 2.2 ng liter^{-1}) and no gradient on another (February 1985; canopy and bottom, 1.3 and 1.0 ng liter^{-1}).

CH_3I production by understory algae does not appear to explain the discrepancy between CH_3I and bromomethane concentration profiles. The algae directly below the dense *Macrocystis* canopy were sparsely distributed and primarily crustose corallines. Although we did not incubate crustose algae, the articulated coralline, *Corallina*, did not produce significant quantities of CH_3I in laboratory incubations (Table 2.1).

Halomethane production and transport from nearshore macroalgae does not seem to explain the uniform [CH_3I] profile. Water transport into the region of the floor of the kelp bed should have resulted in similar profiles for all three compounds. The dominant nearshore macroalgae (by visual inspection) were the red algae *R. californica* (5-10% cover), *C. officinalis* (5%), and *Pterocladia capillacea* (1%) and the brown algae *D. binghamiae* (2%) and *C. osmundacea* (1%). A few individuals (<1%) of the kelps *E. arborea*, *E. menziesii*, and *L. farlowii* were also present. These algae produced bromomethanes in the laboratory yet only CH_3I [concentrations were similar in bottom

and canopy waters (Table 2.1)][e]. Microbial CH_3I production in the sediments may account for these results.

Water flowing from the estuary with the tide was not elevated in CH_3I. However, the dominant algae in the upper Newport Bay estuary, *E. intestinalis* and *Ulva* sp., both produced CH_3I at moderate rates in incubation studies (Table 2.1). Low levels of CH_3I in estuarine water may be due to volatilization. Methyl iodide may also act as a methylating agent in porewater (Ring and Weber 1988). A more thorough investigation of [CH_3I] profiles in estuaries is needed.

The estuary also contained a variety of angiosperms including *Zostera marina* (eel grass), *Spartina foliosa* (cord grass), and *Juncus acutus* (spiny rush). The ability of salt marsh higher plants to produce halocarbons has not been investigated. Enzymatic synthesis of methyl halides, however, has been demonstrated for a terrestrial succulent (ice plant) growing in saline soil (Wuosmaa and Hager 1990). The release of volatile iodine, possibly CH_3I, from bean plant foliage has also been reported (Amiro and Johnston 1989).

Water taken from the submarine canyon (site 6) was not significantly enriched in CH_3I as compared to water from the surface (sites 5 and 7). Marine microbial production of CH_3I has been reported (Manley and Dastoor 1988), thus high halomethane concentrations were expected in an area where seaweed collects and decays. Low [CH_3I] may reflect weak microbial production at this canyon. Alternatively, microbial consumption of any CH_3I produced may have resulted in a low net concentration.

---

[e]edited for clarity.

Surface seawater concentrations of these halomethanes showed a strong cross-shore gradient (kelp canopy, 0.7 km, and 5 km offshore) with the highest concentration in the kelp canopy and the lowest at 5 km (Figure 2.2). Attempts to identify areas of high halomethane production by measuring seawater concentrations (Table 2.2) are limited because measurements reflect net accumulation in an area. Dilution, volatilization, halogen exchange reactions, photolysis, and biodegradation tend to lower concentrations independent from gross production. It is apparent, however, that the *Macrocystis* canopy is a major source of these halomethanes.

Equilibrium calculations for the measured halomethanes showed them to be supersaturated in seawater with respect to marine air. These calculations used literature values of atmospheric concentrations above the open ocean (Class and Ballschmiter 1988; Singh *et al.* 1983) and the previously given partition coefficients. CH_2Br_2 in submarine canyon surface water was an exception; equilibrium calculations showed CH_2Br_2 to be saturated with respect to air at this location[f]. The supersaturation conditions at least partly reflect halomethane macroalgal production in coastal waters. For $CHBr_3$, canopy water was supersaturated on all days sampled even when using a reported atmospheric concentration of 200 pptv (1 pptv = 10^{-12} by volume) for open-ocean air with coastal input (Class and Ballschmiter 1988). Future studies will include measurements of both seawater and overlying air concentration.

---

[f]Calculations with the partition coefficients of Tse *et al.* 1992 give that seawater in the submarine canyon was saturated and the surface seawater above the canyon was slightly undersaturated with respect to overlying air.

Global Estimates

Previous extrapolations (Manley and Dastoor 1988) suggested that on a global basis seaweeds do not directly account for the estimated oceanic source strength of CH_3I (Singh *et al.* 1983). CH_3I production rates presented here from a wider variety of macroalgal species support this conclusion. It is possible, however, that macroalgae are significant indirect producers via microbial decay of seaweed iodocarbons.

Kelps are estimated to comprise two-thirds of the macroalgal biomass (60 Tg FW; DeVooys 1979). Kelps, by sheer mass, should be an important class of macroalgae in the global scheme. Estimates of global production of CH_2Br_2 and $CHBr_3$ by kelp are 1.7 Gg yr^{-1} and 1.0 x 10^2 Gg yr^{-1} when mean production rates (Table 2.1) are used. Monobromomethane production from kelp was estimated to be 0.1 Gg CH_3Br yr^{-1} (Manley and Dastoor 1987). Kelps, therefore, are estimated to produce a total 97 Gg organic Br yr^{-1}, 98% derived from bromoform.

Similar calculations for the nonkelp seaweeds using one-third of the global biomass and the mean values from Table 2.1 provide global production estimates of 0.9 Gg CH_2Br_2 yr^{-1} and 66 Gg $CHBr_3$ yr^{-1}. The contribution of nonkelp macroalgae is estimated at 64 Gg organic Br yr^{-1}, and therefore the total macroalgal input is estimated at 2 x 10^2 Gg yr^{-1} or 1 x 10^9 mol yr^{-1} of organic Br. Volatilization is probably the most important mechanism of bromomethane loss (Helz and Hsu 1978). If we assume that this Br is released into the atmosphere within a year, the input is the same order of magnitude as all known anthropogenic sources (Gschwend *et al.* 1985). These calculations suggest that marine macroalgae produce globally significant amounts of bromomethanes and have an important role in the biogeochemical cycling of bromine.

Table 2.1. Production rates of $CHBr_3$, CH_2Br_2, and CH_3I [ng d^{-1}(g FW)$^{-1}$][g h] from marine macroalgae (n = 3). [Percent dry weight (%DW) is shown for each species.][i]

	$CHBr_3$	CH_2Br_2[d,j]	CH_3I	%DW
		Phaeophyta (brown algae)		
Laminariales (kelps)				
Macrocystis pyrifera	3.0×10^3	2.2×10^2	6.1	10
Laminaria farlowii	2.2×10^3	78	17	15
Egregia menziesii	6.8×10^3	74	3.1	16
Eisenia arborea	1.5×10^4	87	0.89	16
kelp mean:	6.9×10^3	1.1×10^2	6.8	
Nonkelps				
Dictyota binghamiae	0.0*	0.44*	0.25	18
Cystoseira osmundacea	5.6×10^2	1.5×10^2	2.2	15
		Rhodophyta (red algae)		
Corallina officinalis	4.8×10^2	48	0.12*	56
Pterocladia capillacea	1.0×10^4	2.4×10^2	1.4	26
Rhodymenia californica	1.2×10^4	81	0.32*	24
		Chlorophyta (green algae)		
Ulva sp.	3.6×10^4	1.9×10^2	1.2	18
Enteromorpha intestinalis	4.6×10^3	1.8×10^2	0.52	8
non-kelp mean:	9.1×10^3	1.3×10^2	0.86	

*production not significant compared to control ($p < 0.05$).

[g] printer's error in original publication is corrected.

[h] Based on 24 hr production, see Chapter 3 for values based on 12 hr photoperiod.

[i] added for clarity.

[j] See Chapter 3 for CH_2Br_2 values calculated with partition coefficients of Tse *et al.* 1992 and salting-out coefficient of 1.2. Values in Table 3.6 are divided by 3.16 (0.049 seawater @28°C) except *M. pyrifera* and *Ulva* sp. which are divided by 2.97 (0.046 seawater @26.5°C).

Table 2.2. Seawater halomethane concentrations (ng liter^{-1}) (SD, *n* in parentheses) from various coastal sites. Details given in Figure 2.1 and text.

location (site)	[$CHBr_3$]	[CH_2Br_2][d,k]	[CH_3I]
14 September 90			
Kelp canopy (1)	516 (90, 4)	8.5 (1.4,5)	1.4 (0.31, 5)
Bed bottom (2)	292 (96, 3)	6.2 (0.67, 4)	1.4 (0.33, 3)
Outside canopy (3)	131 (17, 4)	4.0 (0.44, 4)	0.97 (0.19, 3)
Estuary (4)	18 (12, 3)	12 (1.9, 3)	0.37 (0.14, 3)
8 August 90			
Kelp canopy (1)	422 (68, 3)	10 (0.95, 3)	1.3 (0.081, 3)
Above canyon (5)	12 (1.4, 2)	0.94 (0.37, 2)	0.54 (0.092, 2)
Canyon bottom (6)	11 (5.2, 3)	1.4 (0.57, 4)	0.53 (0.12, 3)
14 August 90			
Kelp canopy (1)	124 (49, 4)	10 (3.0, 5)	1.1 (0.22, 4)
Outside canopy (3)	43 (20, 3)	6.7 (2.1, 3)	0.81 (0.021, 3)
Outer coastal (7)	22 (6.5, 3)	2.4 (0.67, 3)	0.49 (0.14, 4)

[k] CH_2Br_2 values calculated with partition coefficients of Tse *et al.* 1992 and salting-out coefficient of 1.2 give the following ([CH_2Br_2], SD): 9/14/90: kelp canopy (2.8, 0.46); bed bottom (2.1, 0.22); outside canopy (1.3, 0.14); estuary (3.8, 0.62). 8/8/90: kelp canopy (3.4, 0.31); above canyon (0.31, 0.12); submarine canyon (0.44, 0.19). 8/14/90: kelp canopy (3.5, 0.99); outside bed (2.2, 0.67); offshore (0.79, 0.22).

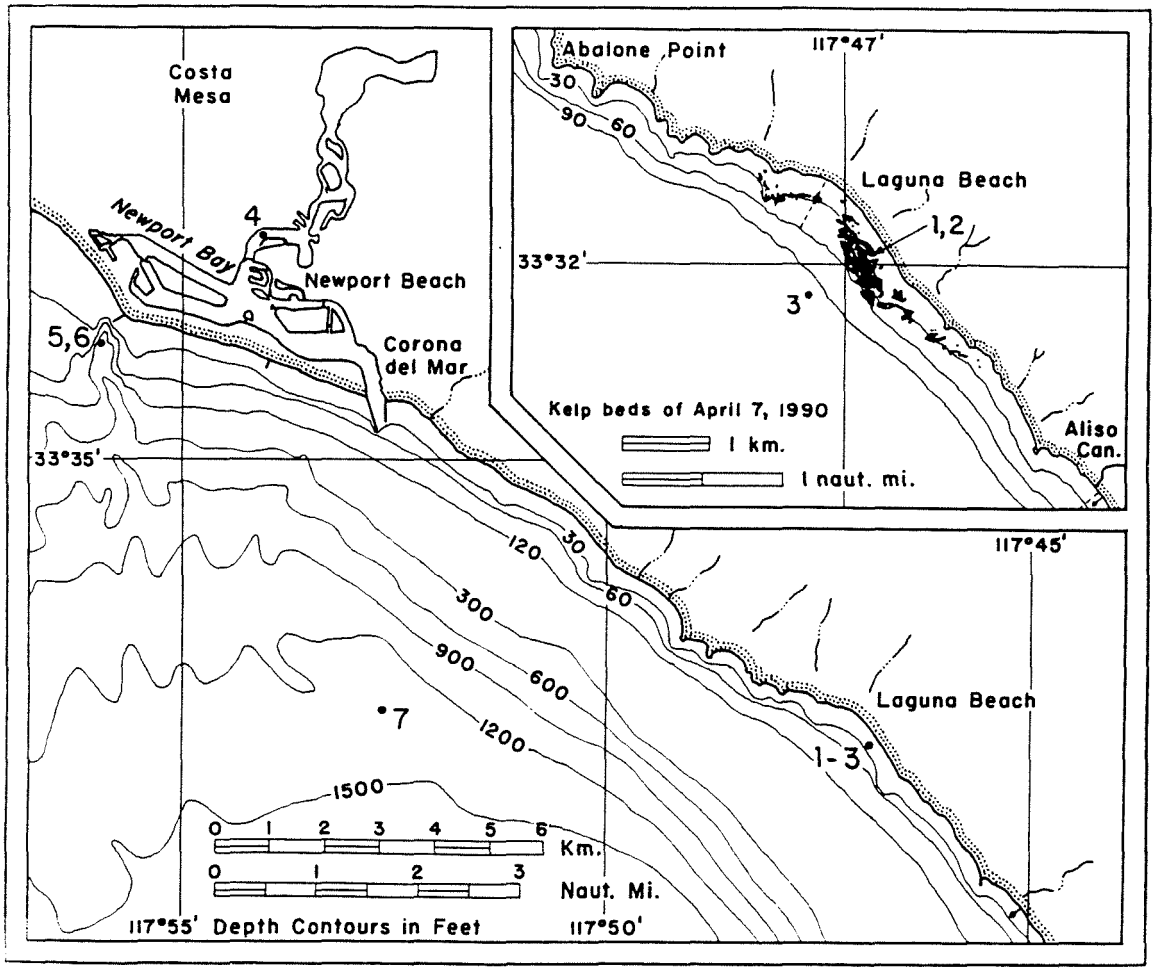

Figure 1. Coastal sites (Orange County, California) where seawater samples were obtained for $CHBr_3$, CH_2Br_2, and CH_3I analysis. Site 1 was in a kelp canopy (0.2 km from shore), site 2 at the floor of the kelp bed, and site 3 outside the kelp canopy (0.7 km offshore). Site 4 was in an estuary, sites 5 and 6 were above and in a submarine canyon, and site 7 was 5 km offshore (Depth contours in feet, 60 ft @ 18 m).

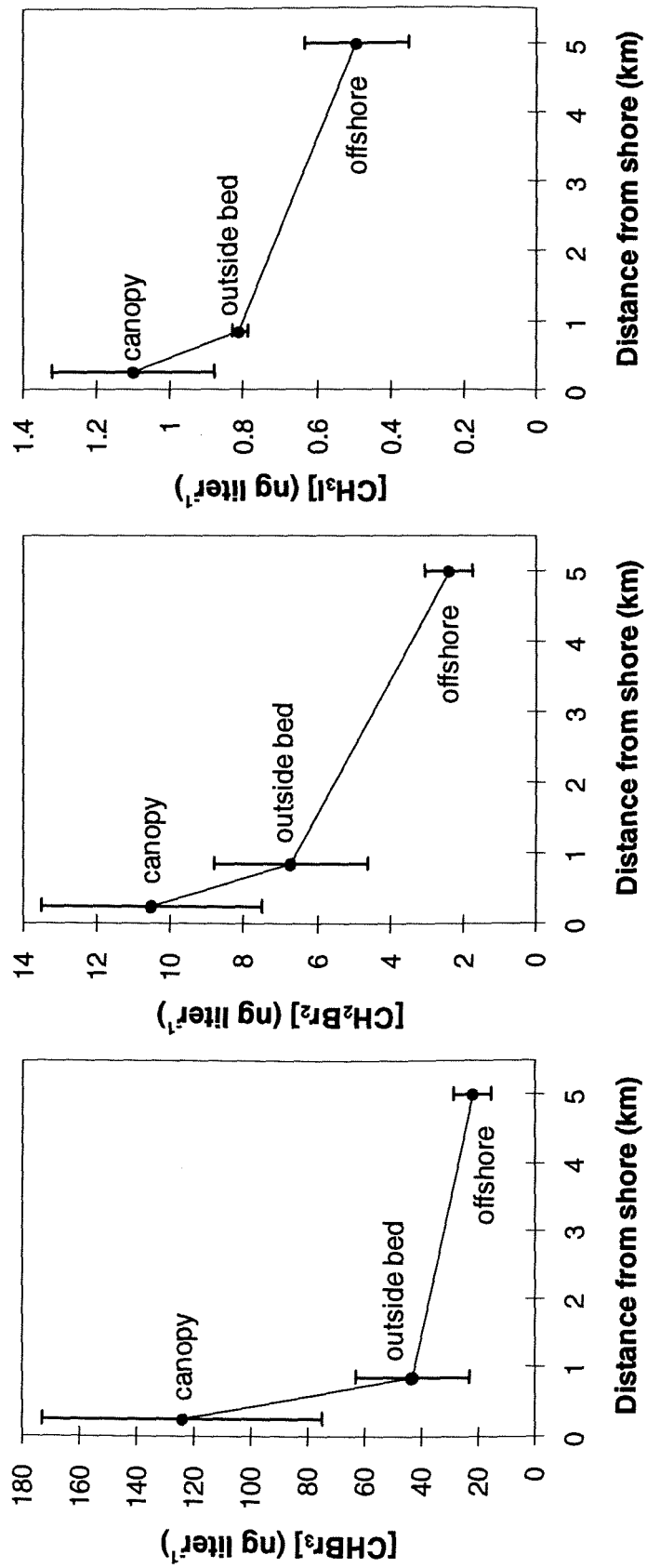

Figure 2.2. $CHBr_3$, CH_2Br_2, and CH_3I surface seawater concentrations (± 1 SD) as a function of distance from the shore, including a sample taken from the center of a dense *Macrocystis pyrifera* canopy. See Figure 2.1 for map. Samples collected 14 August 1990.

References

Amiro, B.D. & Johnston, F. L. (1989). Volatilization of Iodine from Vegetation. *Atmos. Environ.* **23**, 533-538.

Arnold, K.E. & Manley, S.L. (1985). Carbon Allocation in *Macrocystis pyrifera* (Phaeophyta): Intrinsic Variability in Photosynthesis and Respiration. *J. Phycol.* **21**, 154-167.

Class, T. & Ballschmiter, K. (1988). Chemistry of Organic Traces in Air VIII: Sources and Distribution of Bromo- and Bromochloromethanes in Marine Air and Surfacewater of the Atlantic Ocean. *J. Atmos. Chem.* **6**, 35-46.

De Vooys, C.G.N. (1979). Primary Production in Aquatic Environments. In: *The Global Carbon Cycle* (Bolin, B., Degens, E.T., Kempe, S., and Ketner, P. eds.), John Wiley & Sons, NY, pp. 259-292.

Fogelqvist, E., & Krysell, M.. (1991). Naturally and Anthropogenically Produced Bromoform in the Kattegatt, a Semi-Enclosed Oceanic Basin. *J. Atmos. Chem.* **13**, 315-324.

Gschwend, P.M., MacFarlane, J.K. & Newman, K.A. (1985). Volatile Halogenated Organic Compounds Released to Seawater from Temperate Marine Macroalgae. *Science* **227**, 1033-1035.

Helz, G.R. & Hsu, R.Y. (1978). Volatile Chloro- and Bromocarbons in Coastal Waters. *Limnol. Oceanogr.* **23**, 858-869.

Hunter-Smith, R.J., Balls, P.W., & Liss, P.S. (1983). Henry's Law Constants and the Air-Sea Exchange of Various Low Molecular Weight Halocarbon Gases. *Tellus* **35B**, 170-176.

Lovelock, J.E. (1975). Natural Halocarbons in the Air and in the Sea. *Nature* **256**, 193-194.

McFarland, W.N. and Prescott, J. (1959). Standing Crop, Chlorophyll Content, and *in Situ* Metabolism of a Giant Kelp Community in Southern California. *Inst. Mar. Sci., Univ. Texas* **6**, 109-132.

Mackay, D., and W.Y. Shiu. (1981). A Critical Review of Henry's Law Constants for Chemicals of Environmental Interest. *J. Phys. Chem. Ref. Data* **10**, 1175-1199.

Manley, S.L. & Dastoor, M.N. (1987). Methyl Halide (CH_3X) Production from the Giant Kelp, *Macrocystis* and Estimates of Global CH_3X Production by Kelp. *Limnol. Oceanogr.* **32**, 709-715.

Manley, S.L., and M.N. Dastoor. (1988). Methyl Iodide (CH_3I) Production by Kelp and Associated Microbes. *Mar. Biol.* **98,** 447-482.

Nicholson, B.C., Maguire, B.P. & D. B. Bursill. (1984). Henry's Law Constants for the Trihalomethanes: Effects of Water Composition and Temperature. *Environ. Sci. Technol.*, **18**, 518-521.

Penkett, S.A., Jones, B.M.R., Rycroft, M.J. & Simmons, D.A. (1985). An Interhemispheric Comparison of the Concentrations of Bromine Compounds in the Atmosphere. *Nature* **318**, 550-553.

Rasmussen, R.A., M.A.K. Khalil, R. Gunawardena, and S.D. Hoyt. (1982). Atmospheric Methyl Iodide (CH_3I). *J. Geophys. Res.* **87,** 3086-3090.

Ring, R.M., and J.H. Weber. (1988). Methylation of Tin (II) by Methyl Iodide Under Simulated Estuarine Conditions in the Absence and Presence of Fulvic Acid. *Sci. Total Environ.* **68**, 225-239.

Singh, H.B., Salas, L.J. & R.E. Stiles. (1983). Methyl halides in and over the eastern pacific (40°N-32°S). *J. Geophys. Res.* **88**, 3684-3690.

Theiler, R., Cook, J.C., Hager, L.P. & Siuda, J.F. (1978). Halohydrocarbon Synthesis by Bromoperoxidase. *Science* **202**, 1094-1096.

Wever, R., Tromp, M.G.M., Krenn, B.E., Marjani, A. & Tol, M.V. (1991). Brominating Activity of the Seaweed *Ascophyllum nodosum*: Impact on the Biosphere. *Environ. Sci. Technol.* **25**, 446-449.

Wuosmaa, A. & Hager, L.P. (1990). Methyl Chloride Transferase: A Carbocation Route for Biosynthesis of Halometabolites. *Science* **249**, 160-162.

Chapter Three

Macroalgal Production of Bromoform and Dibromomethane

Introduction

Brominated Methanes in the Environment

Brominated methanes are volatile, halogenated organic compounds present in the atmosphere in trace amounts (i.e., pptv; part per trillion by volume). Terrestrial and marine sources of brominated methanes deliver bromine to the atmosphere where it may become involved in catalytic destruction of ozone (see Chapter 1). Bromine species probably cause a significant amount of global ozone loss (U.N. Environmental Programme 1992). Increased ultraviolet radiation caused by stratospheric ozone loss might negatively effect human, animal, and marine ecosystem health. There are additional concerns because changes in tropospheric and stratospheric ozone are predicted to affect climate (Ramanathan *et al.* 1985; Lacis *et al.*). Changes in concentrations of ozone-depleting trace gases (e.g., halogenated methanes, chlorofluorocarbons) could have cumulative effects on climate rivaling even the predicted effects from changes in carbon dioxide concentrations (Ramanathan *et al.* 1985). An accurate biogeochemical picture of brominated methanes is needed to predict their atmospheric and climatic effects. Furthermore, an understanding of the biogenic sources of brominated methanes provides a context in which to evaluate impacts from anthropogenic emissions.

This study focuses on two brominated methanes, bromoform ($CHBr_3$) and dibromomethane (CH_2Br_2). These compounds are destroyed primarily in the troposphere,

releasing three and two bromine atoms, respectively. Bromoform is apparently the major natural source of bromine to the atmosphere (Penkett *et al.* 1985). Sheridan *et al.* (1993) suggested $CHBr_3$ to be the key organobromide involved in springtime ozone losses in Arctic surface layers. Dibromomethane has been observed near the tropical tropopause, the region where chemical constituents may transfer between troposphere and stratosphere (Wayne 1985, p. 62). Dibromomethane was estimated to contribute 7% of the total organic bromine in that region (Schauffler *et al.* 1993). Bromoform and CH_2Br_2 are produced naturally by marine algae (Gschwend 1985), and interest in Arctic ozone loss has encouraged investigation of brominated methane release from polar marine algae (e.g., Sturges *et al.* 1992; Schall *et al.* 1994; Nightingale *et al.* 1995). Bromoform is produced anthropogenically as a by-product of water, wastewater, and especially seawater chlorination (Helz and Hsu 1987; Kristiansen *et al.* 1994). Dibromomethane may be produced anthropogenically for use in future fire extinguishers and fumigants (Mellouki *et al.* 1992).

Oceanic concentrations of $CHBr_3$ and CH_2Br_2 were generally 20-50% supersaturated relative to overlying air with very large supersaturations of up to 800-1000% in coastal and coastally influenced waters (J. Lobert, unpublished results). The oceans thus appear to be an important global source of $CHBr_3$ and CH_2Br_2 to the atmosphere, and marine algae may be dominant producers of $CHBr_3$ and CH_2Br_2 measured in marine waters.

Methyl bromide (CH_3Br; MeBr), another important brominated methane, is probably the largest reservoir of atmospheric gaseous bromine (Khalil *et al.* 1993).

Methyl bromide is destroyed primarily in the troposphere, but a significant fraction survives transport to the stratosphere. Free bromine is released in the stratosphere primarily through reaction with hydroxyl radical. Methyl bromide is produced naturally by algae (Manley and Dastoor 1987) and is produced anthropogenically as an agricultural and structural fumigant. Anthropogenic sources account for only ~25% of atmospheric MeBr (U.N. Environmental Programme 1992).

Methyl bromide fumigation may be phased out because of its potential to destroy ozone (Chapter 1). Proposed regulation, however, has been debated on grounds that data are too incomplete to justify the economic consequences. The biogeochemical cycling of MeBr is indeed poorly understood. For example, oceanic waters were once considered supersaturated with MeBr and thus a net source of this compound to the atmosphere (Singh *et al.* 1983; Singh and Kanakidou 1993). Data now show (Lobert *et al.* 1995) that many oceanic waters are undersaturated and the global oceans are a small net sink for atmospheric MeBr. Biomass burning has recently been estimated to release approximately 30 Gg MeBr/yr into the atmosphere (Manö and Andreae 1994). This source, however, does not balance the MeBr budget (Anbar *et al.*, in press), and a large, perhaps natural, source of MeBr remains to be identified. More information is clearly needed regarding biogeochemical cycling of brominated methanes to ensure sound regulatory decisions.

Biogenic Production of Brominated Methanes

Marine macroalgae (seaweeds) are associated with elevated seawater concentrations of brominated methanes (Class and Ballschmiter 1988; Klick 1992; Manley *et al.* 1992). Seaweeds probably produce halogenated organics as part of a defense

system against microorganisms (McConnell and Fenical 1977), herbivores (Gschwend *et al.* 1985), or excess hydrogen peroxide (Collén *et* al. 1994). Halogenated organics may also be intermediates of metabolic processes involving nonhalogenated compounds (Krenn *et al.* 1989) or perhaps result from fortuitous side reactions of halogenating enzymes with broad substrate specificity (Gschwend *et al.* 1985). Early studies observed a suite of halogenated compounds, including $CHBr_3$ and CH_2Br_2, in macroalgal extracts (Moore 1977; McConnell and Fenical 1977). More recent studies have observed brominated methanes from macroalgal incubations (e.g., Gschwend *et al.* 1985; Manley *et al.* 1992; Schall *et al.* 1994). Bromoform tends to predominate the products followed by CH_2Br_2. Chlorodibromomethane ($ClCHBr_2$) and bromodichloromethane ($BrCHCl_2$) are also often observed.

Biochemical evidence supports that macroalgae produce brominated methanes, but the mechanisms have not been fully elucidated. Production of methyl halides (CH_3X; X = Br, Cl, I) appears to be distinct from production of polyhalogenated methanes (e.g., CH_2Br_2, $CHBr_3$). Methyl halide production evidently results from a methyl transferase that catalyzes the methylation of iodide, bromide, and chloride ions (White 1982; Wuosmaa and Hager 1990; Harper 1993). Wuosmaa and Hager (1990) suggested that methyl transferase may be broadly distributed among marine algae; however, Harper (1993) has criticized their methodology.

Polyhalogenated methanes are evidently produced by haloperoxidases. Haloperoxidases are a class of peroxidase enzyme that catalyze halide oxidation in the presence of hydrogen peroxide (H_2O_2), resulting in the halogenation of suitable organic

compounds. The name of the haloperoxidase indicates the range of halides the enzyme will utilize *in vitro*, e.g., chloroperoxidase will utilize chloride, bromide, or iodide in halogenation reactions, bromoperoxidase will utilize bromide or iodide, and iodoperoxidase will utilize only iodide (Neideman and Geigert 1986). Some haloperoxidases are iron heme proteins (Pedersén 1976; Manthey and Hager 1981) while others contain vanadium as a prosthetic group. Organisms containing vanadium haloperoxidases include the brown seaweeds *Laminaria saccharina* (de Boer *et al.* 1986a), *Ascophyllum nodosum* (de Boer *et al.* 1986b), and *M. pyrifera* (Butler *et al.* 1990), the red marine algae *Ceramium rubrum* (Krenn *et al.* 1987) and *Corallina pilulifera* (Krenn *et al.* 1989a), the lichen *Xanthoria Parietina* (Plat *et al.* 1987), and the terrestrial fungus *Curvularia inaequalis* (Wever *et al.* 1993). Both iron (Theilier *et al.* 1978; Beissner *et al.* 1981) and vanadium (Itoh and Shinya 1994) bromoperoxidases produce $CHBr_3$ and CH_2Br_2 *in vitro*.

The location of halogenation within an alga is unknown (Klick 1993), but the locale might indicate the natural haloperoxidase substrate and provide clues to halogenation function. Wever *et al.* (1991), for example, hypothesized that vanadium bromoperoxidase (V-BrPO) in *A. nodosum* uses surface water H_2O_2 because V-BrPO is located on the algal surface. However, *A. nodosum* apparently has two types of V-BrPO, both primarily associated with fruiting bodies (receptacles). One type (bromoperoxidase I) is located inside receptacles and the other type (bromoperoxidase II) is associated with receptacle surfaces (Krenn *et al.* 1989b). Bromoperoxidase activity in *A. nodosum* was detected in cell walls between the cortex and the medulla (inner cellular layers; see North

1994) and in cell walls of the thallus surface (Vitler 1983b). *M. pyrifera* was also observed to contain V-BrPO in cortical and surface regions; however, activity was found in protoplasts free of cell walls (Butler *et al.* 1990).

Formation of polyhalogenated methanes involves enzymatic halogenation of compounds with two or more carbons (C-2 or greater) (e.g., McConnell and Fenical 1977; Theiler *et al.* 1978; Beissner *et al.* 1981) which either spontaneously decompose or are enzymatically converted to halomethanes (e.g., Moore 1977; Harper 1993). Bromoform has been shown to form nonenzymatically from enzymatic bromination of C-7 and C-8 compounds (Beissner *et al.* 1981). Whether haloperoxidases form an enzyme-bound halogenating intermediate or generate hypohalous acid (HOCl, HOBr) which then reacts nonspecifically with nucleophilic acceptors is an issue of debate (Harper 1993).

Wever *et al.* (1991) subscribe to the theory that HOBr is released from the enzyme with subsequent nonenzymatic reaction of dissolved organic matter by the haloform reaction. The haloform reaction is commonly discussed with regard to water chlorination. The following haloform reaction scheme is simplified from Morris (1985), where X = Cl or Br:

$$RCOCH_3 \xrightarrow[HOX]{OH^-} RCOCH_2X \xrightarrow[HOX]{OH^-} RCOCHX_2 \xrightarrow[HOX]{OH^-} RCOCX_3$$

$$RCOCX_3 + H_2O \longrightarrow RCOOH + \mathbf{CHX_3}$$

Soedjak and Butler (1990), however, noted that accumulation of HOBr (determined spectrophotometrically as $HOBr/Br_2/Br_3^-$) occurred only in the absence of a halogen acceptor, e.g., with enzyme stored in water or non-amine containing buffer. They

concluded that build-up of $HOBr/Br_2/Br_3^-$ in the absence of organics does not necessarily imply that HOBr is the brominating species and that an enzyme bound intermediate remains plausible. Soedjak and Butler (1990) have proposed the following reaction scheme for V-BrPO organic bromination highlighting that the intermediate has not yet been identified:

$$H_2O_2 + Br^- \xrightarrow{\text{V-BrPO}} \text{"intermediate"} \xrightarrow{k_1\ \text{organic}} \text{Br-organic}$$

(i.e. HOBr, Br_3^-, Enz-OBr, Enz-Br)

Soedjak and Butler (1990) also suggested that the actual bromide oxidant may not be H_2O_2 because $HOBr/Br_2/Br_3^-$ accumulation occurs only at low pH with H_2O_2, but accumulation is obtained at higher pH when using peracetic acid.

Addition of H_2O_2, whether or not it is normally used *in vivo*, was observed to affect production of organobromides from the red alga *Meristiella gelidium* (Collén *et al.* 1994). Production of several halocarbons, including $CHBr_3$ and CH_2Br_2, increased with addition of 1 mM H_2O_2 compared to control cultures. Hydrogen peroxide diffuses through cell membranes (Frimer *et al.* 1983), but catalase, which consumes H_2O_2, does not (Collén *et al.* 1994). Addition of catalase did not halt increased production of halocarbons associated with adding H_2O_2. Collén *et al.* interpreted this result as indication of an intracellular source of H_2O_2 available to the bromoperoxidase enzyme. Collén *et al.* also added sodium azide (NaN_3) to cultures. Sodium azide is a catalase inhibitor; thus additional H_2O_2 should have been available to the enzyme and perhaps cause increased halomethane production. However, Collén *et al.* found decreased halocarbon production upon addition of sodium azide. Azide inhibits iron-containing enzymes (e.g., iron heme

peroxidases, cytochromes) (Pedersén 1976; Vitler 1983a), thus this result may indicate that the bromoperoxidase of *M. gelidium* contains an iron heme instead of vanadium.

Hydrogen peroxide can be produced both external and internal to an alga. Photochemical reactions produce H_2O_2 in sunlit waters through photooxidation of dissolved organic matter yielding higher concentrations in surface waters relative to dimly lit waters at depth (Cooper *et al.* 1988). This distribution could influence brominated methane production if bromoperoxidases rely primarily on external H_2O_2 supplies. Biological release of H_2O_2 has additionally been observed from certain cyanobacteria (Patterson and Myers 1973; Dubinin *et al.* 1992), microalgae (Zepp *et al.* 1987), and marine eukaryotic phytoplankton (Palenik *et al.* 1987). Marine phytoplankton could potentially introduce significant amounts of H_2O_2 into the marine environment (Palenik *et al.* 1987).

Photosynthesis and photorespiration can produce intracellular H_2O_2. Hydrogen peroxide production occurs during photosynthesis when electrons of Photosystem I are donated to O_2 instead of to $NADP^+$. This reaction is sometimes termed the "Mehler reaction" or "pseudocyclic photophosphorylation." Oxygen reduction with subsequent H_2O_2 production is expected when the ratio of ATP/NADPH is lowered. This ratio may be lowered by a variety of factors including environmental stress or plant illness (Elstner 1987).

Photorespiration is a complex metabolic pathway resulting from the dual action of ribulose-1,5-bisphosphate carboxylase (Rubisco), the enzyme responsible for fixing carbon dioxide (CO_2). Rubisco generally acts as a carboxylase (fixing CO_2), but it can also act as

an oxygenase (incorporating O_2) depending on the CO_2/O_2 ratio. If Rubisco acts as an oxygenase, glycolate is formed which can potentially leak from cells, losing valuable carbon. Photorespiration has apparently evolved to salvage some glycolate carbon by converting it into glyoxylate, a usable carbon form. Hydrogen peroxide is produced during photorespiration when glycolate (CO_2HCH_2OH) is oxidized to glyoxylate (CO_2HCHO) by glycolate oxidase (Tolbert 1980).

Photorespiration is wasteful because it is not 100% efficient at salvaging glycolate. Many photoautotrophs have thus developed ways to maintain a favorable CO_2/O_2 ratio. Bidwell and McLachlan (1985) proposed that seaweeds utilize and concentrate HCO_3^- so that photorespiration normally does not occur. However, not detecting photorespiratory carbon emissions in laboratory experiments does not necessarily indicate absence of photorespiration because carbon uptake and salvage can occur. Additionally, photorespiration may occur under canopy conditions where kelp are exposed to high oxygen tensions (S.L. Manley, personal communication).

Seasonal Patterns of Brominated Methanes

Seasonal variations have been observed in seawater concentrations of volatile halomethanes, including $CHBr_3$ and CH_2Br_2, off the western coast of Sweden (Klick 1992). Klick suggested that temporal and spatial concentration profiles of CH_2Br_2, $CHBr_3$, and $CHBr_2Cl$ indicated a macroalgal source for these compounds. Concentration profiles of CH_2I_2 and CH_2ClI, however, suggested a phytoplankton source for these iodinated species. In contrast to Klick's observations, Gschwend and MacFarlane (1986) did not observe a seasonal pattern for $CHBr_3$ in seawater collected at high tide off the

coast of Cape Cod. Sample aliasing may have obscured a seasonal trend in the Cape Cod study. Samples in the Sweden study were taken weekly and showed strong weekly fluctuations, sometimes comparable to seasonal variations. Cape Cod samples, however, were taken approximately monthly, thus any seasonal trend may have been obscured. Gschwend and MacFarlane (1986) did observe weak seasonality for polybromomethanes in laboratory incubations of the rockweeds *A. nodosum* and *Fucus vesiculosis* taken from the Cape Cod Canal shoreline.

A number of factors including light irradiance, temperature, nutrition, and wave motion cause seasonal variations in algal productivity. These factors interact and contribute to a characteristic summertime deterioration of southern California *M. pyrifera* canopies. Canopy deterioration is associated with elevated temperatures of >20 °C for an excess of two months or with temperatures >24 °C for an excess of one week (North *et al.* 1986). Although photosynthetic capacity in the field (measured as quantity $O_2/cm^2 \cdot hr$) decreases in summer and bottom tissues will degrade when exposed to elevated canopy temperatures, this temperature effect is not direct (Clendenning 1971). In fact, *M. pyrifera* shows a broad photosynthetic temperature range with an optimum at ~20-25 °C for mature blades (Arnold and Manley, 1985). Also, optimum phosphate uptake was observed at 24 °C (Manley 1985).

Although it is difficult to separate temperature and nutrient effects in the field, summertime canopy deterioration appears to be caused by nutrient depletion in waters above the thermocline (Jackson 1977; Zimmerman and Kremer 1984). Waters in the Southern California Bight are stratified in summer with maximum upwelling in spring.

Canopies receive nutrients mostly during winter and nitrate limitation probably causes degraded *M. pyrifera* canopies in summer. The summer nitrate supply appears dominated by episodic, short-duration vertical fluctuations of the thermocline. Investigators observed such numerous daily variations that a single day of intensive sampling per month produced a more accurate picture of nutrient variations than sampling once a day several times each month (Zimmerman and Kremer 1984).

Larger-scale climatic variations also affect *Macrocystis* populations. El Niño events bringing warm equatorial currents (Ingmanson and Wallace 1985) can expose Southern California *Macrocystis* to prolonged periods of elevated temperature and nutrient depletion. Severe nitrogen starvation during these events can reduce photosynthetic capacity, chlorophyll content, and frond growth rates (Gerard 1984). Extended El Niño periods can cause extensive loss of *Macrocystis* populations and change species composition of the kelp bed region (North *et al.* 1986). The contrasting La Niña episodes bring in cold, nutrient-rich water to kelp canopies and enhance the *M. pyrifera* standing crop. Brominated methane release should be affected by climatic variations that substantially change algal standing crop and/or species distributions. *M. pyrifera* standing crop in Orange and San Diego Counties varied by an order of magnitude between 1967 and 1991 (North *et al.* 1993) – the highest biomass during the 1990 La Niña episode and the lowest during a major El Niño (1983). Regional and global brominated methane releases are expected to fluctuate similarly to biomass.

The Giant Kelp, *Macrocystis Pyrifera*

Kelp (brown seaweeds of the order Laminariales) have been estimated as two-thirds of the global macroalgal biomass (De Vooys 1979). Kelp, by sheer weight, should be important contributors of brominated methanes. *Macrocystis* spp. (i.e., Giant Kelp) occur in both hemispheres along temperate-water coasts. They are dominant along Pacific North America and in the southern hemisphere (Australia, New Zealand, South Africa, and both coasts of South America) (see maps in De Vooys 1979; North 1994). *Macrocystis* beds along the coast of Pacific North America range from Baja California to Alaska (North 1971). *Macrocystis pyrifera* is the dominant kelp species in southern California coastal waters. Plants attach to a rocky substrate by a holdfast and grow up to and across the water surface (Figure 3.1). *Macrocystis* forms extensive canopies and "forests." Much of the of the biomass occurs in the canopy located near or at the water surface (47-60% excluding holdfast, McFarland and Prescott 1959; see also Chapter 5). The morphology of this kelp species should thus be conducive to releasing halomethanes into the atmosphere.

Many algae concentrate iodide relative to surrounding seawater, and chloride is the major halide in most, if not all, algae (Shaw 1962), yet bromine is most commonly incorporated into organic compounds by marine biota (Fenical 1981). *M. pyrifera* is about 88% water, and the following halide concentrations have been reported for wet tissues: 140 μM Cl/g, <0.16 μM Br/g, 0.5 μM I/g, and 0.0063 μM F/g (North 1994). Seawater concentrations, in comparison, are approximately 0.55 M Cl, 8.4×10^2 μM Br, 0.5 μM I, and 68 μM F (North 1994).

Materials and Methods

Samples of *M. pyrifera* (Giant Kelp) were collected on seven separate days between May 1994 and February 1995 from surface waters in kelp beds off Dana Point and Laguna Beach, California (CA) (Figure 2.1: Dana Point is not shown, but it located just south of Laguna Beach). The most distal 1.2-1.5 m (4-5 ft) of canopy fronds growing in 14-20 m (45-65 ft) of water were collected by hand. Fronds were taken from several different plants and normally had attached apical meristems (growing tips). Fronds were placed in 10 gallon buckets with kelp-bed seawater and returned by boat to Caltech's Kerckhoff Marine Laboratory (Corona del Mar, CA). Buckets were transported on ice approximately 1.5 hr to the Caltech main campus (Pasadena, CA). Seawater was typically 15-18 °C upon arrival, a physiologically compatible range.

Seawater used in incubations was acquired from a distribution system at the marine lab. The water originated from Newport Bay (Figure 2.1) and was charcoal filtered prior to distribution; it was not further filtered. Seawater was bubbled with N_2 (15-30 min) to remove background halomethanes prior to incubations. The water was entrained with air during transfer to incubation bags and was thus exposed to background halomethanes in the room air; background concentrations were normally below detection. Ten blades with attached bulbs from 2-4 separate fronds were placed in a polyethylene bag (9x15 in; Bradley Plastic Bag Co., Downey, CA). Each bag was fitted with a septa port and closed with a glove bag closure. Blades were incubated without headspace in a refrigerated (15 °C), shaking water bath and were additionally hand shaken prior to removing water samples. Samples were removed by plastic syringe and placed into glass bottles at 0.25, 1,

1.5, and 2 hr. Bottle headspace overlying the seawater was injected (100 µl) into an electron capture gas chromatograph (ECD-GC). Kelp was weighed and the volume of seawater (~ 4L) in each bag was measured at the end of the experiment.

Experiments in May 1994 utilized a gas chromatograph requiring manual injection (HP5880). Samples were placed in 32 ml amber, screw-top vials and stored for up to 48 hr at 4 °C with no headspace to minimize halomethane losses. Prior to analysis, 4 ml of water was exchanged by syringe with ultra high purity helium at 1 atm. Bottles were shaken upside down at 28 °C for at least one hour. Two headspace samples (100 µl) were injected per vial (1 min splitless; oven temp: 40 °C for 2.5 min, ramp 20 °C/min to 100 °C for 0 min, ramp 30 °C/min to 150 °C for 0 min; HP-5 column: 25m x 0.32mm x 1.05µm film thickness; detector 300 °C, injector 200 °C). Standards for calibration were made in capillary chromatography grade hexane from pure $CHBr_3$ and CH_2Br_2.

Experiments after May 1994 utilized a gas chromatograph equipped with a headspace autosampler (HP 5890 Series II Plus, HP7694 headspace autosampler). Experiments were run similarly as described above except that three replicate, 15 ml samples were removed at each time point and placed into 20 ml autosample vials. Standards for calibration were made in seawater (7 concentrations; 3 replicates each) and run exactly as the samples themselves. Bromotrichloromethane ($BrCCl_3$) was added as a reference peak prior to crimp sealing vials. The headspace autosampler was connected directly to the GC column, bypassing the inlet system (HP-624 column, 30m x 0.32mm x 1.8µm film thickness; oven temp: 40 °C for 2.5 min, ramp 15 °C/min to 165 °C for 0 min, ramp 70 °C/min to 220 °C for 4 min; detector 300 °C; autosampler: oven 95 °C; sample

loop 120°C; transfer line 160 °C; loop equilibrium time 0.02 min; loop fill time 0.09 min; vial fill pressure 0 psi).

Experiments investigated effects of light and photosynthetic state on $CHBr_3$ and CH_2Br_2 production. Experiments were performed under three conditions: light, darkness, or light with the photosynthetic inhibitor DCMU (3-(3,4,-dichlorophenyl)-1,1-dimethylurea; Diuron). Experiments consisted of paired bags incubated simultaneously under identical conditions except for the treatment under study (e.g., light versus dark, light versus DCMU). Paired bags contained blades from the same fronds and of similar size and weight. Experiments in light were conducted under cool white fluorescent, full-spectrum fluorescent, or natural sunlight (see Table 3.1 for light intensities). Experiments in darkness were conducted with opaque plastic covering the incubation bags. Photosynthetic inhibition studies were performed under full light. One ml of DCMU was injected (50 μM final concentration) at the start of the experiment from a stock ethanol solution. One ml of ethanol was added to the partner bag to control for possible ethanol effects.

Controls were incubated in light without kelp and sampled at 0.25 and 2 hr. No halomethane production was observed (n = 8). Bags without kelp were spiked with 12 nM CH_2Br_2 and 10 nM $CHBr_3$, incubated for 1 hr, and samples were analyzed for recovery. Recovery was approximately 100% for CH_2Br_2 (HP5880: n = 9, 3 separate bags; HP5890: n = 20, 7 separate bags). Recovery for $CHBr_3$ was approximately 100% when analyzed on the HP5890, but only 75% for samples analyzed on the HP5880. The

affected $CHBr_3$ results (May 1994) were corrected for recovery. Detection limits were approximately 10 ng/L (58 pM) for CH_2Br_2 and 18 ng/L (71 pM) for $CHBr_3$.

Hydrogen peroxide (186 nM) was added after 2 hr for certain incubations and seawater samples were taken approximately 25 min later and analyzed for $CHBr_3$ and CH_2Br_2. Bromoform and CH_2Br_2 concentrations after H_2O_2 addition were compared to the 95% confidence limit of the linear regression of concentrations prior to H_2O_2 addition using a Sigma Plot graphics program. Hydrogen peroxide concentrations in seawater were analyzed using an HPPA (3-(p-hydroxyphenyl)propionic acid) assay (Palenik and Morel 1988) on a Shimadzu RF-540 spectrofluorophotometer (excitation wavelength = 320 nm, slit width = 2 nm; emission wavelength = 415nm, slit width = 10 nm). A POPA (4-hydroxyphenylacetic acid) assay (Kok *et al.* 1986) was originally used, but the POPA assay has a detection limit of 30 nM, and a more sensitive assay was needed. The HPPA assay has a reported detection limit of 3 nM (Palenik and Morel 1988), but H_2O_2 could be consistently and reliably detected to about 10 nM in this study. HPPA stock was added to seawater samples and to standards made from serial dilution of 3% H_2O_2 into seawater (25 µl of 2 mM stock into 10 ml seawater). A blank reading was taken prior to adding horseradish peroxidase (HRP) (5 µl of 4.4 units/ml HRP to 10 ml seawater). The effect of DCMU on the HPPA assay was investigated by analyzing the full-emission spectrum of DCMU in seawater under different combinations of HPPA, HRP, and H_2O_2. The presence of DCMU did not cause an additional fluorescence peak that would interfere with readings taken at 415 nm. However, there was more variability in readings from samples containing DCMU which decreased the ability to distinguish low values of H_2O_2.

Hydrogen peroxide concentrations in the presence of DCMU were assayed most reliably above about 50 nM.

Proton nuclear magnetic resonance spectroscopy (NMR) was used to assess whether DCMU reacts directly with H_2O_2. DCMU and H_2O_2 were shaken in 50 ml distilled, deionized water (ddH_2O) with and without horseradish peroxidase (HRP) for 1 hr in room light. DCMU was added from an ethanol stock to a final concentration of 0.17 mM. Hydrogen peroxide was added to achieve a H_2O_2:DCMU ratio approximating incubation conditions (170 nM H_2O_2) or to achieve an equimolar ratio (0.17 mM H_2O_2) to ensure that any reaction that occurred could be detected. The HRP (Type VI-A; Sigma) final concentration was 2 mg/L (500 purpurollamin units/L). The reaction mixture was evaporated to dryness under vacuum. The precipitate was dissolved in 1 ml deuterated chloroform ($CDCl_3$) with 0.1% tetramethylsilane (TMS) as an internal standard. Samples were analyzed by NMR (General Electric QE-300) and chemical shifts were assigned with the assistance of Dr. Robert Johnson and Vidyasankar Sundaresan (Caltech).

Calculations

Calculations for experiments performed on the HP5880 GC-ECD (May 1994; see above for further description) required dimensionless partition coefficients which were obtained by interpolating results of Tse *et al.* (1992). We determined salting-out coefficients by the method of Gossett (1987) and obtained values of 1.23 ± 0.08 for $CHBr_3$ and 1.18 ± 0.03 for CH_2Br_2, consistent with the salting-out coefficient of 1.2 used by Singh *et al.* (1983) for methyl halides. Multiplying the freshwater partition coefficients (Tse *et al.* 1992) by the 1.2 salting-out coefficient gives the following partition

coefficients: $CHBr_3 = 0.031$; $CH_2Br_2 = 0.049$ for seawater at 28 °C. Production rates were determined by linear regression of halomethane mass in the bag over the incubation period (accounting for mass and volume removed at previous time points and normalized by kelp weight) according to the following:

$M_{bg} = C_{bg} V_{bg}$ (at each time point)

$$C_{bg} = C_{bt\,\text{no HS}} = \frac{M_{g+w}}{V_w}$$

$$M_{g+w} = C_g V_g + C_w V_w = C_g V_g + \left(C_g / H\right) V_w = C_g \left(V_g + V_w / H\right)$$

$$C_g = \frac{M_{inj}}{V_{inj}}$$

where,

C_{bg}	=	halomethane concentration in bag (ng/L)
C_g	=	concentration in headspace at equilibrium with water phase (ng/L)
C_w	=	concentration in water at equilibrium with gas phase (ng/L)
$C_{bt\,\text{no HS}}$	=	concentration in bottle prior to addition of headspace (ng/L)
H	=	dimensionless partition coefficient · salting-out coefficient
M_{bg}	=	mass of halomethane in bag (ng)
M_{g+w}	=	total mass in bottle, headspace and water (ng)
M_{inj}	=	mass injected into gas chromatograph (determined by standards)
V_{bg}	=	volume of bag (L)
V_g	=	volume of headspace in bottle (L)
V_w	=	volume of water in bottle after addition of headspace (L)
V_{inj}	=	volume injected (L)

Rate calculations for experiments employing the headspace autosampler (after May 1994; see above for further description) were simplified because standards were made in seawater and run exactly as the samples themselves. Mass in the sample bottle was determined from the standards (instead of from C_g), thus partition coefficients were not required. Production rates were calculated by linear regression of the mass of

halomethane produced in the bag over the time course of incubation (accounting for mass and volume removed at previous time points and normalized by kelp weight) according to the following:

$M_{bg} = C_{bg} V_{bg}$ (at each time point)

$$C_{bg} = C_{sy} = \frac{M_{bt}}{V_{bt}}$$

where

M_{bt}	=	total mass of halomethane in vial (determined from standards)
M_{bg}	=	mass of halomethane in bag
C_{bg}	=	concentration in bag (ng/L)
C_{sy}	=	concentration in syringe used to remove water (ng/L)
V_{bg}	=	volume of bag (L)
V_{bt}	=	volume of seawater in autosample vial (L)

Results and Discussion

M. Pyrifera Bromoform and Dibromomethane Production Rates

Kelp incubations were performed on seven separate days during a nine-month period from May to February 1994-1995. Chromatographic results (Figure 3.2) normalized by kelp weight and plotted against time (Figure 3.3) were used to calculate production rates by linear regression. Median production rates were 171 ng $CHBr_3$/gfwt·day (0.68 nmoles $CHBr_3$/gfwt·day) and 48 ng CH_2Br_2/gfwt·day (0.27 nmoles CH_2Br_2/gfwt·day) based on a 12 hr photoperiod (mean ± SD: 299 ± 348 and 58 ± 38 ng/gfwt·day, respectively $CHBr_3$ and CH_2Br_2) (gfwt = g fresh weight kelp). In no instance was halomethane production observed in seawater controls. Production ranged from 25-1126 ng $CHBr_3$/gfwt·day and 21-173 ng CH_2Br_2/gfwt·day for 19 separate incubations of

10 blades each (Table 3.2; Figure 3.4) based on a 12 hr photoperiod (see darkness effects below). The median is a better estimate of the central value for small observational sets (Kennedy 1984) thus median values were used in further calculations. The large range in production indicates that single-sampling could bias production estimates. Thus, algal production studies using a small number of samples at a single time of year may not accurately reflect the overall release behavior of halogenated methanes.

M. pyrifera produced more $CHBr_3$ than CH_2Br_2 (Figure 3.4). One exception to this pattern occurred on 2/22/95 with the sample giving the lowest $CHBr_3$ release rate (25 ng/gfwt·day). This value, however, was not excluded because no leaks were found in the polyethylene bag and the concomitant CH_2Br_2 production rate (37 ng/gfwt·day) was within the range of the other CH_2Br_2 values. If this lowest $CHBr_3$ rate were excluded, the range would narrow to 39-1126 ng $CHBr_3$/gfwt·day.

Linear production was observed, in general, but some incubations appeared to lag initially (approximately 7 of 19 incubations). In these cases, performing regression only over the linear portion of the curve increased the median production values (192 ng $CHBr_3$/gfwt·day and 57 ng CH_2Br_2/gfwt·day) but did not affect the range. Moreover, most slopes determined in this manner for CH_2Br_2 (6 out of 7) and several for $CHBr_3$ (3 out of 7) were within the 95% confidence interval of slopes calculated by linear regression over the entire 2 hr period. Production values calculated over the entire time were used in further calculations.

Factors Affecting Brominated Methane Production

Light and Photosynthetic State

Clear polyethylene bags used in incubation experiments allowed passage of approximately 66% of light in the biologically important 400-750 nm range and 77% in the 800-1070 nm range (Figure 3.5). The opaque plastic used to cover clear bags during darkness experiments essentially blocked light transmission (<1% for 400-750 nm and 4% for 800-1070 nm) (Figure 3.5). Chlorophyll *a*, present in all algae (Meeks 1974), has peak absorbances at approximately 428 and 660 nm (Danks *et al.* 1983, p. 38). Plastic films were graciously analyzed by Dr. George Rossman (Caltech) using a diode array spectrophotometer.

Light was important for the production of $CHBr_3$ and CH_2Br_2 by *M. pyrifera* (Figure 3.6). Bromoform production was reduced 5 to 19 times in darkness while CH_2Br_2 production was reduced 3 to 6 times compared to simultaneous light incubations under otherwise identical conditions. Blades incubated in darkness produced no $CHBr_3$ or CH_2Br_2 in one instance (Figure 3.6, 5/18/94). A photoperiod should thus be included when calculating daily $CHBr_3$ and CH_2Br_2 production based on short-term incubations; a 12-hour photoperiod was used in this study. In contrast, light has been shown not to affect *M. pyrifera* methyl halide (CH_3X) production (Manley and Dastoor 1987). Perhaps monohalogenated methane production by the proposed methyl transferase system is not constrained by light, unlike polyhalogenated methane production by the V-BrPO system.

The paired incubation method used here for *M. pyrifera* clearly showed a light effect for $CHBr_3$ and CH_2Br_2 production (Figure 3.6). Other researchers have investigated the effect of light on halomethane production with somewhat mixed results.

Light was shown to affect bromination of phenol red by V-BrPO from *A. nodosum*, but not for seven other algal species tested (Wever *et al.* 1991); brominated methane production was not directly monitored in those experiments. In a more recent investigation, release rates of $CHBr_3$ and CH_2Br_2 from the red alga *M. gelidium* were reduced in darkness, but not significantly (Collén *et al.* 1994). Relevant rate differences, however, may have been obscured by large standard deviations in production values. Light was observed to affect $CHBr_3$ and CH_2Br_2 production in the rockweeds *F. vesiculosis* (Klick *et al.* 1993) and *A. nodosum* (Nightingale *et al.* 1995).

Understanding the mechanism of algal brominated production is important to understanding the spatial and temporal distributions of brominated methanes. To directly address whether the observed light effect (Figure 3.6) was photochemical or physiological, algal photosynthetic activity was disrupted for blades incubated in light. Photosynthetic inhibition by DCMU was accompanied by inhibition of $CHBr_3$ and CH_2Br_2 production compared to blades incubated in otherwise identical conditions (Figures 3.7-3.11). There was only one instance of detectable CH_2Br_2 production in the presence of DCMU, but concomitant $CHBr_3$ production was not observed (Figure 3.7 5/25/94; Figure 3.9). Algal photosynthetic activity thus appears critical to release of $CHBr_3$ and CH_2Br_2.

DCMU blocks photosynthetic electron transport after Photosystem II between the plastiquinones Q and R (Avron 1981; Danks *et al.*1983, p.61; Figure 3.12). Therefore, the DCMU effect likely arose from halting H_2O_2 supplied from the Mehler reaction to V-BrPO, the enzyme responsible for organic bromination (see "Hydrogen Peroxide and Brominated Methane Production" below). Photosynthetic inhibition by DCMU was

indicated by a decline in pH and O_2 levels, as expected from cellular respiration (pH 8.18 to 8.09; O_2: ≈5.0 to 3.4 mg/L), whereas pH and O_2 levels increased during incubation of kelp not treated with DCMU, as expected from photosynthesis (pH: 8.22 to 8.34; O_2: ≈5.6 to 5.9 mg/L). Also, photosynthetic inhibition was indicated by a lack of bubbles in incubations treated with DCMU. DCMU was solubilized in ethanol, but injection of ethanol alone (1 ml into 4 L) did not significantly affect production rates.

Kelp blades incubated in sunlight received a light flux 17-40x higher than blades incubated under fluorescent light (Table 3.1). Despite fluctuating light conditions, sunlight incubations displayed similar $CHBr_3$ and CH_2Br_2 production patterns compared to a cool-white fluorescent incubation under stable light intensity (Figure 3.11). Production rates were only about a factor of two higher for sunlight incubations (170 ± 6.3 and 211 ± 14 ng $CHBr_3$/gfwt·day; 35 ± 1.7 and 31 ± 2.3 ng CH_2Br_2/gfwt·day) (± std error) compared to a fluorescent light incubation performed on the same day (106 ± 9.4 ng $CHBr_3$/gfwt·day; 21 ± 1.7 ng CH_2Br_2/gfwt·day; Figure 3.4, 8/19/94; Figure 3.11) despite substantially higher photon flux in sunlight. This production behavior appears consistent with the light intensity required for photosynthetic saturation of *M. pyrifera*. Laboratory fluorescent light fluxes were typically 2/3 below the saturating light intensity of about 80 $\mu E/m^2 \cdot s$ (Arnold and Manley 1987), whereas sunlight was consistently above saturating light intensity (Table 3.1). A no-kelp control in full sunlight showed no brominated methane production.

Production of $CHBr_3$ and CH_2Br_2 under standard cool-white fluorescent light was comparable to production under full-spectrum fluorescent light. Full-spectrum lighting

simulates natural sunlight more closely, particularly in the biologically important 450-675 nm range (Vita-lite product information). Rates did not differ significantly for incubations performed in either type of light (Figure 3.4), and light type did not appear to affect whether production lagged initially (Figures 3.13-3.15). Thus, the light flux from cool-white fluorescent light appeared to adequately stimulate $CHBr_3$ and CH_2Br_2 production.

Potential Factors Affecting Production: Environmental Conditions and Algal Health

Release rates of $CHBr_3$ and CH_2Br_2 were variable over the nine-month sampling period (5/94-2/95), but highest $CHBr_3$ and CH_2Br_2 production rates occurred in late July and early August of 1994 (Figure 3.4). A tendency for higher late-summer production was most apparent for $CHBr_3$. Water temperatures during this time were high (21-22 °C), and canopy conditions were visibly poor (e.g., sparse canopy, unhealthy-looking blades). Klick (1992) also observed peak concentrations of volatile halomethanes, including $CHBr_3$ and CH_2Br_2, in summer associated with visible degradation of the annual seaweeds *Enteromorpha* and *Ceramium.* Higher production in late summer during poor canopy conditions suggests that an alga's physiological state might be important for $CHBr_3$ and CH_2Br_2 release. Higher production may occur during conditions of environmental stress partly because of increased H_2O_2 production (Elstner 1987), but further work is needed to address this hypothesis.

Kelp blades without visible epiphytes were chosen for incubation studies when possible. However, degraded canopy conditions sometimes dictated that the " best" available fronds did support visible epiphytes. Epiphytes (usually bryozoans) were not removed to avoid possible disruption of algal tissues containing V-BrPO enzyme and to

better assess production rates for conditions as they existed. The presence of visible epiphytes on *M. pyrifera* blades apparently did not affect $CHBr_3$ and CH_2Br_2 production. Production rates were not significantly different between blades moderately encrusted (5/18/94) and lightly encrusted (5/25/94) with the common bryozoan epiphyte *Membranipora membranacea* (Figure 3.4, Figures 3.8-3.9). Several unidentified *Foramanifera* (8/1/94) and limited coverage of hydroids on some blade tips (2/16/95) did not appear to alter production rates of $CHBr_3$ and CH_2Br_2 (Figure 3.4). Microscopic inspection of blades was not performed. Gschwend *et al.* (1985) also observed that "heavily epiphytized" plants did not produce more halomethanes than less epiphytized counterparts. *Membranipora* encrustation reportedly does not inhibit photosynthetic capacity in saturating light intensities (Clendenning 1971). However, more light may be needed to provide saturating conditions for densely encrusted blades, and this would be detrimental for blades that were light limited (Woollacott and North 1971). Woollacott and North (1971) additionally report that dense *Membranipora* encrustation can cause buoyancy and flexibility losses, increase grazing pressure, and hinder growth.

We addressed the issue of kelp health directly by incubating highly tattered and unhealthy-looking blades (pictured in Figure 3.16). Unhealthy-looking blades produced $CHBr_3$ (235 ± 36 ng/gfwt·day) and CH_2Br_2 (43 ± 0.6 ng/gfwt·day) (± std error) at rates similar to relatively healthy-looking blades incubated simultaneously under full-spectrum light (146 ± 58 ng $CHBr_3$/gfwt·day; 48 ± 17 ng CH_2Br_2/gfwt·day) (Figure 3.17). The unhealthy-looking blades also produced $CHBr_3$ and CH_2Br_2 at rates similar to two other sets of relatively healthy-looking blades incubated on the same day under cool-white

fluorescent light (188 ± 28 and 206 ± 34 ng $CHBr_3$/gfwt·day; 58 ± 4.3 and 91 ± 14 ng CH_2Br_2/gfwt·day; Figure 3.13; Figure 3.4, 5/25/94). Unhealthy plants seem to produce comparable amounts of $CHBr_3$ and CH_2Br_2 relative to healthier counterparts.

Relatively high rates of $CHBr_3$ and CH_2Br_2 production measured in late July (7/22/94; Figure 3.4) were associated with seriously degraded canopy conditions. All canopy fronds seemed to contain perforations or "shot-holes" (Clendenning 1971, p.181; p. 340), and most apical meristems were degraded. Sea surface temperature was high (21.1 °C; Table 3.1) and many mysids and isopods were observed. The "shot-holes" may have been caused by bacterial degradation (W.J. North, personal communication). However, degradation alone was not expected to account for high production rates because degradation of drift kelp trapped in a submarine canyon was not associated with elevated concentrations of $CHBr_3$, CH_2Br_2, or CH_3I (see Chapter 2). High $CHBr_3$ and CH_2Br_2 production rates were also measured ten days later (8/1/94; Figure 3.4) when surface seawater temperature again was high (21.6 °C), but in this case blades were free of "shot-holes." This kelp, however, experienced a longer, warmer transport to the laboratory relative to any other sampling day due to traffic delays. Higher halomethane production (Figure 3.4; 8/1/94) conceivably may have resulted from increased H_2O_2 production caused by added environmental stress (Elstner 1987). These relatively high production rates were not simply related to seawater temperature because sea surface temperature was unusually high on 8/19/94 (23.6 °C; Table 3.1), but production rates were substantially lower than rates measured on 7/22/94 and 8/1/94 (Figure 3.4). Interestingly, kelp collected on this day appeared healthier than any previously collected,

which may indicate improved canopy conditions. Summertime canopy fronds experience variable nutritional stress (Zimmerman and Kremer 1984), particularly if internal nitrogen reserves are depleted. Vertical stratification of dissolved nitrate (NO_3^-) is common in southern California kelp beds (Gerard 1982b), and nutrient conditions vary daily in summertime canopies due to vertical movements of the thermocline (Zimmerman and Kremer 1984). Moreover, internal nitrogen reserves accumulate only when growth is nitrogen-saturated (Gerard 1982a,b). Nitrogen starvation may be accompanied by a variety of physiological changes including reduced photosynthetic capacity (Gerard 1984; measured as quantity $O_2/cm^2 \cdot hr$). Differences measured in $CHBr_3$ and CH_2Br_2 release may have reflected physiological differences (e.g., photosynthetic capacity, H_2O_2 production) caused from changes in environmental conditions.

Hydrogen Peroxide and Brominated Methane Production

The V-BrPO enzyme is known to use H_2O_2 as a substrate *in vitro* (e.g., Soedjak and Butler 1990), thus production of $CHBr_3$ and CH_2Br_2 might depend on H_2O_2 concentrations. Hydrogen peroxide was monitored in light and darkness without kelp to assess photochemical production under laboratory incubation conditions (2 hr; 55 $\mu E/m^2 \cdot s$; 15 °C charcoal-filtered seawater). Seawater H_2O_2 concentrations were similar in both light and dark (Table 3.3) indicating that significant photochemical production of H_2O_2 did not occur under these conditions in the absence of kelp.

Bromoform, CH_2Br_2, and H_2O_2 concentrations were monitored concurrently during kelp incubations under conditions of light, darkness, light with DCMU, and light with aniline. Bromoform and CH_2Br_2 production in darkness was reduced relative to

production in light, and production was inhibited by DCMU (Table 3.4), as previously described (Figures 3.5 and 3.6). Increased H_2O_2 concentrations were detected in seawater only during incubations of kelp in light (<10 nM at 0.3 hr to 31 nM at 2.3 hr). Hydrogen peroxide concentrations remained below detection for kelp incubations in darkness, in light with DCMU, and in light with aniline (Table 3.4). Seawater without kelp contained 44 ± 0.75 nM H_2O_2.

Accumulation of H_2O_2 reflects simultaneous photochemical and biological formation and decomposition processes (Zepp *et al.* 1987; Cooper *et al.* 1988; Moffett and Zafiriou 1990, 1993). Increased seawater H_2O_2 concentrations measured during blade incubations in light may have reflected net accumulation from biological production or from photochemical reactions with dissolved organic matter (Cooper *et al.* 1988) introduced to the seawater with kelp addition. Moffett and Zafiriou (1990) concluded that biological processes dominated H_2O_2 decomposition in coastal marine waters and that decay was primarily caused by catalase (apx. 65-80% of H_2O_2 decay) and peroxidase activity (apx. 20-35% of decay). Relatively low seawater H_2O_2 concentrations for incubations of kelp in darkness compared to incubations without kelp in light or darkness (Table 3.3 and Table 3.4) most likely reflect biological H_2O_2 decomposition processes.

Aniline oxidation has been shown to consume H_2O_2 in light in the presence of algae (Zepp *et al.* 1987). Aniline was used to scavenge H_2O_2 as a control to assess the possibility that reduced $CHBr_3$ and CH_2Br_2 production associated with DCMU addition might result from chemical consumption of bulk H_2O_2. Interestingly, limited $CHBr_3$ and CH_2Br_2 production was observed in the presence of aniline after a lag period (Table 3.4;

Figure 3.19). In comparison, no $CHBr_3$ or CH_2Br_2 production was observed in the presence of DCMU for kelp incubated in otherwise identical conditions (Figure 3.18). Bulk H_2O_2 (<50 nM) should have been depleted by the quantity of aniline added (55 μM). However, aniline did not inhibit photosynthesis as evidenced by evolution of oxygen bubbles in the incubation bag. It is thus conceivable that H_2O_2 remained available to V-BrPO through the Mehler reaction and photorespiration. In contrast, DCMU halts internal H_2O_2 production by photosynthesis (Elstner 1987) because electron transport is inhibited between Photosystem II and Photosystem I, prior to the H_2O_2 producing steps (Figure 3.12). Addition of DCMU does lead to singlet oxygen ($^1O_2$) formation which reacts rapidly with organic compounds (Elstner 1987), but it does not lead to H_2O_2 formation. DCMU was also noted to halt photorespiration (Tolbert 1974, p.478), although the mechanism was not explained. Consequently, DCMU can be expected to curtail availability of H_2O_2 to the V-BrPO enzyme. Direct reaction between DCMU and the V-BrPO enzyme is also unlikely. DCMU is a quinone analogue acting at a specific site in the photosynthetic electron transport chain (e.g., Elstner 1987; Figure 3.12) despite participation by a number of quinones in electron transport. Although experiments with purified V-BrPO are needed to exclude entirely the possibility of direct enzyme inhibition, V-BrPO does not use a quinone cofactor, and thus is unlikely to interact directly with DCMU. Thus, DCMU inhibition of algal $CHBr_3$ and CH_2Br_2 production most likely results from DCMU inhibition of photosynthesis and photorespiration.

Nuclear magnetic resonance spectroscopy was also used to assess the possibility that inhibition of $CHBr_3$ and CH_2Br_2 production associated with DCMU addition was an

artifact arising from consumption of bulk H_2O_2 in a manner analogous to reported aniline oxidation in the presence of algae (Zepp *et al.* 1987). DCMU is not as chemically reactive as aniline and thus was not expected to react with H_2O_2; NMR was used to verify this hypothesis. DCMU was incubated with up to equimolar amounts of H_2O_2 in the presence and absence of horseradish peroxidase. NMR spectra for all reaction mixtures showed identical chemical shifts (Figure 3.19, chemical shift assignments in Table 3.5), indicating that H_2O_2 did not significantly oxidize DCMU even at equimolar concentrations in the presence of HRP. This result supports the conclusion that inhibition of $CHBr_3$ and CH_2Br_2 production concomitant with DCMU addition resulted, not from direct depletion of bulk H_2O_2 in solution, but from physiological changes in the alga.

Whether aniline was toxic to the alga is unknown, but this possibility cannot be ruled out. No reports of aniline effects on plant or algal tissues were found in the literature, but aniline is highly toxic to animals. In contrast, DCMU is low to moderately toxic to animals, and it is even permitted as an additive in feed and drinking water of species used for human consumption (Sax 1975, p. 708). Aniline generates methemoglobin (hemoglobin in which the heme iron has been oxidized from Fe^{2+} to Fe^{3+}) which binds oxygen tightly, preventing release to tissues (methemoglobinemia) (Finkel 1983). Whether aniline acts specifically is unclear because methemoglobinemia obscures evidence of direct toxicology (Finkel 1983). Aniline conceivably may affect other iron heme-containing enzymes, including those in algae and plants (e.g., iron heme peroxidases); the affect of aniline on V-BrPO is unknown. Aniline is absorbed through the skin, but its ability to penetrate algal cell walls is unknown. Limited $CHBr_3$ and CH_2Br_2

production in the presence of aniline suggests that some H_2O_2 was available to V-BrPO which further suggests that aniline was not freely permeable.

Hydrogen peroxide was added to kelp incubations to determine whether increased H_2O_2 available to the V-BrPO enzyme would increase $CHBr_3$ and CH_2Br_2 production. Previous experiments in which H_2O_2 was added either to algal cultures (Collén *et al.*1994) or purified V-BrPO enzyme (Wever *et al.* 1991) employed H_2O_2 concentrations of either 1 or 2 mM, substantially above natural background. Natural seawater H_2O_2 concentrations typically range from 10-200 nM (Palenik and Morel 1988) with an average of about 100 nM for well-lit surface waters (Moffett and Zafiriou 1990). In the experiments presented here, 186 nM H_2O_2 was added at the end (2 hr) of a kelp incubation. Enhanced $CHBr_3$ and CH_2Br_2 production after H_2O_2 addition was indicated by subsequent concentrations outside the 95% confidence interval of the linear regression of earlier concentrations.

Addition of H_2O_2 at an environmentally relevant concentration resulted in a significant increase of $CHBr_3$ and CH_2Br_2 for kelp blades incubated in darkness (Figure 3.20). Bromoform and CH_2Br_2 concentrations observed after total addition of 186 nM H_2O_2 were substantially more than what would be expected based on linear regression of concentrations prior to H_2O_2 addition. Observed $CHBr_3$ concentrations were in fact higher than expected from only a 37 nM H_2O_2 addition (Figure 3.20). This result suggests that brominated methane production is limited in darkness by lack of H_2O_2 and supports the hypothesis that $CHBr_3$ and CH_2Br_2 production is related to H_2O_2 concentration.

Bromoform and CH_2Br_2 production continued after H_2O_2 addition for all incubations performed under light (Figures 3.20-3.21) and under light with aniline (Figure

3.18), but measured concentrations were not higher than would be expected based on linear regression of earlier time-points. Ongoing $CHBr_3$ and CH_2Br_2 production in light may have masked small increases of these compounds caused by H_2O_2 addition. Hydrogen peroxide addition to incubations containing aniline was not expected to affect production rates because aniline is expected to rapidly consume H_2O_2 (Zepp *et al.* 1987). No production was observed for DCMU treated blades even after addition of 186 nM H_2O_2 (Figure 3.18). Halomethane production would be expected with H_2O_2 addition if V-BrPO remained functional upon addition of DCMU, unless an intracellular H_2O_2 source is obligatory to the process. Further investigation is necessary to determine the reason for this result.

These results support the idea that the V-BrPO enzyme uses an intracellular peroxide source. The two primary intracellular sources of H_2O_2 are pseudocyclic photophosphorylation (Mehler reaction) and photorespiration. The Mehler reaction is the most likely peroxide source because photorespiration in seaweeds is unlikely in the absence of high O_2/CO_2 ratio (e.g., Bidwell and McLachlan 1985). The seawater pH in these experiments was about 8.2, and seawater O_2 concentrations were reduced by N_2 bubbling (used to remove background halomethanes); therefore, photorespiration is presumed to have been insignificant.

Comparison of Rates to Other Reported Data

Reported production rates of polybrominated methanes for various algal species vary widely (Table 3.6-3.7). The present study incorporated a larger sample size than previous studies (n = 19; 190 total blades). The range of $CHBr_3$ and CH_2Br_2 production

by *M. pyrifera* was similar to that reported for *A. nodosum* by Gschwend *et al.* (1985) (Table 3.6). The median CH_2Br_2 production rate measured here for *M. pyrifera* whole blade incubations was similar to the mean CH_2Br_2 production rate reported for *M. pyrifera* blade disk incubations by Manley *et al.* (1992) (Chapter 2), adjusting those rates for a 12 hr photoperiod and the CH_2Br_2 partition coefficient of Tse *et al.* (1992) (see Table 3.6 and Chapter 2). The highest $CHBr_3$ production rates observed here were similar to the mean *M. pyrifera* $CHBr_3$ production rates of Manley *et al.* (1992), adjusting those rates for a 12 hr photoperiod (Table 3.6). The median $CHBr_3$ production rates reported here, however, are lower than the mean rates of Manley *et al.* (1992) by a factor of nine. The $CHBr_3$ partition coefficients used in these studies were similar (Tse *et al.* 1992 and Nicholson *et al.* 1984) and do not explain the difference in rates.

It is difficult to draw conclusions about rate differences between these two studies given the overall variability in production. A simple seasonal argument does not appear to explain the higher $CHBr_3$ values measured by Manley *et al.* (1992) because highest $CHBr_3$ rates were measured in this study during July and August (1994), whereas *M. pyrifera* was sampled by Manley *et al.* in late May (1991). Measurements of photosynthesis and photorespiration are affected by prior environmental conditions (e.g., day length, night temperature) as well as by leaf age and developmental stage (Steward *et al.* 1971). Rate differences for *M. pyrifera* thus may have arisen from differences in the tissues used because of environmental or physiological factors. Differences in analytical instruments or incubation technique may also have contributed to rate differences. Manley *et al.* used blade disk incubations whereas this study used whole blade incubations. Blade disks in

Manley *et al.* (1992) were taken centrally from three mature blades from separate *M. pyrifera* fronds and preequilibrated for 1 hr before use to minimize wounding effects. Furthermore, methyl halide production appears unaffected by tissue wounding or desiccation (Manley *et al.* 1988), thus the blade disk method alone was not expected to cause substantial production differences. Photosynthesis and respiration measurements using blade disks show substantial variations within and between blades (Arnold and Manley 1980). The variability present in photosynthesis and respiration apparently is related to differing proportions of photosynthetic and structural tissues along the blade length. Analogous variations possibly exist in V-BrPO coverage that could lead to higher brominated methane production from certain regions within a blade, but such physiological variation would be expected to affect both $CHBr_3$ and CH_2Br_2 production rates.

Regional Estimates of Brominated Methane Production

Southern California *M. pyrifera* populations have been monitored since the early 1950's. There is thus a useful opportunity to estimate regional production from this algal species. Between 1967 and 1991, *M. pyrifera* biomass has fluctuated by more than an order of magnitude along the coasts of Orange and San Diego Counties (~100 mile coastal length from Huntington Beach to Imperial Beach; Figure 3.22). Area values reported by North *et al.* (1993) were converted into mass estimates assuming an average bed density of 6 kg/m^2 (see Chapter 5). The lowest standing crop was recorded during a 1984 El Niño episode with an estimated 4.2×10^9 gfwt (0.70 km^2); the highest biomass was observed during a 1990 La Niña episode with an estimated 9.0×10^{10}gfwt (15 km^2). The

average biomass over this time period was $3.9x10^{10}$ gfwt (6.5 km^2) (Table 3.8). *Macrocystis* comprises about 1/2 of the macroalgal biomass in this region. Of the remainder, approximately 3/4 is kelp and 1/4 is non-kelp species (W.J. North, personal communication). If other regional macroalgal species release $CHBr_3$ and CH_2Br_2 at rates similar to *Macrocystis*, the estimates given below would approximately double for bromine release from all macroalgae in the region.

Estimates of regional production by *M. pyrifera* range from $3.1x10^5$–$6.7x10^6$g Br/yr with an average of $2.9x10^6$ g Br/yr, using the biomass estimates given above and the median $CHBr_3$ and CH_2Br_2 production rates measured from this work (Table 3.9). Bromoform comprises 79% of this average bromine release by *M. pyrifera*. The large range in emission values reflects the biomass range measured over two decades and encompasses biomass fluctuations expected from climatic changes such as El Niño events. Bromine emission estimates assume that volatilization is the fate of brominated methanes produced in the water-column. Volatilization appears to be the dominant loss process for halocarbons, although chemical or biological losses may also occur (see Chapters 1 and 6).

Methyl bromide (CH_3Br; MeBr) production by *M. pyrifera* was not measured in the experiments reported here, but it was determined by Manley and Dastoor (1987). They performed tissue disk and field experiments and observed production rates of 4.3 ng MeBr/gfwt·day and 8.6 ng MeBr/gfwt·day, respectively. Based on their laboratory production estimates and the average *M. pyrifera* standing crop (Table 3.8), MeBr algal production in Orange and San Diego Counties would only amount to $5x10^4$ g Br/yr. The additional bromine from MeBr is small relative to bromine from $CHBr_3$ and CH_2Br_2 (≈2%;

Table 3.9) and thus does not strongly influence regional or global estimates of kelp emissions. Moreover, this algal source of MeBr is insignificant relative to regional fumigant use. For example, $1.2x10^8$ g Br was released in 1993 from MeBr fumigation in Orange and San Diego Counties alone (State of CA 1995; Table 3.10), assuming release to the atmosphere was half of that applied (U.N. Environmental Programme 1992). Bromine from MeBr fumigation dominates bromine from macroalgae in the region of Orange and San Diego Counties. This will not be the case everywhere (e.g., polar regions). North America and Europe account for 90% of all MeBr use. The state of California alone accounts for about 10% ($2.8x10^9$ g Br in 1993; State of CA 1995) of the total bromine emitted worldwide from MeBr fumigation ($2.5x10^{10}$ g Br in 1990; U.N. Environmental Programme 1992). Biomass burning would further contribute MeBr to the region (Manö and Andreae 1994) both naturally and anthropogenically; the quantity of this source was not estimated.

Phytoplankton may also release brominated methanes to the atmosphere. Tokarczyk and Moore (1994) measured significant organohalogen production by two species of phytoplankton in laboratory incubations. Highest production occurred during the exponential growth phase and declined during stationary and death phases. However, eight other tested phytoplankton species did not produce organohalogens. It is thus difficult to interpret these results, and no attempts were made to extrapolate laboratory phytoplankton production to a regional or global scale.

Another regional source of anthropogenic brominated methanes is from water chlorination by-products (Helz and Hsu 1978; Morris 1985). Seawater used for industrial

cooling water is often chlorinated to inhibit biofouling. Freshwater and wastewater may be chlorinated to disinfect water before drinking or release into the environment. Hypobromous acid quickly forms when chlorine is added to waters containing bromine ($HOCl + Br^- \longrightarrow HOBr + Cl^-$) (Helz and Hsu 1978); brominated by-products may then form through the haloform reaction (see p. 3-6). For this study, chlorine use data were collected from major drinking water suppliers, water treatment facilities, and power-generating facilities in Orange and San Diego Counties for direct comparison to algal inputs from this same region (several facilities in this region use alternatives to chlorination). Chlorination produces about 0.1% brominated by-products from freshwater and about 1% for seawater (Gschwend *et al.* 1985); although values vary (Helz and Hsu 1978; Bean *et al.* 1980; Cooper *et al.* 1983; Samsone and Kearney 1985; Amy *et al.* 1990). Estimates were not made of bromine emissions from pool chlorination (Copaken 1987). I estimated that approximately 7.9×10^6 g Br/yr was released as by-products of water chlorination in Orange and San Diego Counties (Table 3.10), which is roughly similar to the average estimate of bromine release by *M. pyrifera* in that region (Table 3.9).

Global Estimates of Brominated Methane Production

Extrapolating production to a global scale is more tentative because global biomass has been only roughly estimated; indeed, the biomass estimate is most likely the largest source of estimate error. De Vooys (1979) estimated the total macroalgal standing crop as 60 Tg with 2/3 of that biomass comprised of kelp species (40 Tg). Biomass estimates that account for seasonal or species differences were not found in the literature,

but these factors can affect halomethane release. Given these caveats, global bromine emissions from kelp are estimated as $3.0x10^9$g Br/yr from $CHBr_3$ and CH_2Br_2, assuming 40 Tg for global kelp biomass and that median *M. pyrifera* release rates are representative of other kelp species (Table 3.11). Bromoform contributes about 80% of the estimated total bromine produced by kelp worldwide.

Marine algae appear to be an important part of the global bromine cycle based on their combined bromine emissions. Estimates of bromine emissions from a few groups of algae are on the order of 10^{10} to 10^{11} g Br/yr (Table 3.11). Combined bromine emissions by kelp (this study), non-kelp macroalgae (Nightingale *et al.* 1995), and ice algae communities (Sturges *et al.* 1992) are conservatively estimated at $1x10^{10}$g Br/yr for just these algal groups. The upper estimate of bromine emissions is $2x10^{11}$ g Br/yr from kelp and nonkelp macroalgae (Manley *et al.* 1992) and ice algae communities (Sturges *et al.* 1992) (Table 3.11). The estimated global input of $CHBr_3$ to the atmosphere based on atmospheric measurements is on the order of 10^{12} g $CHBr_3$/yr, which greatly exceeds anthropogenic inputs (Penkett *et al.* 1985; Krysell 1991). Presuming this estimate is approximately correct, $CHBr_3$ sources are not yet fully budgeted. Phytoplankton may be an additional bromine source but, as mentioned above, more information is required before an adequate assessment can be made.

Anthropogenic bromine emissions were estimated as ~$7x10^{10}$ g Br/yr (Table 3.12). This estimate is based on global emissions of MeBr, ethylene dibromide ($C_2H_4Br_2$; EDB), Halon 1301 (CF_3Br), Halon 1211 (CF_2ClBr), and brominated by-products from water chlorination. The 1990 value for Halon 1301 emissions was used (McCulloch 1992), but

it should be noted that U.S. manufacture of this flame retardant was halted at the end of 1994 (Great Lakes Chemical, personal communication). Methyl bromide from biomass burning (Manö and Andreae 1994) was included with anthropogenic sources for comparison to algal emissions. A value of $<6x10^9$ g Br/yr from EDB was used in this analysis, which is half the lowest estimate of Yung *et al.* (1980). This value is within the range of $4.2x10^8$ to $1.9\ x10^{10}$ g Br/yr from EDB conversion to MeBr given unreferenced by Butler (1995). The EDB values given in Yung *et al.* (1980) were based on data published in the 1976 Minerals Yearbook (Foster 1978), but use of EDB has since declined. Ethylene dibromide is used as an agricultural fumigant and as a leaded gasoline additive. However, U.S. fumigation use was banned in 1984, and its use as a gasoline additive has declined world-wide with the decline of leaded gasoline. Bromine sales have in fact steadily decreased since 1979 due largely to regulations regarding lead in leaded gasoline (Lyday 1992). The values given in Yung *et al.* (1980) were $1.2x10^{10}$ to $1.2x10^{11}$ g Br/yr from EDB. A value of $\leq 1.0x10^{11}$ was referenced to Yung *et al.* (1980) in the frequently cited paper by Gschwend *et al.* (1985). This outdated EDB value is often the ultimate source of a quoted value of $\sim 10^{11}$ g Br/yr coming from anthropogenic sources.

Comparing estimates for anthropogenic and algal bromine emissions (Table 3.11, Table 3.12), values are of similar magnitude ($\sim 10^{10}$-10^{11} g Br/yr). Algae thus appear to contribute significantly to the global bromine cycle. Natural and anthropogenic bromine emissions, however, have important differences. Biogenic brominated methane emissions, for example, may differ regionally due to season and species distribution. Also, $CHBr_3$

dominates biogenic organobromide emissions while MeBr dominates anthropogenic ones. These two compounds have different atmospheric fates.

The atmospheric fate of MeBr is distinct from the polybrominated methanes because of its longer atmospheric lifetime. The atmospheric lifetime of MeBr is on the order of 1.2 yr (Lobert *et al.*1995) whereas $CHBr_3$ and CH_2Br_2 have relatively short atmospheric lifetimes. The atmospheric lifetime of $CHBr_3$ is on the order of 0.05 yr (Penkett *et al.* 1985) and CH_2Br_2 is approximately 0.40 yr (Mellouki *et al.* 1992). Most MeBr is destroyed in the troposphere, but enough is transported to the stratosphere to play a significant role in stratospheric ozone depletion. MeBr has been estimated to contribute 54% of the total organic bromine near the tropical tropopause, and CH_2Br_2 was estimated to contribute 7% (Schauffler *et al.* 1993). The relatively short atmospheric lifetimes of $CHBr_3$ and CH_2Br_2 imply that these compounds are largely destroyed in the troposphere. Significant transport to the stratosphere is believed to be unlikely, particularly for $CHBr_3$ (Penkett *et al.* 1985). Accordingly, the atmospheric role of biogenic brominated methanes is probably tropospheric because biogenic emissions appear to be dominated by $CHBr_3$ (e.g., approximately 80% of kelp emissions; Table 3.11). However, Li *et al.* (1994) suggest that total organic bromine, and not only MeBr, should be salient to ozone cycling in the stratosphere and the troposphere partly because brominated methane species might reach higher altitudes than expected from their relatively short atmospheric lifetimes. Shorter-lived brominated methanes may thus have larger roles in the stratosphere and troposphere than previously believed. Defining the

role of biogenic brominated methanes will continue as understanding of the global bromine cycle progresses.

Conclusions

Bromoform and dibromomethane were produced during whole blade incubations of Giant Kelp, *Macrocystis pyrifera* with median rates of 171 ng $CHBr_3$/gfwt·day (0.68 nmoles $CHBr_3$/gfwt·day) and 48 ng CH_2Br_2/gfwt·day (0.27 nmoles CH_2Br_2/gfwt·day) based on a 12 hr photoperiod. Production ranged from 21-173 ng CH_2Br_2/gfwt·day and 25-1126 ng $CHBr_3$/gfwt·day for 19 separate incubations (190 blades total) over a period from May 1994 to February 1995. The large range in production indicates that a long-term sampling strategy may be necessary to reflect accurately the overall release behavior of halogenated methanes.

Light and photosynthetic activity affected $CHBr_3$ and CH_2Br_2 production. Darkness reduced production rates relative to $CHBr_3$ and CH_2Br_2 production by kelp incubated simultaneously in light. Production was inhibited in light by addition of the photosynthetic inhibitor, DCMU. DCMU probably affected the vanadium bromoperoxidase enzyme by halting photosynthetic production of H_2O_2. Hydrogen peroxide concentrations and the effect of adding additional H_2O_2 to different kelp treatments (i.e., light, dark, light/DCMU, light/aniline) suggested that internal H_2O_2 is available to vanadium bromoperoxidase. The likely H_2O_2 source is from photosynthesis, specifically pseudocyclic photophosphorylation (Mehler reaction).

The release behavior of $CHBr_3$ and CH_2Br_2 suggested that the physiological state of the alga was important to the production of these compounds. Environmental factors

affecting kelp physiology (e.g., health, light, season, climate, etc.) may therefore ultimately affect release of these brominated methanes to the atmosphere.

Anthropogenic bromine emissions appear to dominate algal emissions in southern California. A regional estimate of 3.0×10^6 g Br/yr was calculated for $CHBr_3$, CH_2Br_2, and MeBr production by *M. pyrifera* along Orange and San Diego Counties. Bromoform contributed 77% of this regional, *M. pyrifera* bromine source. Anthropogenic bromine emissions in this region are about 10^8 g Br/yr from MeBr fumigation alone. California accounts for approximately 10% of global MeBr use, thus this pattern of MeBr domination is not expected for all coastal regions, but it may be representative of other areas with dense urban and agricultural development.

Table 3.1. Experimental light flux, type of light (cool-white fluorescent, full-spectrum fluorescent, or sunlight) and seawater surface temperature in the kelp bed on the day of kelp collection.

date of collection	Surface Temp (°C)	incubation light type	incubation light flux ($\mu E/m^2 \cdot s$)
5/18/94	18.7	full-spectrum	36
5/25/94	18.7	cool-white	56
		full-spectrum	65
7/22/94	21.1	cool-white	52
8/1/94	21.6	cool-white	54
8/19/94	23.6	sunlight	1500 - 2166
		sunlight	927 - 1756
		cool-white	54
2/16/95	18.1	cool-white	55
2/22/95	18.1	cool-white	55
		full-spectrum	54

Table 3.2. *M. pyrifera* laboratory production rates of $CHBr_3$ and CH_2Br_2 for whole blades collected May 1994 to February 1995 and incubated in light (n = 19; 190 blades). Rates are based on a 12 hr photoperiod and calculated by linear regression; see Figure 3.4 for further description (gfwt = g fresh weight).

	median (ng/gfwt·day)	range (ng/gfwt·day)
$CHBr_3$	171	25.4 - 1126
CH_2Br_2	47.6	21.5 - 173

Table 3.3. Seawater H_2O_2 concentrations (nM ± SD) for incubations without kelp in light or darkness (n = 3 at each time point). Seawater H_2O_2 concentrations were not significantly higher in light compared to darkness when kelp was absent.

time (hr)	light, no kelp nM H_2O_2	dark, no kelp nM H_2O_2
0.25	21 ± 0	21 ± 0
1.0	24 ± 1.8	22 ± 1.3
1.5	25 ± 0.5	26 ± 1.3
2.0	25 ± 1.6	25 ± 3.9

Table 3.4. Seawater H_2O_2 concentrations (nM ± SD; n = 3 at each time point) and $CHBr_3$ and CH_2Br_2 production rates by *M. pyrifera* blades collected 2/15/95. Results are shown for different kelp incubation treatments (light, dark, light with DCMU, or light with aniline). H_2O_2 was reliably detected above apx.10 nM unless DCMU was present, then reliable detection limit was above apx. 50 nM H_2O_2. "ND" (not detected) indicates a "zero" spectrofluorophotometer reading, whereas a nonzero reading below the limit of reliable detection is indicated by the "<" symbol (e.g., < 10 nM). Seawater [H_2O_2] was 44 nM prior to placement in incubation bags with kelp (see text). See also Figures 3.18 and 3.20-3.21 for $CHBr_3$ and CH_2Br_2 production. See Figure 3.4 for description of rate calculation.

Light		Dark		DCMU		Aniline	
time (hr)	nM H_2O_2	time (hr)	nM H_2O_2	time (hr)	nM H_2O_2	time (hr)	nM H_2O_2
0.28	< 10	0.42	ND	0.37	ND	0.48	ND
1.72	45 ± 6.0	1.7	ND	1.13	ND	2.13	ND
2.25	31 ±0.75	2.5	ND	1.68	ND		
				2.1	ND		
$CHBr_3$ and CH_2Br_2 Production Rates (ng/gfwt·day ± std error)							
$CHBr_3$	CH_2Br_2	$CHBr_3$	CH_2Br_2	$CHBr_3$	CH_2Br_2	$CHBr_3$	CH_2Br_2
172 ± 19	54 ± 5.2	9.0 ± 1.2	8.5±0.15	ND	ND	20 ± 8.7*	21 ± 2.2*

* substantial lag

Table 3.5. Proton NMR chemical shifts of DCMU. Description refers to NMR spectra shown in Fig. 3.18. Proton assignment refers to inset of Fig. 3.18.

chemical shift (ppm)	description	proton assignment
1.609	singlet	methyl
6.341	broadened	amide
7.244	quartet	C(6)
7.346	doublet	C(5)
7.645	doublet	C(2)

Table 3.6. Published $CHBr_3$ and CH_2Br_2 production rates from various kelp and rockweeds (Division Phaeophyta; brown algae) to compare to rates measured in this study (bold). Number of replicates used to determine rate is noted. Rates are per g dry weight (gdwt); see Table 3.2 for per g fresh weight values measured in this study.

species	**$CHBr_3$** ng/gdwt·day	**CH_2Br_2** ng/gdwt·day	study description
Kelp (Order Laminariales)			
Macrocystis pyrifera	**$1.7x10^3$** ($2.5x10^2$ - $1.1x10^4$)	**$4.8x10^2$** ($2.1x10^2$ - $1.7x10^3$)	this study; median (range), n=19[a]
Macrocystis pyrifera	$1.5x10^4$	$3.7x10^2$	Manley *et al.* 1992; mean, n=3[b]
Laminaria farlowii	$7.3x10^3$	82	
Egregia menziesii	$2.1x10^4$	73	
Eisenia arborea	$4.7x10^4$	86	
Laminaria saccharina	$4.8x10^2$ ($1.4x10^2$ - $1.0x10^3$)	55 (13 - $1.2x10^2$)	Schall *et al.* 1994; mean (range), n=4[c]
Laminaria saccharina	$3.0x10^4$	$2.5x10^3$	Nightingale *et al.* 1995; n=1
Laminaria digitata	94 ($7.8x10^2$ - $1.1x10^3$)	86 (75 - 96)	Nightingale *et al.* 1995; mean (range), n=2;
Rockweed (Order Fucales)			
Ascophyllum nodosum	$4.5x10^3$ ($1.5x10^2$ - $1.2x10^4$)	$6.8x10^2$ (ND - $2.1x10^3$)	Gschwend *et al.* 1985; mean (range), n=8
Fucus vesiculosis	$2.2x10^3$ ($1.4x10^2$ - $4.7x10^3$)	84 (ND - $5.9x10^2$)	Gschwend *et al.* 1985; n=7, ND = not detected
Fucus vesiculosis	$5.9x10^2$	$2.4x10^2$	Klick 1993; n=1
Fucus distichus	$1.2x10^2$ (30 - $2.0x10^2$)	54 (11 - $1.8x10^2$)	Schall *et al.* 1994; mean (range), n=4[c]
Ascophyllum nodosum	$4.7x10^2$	79	Nightingale *et al.* 1995; n=1
Fucus serratus	$1.1x10^3$	45	
Pelvetia canalicuta	$2.8x10^2$	59	

[a] Converted from fresh weight calculations using 10% dry weight from measurements in Chapter 2 (Table 2.1).

[b] Rates adjusted for 12 hr photoperiod. CH_2Br_2 rates additionally adjusted for Tse *et al.* (1992) partition coefficient. See Table 3.7 for description. See Chapter 2 for % dry weight values.

[c] Converted from fresh weight calculations assuming 15% dry weight.

Table 3.7. Published $CHBr_3$ and CH_2Br_2 production rates for various red, green, and brown algae. See Table 3.6 for kelp and rockweed rates and further description.

species	**$CHBr_3$** ng/gdwt·day	**CH_2Br_2** ng/gdwt·day	study description
Rhodophyta (red algae)			
Gigartina stellata	ND - $2.1x10^3$	ND	Gschwend *et al.* 1985; range, n=3.
Chondrus crispus	ND	ND	Gschwend *et al.* 1985; n=2 (ND = not detected)
Corallina officinalis	$4.3x10^2$	14	Manley *et al.* 1992; mean, n=3[a]
Pterocladia capillacea	$1.9x10^4$	$1.5x10^2$	
Rhodymenia californica	$2.5x10^4$	53	
Chlorophyta (green algae)			
Gigartina stellata	$3.3x10^2$	3.0	Nightingale *et al.* 1995; n=1
Corallina officinalis	$1.1x10^2$	1.2	
Polysiphonia lanosa	$1.7x10^2$	ND	
Ulva lactuca	$1.7x10^3$ - $1.4x10^4$	ND - $2.5x10^2$	Gschwend *et al.* 1985; range, n=2
Enteromorpha linza	ND - $8.5x10^2$	$3.0x10^2$	(ND = not detected)
Ulva sp.	$1.0x10^5$	$1.8x10^2$	Manley *et al.* 1992; mean, n=3[a]
Enteromorpha intestinalis	$2.9x10^4$	$3.6x10^3$	
Ulva lactuca	$1.1x10^3$	ND	Nightingale *et al.* 1995; n=1
Enteromorpha sp.	$5.0x10^2$	38	
Cladophora albida	ND	1.6	
Phaeophyta (brown algae)			
Dictyota binghamiae	ND	ND	Manley *et al.* 1992; mean, n=3[a]
Cystoseira osmundacea	$1.9x10^3$	$1.6x10^2$	(ND = not detected)
Desmarestia aculeata	23 (18 - 30)*	6 (4 - 11)	Schall *et al.* 1994; mean (range), n=4[b]; *n=3

[a] Rates adjusted for 12 hr photoperiod by dividing original rates (see Table 2.1) by two. CH_2Br_2 rates additionally adjusted for Tse *et al.* (1992) partition coefficient at temperature of halomethane extraction by dividing original rates by 3.16 (partition coefficient = 0.049 @ 28 °C) for all algae except *M. pyrifera* and *Ulva* sp. for which rates were divided by 2.97 (partition coefficient = 0.046 @ 26.5 °C).

[b] Corrected from fresh weight calculations assuming 15% dry weight.

Table 3.8. Range (low-high) and average estimated *M. pyrifera* standing crop from 1963-1991 for Orange and San Diego Counties. Standing crop range was associated with climatic features (El Niño and La Niña episodes). Biomass estimates (g) were based on areas (km^2) from North *et al.* (1993) and *M. pyrifera* bed density of 6 kg/m^2 (see Chapter 5).

year (description)	*M. pyrifera* coverage (km^2)	*M. pyrifera* biomass (g)
1984 (low; El Niño)	0.70	$4.2x10^9$
1990 (high; La Niña)	15	$9.0x10^{10}$
1963-1991 (average)	6.5	$3.9x10^{10}$

Table 3.9. Regional estimates of bromine emissions from $CHBr_3$, CH_2Br_2, and MeBr production by *M. pyrifera* along Orange and San Diego Counties. Biogenic emissions (g Br/yr) were based on regional biomass estimates (Table 3.8), *M. pyrifera* median $CHBr_3$ and CH_2Br_2 production rates (Table 3.2), and *M. pyrifera* MeBr laboratory production rates from Manley and Dastoor (1987) (see text). $CHBr_3$ dominates these emissions.

M. pyrifera biomass estimate (g)	g Br/yr from CH_3Br	g Br/yr from CH_2Br_2	g Br/yr from $CHBr_3$	Regional emissions (g Br/yr)
$4.2x10^9$ (low)	$5.5x10^3$	$6.7x10^4$	$2.5x10^5$	$3.2x10^5$
$9.0x10^{10}$ (high)	$1.2x10^5$	$1.4x10^6$	$5.3x10^6$	$6.9x10^6$
$3.9x10^{10}$ (average)	$5.1x10^4$	$6.2x10^5$	$2.3x10^6$	$3.0x10^6$

Table 3.10. Regional estimates of bromine emissions (g Br/yr) from two major anthropogenic sources in Orange and San Diego Counties for comparison with *M. pyrifera* bromine emissions in the same region (see Table 3.9). MeBr dominates these emissions.

Br source	g Br/yr
methyl bromide fumigation [a]	1.2×10^8
water chlorination by-products [b]	$\approx 7.9 \times 10^6$
sum	1.3×10^8

[a] State of California Department of Pesticide Regulation Annual Pesticide Use Report 1993 (Draft), assuming half of application is emitted to the atmosphere.

[b] Calculations assume 0.1% brominated by-products from freshwater and wastewater chlorination and 1% brominated by-products from seawater chlorination (Gschwend 1985). Water chlorination information was graciously provided from the following Orange and San Diego County companies:

Metropolitan Water District of Southern California
Southern California Edison (El Segundo, Huntington Beach, Redondo, and San Onofre)
San Diego Gas and Electric
Orange County Sanitation District
City of San Diego Metropolitan
San Diego County Sanitation Districts
City of Fallbrook
City of Encino
City of Escondido

Table 3.11. Global estimates of bromine emissions by selected algal groups. Estimates were based on published $CHBr_3$ and CH_2Br_2 algal production rates and rates measured in this study for *M. pyrifera* (bold) (see Table 3.6-3.7). Global emission estimates are derived by extrapolating production rates based on biomass (g) or area coverage (km^2). $CHBr_3$ is the dominant bromine source.

algal type	extrapolation basis	g Br/yr
kelp	$4x10^{13}$ g [a]	**$3.0x10^{9}$** [b] – $4.8x10^{10}$ [c]
non-kelp macroalgae	$2x10^{13}$ g [a]	$8.2x10^{8}$ [d] – $3.2x10^{10}$ [c]
ice algae community [e]	$2.3x10^{7}$ km^2	$9.5x10^{9}$ – $1.4x10^{11}$
sum		$1x10^{10}$ – $2x10^{11}$

[a] De Vooys (1977).
[b] this study.
[c] Manley *et al.* (1992) (Chapter 2), adjusted as described in Table 3.7.
[d] Nightingale *et al.* (1995). Rates per gfwt (Table 3.6-3.7) converted by the following % dry weight values (P. Nightingale, personal communication): *L. saccharina* 12; *L. digitata* 18 (5/21/90), 14 (5/23/90); *A. nodosum* 28; *F. serratus* 24; *P. canalicuta* 25; *G. stellata* 32; *C. officinalis* 65; *P. lanosa* 23; *U. lactuca* 24; *Enteromorpha sp.* 14; *C. albida* 31.
[e] bromine emissions based on $CHBr_3$ production estimates of Sturges *et al.* (1992).

Table 3.12. Global estimates of bromine emissions from anthropogenic sources for comparison to estimates of global biogenic emissions (see Table 3.11 and text). MeBr is the dominant bromine source.

bromine source	g Br/yr	reference
CH_3Br fumigation	$2.5x10^{10}$	U.N. Environmental Programme 1992[b]
CH_3Br biomass burning	$2.5x10^{10}$	Manö and Andreae 1994
$C_2H_2Br_2$	$< 6.0x10^9$	Yung *et al.* 1980[a]
CF_3Br (Halon 1301)	$4.6x10^9$	McCulloch 1992[b]
CF_2ClBr (Halon 1211)	$1.6x10^9$	McCulloch 1992[b]
seawater chlorination	$6x10^8$	Gschwend *et al.* 1985
freshwater chlorination	$4x10^9$	Gschwend *et al.* 1985
sum	$\approx 7x10^{10}$	

[a] half the lowest estimate (see text).
[b] 1990 emission estimates.

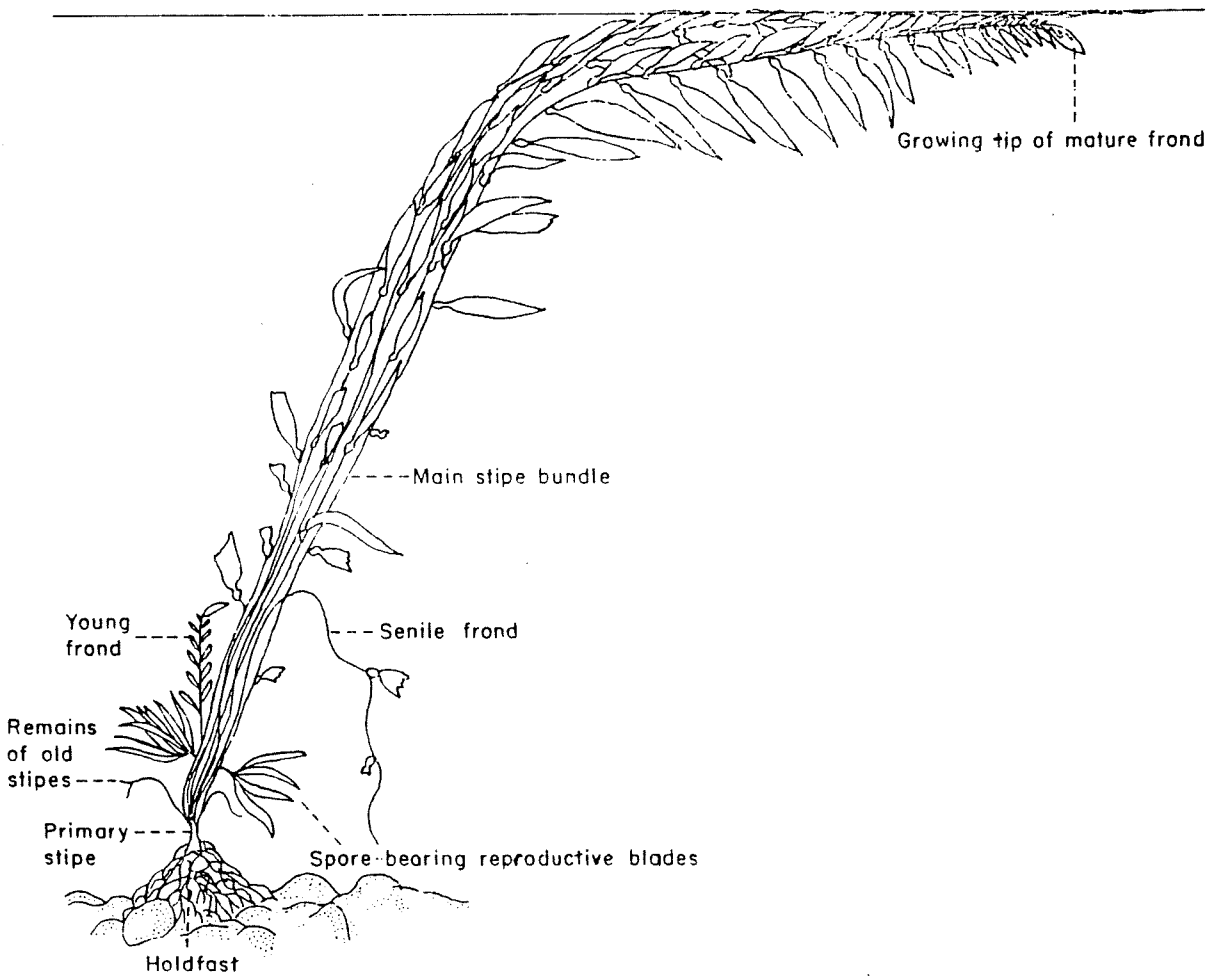

Figure 3.1. Diagram of a *M. pyrifera* canopy frond (adapted from North 1994).

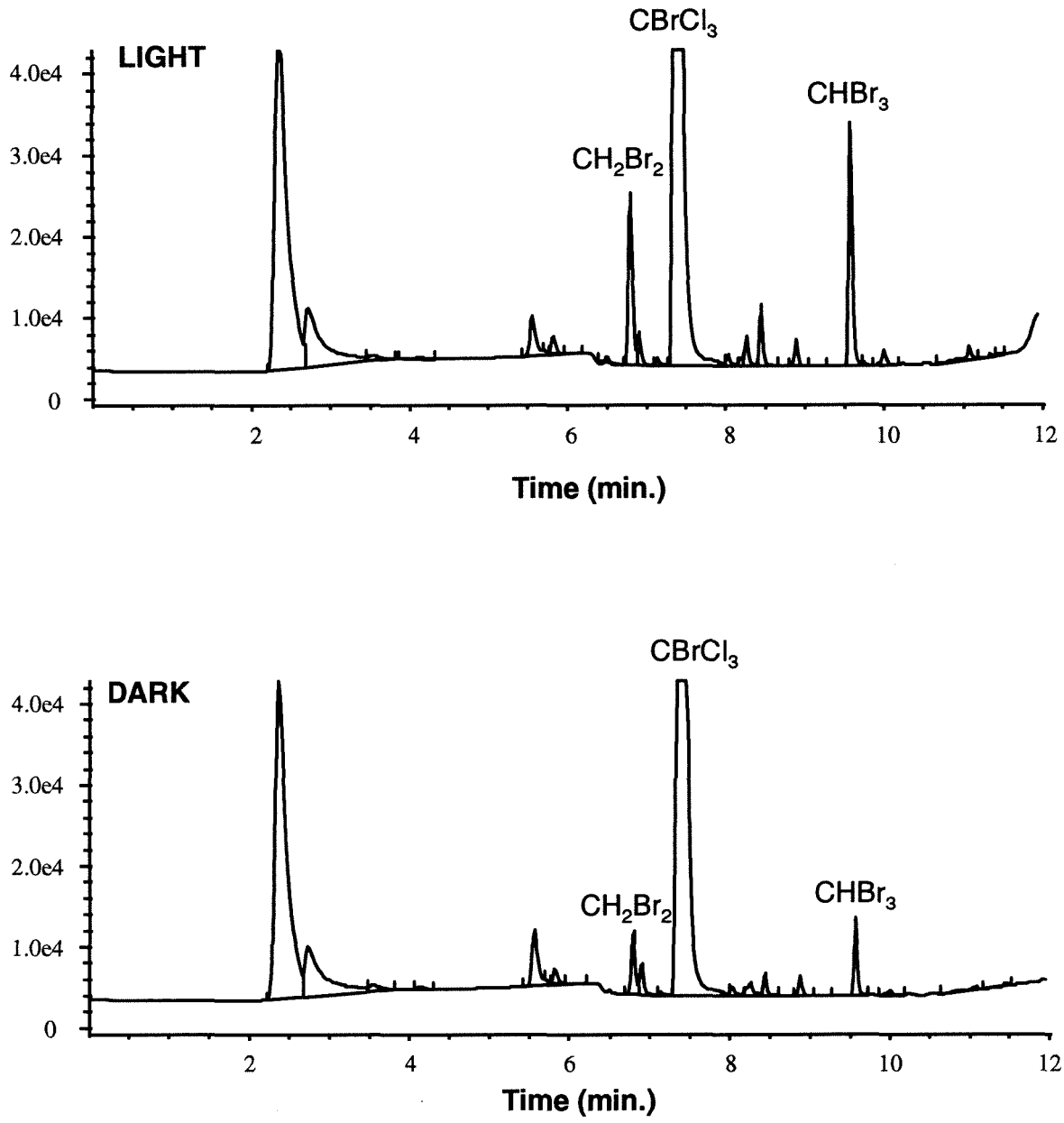

Figure 3.2. Halomethane analysis by gas chromatography of headspace overlying seawater. Upper chromatogram shows CH_2Br_2 and $CHBr_3$ peaks from seawater incubated with *M. pyrifera* under cool-white fluorescent light for 2 hr. Lower chromatograph shows seawater incubated with *M. pyrifera* in darkness for 2 hr under otherwise identical conditions. $CHBrCl_3$ is a reference peak.

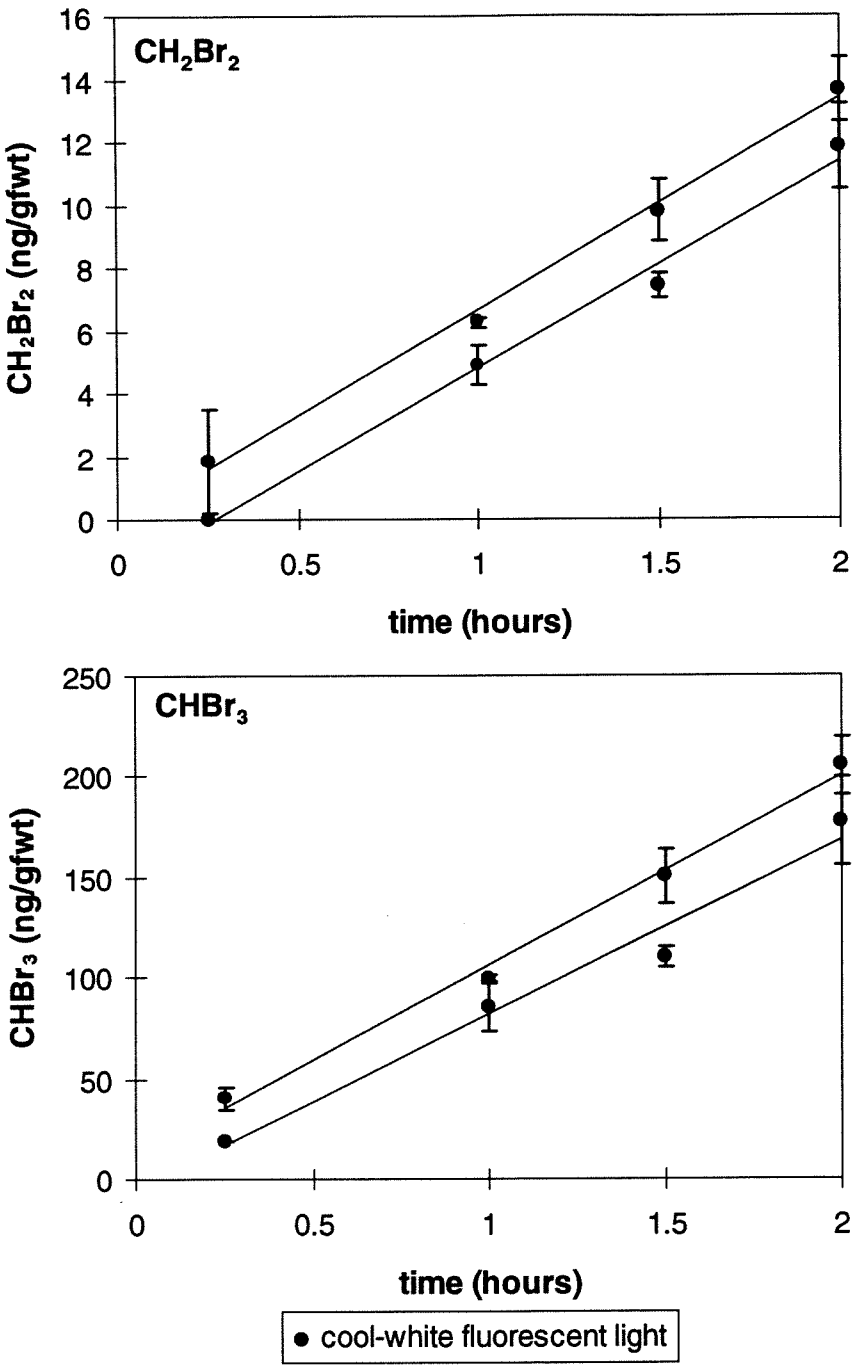

Figure 3.3. *M. pyrifera* laboratory production of CH_2Br_2 and $CHBr_3$ for blades collected 7/22/94. Linear regression (solid lines) was used to determine production rates shown in Fig. 3.4. Blades of similar size and weight were incubated simultaneously in identical conditions under cool-white fluorescent light (gfwt = g fresh weight). Error bars are SD of 3 replicate samples.

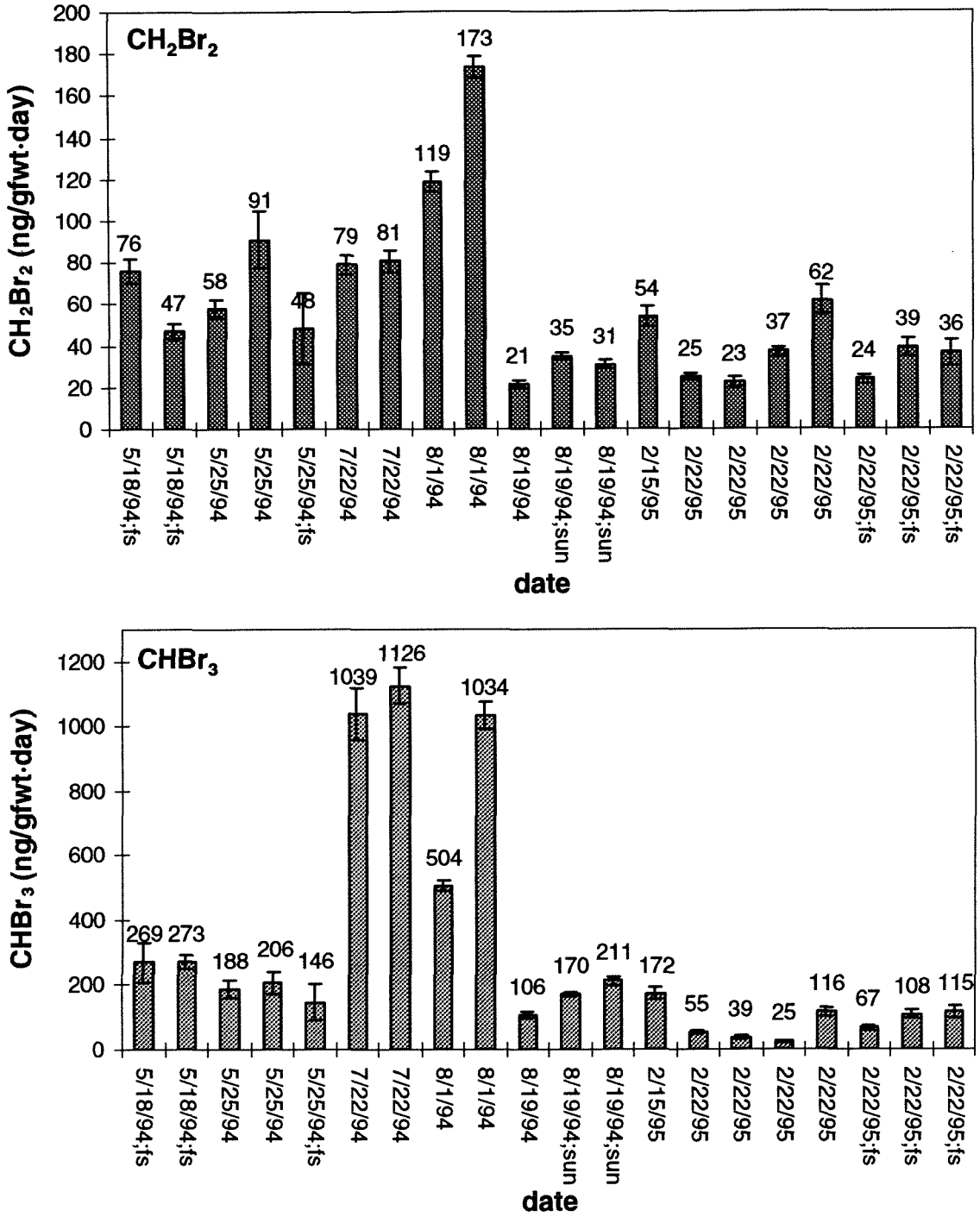

Figure 3.4. *M. pyrifera* laboratory production rates of CH_2Br_2 and $CHBr_3$ for blades collected May 1994 to February 1995. Rates were determined by linear regression of halomethane produced (ng) per g fresh weight (gfwt) during incubation (2 hr) and converted to daily rates using a 12 hr photoperiod. Blades were incubated in a shaking water bath under cool-white fluorescent light unless otherwise indicated by "sun" or "fs" (full-spectrum fluorescent). Error bars are standard error of regression. See Figs. 3.3, 3.8-3.11, 3.13-3.15, 3.20 for data used in rate calculations.

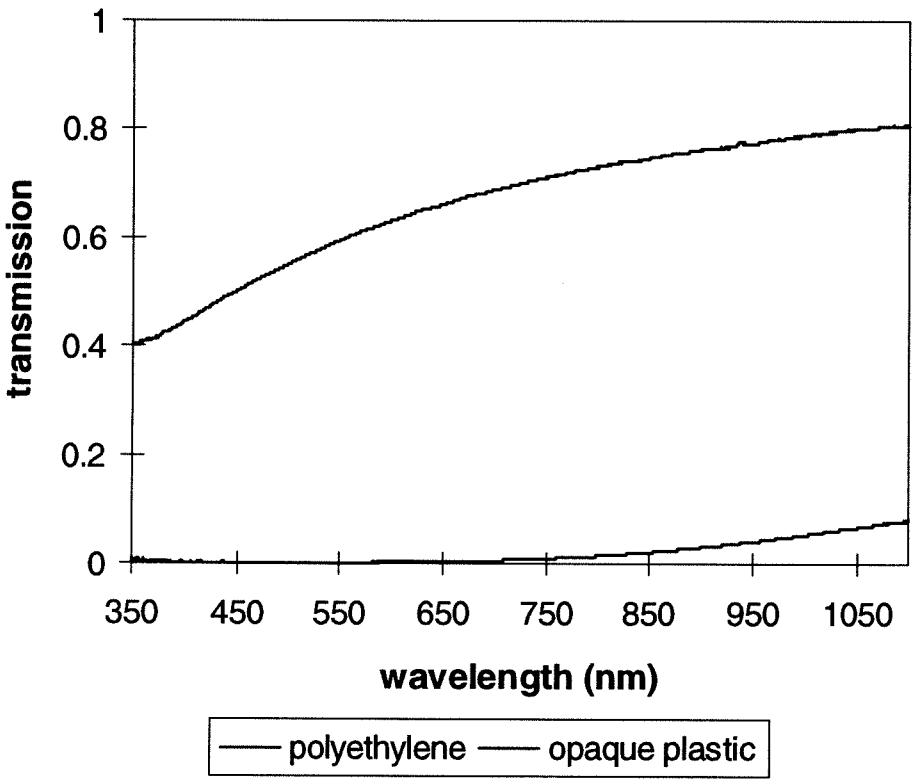

Figure 3.5. Light transmission spectra for plastic films used in incubation studies. Clear polyethylene plastic allowed passage of approximately 66% in the 400-750 nm range and 77% of light in the 800-1070 nm range. Opaque plastic used to cover clear polyethylene bags in darkness incubations essentially blocked light transmission (< 1% for 400-750 nm and 4% for 800-1070 nm).

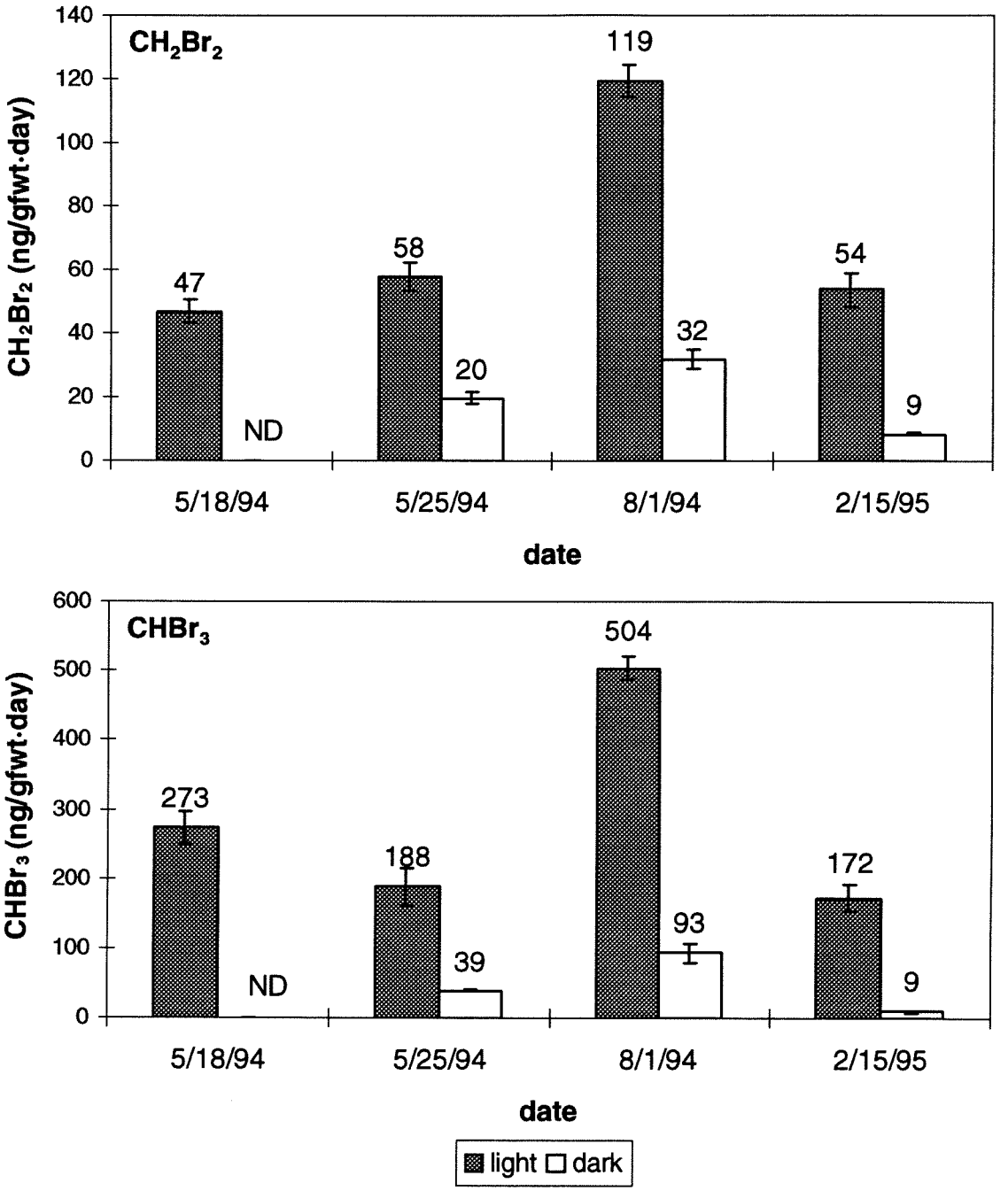

Figure 3.6. *M. pyrifera* laboratory production rates of CH_2Br_2 and $CHBr_3$ for blades incubated under fluorescent light or in darkness. Paired columns represent production during simultaneous incubations in otherwise identical conditions. ND = production not detected. See Figs. 3.8-3.11, 3.20 for data used in rate calculations. See Fig. 3.4 for additional description. Error bars are standard error of regression.

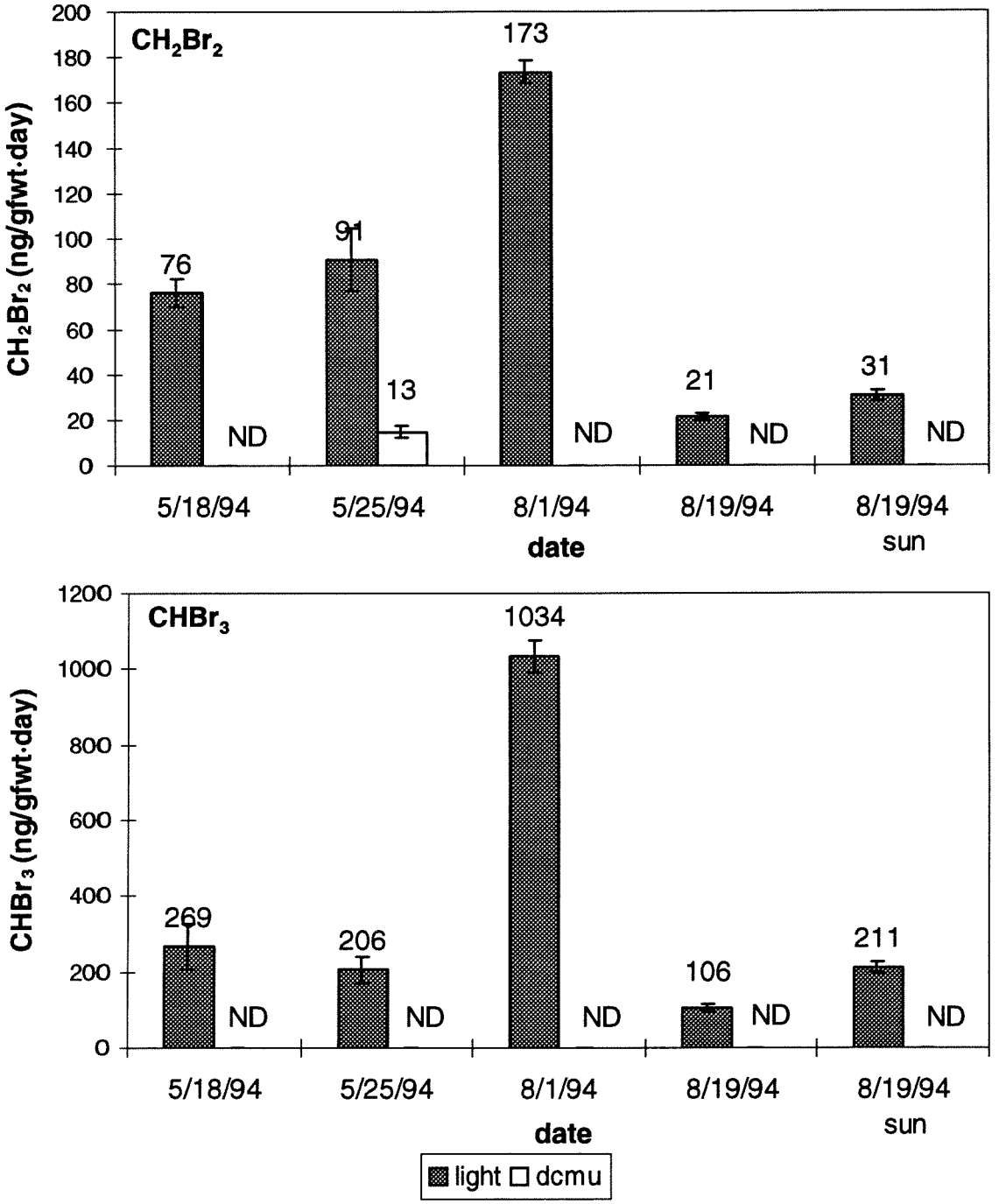

Figure 3.7. *M. pyrifera* laboratory production rates of CH_2Br_2 and $CHBr_3$ for blades incubated under fluorescent light or in sunlight ("sun") with or without the photosynthetic inhibitor DCMU. Paired columns represent production during simultaneous incubations in otherwise identical conditions. ND = production not detected. See Figs. 3.8-3.11 for data used in rate calculations. See Fig. 3.4 for further description. Error bars are standard error of regression.

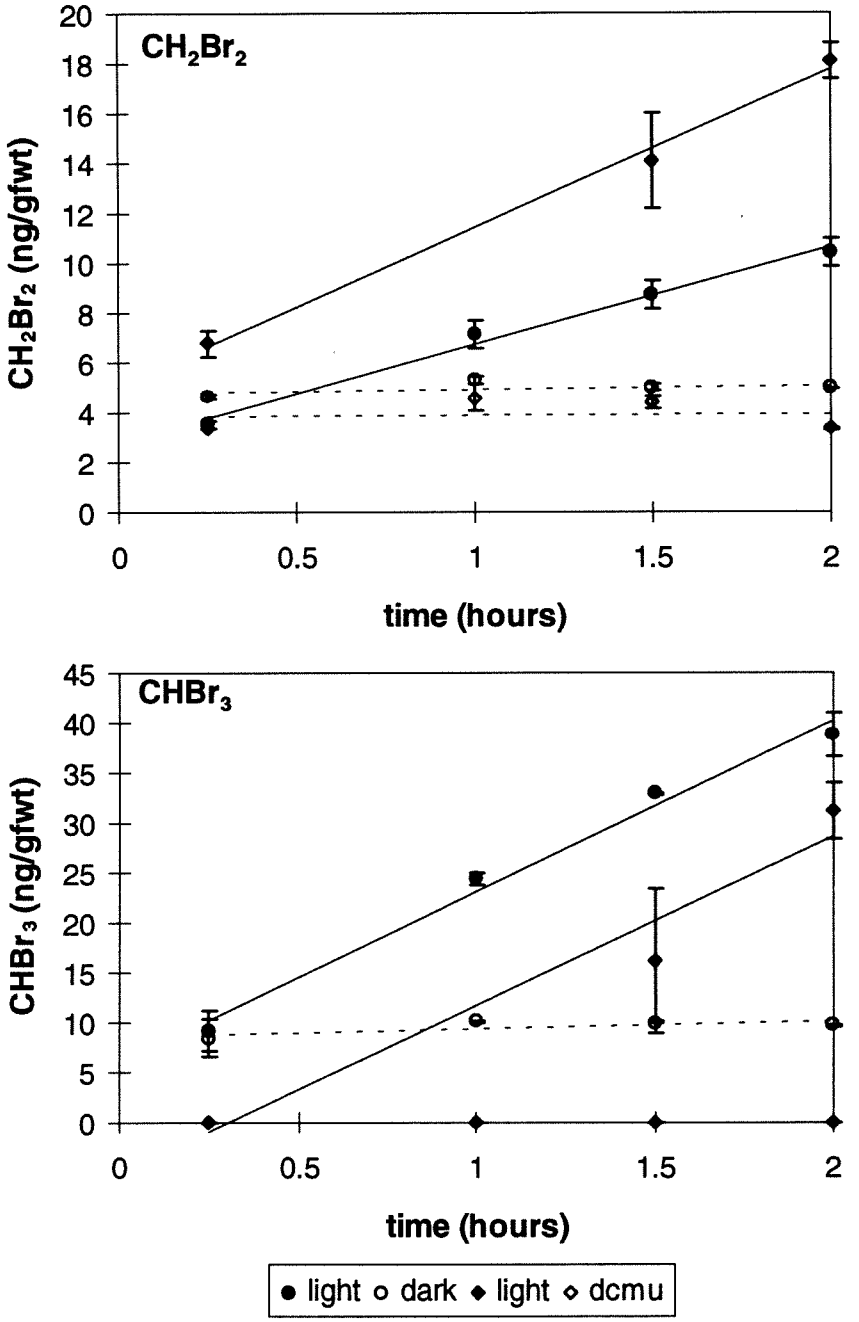

Figure 3.8. *M. pyrifera* laboratory production of CH_2Br_2 and $CHBr_3$ for blades collected 5/18/94. Paired incubations were performed with blades of similar size and weight under simultaneous and identical conditions except for the treatment being examined (darkness or photosynthetic inhibitor, DCMU). Paired incubations have the same symbol (circle or diamond). Incubations were performed under cool-white fluorescent light ("light" and "dcmu") or in darkness ("dark"). Linear regression lines are shown (solid for "light"; dashed for "dark" or "dcmu"). DCMU was dissolved in ethanol; therefore, ethanol was also added to the partner incubation. Not detected values appear as zero on the graph. See Table 3.1 for light flux data. Error bars are SD of two replicate injections of a single sample.

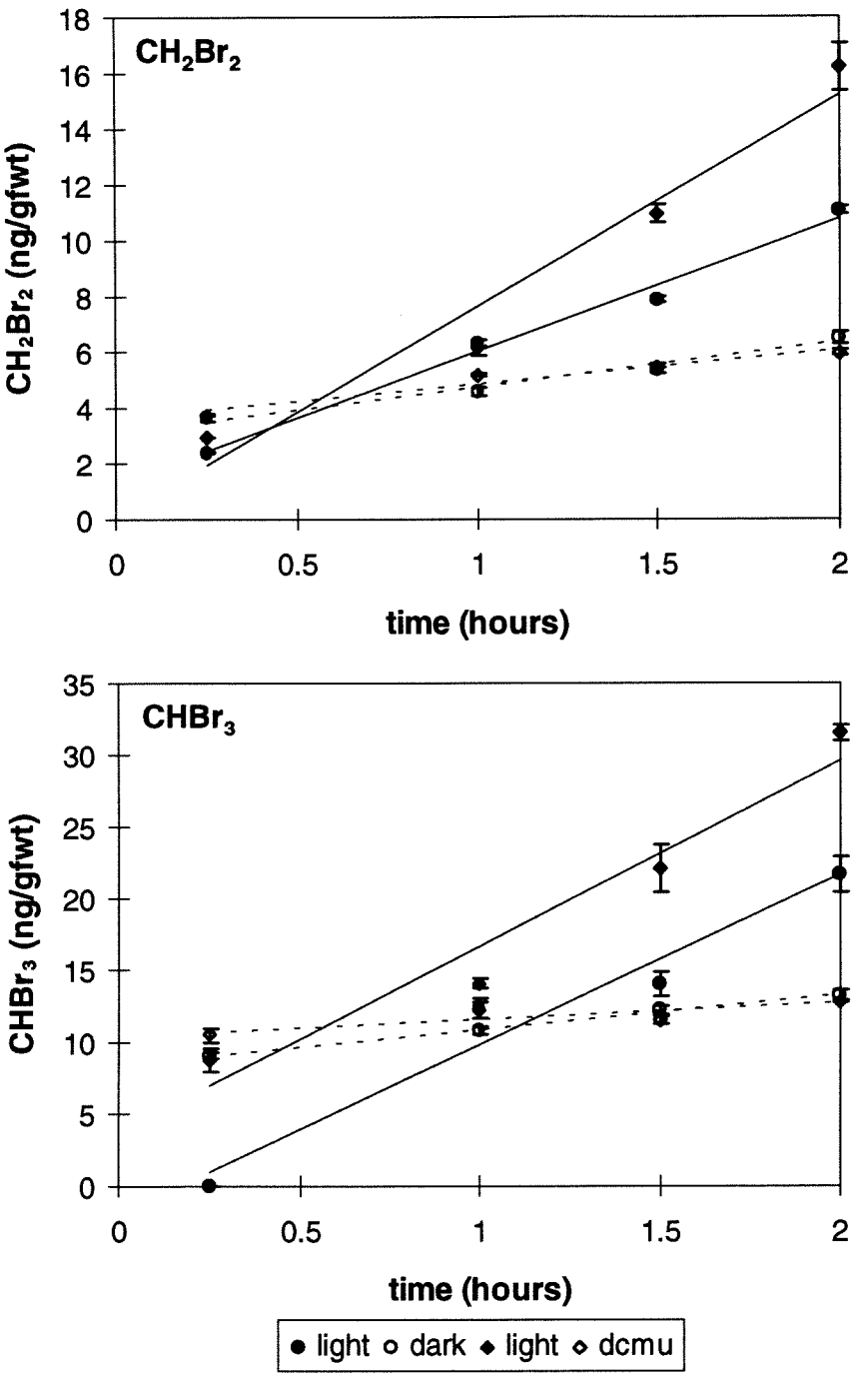

Figure 3.9. *M. pyrifera* laboratory production of CH_2Br_2 and $CHBr_3$ for blades collected 5/25/94. Production appears to lag in one light incubation (solid diamond). Error bars are SD of two replicate injections of a single sample. See Fig. 3.8 for description.

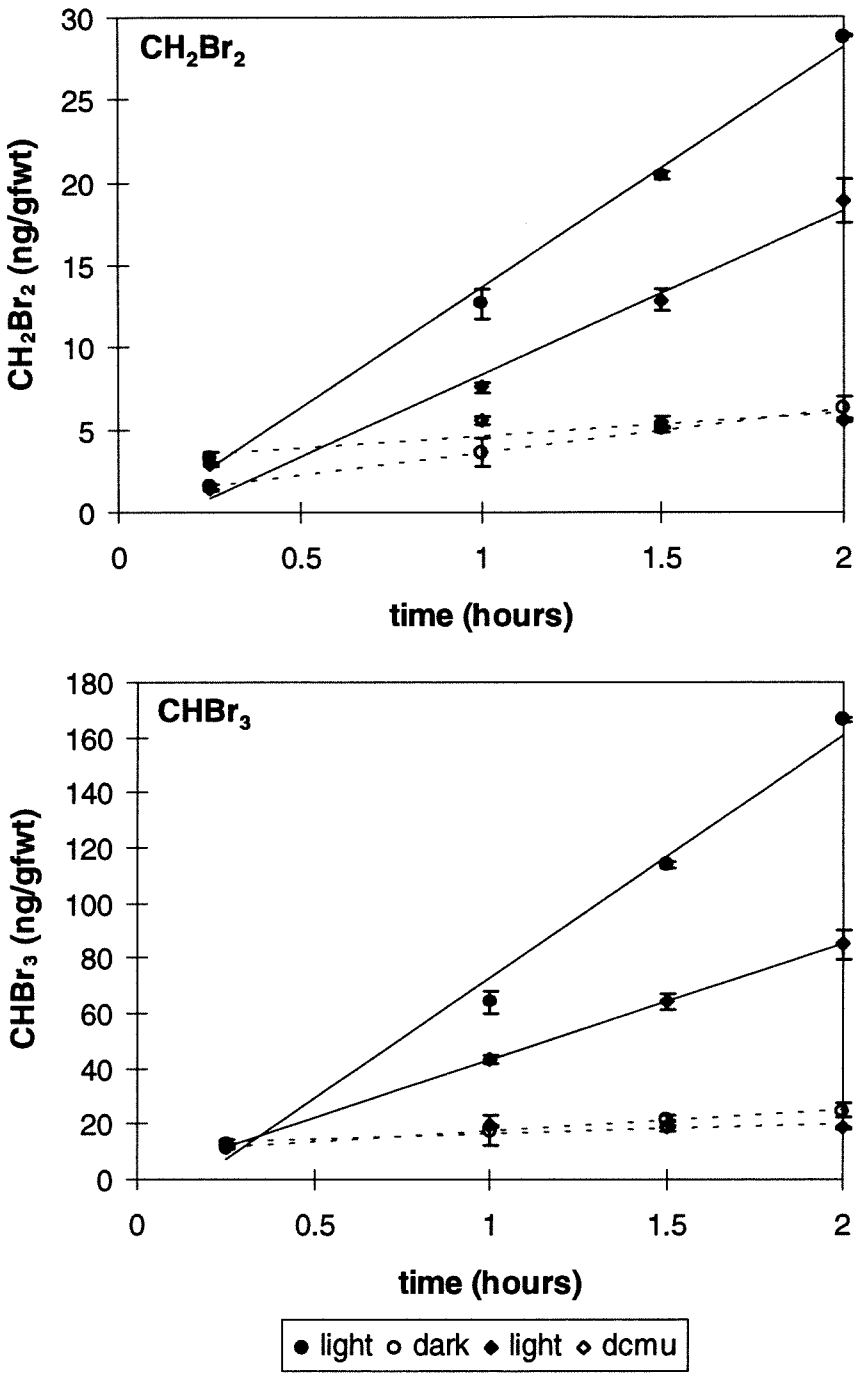

Figure 3.10. *M. pyrifera* laboratory production of CH_2Br_2 and $CHBr_3$ for blades collected 8/1/94. Error bars are SD or three replicate samples. See Figure 3.8 for description.

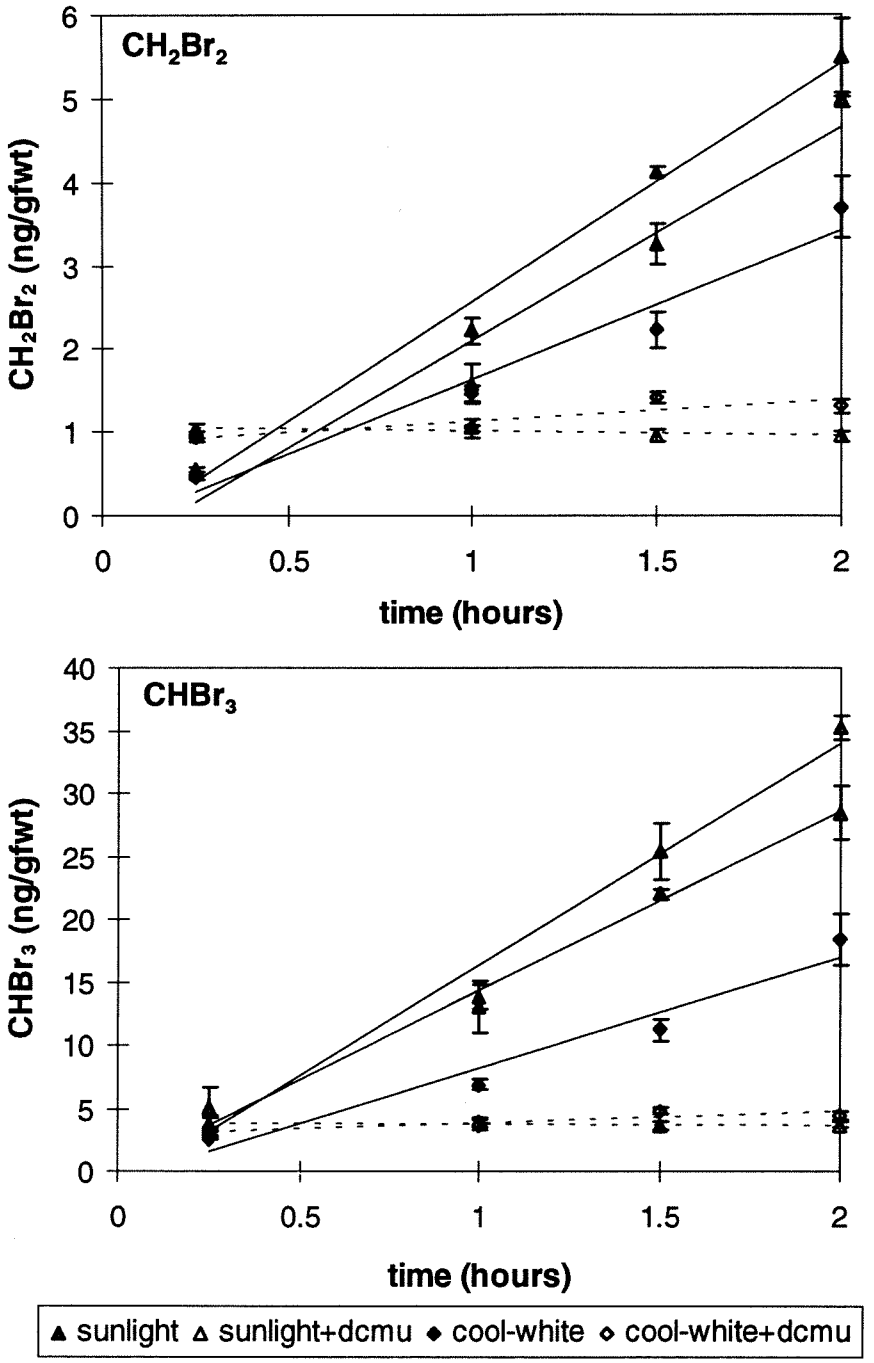

Figure 3.11. *M. pyrifera* laboratory production of CH_2Br_2 and $CHBr_3$ for blades collected 8/19/94. Blades were incubated as described in Fig. 3.8 with additional incubations performed in natural sunlight. See Table 3.1 for light flux data. Error bars are SD or three replicate samples.

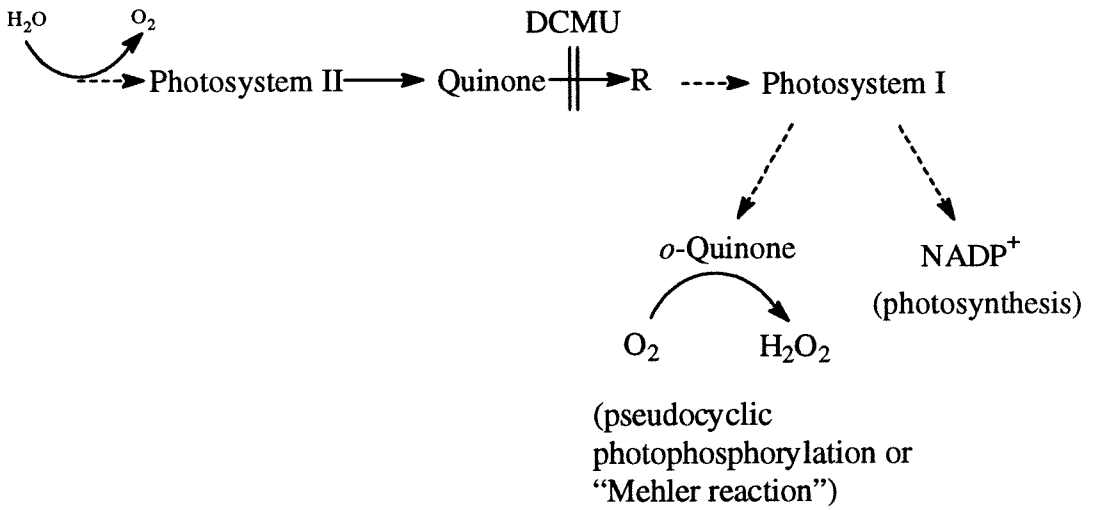

Figure 3.12. Skeleton diagram of the photosynthetic electron transport chain. The reaction scheme shows the site of DCMU action and hydrogen peroxide production from pseudocyclic photophosphorlation, commonly referred to as the "Mehler reaction" (adapted from Elstner 1987).

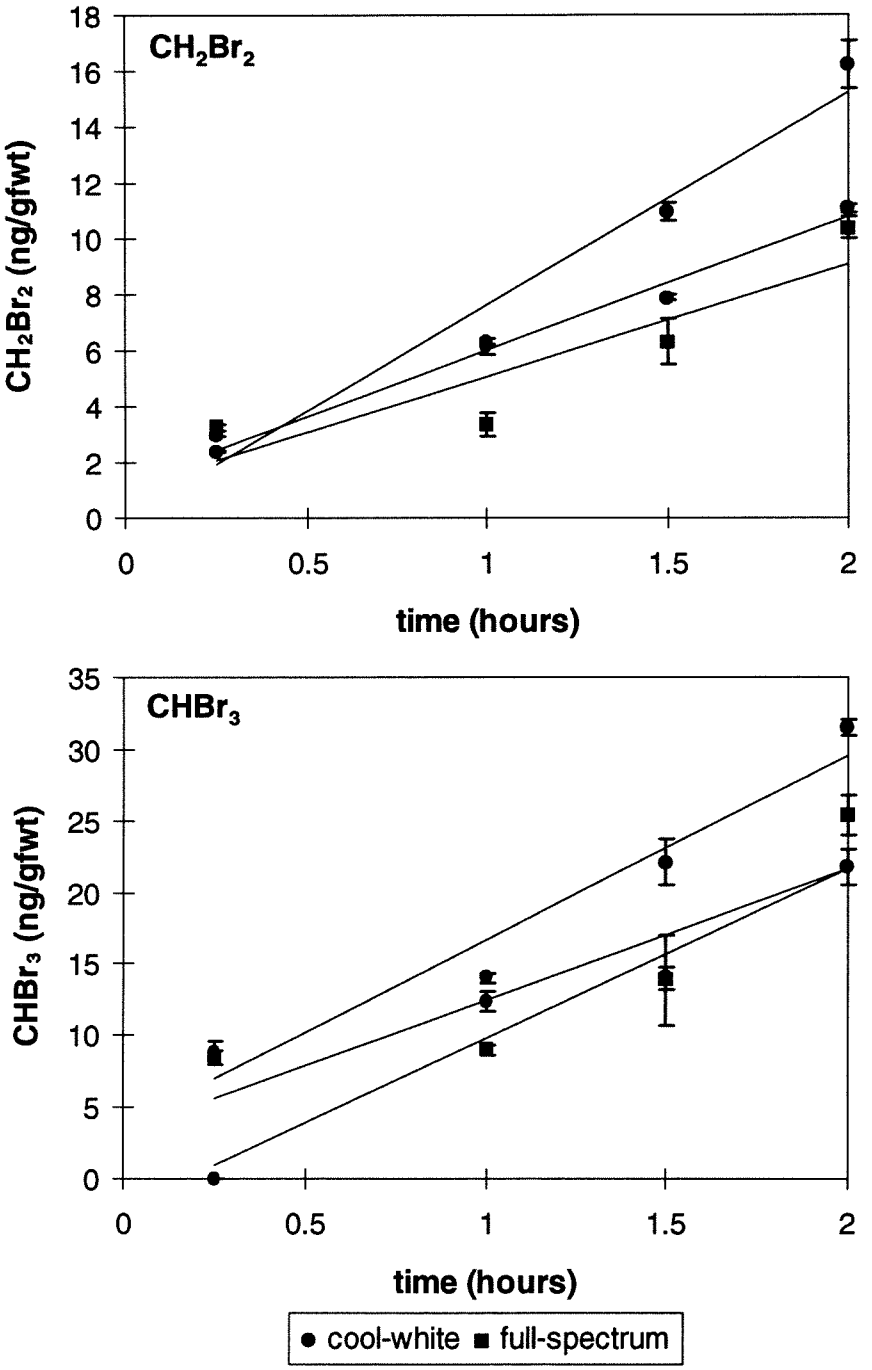

Figure 3.13. *M. pyrifera* laboratory production of CH_2Br_2 and $CHBr_3$ for blades collected 5/25/94 and incubated under conditions of cool-white fluorescent or full-spectrum fluorescent light. The cool-white incubation data are also shown in Fig. 3.9 but are plotted again here for direct comparison to the the full-spectrum incubation. Error bars are SD of three replicate samples. See Fig. 3.4 for production rate comparisons.

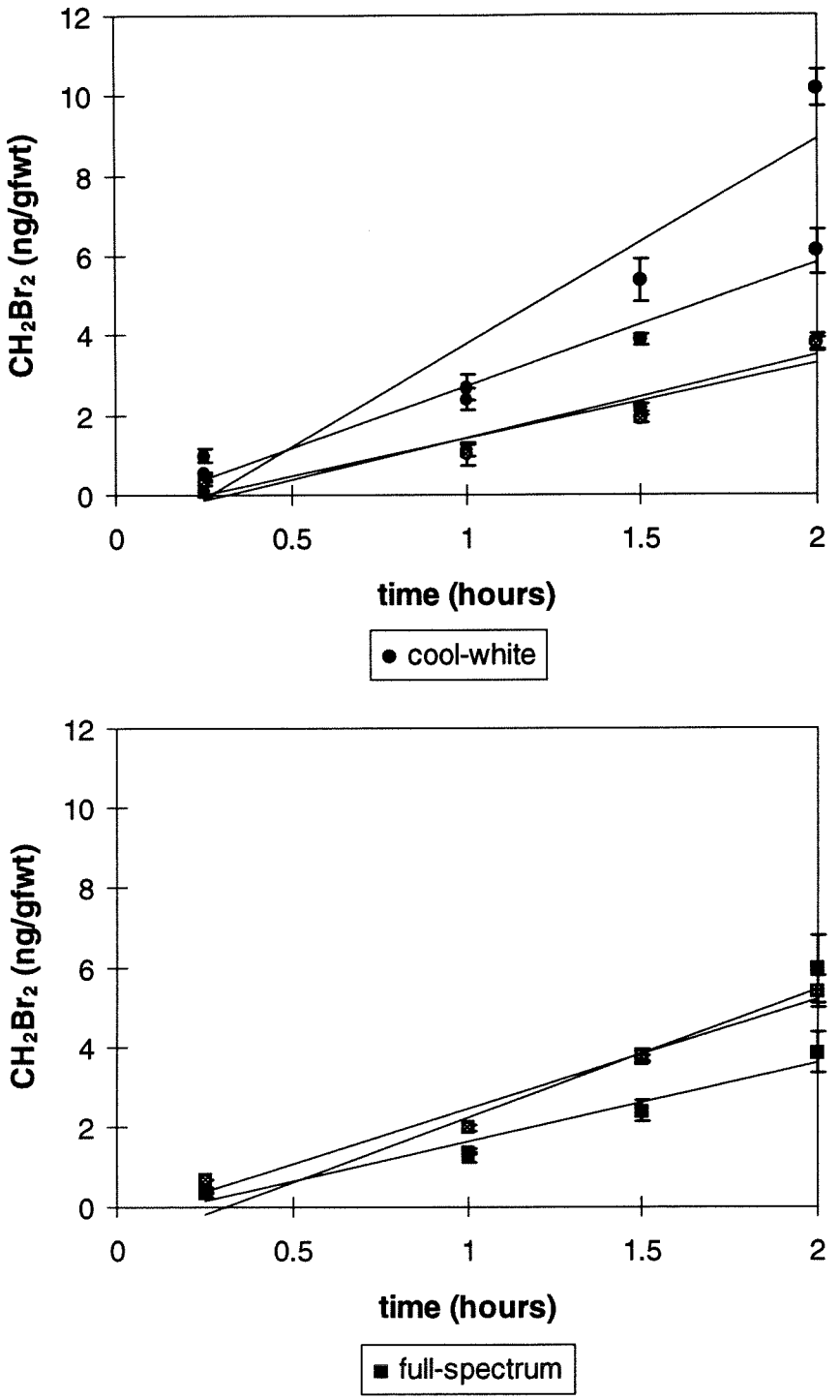

Figure 3.14. *M. pyrifera* laboratory production of CH_2Br_2 for blades collected 2/22/95 and incubated under conditions of cool-white fluorescent (upper graph) or full-spectrum fluorescent (lower graph) light. Production appears to lag for some samples under either type of light. See Figure 3.15 for $CHBr_3$ production. Error bars are SD of three replicate samples.

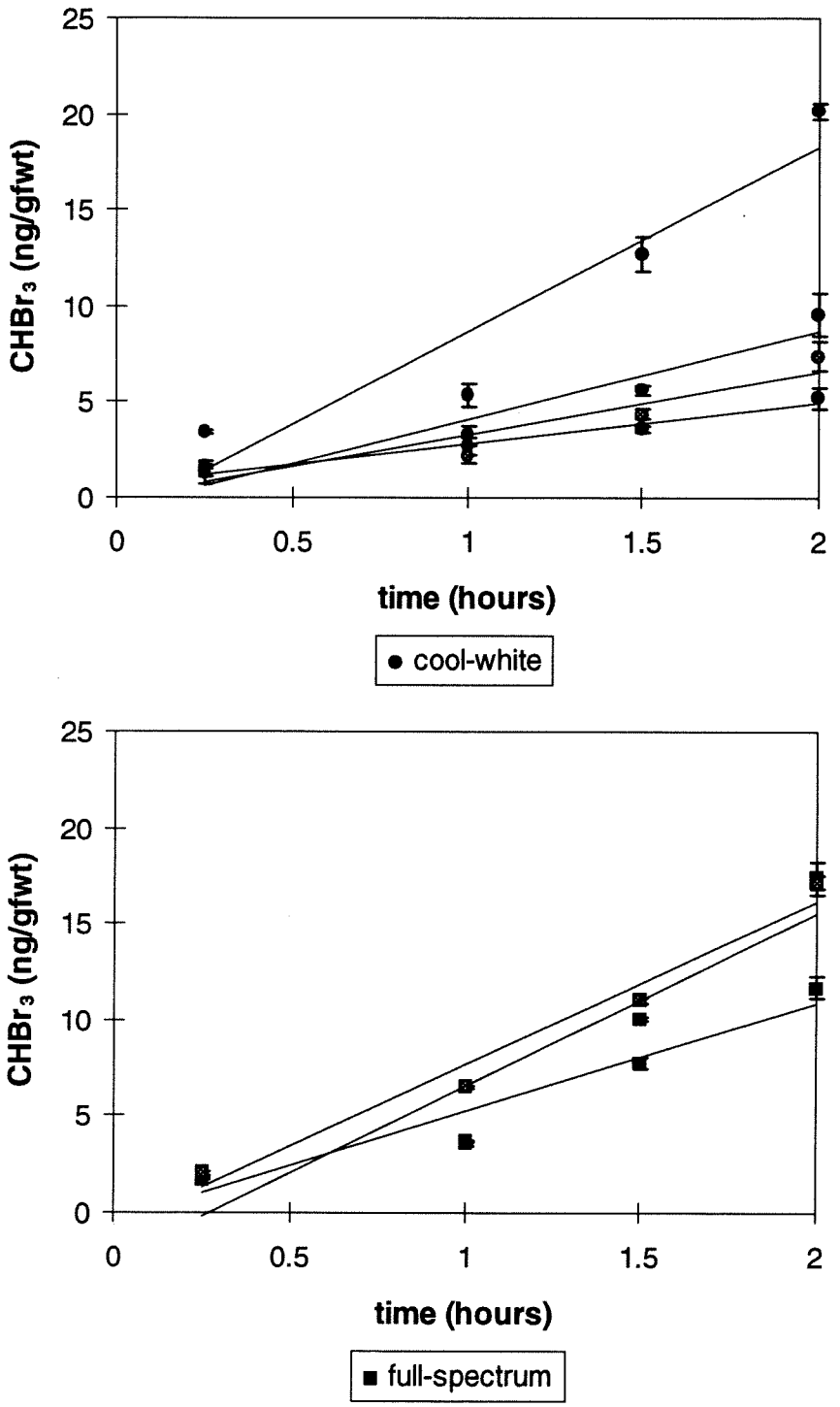

Figure 3.15. *M. pyrifera* laboratory production of $CHBr_3$ for blades collected 2/22/95 and incubated under conditions of cool-white fluorescent (upper graph) or full-spectrum fluorescent (lower graph) light. Production appears to lag for some samples under either type of light. See Figure 3.14 for CH_2Br_2 production. Error bars are SD of three replicate samples.

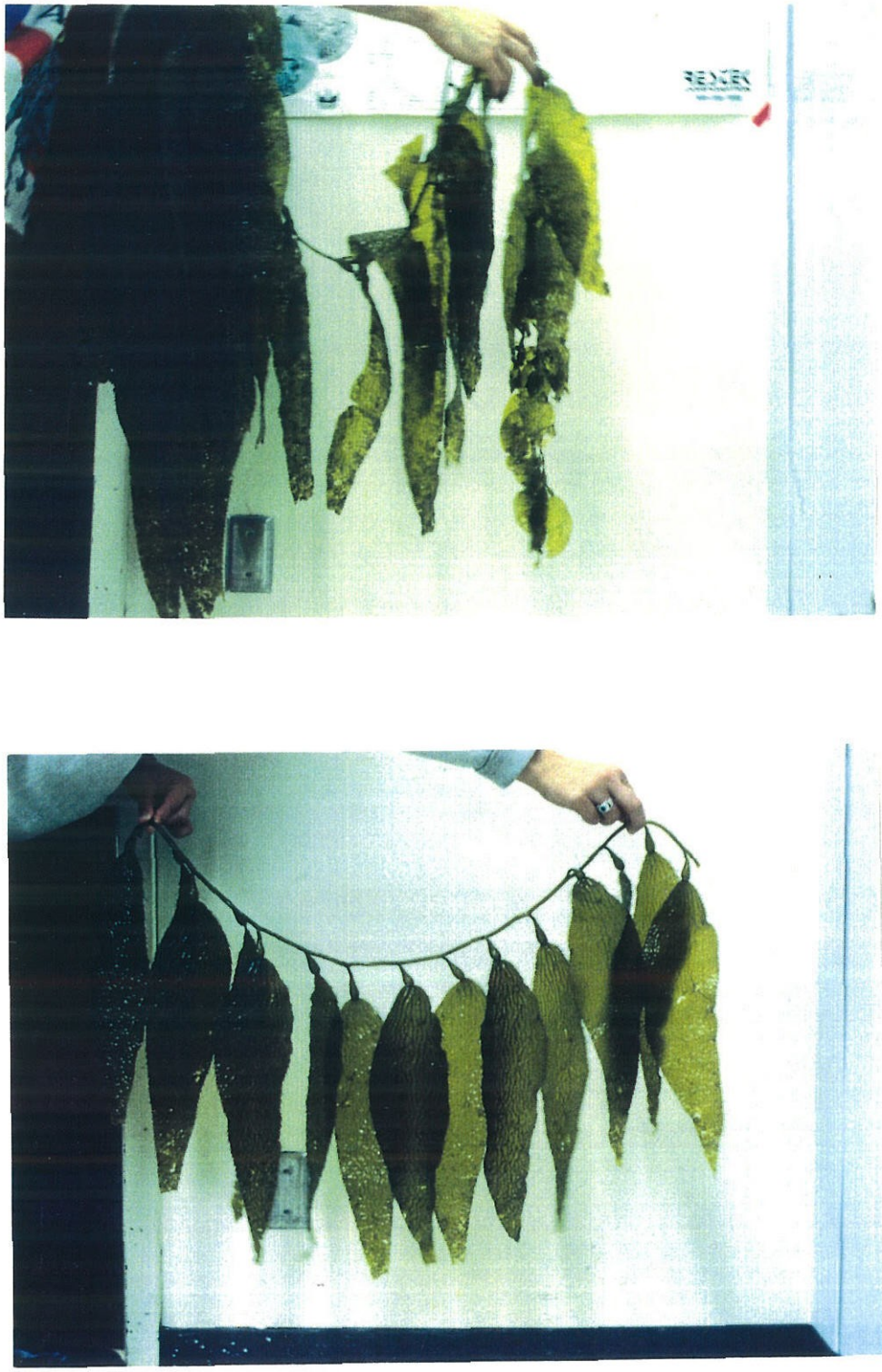

Figure 3.16. Photographs of *M. pyrifera* kelp fronds showing a highly tattered (upper picture) and a more healthy-looking specimen (lower picture).

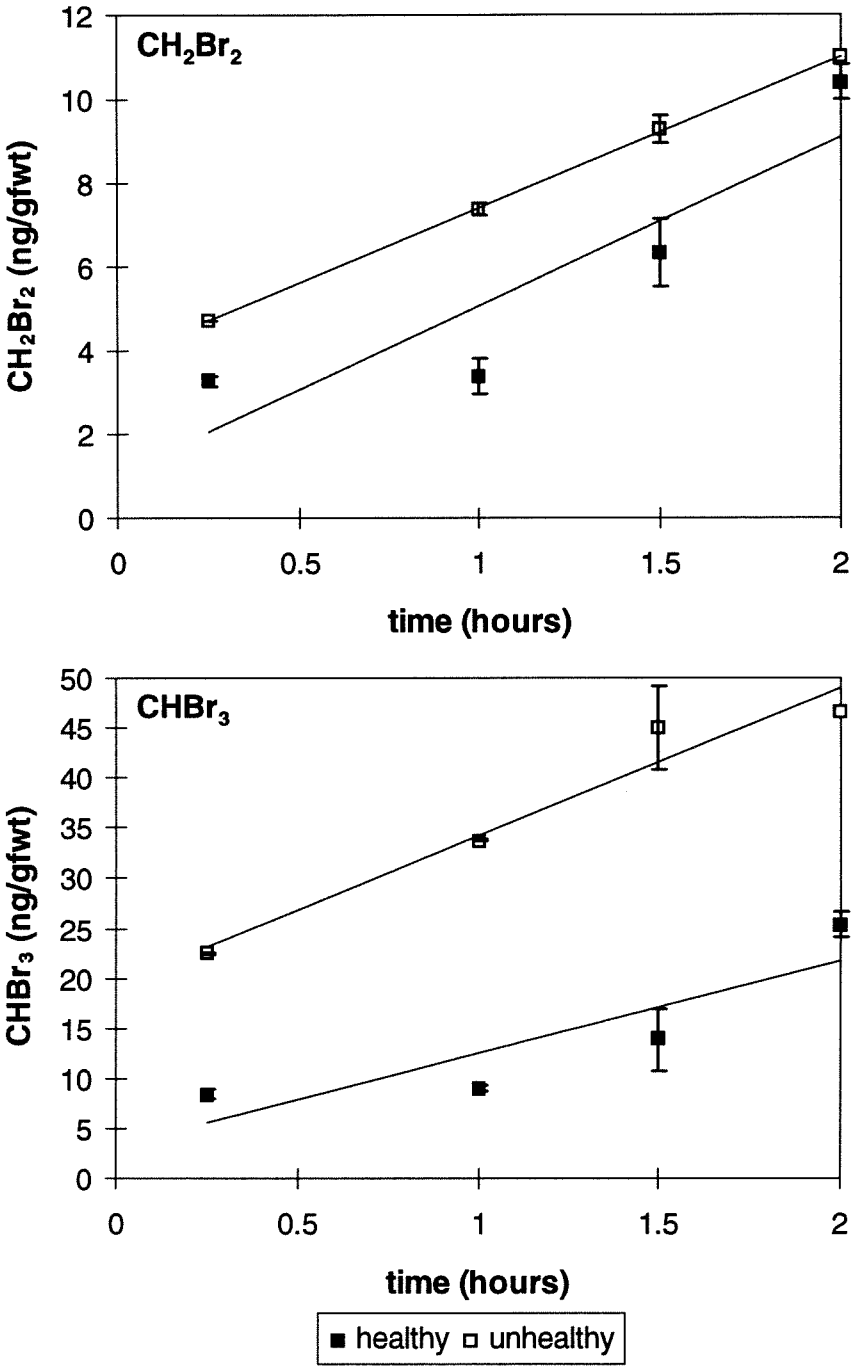

Figure 3.17. *M. pyrifera* laboratory production of CH_2Br_2 and $CHBr_3$ from "healthy" and "unhealthy" looking blades collected 5/25/94 and pictured in Fig. 3.16. Incubations were performed simultaneously under full-spectrum fluorescent light. Data for healthy blades are also shown in Fig. 3.13 for comparison to similar incubations under cool-white light. Error bars are SD two replicate injections of a single sample.

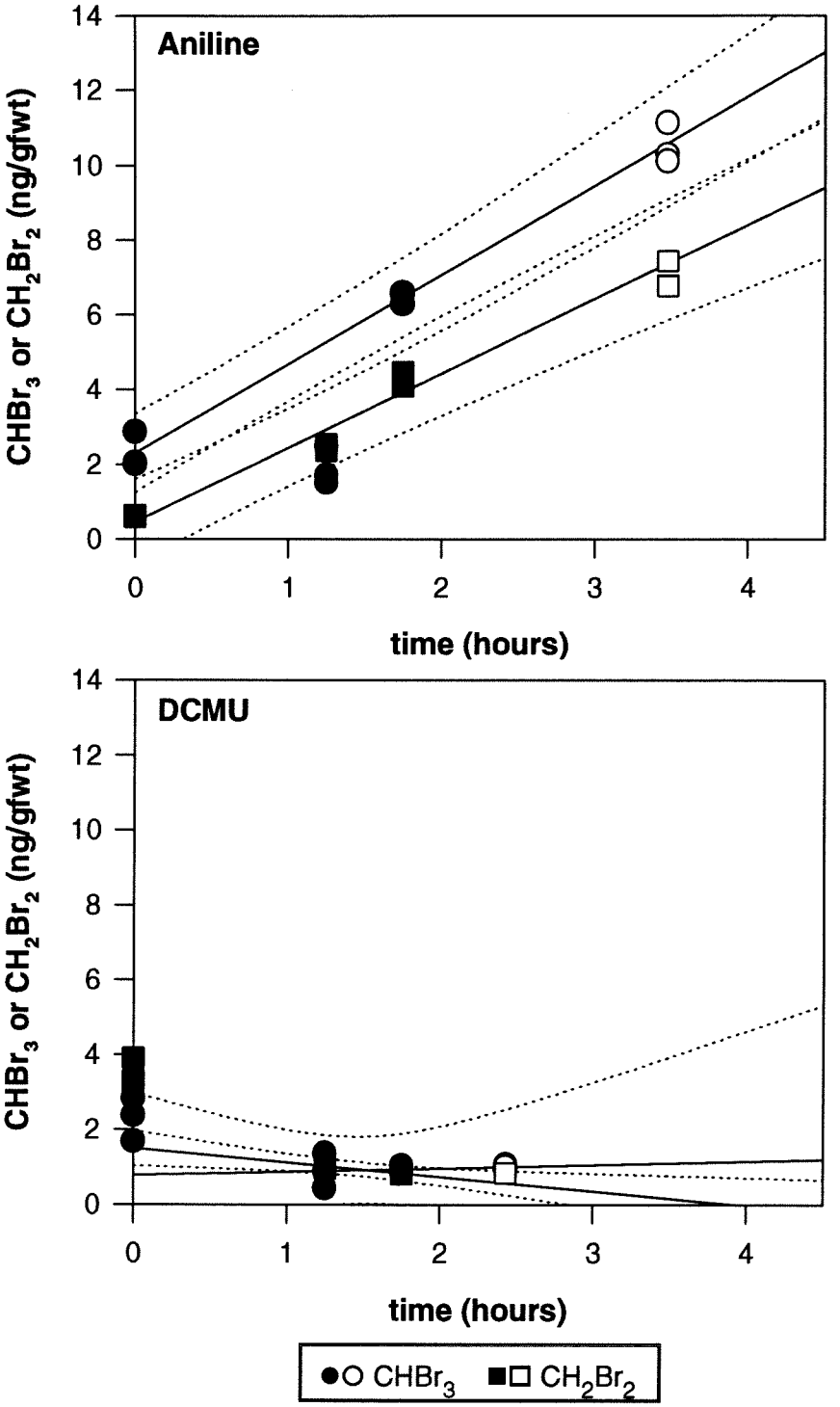

Figure 3.18. *M. pyrifera* laboratory production of CH_2Br_2 and $CHBr_3$ for blades collected 2/15/95 and incubated before (closed symbols) and after (open symbols) addition of 186 nM H_2O_2. Kelp were incubated simultaneously under cool-white fluorescent light with 50 μM aniline (upper graph) or 50 μM DCMU (lower graph) in otherwise identical conditions. The $CHBr_3$ initial DCMU time point was an outlier (determined by Q-test) and not included in the regression (dotted lines).

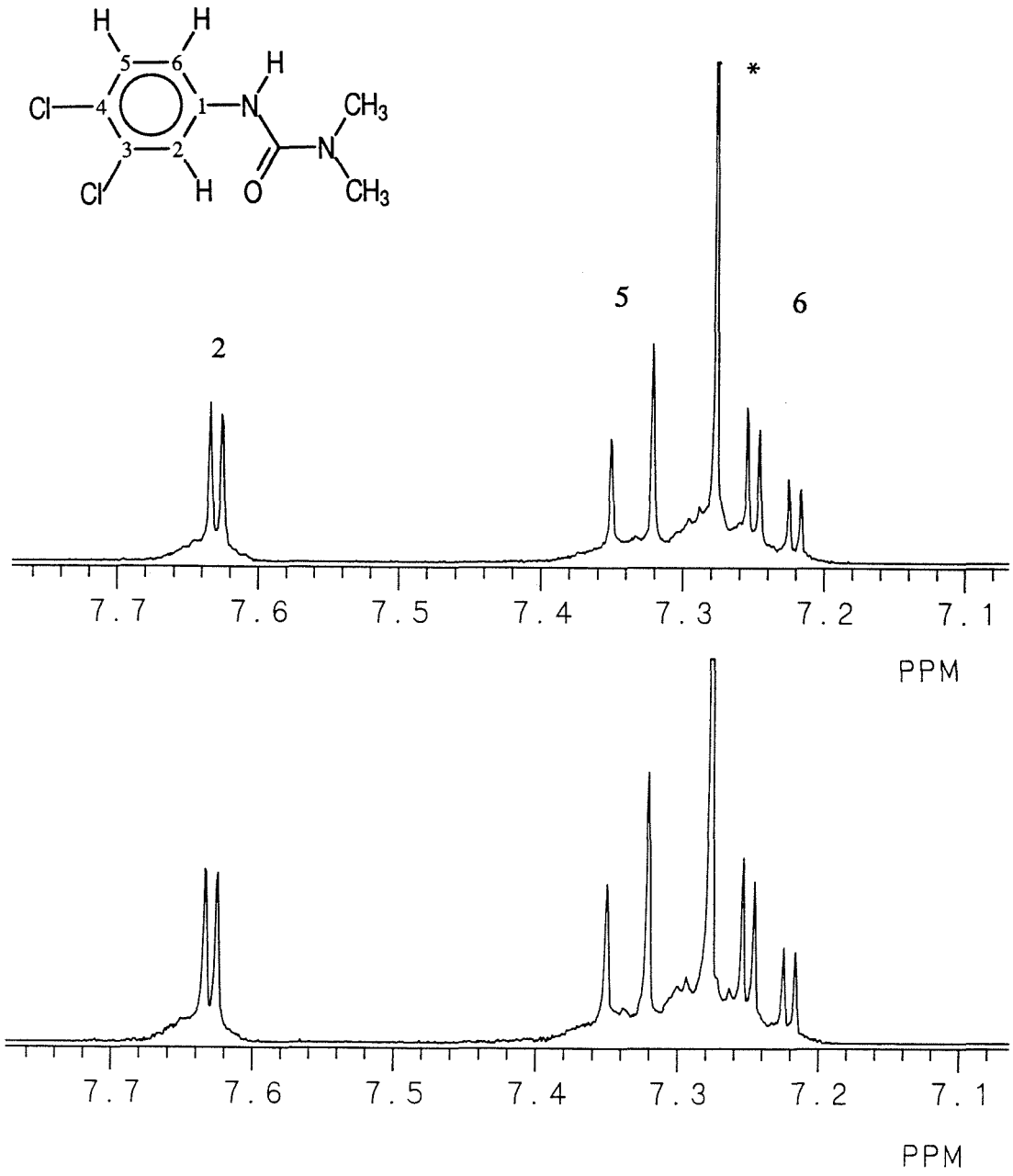

Figure 3.19. Proton NMR spectra of aromatic region of DCMU in $CDCl_3$. Upper spectrum is DCMU (0.17 mM) after 1 hr incubation with horseradish peroxidase (HRP). Lower spectrum is DCMU after 1 hr incubation with equimolar H_2O_2 (0.17 mM) and HRP. Spectra of DCMU dissolved directly into $CDCl_3$ showed identical chemical shifts (not shown). Asterisk denotes $CHCl_3$ resonance. Proton resonances are labeled by adjacent carbon of DCMU (inset), as listed in Table 3.5.

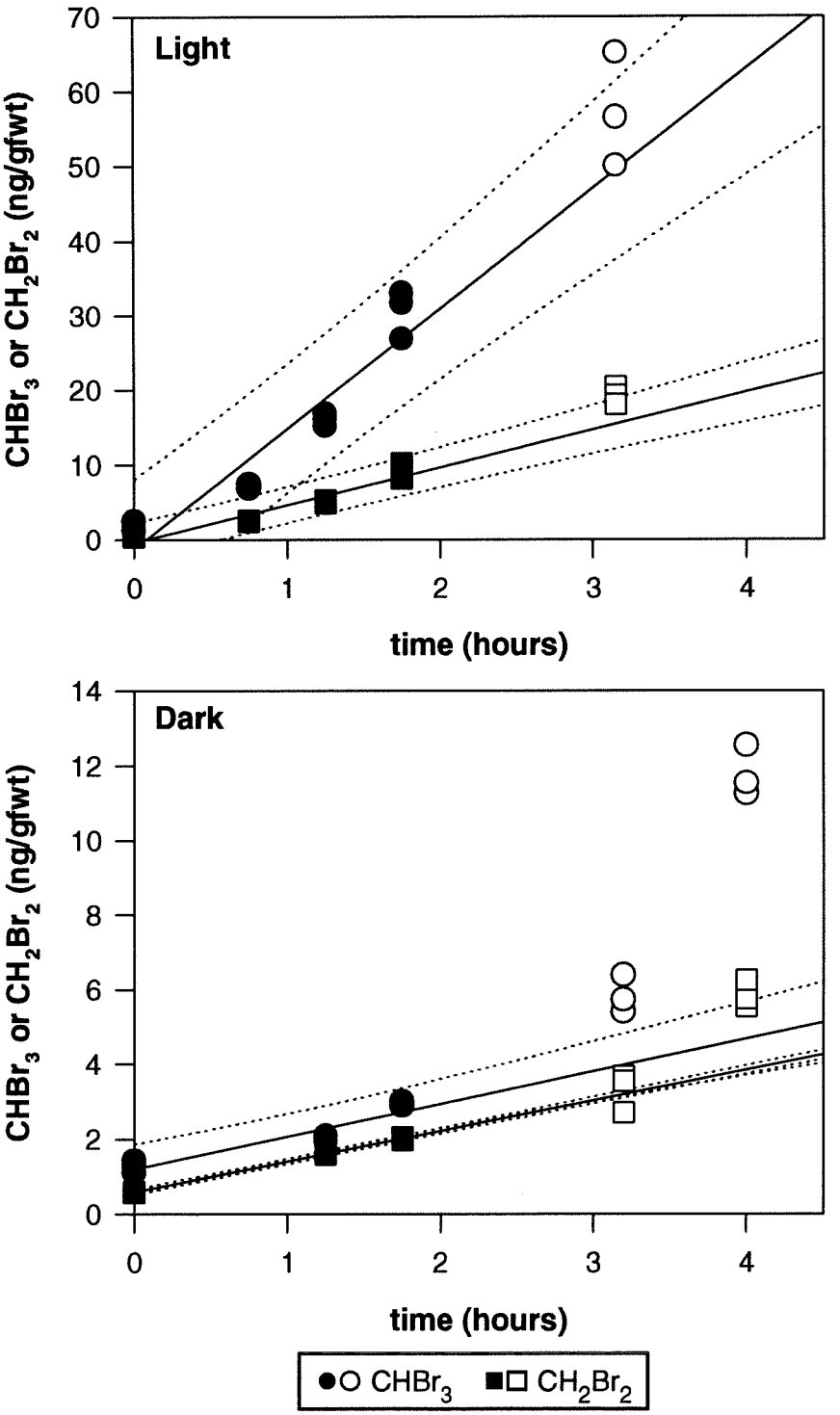

Figure 3.20. *M. pyrifera* laboratory production of CH_2Br_2 and $CHBr_3$ for blades collected 2/15/95 and incubated before (closed symbols) and after (open symbols) addition of 186 nM H_2O_2. Kelp were incubated simultaneously under cool-white fluorescent light (upper graph) or in darkness (lower graph) in otherwise identical conditions. Open symbols outside the 95% confidence limits of the linear regression (dotted lines) indicate enhanced production after peroxide addition.

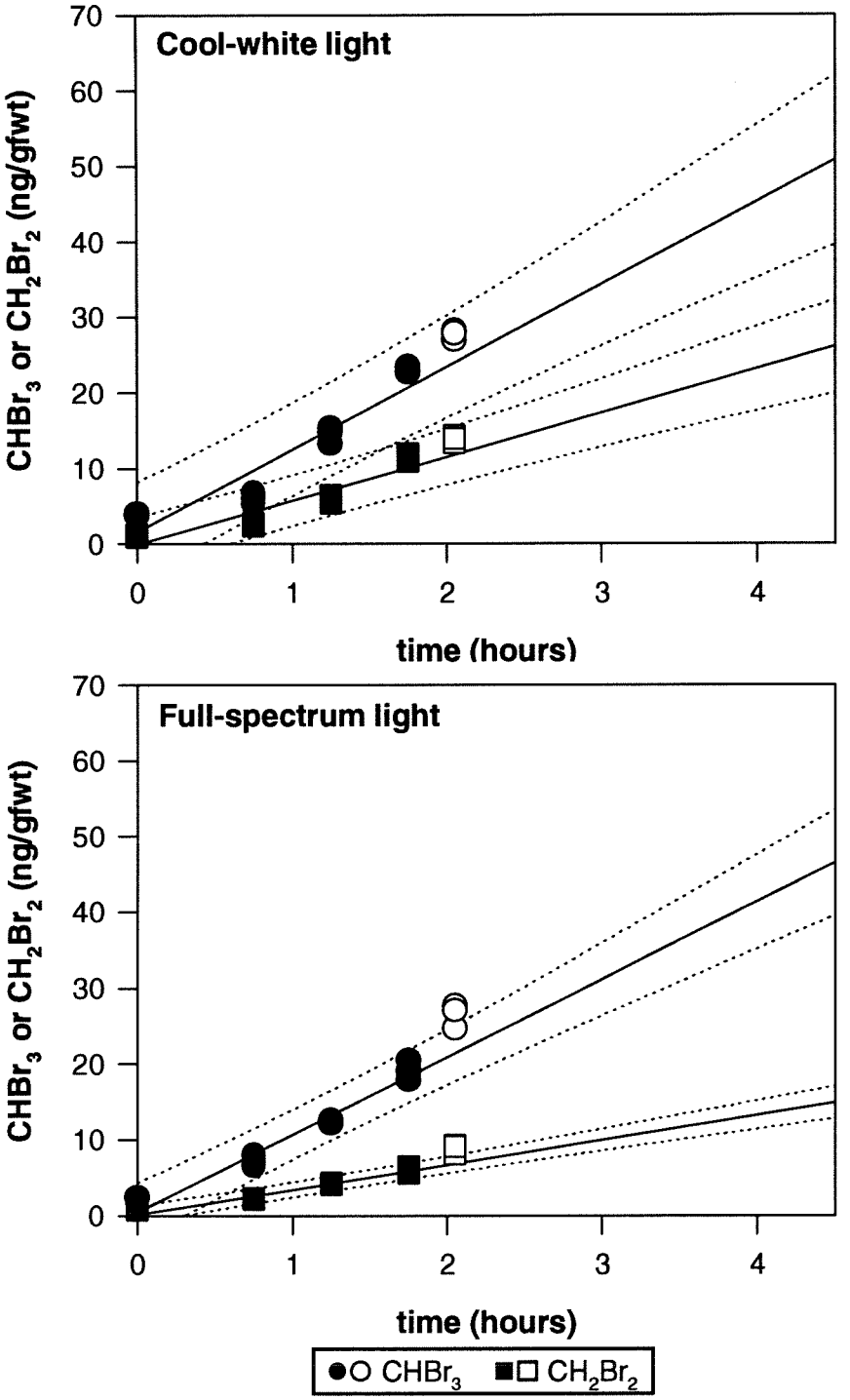

Figure 3.21. *M. pyrifera* laboratory production of CH_2Br_2 and $CHBr_3$ for blades collected 2/15/95 and incubated before (closed symbols) and after (open symbols) addition of 186 nM H_2O_2. Kelp were incubated under cool-white (upper graph) or full-spectrum fluorescent light (lower graph). Open symbols outside the 95% confidence limits of the linear regression (dotted lines) indicate enhanced production after peroxide addition. Data prior to H_2O_2 addition are also presented in Figs. 3.13-3.14.

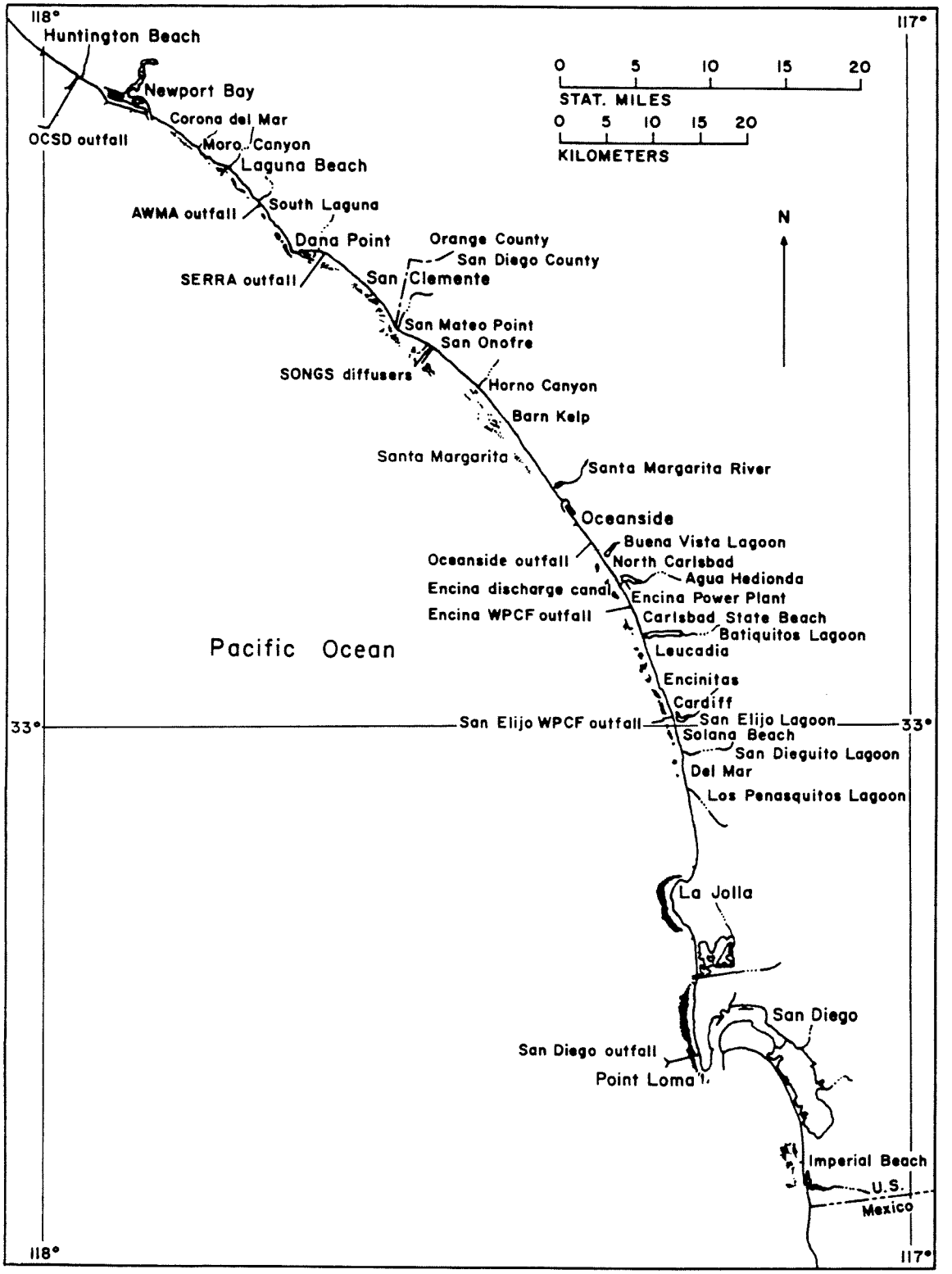

Figure 3.22. Location of *M. pyrifera* kelp beds along the coastline of Orange County and San Diego County, CA (from North *et al.* 1993, used by permission).

References

Amy, G.L., Greenfield, J.H. & Cooper, W.J. (1990). Organic Halide Formation During Water Treatment Under Free Chlorine Versus Chloramination Conditions. In *Water Chlorination Chemistry, Environmental Impact and Health Effects V. 6* (Jolley, R.L., Condie, L.W., Johnson, J.D., *et al.*, Lewis Publishers, Inc., Chelsea, MI, pp. 605-622.

Anbar, A.D., Yung, Y.L., & Chavez, F.P. (in press). Methyl Bromide: Ocean Sources, Ocean Sinks, and Climate Sensitivity. *Glob. Biogeochem. Cycles.*

Arnold, K.E. & Manley, S.L. (1985). Carbon Allocation in *Macrocystis pyrifera* (Phaeophyta): Intrinsic Variability in Photosynthesis and Respiration. *J. Phycol.* **21**, 154-167.

Avron, M. (1981). Photosynthetic Electron Transport and Photophosphorylation. In *The Biochemistry of Plants A Comprehensive Treatise Vol. 8 Photosynthesis* (Stumpf, P.K. and Conn, E.E. eds.), Academic Press, NY, pp. 163-191.

Bean, R.M., Riley, R.G. & Ryan, P.W. (1980). Investigation of Halogenated Components Formed from Chlorination of Marine Water. In *Water Chlorination Environmental Impact and Health Effects V. 2* (Jolley, R.L., Gorchev, H. and Hamilton Jr., D.H. eds.), Ann Arbor Science Publishers, Inc., Ann Arbor, MI, pp. 223-234.

Beissner, R.S., Guilford, W.J., Coates, R.M. & Hager, L.P. (1981). Synthesis of Brominated Heptanones and Bromoform by a Bromoperoxidase of Marine Origin. *Biochemistry* **20**, 3724-3731.

Bidwell, R.G.S. & McLachlan, J. (1985). Carbon Nutrition of Seaweeds: Photosynthesis, Photorespiration and Respiration. *J. Exp. Mar. Biol. Ecol.* **86**, 15-46.

Butler, A., Soedjak, H.S., Polne-Fuller, M., Gibor, A., Boyen, C. & Kloareg, B. (1990). Studies of Vanadium-Bromoperoxidase Using Surface and Cortical Protoplasts of *Macrocystis Pyrifera* (Phaeophyta). *J. Phycol.* **26**, 589-592.

Butler, J.H. (1995). Methyl Bromide Under Scrutiny. *Nature* **376**, 469-470.

Clendenning, K.A. (1971). Photosynthesis and General Development in *Macrocystis*. In *The Biology of Giant Kelp Beds (Macrocystis)* in California (North, W.J. ed.), J. Cramer, Lehre, Germany, pp. 169-190.

Class, T. & Ballschmiter, K. (1988). Chemistry of Organic Traces in Air VIII: Sources and Distribution of Bromo- and Bromochloromethanes in Marine Air and Surfacewater of the Atlantic Ocean. *J. Atmos. Chem.* **6**, 35-46.

Collén, J., Ekdahl, A., Abrahamsson, K. & Pedersén, M. (1994). The Involvement of Hydrogen Peroxide in the Production of Volatile Halogenated Compounds by *Meristiella gelidium*. *Phytochemistry* **36**, 1197-1202.

Cooper, W.J., Villate, J.T., Ott, E.M., Slifker, R.A., Parsons, F.Z. & Graves, G.A. (1983). Formation of Organohalogen Compounds in Chlorinated Secondary Wastewater Effluent. In *Water Chlorination Environmental Impact and Health Effects V. 4 Book 1* (Jolley, R.L. *et al.* eds.), Ann Arbor Science Publishers, Inc., Ann Arbor, MI, pp. 483-497.

Cooper, W.J., Zika, R.G., Petasne, R.G. & Plane, J.M.C. (1988). Photochemical Formation of H_2O_2 in Natural Waters Exposed to Sunlight. *Environ. Sci. Technol.* **22**, 1156-1160.

Copaken, J. (1990). Trihalomethanes: Is Swimming Pool Water Hazardous? In *Water Chlorination Chemistry, Environmental Impact and Health Effects V. 6* (Jolley, R.L., Condie, L.W., Johnson, J.D., *et al.*, Lewis Publishers, Inc., Chelsea, MI, pp. 605-622.

Danks, S.M., Evans, E.H. & Whittaker, P.A. (1983). *Photosynthetic Systems Structure, Function, and Assembly*. John Wiley & Sons, NY.

de Boer, E., Tromp, M.G.M., Plat, H., Krenn, B.E. & Wever, R. (1986a). Vanadium (V) as an essential element for haloperoxidase activity in marine brown algae: purification and characterization of a vanadium (V)-containing bromoperoxidase from *Laminaria saccharina*. *Biochim. Biophys. Acta* **872**, 104-115.

de Boer, E., Van Kooyk, Y., Tromp, M.G.M., Plat, H. & Wever, R. (1986b). Bromoperoxidase from *Ascophyllum Nodosum* - A Novel Class of Enzymes Containing Vanadium as a Prosthetic Group. *Biochim. Biophys. Acta* **869**, 48-53.

De Vooys, C.G.N. (1979). Primary Production in Aquatic Environments. In: *The Global Carbon Cycle* (Bolin, B., Degens, E.T., Kempe, S., and Ketner, P. eds.), John Wiley & Sons, NY, pp. 259-292.

Dubinin, A.V., Zastrizhnaya, O.M. & Gusev, M.V. (1992). Hydrogen Peroxide Production by the Halophilic Cyanobacterium *Microcoleus Chthonoplastes*. *Microbiol.* **61**, 261-266.

Elstner, E.F. (1987). Metabolism of Activated Oxygen Species. In *The Biochemistry of Plants A Comprehensive Treatise, Vol. 11, Biochemistry of Metabolism* (Stumpf, P.K. and Conn, E.E. eds.), Academic Press, NY, pp. 253-315.

Fenical, W. (1981). Natural Halogenated Organics. In: *Marine Organic Chemistry* (Duursma, E.K. and Dawson, R., eds.), Elsevier Scientific, Amsterdam, pp. 375-392.

Finkel, A.J. (1983). Aromatic Nitro and Amino Compounds. In *Hamiliton and Hardy's Industrial Toxicology*, PSF Publishing Co. Inc., Liltleton, pp. 256-261.

Foster, R.J. (1978). Bromine. In *Mineral Yearbook 1976*, United States Department of Interior Bureau of Mines, pp. 229-233.

Frimer, A.A., Forman, A. & Borg, D.C. (1983). H_2O_2-Diffusion Through Liposomes. *Israel J. Chem.* **23**, 442-445.

Gerard, V.A. (1982a). Growth and Utilization of Internal Nitrogen Reserves by the Giant Kelp, Macrocystis Pyrifera, in a Low Nitrogen Environment. *Mar. Biol.* **66**, 27-35.

Gerard, V.A. (1982b). *In situ* Rates of Nitrate Uptake by Giant Kelp, *Macrocystis Pyrifera* (L.) C. Agardh: Tissue Differences, Environmental Effects, and Prediction of Nitrogen-Limited Growth. *J. Exp. Mar. Biol. Ecol.* **62**, 211-224.

Gerard, V.A. (1984). Physiological Effects of El Niño On Giant Kelp in Southern California. *Mar. Biol. Lett.* **5**, 317-322.

Gossett, J.M. (1987). Measurement of Henry's Law Constants for C_1 and C_2 Chlorinated Hydrocarbons. *Environ. Sci. Technol.* **21**, 202-208.

Gschwend, P.M., MacFarlane, J.K. & Newman, K.A. (1985). Volatile Halogenated Organic Compounds Released to Seawater from Temperate Marine Macroalgae. *Science* **227**, 1033-1035.

Gschwend, P.M. & MacFarlane, J.K. (1986). Polybromomethanes: A Year-Round Study of Their Release to Seawater from *Ascophyllum nodosum* and *Fucus vesiculosis*. In *ACS Symposium Series **305**,* 314-322.

Harper, D.B. (1993). Biogenesis and Metabolic Role of Halomethanes in Fungi and Plants. *Metal Ions in Biological Systems* **29**, 345-388.

Helz, G.R. & Hsu, R.Y. (1978). Volatile Chloro- and Bromocarbons in Coastal Waters. *Limnol. Oceanogr.* **23**, 858-869.

Ingmanson, D.E. & Wallace, W.J. (1985). *Oceanography: An Introduction.* Wadsworth Pub. Co., Belmont, CA, pp. 180-182.

Itoh, N. & Shinya, M. (1994). Seasonal Evolution of Bromomethanes from Coralline Algae (Corallinaceae) and its Effect on Atmospheric Ozone. *Mar. Chem.* **45**, 95-103.

Jackson, G.A. (1977). Nutrients and Production of Giant Kelp, *Macrocystis Pyrifera*, off Southern California. *Limnol. Oceanogr.* **22**, 979-995.

Kennedy, J.H. (1984). *Analytical Chemistry*. Harcourt Brace Jovanovich, San Diego, pp. 17.

Khalil, M.A.K., Rasmussen, R.A. & Gunawardena, R. (1993). Atmospheric Methyl Bromide: Trends and Global Mass Balance. *J. Geophys. Res.* **98**, 2887-2896.

Klick, S. (1992). Seasonal Variations of Biogenic and Anthropogenic Halocarbons in Seawater from a Coastal Site. *Limnol. Oceanogr.* **37**, 1579-1585.

Klick, S. (1993). The Release of Volatile Halocarbons to Seawater by Untreated and Heavy Metal Exposed Samples of the Brown Seaweed *Fucus Vesiculosus*. *Mar. Chem.* **42**, 211-221.

Kok, G.L., Thompson, K. & Lazrus, A. (1986). Derivatization Technique for the Determination of Peroxides in Precipitation. *Anal. Chem.* **58**, 1192-1194.

Krenn, B.E., Plat, H. & Wever, R. (1987). The Bromoperoxidase from the Red Alga *Ceramium Rubrum* Also Contains Vanadium as a Prosthetic Group. *Biochim. Biophys. Acta* **912**, 287-291.

Krenn, B.E., Izumi, Y., Yamada, H. & Wever, R. (1989a). A Comparison of Different (Vanadium) Bromoperoxidases; the Bromoperoxidase from *Corallina Pilulifera* is Also a Vanadium Enzyme. *Biochim. Biophys. Acta* **998**, 63-68.

Krenn, B.E., Tromp, M.G.M. & Wever, R. (1989b). The Brown Alga Ascophyllum Nodosum Contains Two Different *Vanadium Bromoperoxidases*. *J. Biol. Chem.* **264**, 19287-19292.

Kristiansen, N.K., Froshaug, M., Aune, K.T. & Becher, G. (1994). Identification of Halogenated Compounds in Chlorinated Seawater and Drinking Water Produced Offshore Using N-Pentane Extraction and Open-Loop Stripping Technique. *Environ. Sci. Technol.* **28**, 1669-1673.

Krysell, M. (1991). Bromoform in the Nansen Basin in the Arctic Ocean. *Mar. Chem.* **33**, 187-197.

Lacis, A.A., Wuebbles, D.J. & Logan, J.A. (1990). Radiative Forcing of Climate by Changes in the Vertical Distribution of Ozone. *J. Geophys. Res.* **95**, 9971-9981.

Li, S.-M., Yokouchi, Y., Barrie, L.A., Muthuramu, K., Shepson, P.B., Bottenheim, J.W., Sturges, W.T. & Landsberger, S. (1994). Organic and Inorganic Bromine Compounds and Their Composition in the Arctic Troposphere During Polar Sunrise. *J. Geophys. Res.* **99**, 25415-25428.

Lobert, J.M., Butler, J.H., Montzka, S.A., Geller, L.S., Myers, R.C. & Elkins, J.W. (1995). A Net Sink For Atmospheric CH_3Br in the East Pacific Ocean. *Science* **267**, 1002-1005.

Lyday, P.A. (1992). Bromine. In *Mineral Yearbook 1992*, United States Department of the Interior Bureau of Mines, pp. 259-269.

Manley, S.L., Goodwin, K. & North, W.J. (1992). Laboratory Production of Bromoform, Methylene Bromide and Methyl Iodide by Macroalgae and Distribution in Nearshore Southern California Waters. *Limnol. Oceanogr.* **37**, 1652-1659.

Manley, S.L. & Dastoor, M.N. (1987). Methyl Halide (CH_3X) Production from the Giant Kelp, *Macrocystis* and Estimates of Global CH_3X Production by Kelp. *Limnol. Oceanogr.* **32**, 709-715.

Manley, S.L., and M.N. Dastoor. (1988). Methyl Iodide (CH_3I) Production by Kelp and Associated Microbes. *Mar. Biol.* **98,** 447-482.

Manley, S.L. (1985). Phosphate Uptake by Blades of *Macrocystis Pyrifera* (Phaeophyta) *Bot. Mar.* **18**, 237-244.

Manö, S. & Andreae, M.O. (1994). Emission of Methyl Bromide from Biomass Burning. *Science* **263**, 1255-1257.

Manthey, J.A. & Hager, L.A. (1981). Purification and Properties of Bromoperoxidase from *Penicillus Capitatus*. *J. Biol. Chem.* **256**, 11232-11238.

McConnell, O. & Fenical, W. (1977). Halogen Chemistry of the Red Alga *Asparagopsis*. *Phytochemistry* **16**, 367-374.

McCulloch, A. (1992). Global Production and Emissions of Bromochlorodifluoromethane and Bromotrifluoromethane (Halons 1211 and 1301). *Atmos. Environ.* **26A**, 1325-1329.

McFarland, W.N. and Prescott, J. (1959). Standing Crop, Chlorophyll Content, and *in Situ* Metabolism of a Giant Kelp Community in Southern California. *Inst. Mar. Sci., Univ. Texas* **6**, 109-132.

Meeks, J.C. (1974). Chlorophylls. In *Algal Physiology and Biochemistry* (Stewart, W.P.D. ed.), University of California Press, Berkeley, pp. 161-175.

Mellouki, A., Talukdar, R.K., Schmoltner, A., Gierczak, T., Mills, M.J., Solomon, S. & Ravishankara, A.R. (1994). Atmospheric Lifetimes and Ozone Depletion Potentials of Methyl Bromide (CH_3Br) and Dibromomethane (CH_2Br_2). *Geophys. Res. Lett.* **19**, 2059-2062.

Moffett, J.W. & Zafiriou, O.C. (1990). An Investigation of Hydrogen Peroxide Chemistry in Surface Waters of Vineyard Sound with $H_2{}^{18}O_2$ and $^{18}O_2$. *Limnol. Oceanogr.* **35**, 1221-1229.

Moffett, J.W. & Zafiriou, O.C. (1993). The Photochemical Decomposition of Hydrogen Peroxide in Surface Waters of the Eastern Caribbean and Orinoco River. *J. Geophys. Res.* **98**, 2307-2313.

Moore, R.E. (1977). Volatile Compounds from Marine Algae. *Acc. Chem. Res.* **10**, 40-46.

Morris, J.C. (1985). Reaction Dynamics in Water Chlorination. In *Water Chlorination Chemistry, Environmental Impact and Health Effects V. 5* (Jolley, R.L., Bull, R.J., Davis, W.P., Katz, S., Roberts Jr., M.H. and Jacobs, V.A. eds.), Lewis Pub., Inc., Chelsea, MI, pp. 701-712.

Neideman, S.L. & Geigert, J. (1986). *Biohalogenation: Principles, Basic Roles and Applications*. Ellis Horwood Ltd., Chichester, pp. 46.

Nicholson, B.C., Maguire, B.P. & Bursill, D. B.. (1984). Henry's Law Constants for the Trihalomethanes: Effects of Water Composition and Temperature. *Environ. Sci. Technol.*, **18**, 518-521.

Nightingale, P.D., Malin, G. & Liss, P.S. (1995). Production of Chloroform and Other Low Molecular Weight Halocarbons by Some Species of Macroalgae. *Limnol. Oceanogr.*, **40**, 680-689.

North, W.J. (1971). *The Biology of Giant Kelp Beds (Macrocystis) in California.* Beihefte Zur Nova Hedwigia 32. J. Cramer, Lehre, Germany.

North, W.J., Jackson, G.A. & Manley, S.A. (1986). *Macrocystis* and Its Environment, Knowns and Unknowns. *Aquat. Bot.*, **26**, 9-26.

North, W.J., James, D.E. & Jones, L.G. (1993). History of Kelp Beds (*Macrocystis*) in Orange and San Diego Counties, California. *Hydrobiologia* **260/261**, 277-283.

North, W.J. (1994). Review of *Macrocystis* Biology. In: *Biology of Economic Algae* (Akatsuka, I., ed.), SPB Academic Publishing, Hague, Netherlands, pp. 447-527.

Palenik, B., Zafiriou, O.C. & Morel, F.M.M. (1987). Hydrogen Peroxide Production by a Marine Phytoplankter. *Limnol. Oceanogr.* **32**, 1365-1369.

Palenik, B. & Morel, F.M.M. (1988). Dark Production of H_2O_2 in the Sargasso Sea. *Limnol. Oceanogr.* **33**, 1606-1611.

Patterson, C.O.P. & Myers, J. (1973). Photosynthetic Production of Hydrogen Peroxide by *Anacystis nidulans*. *Plant Physiol.* **51**, 104-109.

Pedersén, M. (1976). A Brominating and Hydroxylating Peroxidase form the Red Alga *Cystoclonium Purpureum*. *Physiol. Plant* **37**, 6-11.

Penkett, S.A., Jones, B.M.R., Rycroft, M.J. & Simmons, D.A. (1985). An Interhemispheric Comparison of the Concentrations of Bromine Compounds in the Atmosphere. *Nature* **318**, 550-553.

Plat, H., Krenn, B.E. & Wever, R. (1987). The Bromoperoxidase From the Lichen *Xanthoria Paretina* is a Novel Vanadium Enzyme. *The Biochemical Journal* **248**, 277-279.

Ramanathan, V., Cicerone, R.J., Singh, H.B. & Kiehl, J.T. (1985). Trace Gas Trends and Their Potential Role in Climate Change. *J. Geophys. Res.* **90**, 5547-5566.

Sansone, F.J. & Kearney, T.J. (1985). Chlorination Kinetics of Surface and Deep Tropical Seawater. In *Water Chlorination Chemistry, Environmental Impact and Health Effects V. 5* (Jolley, R.L., Bull, R.J., Davis, W.P., Katz, S., Roberts Jr., M.H. and Jacobs, V.A. eds.), Lewis Publishers, Inc. Chelsea, MI, pp. 737-754.

Sax, N.I. (1975). *Dangerous Properties of Industrial Materials*. Van Norstrand Reinhold Co., NY.

Schall, C., Laturnus, F. & Heumann, K.G. (1994). Biogenic Volatile Organoiodine and Organobromine Compounds Released from Polar Macroalgae. *Chemosphere* **28**, 1315-1324.

Schauffler, S.M., Heidt, L.E., Pollock, W.H., Gilpin, T.M., Vedder, J.F., Solomon, S., Lueb, R.A. & Atlas, E.L. (1993). Measurements of Halogenated Organic Compounds Near the Tropical Tropopause. *Geophys. Res. Lett.* **20**, 2567-2570.

Shaw, T.I. (1962). Halogens. In: *Physiology and Biochemistry of Algae* (Lewin, R.A., ed.), Academic Press, NY, pp. 247-253.

Sheridan, P.J., Schnell, R.C., Zoller, W.H., Carlson, N.D., Rasmussen, R.A., Harris, J.M. & Severing, H. (1993). Composition of Br-Containing Aerosols and Gases Related

to Boundary Layer Ozone Destruction in the Arctic. *Atmos. Environ.* **27A**, 2839-2849.

Singh, H.B. & Kanakidou, M. (1993). An Investigation of the Atmospheric Sources and Sinks of Methyl Bromide. *Geophys. Res. Lett.* **20**, 133-136.

Singh, H.B., Salas, L.J. & R.E. Stiles. (1983). Methyl Halides in and Over the Eastern Pacific (40°N-32°S). *J. Geophys. Res.* **88**, 3684-3690.

Soedjak, H.S. & Butler, A. (1990). Characterization of Vanadium Bromoperoxidase from *Macrocystis* and *Fucus*: Reactivity of Vanadium Bromoperoxidase Toward Acyl and Alkyl Peroxides and Bromination of Amines. *Biochemistry* **29**, 7974-7981.

State of California Department of Pesticide Regulation (1995). Annual Pesticide Use Report by County, January to December 1993 (Draft).

Steward, F.C., Craven, C.G., Weerasinghe, S.P.R. & Bidwell, R.G.S. (1971). Effects of Prior Environmental Conditions on the Subsequent Uptake and Release of Carbon Dioxide in the Light. *Can. J. Bot.* **49**, 1999-2007.

Sturges, W.T., Cota, G.F. & Buckley, P.T. (1992). Bromoform Emission from Arctic Ice Algae. *Nature* **358**, 660-662.

Theiler, R., Cook, J.C., Hager, L.P. & Siuda, J.F. (1978). Halohydrocarbon Synthesis by Bromoperoxidase. *Science* **202**, 1094-1096.

Tokarczyk, R. & Moore, R.M. (1994). Production of Volatile Organohalogens by Phytoplankton Cultures. *Geophys. Res. Lett.* **21**, 285-288.

Tolbert, N.E. (1974). Photorespiration. In *Algal Physiology and Biochemistry* (Stewart, W.P.D. ed.), University of California Press, Berkeley, pp. 474-504.

Tolbert, N.E. (1980). Photorespiration. In *The Biochemistry of Plants A Comprehensive Treatise* (Stumpf, P.K. and Conn, E.E. eds.), Academic Press, NY, pp. 488-521.

Tse, G., Orbey, H. & Sandler, S.I. (1992). Infinite Dilution Activity Coefficients and Henry's Law Coefficients of Some Priority Water Pollutants Determined by a Relative Gas Chromatographic Method. *Environ. Sci. Technol.* **26**, 2017-2022.

U.N. Environment Programme. (1992). Montreal Protocol Assessment Supplement. Methyl Bromide: Its Atmospheric Science, Technology and Economics. Nairobi, Kenya.

Vitler, H. (1983a). Peroxidases from Phaeophyceae III: Catalysis of Halogenation by Peroxidases from *Ascophyllum Nodosum* (L.) Le Jol. *Bot. Mar.* **26**, 429-435.

Vitler, H. (1983b). Peroxidases from Phaeophyceae IV. *Bot. Mar.* **26**, 451-455.

Wayne, R.P. (1985). *Chemistry of Atmospheres*. Clarendon Press, Oxford.

Wever, R., Tromp, M.G.M., Krenn, B.E., Marjani, A. & Tol, M.V. (1991). Brominating Activity of the Seaweed *Ascophyllum nodosum*: Impact on the Biosphere. *Environ. Sci. Technol.* **25**, 446-449.

Wever, R., Plat, H. & de Boer, E. (1993). The Chloroperoxidase from the Fungus *Curvularia Inaequalis* - A Novel Vanadium Enzyme. *Biochim. Biophys. Acta* **1161**, 249-256.

White, R.H. (1982). Biosynthesis of Methyl Chloride in the Fungus *Phellinus Pomaceus*. *Arch. Microbiol.* **132**, 100-102.

Woollacott, R.M. & North, W.J. (1971). Bryozoans of California and Northern Mexico Kelp Beds. In *The Biology of Giant Kelp Beds (Macrocystis)* in California (North, W.J. ed.), J. Cramer, Lehre, Germany, pp. 455-478.

Wuosmaa, A. & Hager, L.P. (1990). Methyl Chloride Transferase: A Carbocation Route for Biosynthesis of Halometabolites. *Science* **249**, 160-162.

Yung, Y.L., Pinto, J.P., Watson, R.T. & Sander, S.P. (1980). Atmospheric Bromine and Ozone Perturbations in the Lower Stratosphere. *J. Atmos. Sci.* **37**, 339-353.

Zepp, R.G., Skurlatov, Y.I. & Pierce, J.T. (1986). Algal-Induced Decay and Formation of Hydrogen Peroxide in Water: Its Possible Role in Oxidation of Anilines by Algae. In *ACS Symposium Series* **327**, 215-224.

Zimmerman, R.C. & Kremer, J.N. (1986). *In situ* Growth and Chemical Composition of the Giant Kelp *Macrocystis Pyrifera*: Response to Temporal Changes in Ambient Nutrient Availability. *Mar. Ecol. Prog. Ser.* **27**, 277-285.

Chapter Four

Marine Microbial Degradation of Bromoform and Dibromomethane

Introduction

Oceanic halomethanes are an important source of reactive halogens to the atmosphere. Bromoform ($CHBr_3$) and dibromomethane (CH_2Br_2) are two volatile brominated methanes naturally produced by marine macroalgae (Chapters 2 and 3) and phytoplankton (Sturges *et al.* 1992). Bromine atoms from $CHBr_3$ and CH_2Br_2 are released primarily in the troposphere (surface region to 10-15 km in height) where they can react catalytically to destroy ozone. Destruction of tropospheric ozone in the Arctic spring appears mediated in part by $CHBr_3$ emissions (Sheridan *et al.* 1993), and ozone destruction may affect climate in a complex manner (Ramanathan *et al.* 1985). Attention has thus focused on the roles of $CHBr_3$ and related compounds in the bromine biogeochemical cycle.

The potential of a particular halocarbon to destroy ozone depends in part on its atmospheric lifetime and supply to the atmosphere. Longer-lived halocarbons are more likely to survive transport into the stratosphere where they can participate in reactions that deplete stratospheric ozone. Estimates of atmospheric lifetime (or residence time) are primarily based on destruction rates by photochemical processes and hydroxyl radical determined from laboratory experiments and model results. Such estimates generally do not include biological destruction mechanisms. Microbial degradation of volatile halogenated compounds, however, has been observed in a number of bacterial systems

(Bouwer *et al.* 1981, Oremland *et al.* 1994ab). Microbial systems might be significant sinks that need to be included in calculations of halocarbon atmospheric lifetimes.

Microorganisms are key players in most biogeochemical cycles, particularly with compounds of natural origin. Microbial activities may thus affect the supply of volatile organic compounds to the atmosphere. For example, terrestrial microbial degradation could consume brominated methanes from the atmospheric reservoir. Oceanic microbial sinks, if they exist, could consume brominated methanes at a production source and thereby reduce the supply of halogenated organics available to the atmosphere. It is thus important to identify and quantify microbial sinks to accurately evaluate the impact of brominated methane emissions on ozone concentrations. We investigated microbial degradation of $CHBr_3$ and CH_2Br_2 in a marine environment and considered the environmental importance of such degradation processes.

A number of microorganisms have been shown to degrade halomethanes. Microorganisms that utilize single-carbon organic compounds for growth (methylotrophs) appear particularly successful at halomethane dehalogenation. The methanotroph *Methylosinus trichosporium* OB3b, for example, degraded the brominated methanes CH_3Br, CH_2Br_2, and $CHBr_3$ (Bartnicki and Castro 1994). The order of reactivity was $CH_3Br > CH_2Br_2 \approx CHBr_3$. The methane monooxygenase enzyme of methanotrophic bacteria (methylotrophs that utilize methane as the sole source of carbon and energy) degrades a variety of halogenated compounds in a cometabolic reaction. Cometabolic transformations fortuitously arise from enzymes with broad substrate specificity (Stirling and Dalton 1979). Halomethane cometabolism does not directly benefit the organism because the halomethane is transformed into a compound that cannot be further utilized.

Halomethane transformation may result, however, in compounds that can be further utilized by the microorganism. Such dehalogenations enable microbial growth. For example, a *Hyphomicrobium* strain was able to use methyl chloride (CH_3Cl) as a growth substrate (Hartmans *et al.* 1986). Dichloromethane (CH_2Cl_2) was utilized as the sole carbon and energy source by a consortia of anaerobic bacteria (Braus-Stromeyer *et al.* 1993). Some facultative methylotrophs of the genera *Pseudomonas* (Brunner *et al.* 1980, LaPat-Polasko *et al.* 1984), *Hyphomicrobium* (Stucki *et al.* 1981), and *Methylobacterium* (Scholtz *et al.* 1988) are able to utilize CH_2Cl_2 for carbon and energy under aerobic conditions. *Pseudomonas* sp. strain LP was reported to simultaneously utilize CH_2Cl_2 and acetate (LaPat-Polasko *et al.* 1984).

The dichloromethane dehalogenase enzyme mediated CH_2Cl_2 dehalogenation in the above examples. The enzyme is strongly induced in response to CH_2Cl_2 and requires reduced glutathione (GSH) as a cofactor. Dehalogenation is thought to proceed according to the following stoichiometry (Leisinger and Bader 1993):

$$CH_2X_2 + H_2O \longrightarrow HCOH + 2HX$$

The reaction produces formaldehyde (HCOH), a central metabolite for methylotrophic bacteria. The bacteria can thus grow with CH_2Cl_2 as their only carbon and energy source. Purified dichloromethane dehalogenase has a narrow substrate range, using dihalomethanes only (CH_2Cl_2, CH_2Br_2, CH_2I_2, CH_2BrCl) (Leisinger *et al.* 1993). The apparent Michaelis constant, K_m, is 13 μM CH_2Br_2 for purified dichloromethane dehalogenase from *Hyphomicrobium* sp. strain DM2 (Kohler-Staub and Leisinger 1985). Cell extracts and whole cells of strain DM2 dehalogenated CH_2Br_2 (Stucki *et al.* 1981), but neither DM2 nor *Methylobacterium* sp. strain DM4 grew on CH_2Br_2 (Scholtz *et al.*

1988). Strain DM11, later renamed *Methylophilus leisingerii* (Doronina *et al.* 1994), was reported to grow on CH_2Br_2 (Scholtz *et al.* 1988). This facultative methylotroph was isolated from CH_2Cl_2-contaminated groundwater, grows significantly faster on CH_2Cl_2 than other facultative methylotrophs, and has a separate "group B" type of CH_2Cl_2 dehalogenase (Leisinger *et al.* 1993). The ability to dehalogenate CH_2Cl_2 does not appear to be an inherent property of any specific group of methylotrophs and probably arises in natural populations exposed to this compound over extended periods (Stucki *et al.* 1981).

Pursuit of dehalogenating bacteria has often focused on polluted sites. Marine and estuarine sites may also harbor microbes with dehalogenating ability because the organisms evolved in a halide-rich environment. Seawater halide concentrations are $19x10^3$ mg/L Cl (0.55 M), 67 mg/L Br (0.84 mM), and 0.06 mg/L I (0.34 μM as IO_3^-) (North 1994) compared to <10 mg/L Cl commonly found in freshwater (van der Leeden *et al.* 1990, p.423). Marine microbes, in addition, exist where organic halogens are produced naturally; indeed, marine life constitutes the largest source of natural halogenated organics (Gribble 1992). Selected species of marine bacteria, cyanobacteria, algae, sponges, mollusks, coelenterates, and worms have been found to produce halogenated compounds containing from 1 to 30 carbons. Bromine is the most commonly found halogen in these molecules (Fenical 1981).

Little is known about the ability of bacteria to degrade $CHBr_3$ and CH_2Br_2 in the environment. Natural algal sources may provide selective pressure for microbes to develop enzyme systems capable of $CHBr_3$ and CH_2Br_2 degradation. Kelp beds are naturally enriched with $CHBr_3$ and CH_2Br_2 (Manley *et al.* 1992; Chapter 2); therefore, microbial degradation may occur there. Significant microbial degradation of brominated

methanes in the water column could alter estimates of the amounts reaching the atmosphere from macroalgal production. Global brominated methane production by macroalgae is usually estimated by extrapolating production rates per mass of algae to the global mass of algae (10^{12} g fresh weight, De Vooys 1979; see Chapters 2 and 3). Global brominated methane production by phytoplankton is usually estimated by extrapolating production rates per liter seawater (or mass chlorophyll) to the area of phytoplankton coverage. Global estimates normally assume that all of a compound produced eventually enters the atmosphere because chemical water column sinks are relatively slow (see Chapter 1). Microbial water column sinks apparently have not been investigated. The purpose of this investigation was to determine the existence, character, and extent of $CHBr_3$ and CH_2Br_2 microbial degradation at a site of brominated methane production, a *Macrocystis pyrifera* kelp bed.

Some researchers have investigated kelp-associated microbial communities although they mostly focused on microbial roles in the detrital food chain (Mazure and Field 1980; Lucas *et al.* 1981). A diverse epiphytic community was found on *Ascophyllum nodosum* kelp blades including bacteria, diatoms, and cyanobacteria (Cundell *et al.* 1977). Scotten (1971) performed a 22 month microbiological survey of *M. pyrifera* kelp beds and found bacteria to represent a large majority of the epiphytic community living on *M. pyrifera* blades. The same types of bacteria found on blade surfaces were also found in the surrounding kelp-bed waters. Epiphytic bacteria were typically Gram negative rods with a few cocci, spirilla, and a "very few" Gram positive rods. Many motile bacteria were observed.

Scotten observed mostly aerobic or microaerophilic bacteria, but a few facultative aerobes and anaerobic bacteria were found. Chan and McManus (1969) observed a high incidence of hydrogen sulfide (H_2S) production among bacteria isolated from blades of *A. nodosum* and *Polysiphonia lanosa*. Eight out of nine isolates from *A. nodosum* and seven out of eight from *P. lanosa* were able to produce H_2S while only four out of eight bacteria isolated from kelp-bed seawater showed this ability. Chan and McManus noted that algae excrete many complex organic compounds that contain sulfur.

Scotten (1971) observed strong growth of bacteria from kelp on proteinaceous media such as peptone broth, yeast extract, and casein hydrolysate, but little utilization of carbohydrates or polyalcohols. Scotten's observation of weak growth on carbohydrates is curious considering sugars are the major kelp exudates (e.g., alginic acid, North 1971; mannitol, Koop *et al.* 1982). Other research indicated that a large proportion of kelp-associated bacteria readily use carbohydrates (Koop *et al.* 1982). Scotten also found that bacteria grew poorly on agar containing kelp homogenate due to "inhibitory materials" present in the homogenate. Kelp exudation of these "inhibitory materials" appeared strongest in winter months. Bacterial populations on kelp surfaces were correspondingly low in winter and increased with warmer seawater temperatures. Bacterial densities in surrounding waters showed no apparent correlation with seasonal temperature.

A. nodosum also was found to exude materials inhibitory to microbial growth. Low colonization of the *A. nodosum* holdfast was associated with high tannin production (Cundell *et al.* 1977). The most numerous and diverse epiphytic populations occurred at the midregion, an area of low tannin production. Bacterial cell coverage was approximately 10^6-10^9 cells/cm^2. Cundell *et al.* (1977) concluded that microflora

(prokaryotic and eukaryotic) colonization of a seaweed surface probably depends on nutrient availability, blade age and antibiotic properties, and incident light.

Materials and Methods

Seawater containing the Giant Kelp, *Macrocystis pyrifera*, was collected from southern California kelp beds on several separate occasions during 1993-1995. Kelp was removed from seawater upon return to the laboratory. Bacteria (plus other particles) were concentrated by a cell concentrator (Pellicon cassette tangential flow filtration system; Millipore 0.22 μm Durapore cassette) or by serial filtration and suspension of material captured on 10, 1, and 0.2 μm, 142 mm diameter filters (polycarbonate; Poretics Co.) (equipment loaned by Dr. Margo Haygood and Dr. Brad Tebo, Scripps Institute of Oceanography). Seawater concentrated in this manner (10 ml) (hereafter referred to as "concentrated seawater") was incubated on a rotary shaker (200 rpm) in glass vials (38 ml) at room temperature (23 °C) in the dark. Nonconcentrated seawater of unusual turbidity (6/27/94) was additionally incubated with CH_2Br_2 (1 μM). Samples were spiked with different concentrations of CH_2Br_2, $CHBr_3$, or both CH_2Br_2 and $CHBr_3$. Samples and formaldehyde-killed controls were monitored over time by injecting bottle headspace (100 μl) into an electron-capture gas chromatograph (Shimadzu 14-A ECD-GC; 175 °C oven; 200 °C inlet; 60 m Restek 502.1 column, helium carrier gas). Degradation products were not monitored. Samples were centrifuged and resuspended in 1 ml double distilled water (ddH_2O) prior to protein assay (BioRad DC Microassay).

Seawater concentrations of $CHBr_3$ and CH_2Br_2 were calculated from interpolated equilibrium partition coefficients of Tse *et al.* (1992). We determined salting-out

coefficients by the method of Gossett (1987) and obtained values of 1.23 ± 0.08 for $CHBr_3$ and 1.18 ± 0.03 for CH_2Br_2, consistent with the salting-out coefficient of 1.2 used by Singh *et al.* (1983) for methyl halides. Multiplying the freshwater partition coefficients by the 1.2 salting-out coefficient gives the following partition coefficients: $CHBr_3$ = 0.023; CH_2Br_2 = 0.040 for seawater at 23 °C. Partition coefficients were 0.28 for CH_3Br (Singh *et al.* 1983) and 0.097 for CH_2Cl_2 (Gossett 1987 multiplied by the 1.2 salting-out coefficient) for seawater at 23 °C.

Rates were determined by linear regression over the period of degradation (i.e., after lag) and were corrected for loss observed in dead controls. Degradation rates were determined from the total mass degraded (water and gas phase) per time per volume of concentrated seawater and then multiplied by the seawater concentration factor. The fraction of total mass in the headspace was 10% for CH_2Br_2 and 6.1% for $CHBr_3$, for 28 ml headspace and 10 ml seawater at 23 °C.

Standards of $CHBr_3$, CH_2Br_2, and CH_2Cl_2 were made in CH_3OH by serial dilution of neat compound. Halomethanes were added to microbial samples from a solution in double distilled water made by serial dilution of neat compound (order of 10 µl water solution added to samples). CH_3Br standards were made from pure gas diluted in air. Pure CH_3Br gas was added directly to seawater samples.

Dibromomethane-degrading samples were spiked with $CHBr_3$, dichloromethane (CH_2Cl_2), or methyl bromide (CH_3Br) after CH_2Br_2 depletion and monitored for degradation. Dibromomethane-degrading samples were divided and filtered (1.8 or 11 µm pore size) or treated with an inhibitor (acetylene (878 mM); cycloheximide (350 mg/ml); chloramphenicol (260 mg/ml); tetracycline/carbenicillin (50 mg/ml each); formaldehyde

(3.4%)). Treated and untreated pairs were respiked and monitored for CH_2Br_2 degradation.

Attempts were made to isolate CH_2Br_2-degrading organisms. Samples of actively-degrading, concentrated seawater were incubated in liquid media or spread on agar (1.5%). The following media were used: seawater (0.2 μm filter sterilized), Hypho (Harder *et al.* 1973), "337" (Poindexter 1992, pp. 2190), nitrate mineral salts (NMS) (Whittenbury *et al.* 1970), and marine broth (Difco). Salt was added typically to a 1.5% final concentration for Hypho, NMS, and "337" media; 1% salt was used for growing *Methylobacter marinus* A45 on NMS. A vitamin mixture (Staley 1968) was added to all media except marine broth. Seawater and Hypho carbon sources were CH_2Br_2 (57 μM) and CH_3OH (0.5%), CH_2Br_2 alone (57 μM or 114 μM), or no added carbon. Additional agar plates were stored with CH_2Br_2 vapor by adding a few μl of liquid CH_2Br_2 to a small glass vial in a metal canister. NMS was used to isolate methanotrophic bacteria (20 μM Cu as $CuSO_4 \cdot 5H_2O$; 57 μM CH_2Br_2 ; 20% CH_4 atmosphere for liquid cultures, 50% CH_4 atmosphere for plates). Media "337" under a nitrogen (N_2) atmosphere was used to isolate *Hyphomicrobium* sp. (0.5% CH_3OH; 1 μM CH_2Br_2). Plates were incubated at room temperature (23 °C) except for *M. marinus* A45 which was incubated at 37 °C.

Methanotroph isolation from kelp blade surfaces was also attempted. Kelp blades were swabbed or blades were broken allowing the intercellular fluids to flow onto sterile swabs. The swabs were vortexed in sterile seawater and swab suspension was added to liquid NMS media (20% CH_4 atmosphere). Media were shaken (200 rpm) for 12 days, spread onto NMS agar plates with CH_2Br_2 (57 μM), and stored under a 50:50 air:CH_4 atmosphere. Promising colonies were streaked for isolation.

Liquid cultures were shaken (200 rpm) and headspace was monitored over time by ECD-GC. Spread-plate colonies were picked with sterile toothpicks and streaked for isolation. Isolated colonies were checked for growth differences on plates with and without CH_2Br_2. Colonies showing promising growth differences on plates were tested in liquid media for CH_2Br_2 degradation. A series of methanol (CH_3OH) utilizing organisms additionally were tested in liquid media by growing on limited CH_3OH (0.05%) with CH_2Br_2 (10 μM). The strategy was to detect methylotrophic organisms that might turn to CH_2Br_2 for growth or degrade it in a cometabolic process once methanol was depleted.

Results and Discussion

Marine Microbial Brominated Methane Degradation

Microorganisms in concentrated kelp-bed seawater degraded CH_2Br_2 to nondetectable levels ($\leq$ 0.002 μM in water phase) (Figures 4.1-4.8). Even a nonconcentrated sample of particularly turbid water (6/27/94) degraded CH_2Br_2 within one month. Degradation typically occurred after a few days lag period (Figures 4.1-4.2). This lag period suggests that microbial activity does not interfere with short-term experiments (2 hr) in our laboratory on the production of brominated methanes by macroalgae (see Chapter 3).

Dibromomethane degradation was more rapid with subsequent additions of the compound as compared to its initial disappearance (Figures 4.1-4.2). Degradation rates with the second addition of CH_2Br_2 (or "spike") were up to 67 times faster than rates measured originally (Table 4.1). Degradation rates and initial concentrations were proportional for the second, third, and fourth spikes suggesting that degradation rates did

not continue to increase, but had stabilized. Rapid CH_2Br_2 degradation in acclimated samples may indicate growth of CH_2Br_2-degrading organisms and/or induction of enzyme systems capable of degrading CH_2Br_2. Increased degradation rates by acclimated cultures was also pronounced for rates based on per μg protein partly because protein concentrations declined over the time course of the experiment (Table 4.1). Cell lysis and protease action could cause protein concentrations to decline. It is not known what proportion of total protein was attributable to bacterial cells in these mixed assemblages.

Bromoform was not degraded in kelp-bed seawater enrichments. Microbes that can utilize multiple substrates often deplete a preferred substrate before turning to the next favored substrate. Bromoform degradation, however, was not observed for samples spiked with $CHBr_3$ and CH_2Br_2 (Figures 4.4-4.8) or with $CHBr_3$ alone (Figure 4.9). Concentrated seawater incubated for 39 days showed no significant biological $CHBr_3$ degradation relative to controls even though CH_2Br_2 had been depleted for a month (Figures 4.7-4.8). Bouwer *et al.* (1981) also did not observe degradation of the trihalomethanes $CHBr_3$, $CHBrCl_2$, or $CHClBr_2$ even after 25 weeks of aerobic incubation of sewage effluent enrichments. They did, however, measure anaerobic microbial degradation of $CHBrCl_2$ and $CHClBr_2$ in batch cultures, and they found evidence of microbial $CHBr_3$ degradation in an anaerobic aquifer.

Environments naturally or anthropogenically enriched with a compound often harbor microbes capable of degrading that compound. Microbes able to degrade CH_2Br_2 in these enrichments seemed unable to degrade $CHBr_3$. The lack of $CHBr_3$ degradation was surprising considering that enriched $CHBr_3$ concentrations were observed in kelp beds (see Chapter 2) and that more $CHBr_3$ was produced than CH_2Br_2 by macroalgae (see

Chapter 3). Bromoform, however, appears resistant to microbial attack in these enrichments. The lack of microbial degradation may indicate that $CHBr_3$ is difficult to biochemically dehalogenate or it may be testimony to its biocidal strength. It is possible that the brominated methane concentrations observed in kelp-bed seawater reflect not only enhanced $CHBr_3$ production by macroalgae but also CH_2Br_2 degradation in the water column or on blade surfaces.

Seawater samples showing active degradation of CH_2Br_2 were divided and spiked with either CH_2Br_2 (10 μM), CH_2Cl_2 (11 μM), $CHBr_3$ (10 μM) or methyl bromide (CH_3Br; 29 μM) (water phase concentrations). Dibromomethane and CH_2Cl_2 were degraded within a week. Significant CH_3Br or $CHBr_3$ degradation was not observed (Table 4.2) relative to control losses. Interestingly, this pattern of degradation is consistent with the narrow substrate range observed for dichloromethane dehalogenase enzymes.

Nonbiological loss observed in some sample vials (e.g., Figure 4.4) was probably from leaks or adsorption to septa and glass surfaces. Chemical degradation is less likely. Photolytic reactions were precluded by incubating in darkness, and both halide substitution and hydrolytic reactions are slow. The half-life for halide substitution of $CHBr_3$ is 1.3-18.5 yr in 25 °C seawater (Geen 1992). The half-life for hydrolysis of CH_2Br_2 is 183 yr and for $CHBr_3$ 686 yr in 25 °C freshwater (Mabey and Mill 1978).

Microbial Isolation and Inhibition

Degradation activity was maintained for over 2 months in the same enrichments by respiking the sample approximately once a week with up to 62 μM CH_2Br_2. Degradation activity was also maintained by transferring aliquots of enrichment to new vials of CH_2Br_2-

spiked, sterile seawater. Enrichments formed small flocs but never became visibly turbid. Aerobic conditions were maintained in long-term enrichments by swirling open vials in a sterile hood prior to respiking, in addition to shaking during incubation. Oxygen consumption should have been low based on the small amount of visible biomass.

Attempts to isolate bacteria using CH_2Br_2 as the sole carbon and energy source were unsuccessful. Different CH_2Br_2 concentrations (57, 114 μM, and 57 μM + CH_2Br_2 vapor) and agar salinities were used (1.5 and 3.0%) for Hypho and seawater plates. Microbial growth generally appeared similar on plates with or without CH_2Br_2. A few promising organisms were isolated, but they did not degrade CH_2Br_2 in liquid culture. Several of the "promising" organisms were apparently agar-degraders based on small depressions made in the agar and inability to grow in liquid media. The inability to isolate pure cultures may indicate that the microorganisms which degraded CH_2Br_2 in kelp-bed seawater were not utilizing CH_2Br_2 for growth; instead, degradation may have been a cometabolic process. Alternatively, a microbial consortium may have caused degradation, thus pure cultures would not degrade CH_2Br_2. Synergistic-consortia and mixotrophic-cometabolism may actually dominate marine systems in nature (Sieburth 1988).

Dichloromethane dehalogenase activity in some facultative methylotrophs is consistent with the degradation pattern we observed (dihalomethanes only). Enrichments with CH_3OH as a substrate were thus established from CH_2Br_2-degrading seawater. Dibromomethane degradation, however, was not observed after aliquots of CH_2Br_2-degrading seawater were transferred to CH_3OH/CH_2Br_2 liquid media (Hypho or "337"), even though microbial flocs were formed in the CH_3OH media. A number of marine methylotrophic bacteria were isolated by streak-plating (Chistoserdov *et al.* 1995), but

these isolates did not degrade CH_2Br_2 (10 μM) when grown to turbidity on limited CH_3OH (0.05%) in liquid Hypho media. Only transfer of enriched seawater to sterile seawater maintained CH_2Br_2 degradation. Degradation was observed in enrichments even after a month of CH_2Br_2 depletion. Dibromomethane degradation in seawater occurred in the presence and absence of CH_3OH or CH_4, thus the presence of these compounds did not inhibit degradation. Microscopic examination of concentrated seawater showed an array of prokaryotic and eukaryotic organisms as well as kelp debris. Cellular break-down products as well as kelp sugars would have been available as growth substrates for these organisms. Inability to obtain an isolate may indicate that CH_2Br_2 was degraded in a cometabolic process in which the proper growth substrate or balance of substrates was not identified. The CH_2Br_2-degrading organisms may also have been "nonculturable." Only a small fraction of natural microbial populations can be cultured in the laboratory.

Methanotrophs (CH_4-oxidizers) or nitrifiers (NH_4-oxidizers) were logical candidates for CH_2Br_2 degradation. Halomethane degradation by CH_4 and NH_4-oxidizing bacteria is a cometabolic process resulting from broad substrate specificity of CH_4 and NH_4 monooxygenase enzymes; cell growth is not supported. A marine nitrifier, *Nitrosococcus oceanus*, was reported to degrade CH_3Br (Rasche *et al.* 1990). Certain methanotrophs degraded brominated methanes in our laboratory. *Methylobacter marinus* A45 (previously called *Methylomonas* sp. strain A45) degraded CH_2Br_2 and CH_3Br. Strain E-2 degraded $CHBr_3$. Brominated methane degradation was not observed by *Methylomicrobium albus* BG8 (previously called *Methylomonas albus* BG8) or strain E-1 (Table 4.3). Strains E-1 and E-2 are uncharacterized marine methanotrophs isolated from a submerged eel grass bed by K.S. Smith. These four isolates were grown under copper

conditions (10 μM) that should have resulted in pMMO expression. *M. marinus* A45 and *M. albus* BG8 contain only the particulate form of the methane monooxygenase enzyme (pMMO). Brominated methanes were added individually to culture vials to avoid possible competition between halogenated substrates. Degradation of all three compounds (i.e., CH_3Br, CH_2Br_2, $CHBr_3$) by the same strain was not observed (Table 4.3). Degradation of all three compounds has been reported for *Methylosinus trichosporium* OB3b (Bartnicki and Castro 1994) grown under conditions to express the soluble form of the methane monooxygenase (sMMO).

Methanotrophic isolates, however, were not obtained from kelp blade surfaces or intercellular mucous. Lacking an isolate, we turned to inhibitor studies to examine whether methanotrophs or nitrifiers might be responsible for CH_2Br_2 degradation in kelp-bed seawater. Acetylene inhibits monooxygenase enzymes and thus would halt cometabolism of CH_2Br_2 by CH_4 and NH_4-oxidizers, both of which use monooxygenases for their cometabolic activities. Non-methane methylotrophic growth (e.g., using methanol) is not affected by acetylene (Oremland and Capone 1988). Acetylene also inhibits nitrogenase and N_2O-reductase and thus inhibits nitrogen fixation and denitrification (Oremland and Capone 1988). In addition, acetylene concentrations used in this investigation (878 mM) should have been high enough to inhibit methanogenesis (M. Lidstrom, personal communication). Acetylene did not halt CH_2Br_2 degradation in actively-degrading seawater enrichments (Table 4.4) or when added at the start of incubation (Figure 4.10). This result precludes a number of microbial processes from contributing to CH_2Br_2 degradation, including methanotrophy, nitrification, denitrification, nitrogen fixation, and methanogenesis. This result does not exclude the possibility that

obligate or facultative methylotrophic bacteria (except methanotrophs) contribute to CH_2Br_2 degradation.

A marine amoeba originally found feeding on macroalgae was reported to use haloalkanes as a sole carbon source. This organism, *Trichosphaerium* I-7, was maintained on 1-chlorooctadecane and 1-bromooctadecane in the laboratory (Kaska *et al.* 1991). Inhibitor studies were used to examine the possibility that similar eukaryotic organisms degraded CH_2Br_2 in kelp-bed seawater. An eukaryotic protein synthesis inhibitor, cycloheximide, was added to seawater enrichments that had degraded CH_2Br_2. Cycloheximide did not impede degradation of subsequently added CH_2Br_2 (Table 4.4). Microscopic observation of long-term incubations revealed few, if any, eucaryotic organisms although eucaryotes were abundant at the start of incubation. These results, in combination with those from chloramphenicol studies (discussed below), indicate that bacteria and not eucaryotes were degrading CH_2Br_2 in seawater enrichments. Formaldehyde halted degradation of actively degrading cells, further confirming that CH_2Br_2 degradation was biologically mediated.

Enzymes can be inducible (synthesized in response to a compound) or constitutive (continuously present). Enzymes involved in carbon and energy source catabolism are often inducible, while key enzymes involved in growth under all nutritional conditions are often constitutive (Brock and Madigan 1991, pp.171-174). The ability of chloramphenicol, a prokaryotic protein synthesis inhibitor, to inhibit CH_2Br_2 degradation depended on the metabolic condition of the enrichment sample. Chloramphenicol inhibited degradation of CH_2Br_2 when added at the start of the incubation (Figure 4.10). In contrast, chloramphenicol added to actively-degrading cells did not halt CH_2Br_2

degradation (Table 4.5). The broad spectrum antibiotics tetracycline and carbenicillin similarly did not inhibit degradation when added to actively-degrading cultures (Table 4.4). Chloramphenicol also inhibited CH_2Br_2 degradation when added to cells that had been incubated an additional eight days after CH_2Br_2 depletion. A paired sample that did not receive chloramphenicol did degrade CH_2Br_2. Dibromomethane concentrations decreased in both vials after 2.5 days, but further degradation was not observed in the chloramphenicol treated sample (Figure 4.11; Table 4.5). Methane was added to these samples during the period of CH_2Br_2 depletion. The strategy was that CH_4 might be a growth substrate for the degrading organisms and its addition might keep the culture metabolically active during CH_2Br_2 depletion. However, inhibition studies with acetylene later ruled out methanotrophic involvement in CH_2Br_2 degradation, thus CH_4 could not have been a growth substrate for the CH_2Br_2-degrading cells. The chloramphenicol results thus indicate that CH_2Br_2 degradation requires protein synthesis which suggests that degradation is either induced by CH_2Br_2 and/or requires microbial growth.

Open-ocean bacteria primarily exist as free-living cells (Yanagita 1990); however, more attached bacteria are expected in a kelp bed because of increased availability of particle surfaces. The proportion of attached bacteria appears to increase with the amount of particulate material (Kirchman 1993, p. 322). Dibromomethane degradation observed in these experiments was particle-associated. Filtering through 1.2 or 11 μm filters initially halted degradation (Table 4.4), but degradation was reestablished after about two additional weeks of incubation. These were relatively large pore size filters; a 0.2 μm filter is normally used for sterilization. This result indicates that bulk CH_2Br_2 degradation is associated with particles >1.2 μm and that some free-living cells passed through the

filter to reestablish degradation. Particle-associated activity conceivably could have lead to inoculum differences in these experiments because of unequal partitioning between vials. Nonhomogeneous inoculum may be the reason degradation rates sometimes varied between vials within a single experiment (Figures 4.7-4.8; Table 4.6) and why degradation was sometimes not detected for a single sample vial while it was detected for the other vials in that experiment (Figures 4.2, 4.3, and 4.8). Particle-associated activity in laboratory incubations raises the possibility that CH_2Br_2-degrading bacteria may be attached to kelp surfaces in the environment.

Favorable nutrient conditions cause coastal and upwelling regions to harbor more bacteria than open-ocean areas. Coarse filtered (62 μm) seawater had a reported cell density of approximately $1.5x10^6$ cells/ml for an S. African kelp-bed (*Ecklonia maxima* and *Laminaria pallida*) measured by acridine orange direct counting (Linley *et al.* 1981). Open-ocean cell densities range from approximately $1x10^1$ to $8x10^3$ cells/ml (Oppenheimer 1961, p.18). We assayed seawater for total protein immediately after the seawater concentration step (5/18/94 and 7/5/95). Protein concentrations were 643 and 3247 μg/L in the concentrated seawater (Table 4.6) which correspond to 7.6 and 54 μg protein/L seawater, respectively. These protein concentrations would represent $5x10^7$ and $4x10^8$ cells/L seawater assuming that all the protein is bacterial, that bacterial cells are half protein (dry weight), that dry cell weight is 30% wet cell weight (Schlegel 1993), and a cell weighs $1x10^{-12}$ g (Bailey and Ollis 1986, pg. 5). Protein assays, however, measured total protein in samples that included phytoplankton and kelp cellular debris in addition to a mixed bacterial population. Cell densities are overestimated primarily by the proportion of nonbacterial protein present in the sample, for which we have no estimate. Protein

concentrations sharply declined after 39 days of incubation (3247 μg/L to 810 μg/L; 7/5/95). Cell die-off and protease action could cause protein concentrations to decrease.

Rates of Dibromomethane Degradation by Marine Microorganisms

Dibromomethane degradation rates were measured in separate laboratory seawater incubations conducted between June 1993 and June 1995. Rates ranged from 0.11 nmoles CH_2Br_2/day·L seawater (19.1 ng/ day·L seawater) to 73 nmoles CH_2Br_2/day·L seawater ($1.27x10^4$ ng/ day·L seawater), depending in part on the initial CH_2Br_2 concentration (Table 4.6). Microbial degradation rates increased with increasing initial CH_2Br_2 concentration for 1.1 - 4.1 μM CH_2Br_2 (Figure 4.12) indicating that these concentrations were probably below saturation (i.e., concentrations were below or not much above the K_s, the half-saturation constant). Degradation rates also tended to increase between 5 and 10 μM CH_2Br_2, although there is scatter (Figure 4.13). To estimate the maximum sink contributed by bacteria, 10 μM was assumed below saturation in the following calculations.

Laboratory degradation rates were extrapolated linearly to environmental conditions assuming experimental concentrations were below saturation and based on seawater CH_2Br_2 concentrations measured in a *M. pyrifera* canopy (3.2 ng/L, 0.018 nM; Manley *et al.* 1992, using partition coefficient of Tse *et al.* 1992; Chapter 2). Estimated microbial degradation in the kelp-bed water column at this CH_2Br_2 concentration (0.018 nM) ranged from $1.8x10^{-6}$ to $1.4x10^{-4}$ nmoles/day·L seawater ($3.2x10^{-4}$ to 0.023 ng/day·L seawater) (Table 4.7). This range was based on the range of CH_2Br_2 degradation rates measured in the laboratory (minimum: 0.11 nmoles/day·L seawater, occuring at 1.1 μM CH_2Br_2 initial concentration; maximum: 73 nmoles/day·L seawater, occuring at 9.9 μM

CH_2Br_2 initial concentration). These rates are probably maximum estimates because laboratory conditions are expected to optimize degradation.

Seawater collected on 6/27/94 showed a high degradation rate (31 nmoles/day·L seawater) for a low initial concentration (0.77 μM) (Table 4.6). Seawater on this day was particularly turbid and little was filtered because it clogged the system (only six-fold concentration). Protein concentrations were high for seawater samples taken immediately after the concentration step (2448 and 2854 μg protein/L concentrated seawater; Table 4.6). Seawater in the kelp bed was warm (21.1 °C, Table 4.6), cloudy, and contained an abundance of shrimp and flatworms. The high degradation rate (per liter seawater) observed on this day was not considered representative of ordinary kelp bed conditions.

Significant microbial degradation of CH_2Br_2 in the kelp-bed water column could reduce the amount of brominated methanes escaping to the atmosphere. We measured CH_2Br_2 degradation by bacteria from a kelp bed, a site of CH_2Br_2 production. A further motivation for this study, once the existence of microbial degradation had been established, was to evaluate whether microbial degradation of CH_2Br_2 might be environmentally significant. Maximum microbial degradation in the kelp-bed water column was estimated as 0.023 ng CH_2Br_2/day·L seawater (1.35×10^{-4} nmoles/day·L seawater) at CH_2Br_2 canopy concentrations. The macroalga *M. pyrifera* produced 48 ng CH_2Br_2/day·g fresh kelp in laboratory incubations (median rate, see Chapter 3). This production rate translates to 19 ng CH_2Br_2/day·L seawater (0.11 nmoles/day·L seawater) produced in the kelp-bed water column, assuming a bed density of 0.40 kg/m^3 averaged over the kelp-bed water column (see Chapter 5). Marine microbial degradation in the water column is thus estimated to be only 0.1% of macroalgal production, at maximum

(Table 4.7). Even the anomalously high rates observed on 6/27/94 would account for only 0.7% of macroalgal production (0.13 ng CH_2Br_2 degraded/day·L seawater at 3.2 ng/L CH_2Br_2).

Microbial degradation of 0.018 nM CH_2Br_2 would take 136 days at the estimated degradation rate of $1.35x10^{-4}$ nmoles CH_2Br_2/ day·L seawater, based on the extrapolated maximum laboratory degradation rate of 73 nmoles CH_2Br_2/day·L seawater. Based on this extrapolation, microbial degradation could be faster than hydrolysis or halide substitution but slower than volatilization, as shown in Table 6.1. It is noteworthy that Moore and Tokarczyk (1993) observed CH_2Br_2 distributions in the northwest Atlantic Ocean that indicated more pronounced consumption of CH_2Br_2 in deep waters relative to $CHBr_3$. Investigations of microbial CH_2Br_2 degradation in open-ocean environments may assess whether microbial CH_2Br_2 degradation of contributes to oceanic CH_2Br_2 profiles.

These results indicate that microbial CH_2Br_2 degradation is insignificant in the kelp-bed water column compared to macroalgal production. Not only are dibromomethane degradation rates small compared to production, but rates are well within the error of the production estimate itself. The likely habitat, however, of kelp-associated microbes is kelp surfaces. Longshore current velocities through a well-developed kelp bed are on the order of 1 cm/s; thus the residence time of kelp-bed water is on the order of a several days for kelp beds between 1-7 km long (Jackson and Winant 1983). Attachment to kelp surfaces would ensure that bacteria remain in the relatively nutrient-rich kelp environment. Diverse microbial communities have been identified on kelp surfaces including bacteria, diatoms, and cyanobacteria (Cundell *et al.* 1977). Particle-associated degradation in the laboratory (Table 4.4) supports the hypothesis that CH_2Br_2-degrading

bacteria are attached to surfaces in the environment. Bacteria attached to kelp presumably would experience higher CH_2Br_2 concentrations than free-living cells, and high concentrations at blade surfaces might sustain appreciable CH_2Br_2 degradation. Attached bacteria degrading CH_2Br_2, but not $CHBr_3$, might help maintain the concentration disparity observed between CH_2Br_2 and $CHBr_3$ in kelp beds and surrounding areas (e.g., Manley *et al.* 1992, Klick 1992). However, estimates of macroalgal production determined from kelp incubations would remain unchanged even if significant CH_2Br_2 degradation occurs on blade surfaces. Measurements in this case would record net production, with no change in values.

Conclusions

The existence, character, and extent of $CHBr_3$ and CH_2Br_2 degradation by kelp-associated microorganisms was investigated. While both $CHBr_3$ and CH_2Br_2 are released by macroalgae, only CH_2Br_2 was degraded in seawater enrichments. Dibromomethane degradation typically began after a few day lag period and was rapid thereafter. Microbial degradation was observed only for dihalomethanes: CH_2Br_2 and CH_2Cl_2 were degraded, but $CHBr_3$ and CH_3Br were not. The pattern of $CHBr_3$ and CH_2Br_2 loss in seawater concentrated from a kelp bed suggests that microbial activity does not interfere with our short-term experiments on the production of brominated methanes by macroalgae.

Inhibitor studies indicated that eukaryotic organisms and a number of microbial processes, including nitrification and methanotrophy, did not contribute to CH_2Br_2 degradation. Dibromomethane degradation appeared associated with particles > 1.2 μm. This result indicates that a homogenous inoculum may be difficult to achieve in incubation

experiments. Furthermore, particle-associated activity in sample vials supports the idea that CH_2Br_2-degrading bacteria may be attached to kelp surfaces in the environment.

Development of detectable CH_2Br_2 degradation required protein synthesis. Chloramphenicol inhibited development of CH_2Br_2 degradation when added initially to cultures, and it blocked sustained degradation after cultures had been depleted of CH_2Br_2 for several days. Chloramphenicol did not inhibit CH_2Br_2 degradation when cultures were actively degrading; i.e., once protein synthesis and/or growth had occurred, the chloramphenicol had no effect. Therefore, either enzyme synthesis (induction) and/or growth was required for degradation.

Dibromomethane degradation rates ranged from 0.11 to 73 nmoles CH_2Br_2/day·L seawater in kelp-bed seawater incubations. Degradation rates tended to increase with initial CH_2Br_2 concentration indicating that experimental concentrations were most likely below saturation of the degradation process. Degradation rates were extrapolated under this assumption to 0.018 nM CH_2Br_2 (3.2 ng/L), a typical seawater concentration in a *M. pyrifera* kelp bed (Manley *et al.* 1992 values using the partition coefficient of Tse *et al.* 1992). Estimated maximum microbial degradation in the kelp bed was thus 0.023 ng CH_2Br_2/day·L while macroalgal production was an estimated 19 ng CH_2Br_2/day·L seawater (Chapter 3). Microbial CH_2Br_2 degradation thus represents only 0.1% of *M. pyrifera* CH_2Br_2 production, well within the error of the production estimate itself. Microbial degradation of 0.018 nM CH_2Br_2 would take 136 days at a degradation rate of $1.35x10^{-4}$ nmoles CH_2Br_2/ day·L seawater. These estimates suggest that microbial degradation could be faster than hydrolysis or halide substitution but slower than

volatilization. Although microbial degradation of CH_2Br_2 occurs, these results suggest it is probably an insignificant water column sink within the kelp bed.

Microbes attached to kelp surfaces conceivably could encounter elevated CH_2Br_2 concentrations and significant degradation may occur at the blade interface. If this were the case, $CHBr_3$ and CH_2Br_2 concentrations observed in kelp beds and surrounding waters may reflect not only enhanced macroalgal production of $CHBr_3$, but also microbial degradation of CH_2Br_2 as it occurs on blade surfaces. Measured macroalgal production in this case would reflect net production from kelp with associated microbes, but production estimates themselves would remain unchanged.

Table 4.1. CH_2Br_2 microbial degradation rates for individual samples in Figs. 4.1-4.2. Initial CH_2Br_2 degradation was slower than subsequent degradation. Rates were calculated by linear regression over the period of degradation (i.e., after lag) and corrected for losses in dead controls. Rates were determined from total mass degraded (water and gas phase) per time per volume of concentrated seawater and then multiplied by seawater concentration factor (see Table 4.6). Rates per μg protein were normalized by protein concentration in each sample vial; where values are not given, protein concentration was not determined. C_w is water phase concentration. Data for "spike #1" are also given in Table 4.6. See Table 4.6 for explanation of minimum values (≥).

spike #	initial C_w (μM)	nmoles CH_2Br_2/day· L seawater	protein conc. (μg/L)	nmoles CH_2Br_2/day· μg protein
3/1/94 a				
1	0.87	1.1		
2	1.3	14		
3	1.1	≥ 60		
4	1.1	≥ 62		
3/1/94 b				
1	0.84	1.2		
2	1.2	18		
3	1.1	≥ 60		
4	1.5	≥ 80		
3/1/94 c				
1	0.82	0.89		
2	1.4	21		
6/27/94 a				
1	0.76	29	2448[a]	0.071
2	1.7	82		
3	2.1	≥ 123	1115	≥ 0.66
6/27/94 b				
1	0.78	30		
2	2.5	≥ 517		
3	7.7	≥ 1516		
6/27/94 c				
1	0.77	31	2854[ab]	≥ 0.065[b]
2	2.0	≥ 408		
3	7.6	≥ 1612	1189[b]	≥ 7.9[b]

[a] Protein concentration assay performed on half of original sample (5ml); other half was respiked with CH_2Br_2 and monitored for further degradation.

[b] Sample average for 6/27/94 b and c.

Table 4.2. Microbial degradation of several halomethanes in concentrated CH_2Br_2-enriched seawater from a *M. pyrifera* kelp bed. (+) represents disappearance of compound from sample vials; (–) represents insignificant loss relative to controls. C_w is water phase concentration.

compound	initial C_w (μM)	degradation
CH_2Br_2	10	+
CH_2Cl_2	11	+
$CHBr_3$	10	–
CH_3Br	29	–

Table 4.3. Brominated methane degradation by methanotroph laboratory isolates. Organism description and enzyme characteristics are noted. (+) represents disappearance of compound from sample vials; (-) represents insignificant loss relative to formaldehyde killed controls. C_w is water phase concentration.

	CH_2Br_2		$CHBr_3$		CH_3Br	
strain name environment; MMO type	C_w (μM)	deg.	C_w (μM)	deg.	C_w (μM)	deg.
Methylobacter marinus A45 marine; pMMO	6.3 4.2	+ +	4.6 1.8	– –	18	+
Methylobacter albus BG8 nonmarine; pMMO	6.3	–	4.6	–	18	–
E-1 marine; not characterized	6.3	–	4.6	–		
E-2 marine; not characterized	6.3	–	4.6	+		

Table 4.4. Action of inhibitors on CH_2Br_2 degradation for kelp-bed seawater enriched on CH_2Br_2. Acetylene, tetracycline/carbenicillin, filtration, and formaldehyde treatments were performed on actively-degrading samples. Cycloheximide was added several days after CH_2Br_2 depletion to maximize effectiveness of this protein synthesis inhibitor. Particle-associated activity was evaluated by passing samples through filters of relatively large pore size.

inhibitor	inhibitory action	CH_2Br_2 degradation
acetylene	e.g., monooxygenase enzymes	+
cycloheximide	eukaryotic protein synthesis	+
tetracycline/carbenicillin	prokaryotic protein synthesis/ cell wall synthesis	+
filtration (1.2 μm or 11 μm)	removes cells	–/+[a]
formaldehyde	cell death	–

[a] Degradation was inhibited initially but was reestablished after about two weeks (see text for discussion).

Table 4.5. Action of the prokaryotic protein synthesis inhibitor, chloramphenicol, on CH_2Br_2 enriched kelp-bed seawater. The ability of chloramphenicol to inhibit CH_2Br_2 degradation depended on enrichment sample condition indicating that detectable CH_2Br_2 degradation required protein synthesis (see text for discussion). See Figures 4.10 and 4.11.

treatment conditions	CH_2Br_2 degradation
chloramphenicol added after degradation established	+
chloramphenicol added initially to enrichment	–
several days of CH_2Br_2 depletion then chloramphenicol added	+
several days of CH_2Br_2 depletion, no chloramphenicol added	–[a]

[a] Initial loss observed but not sustained, see Figure 4.11.

Table 4.6. Degradation rates for all seawater samples showing CH_2Br_2 degradation (Figs. 4.1-4.9; 4.11). Minimum rates (≥) included a "zero" value in the linear regression; it is thus unknown when degradation to nondetectable level precisely occurred. Protein concentrations are total protein in the enrichment (prokaryotic and eukaryotic). Samples combined for determination of protein concentration are shown as mean ± SD. Kelp bed surface seawater temperature on date of collection and factor seawater was concentrated are shown. C_w is water phase concentration. See Table 4.1 for rate calculations.

date	initial C_w (µM)	nmoles/day·L seawater	nmoles/day·ug protein	total protein (µg/L conc sea)	conc factor	temp (°C)
7/27/93	8.9	7.3	1.8	620	156	21.1
	9.3	7.5				
	14	12				
8/18/93	9.1	≥ 10	≥ 2.0	1069	213	18.9
	9.1	≥ 10				
	9.4	≥ 10	≥ 2.8	789		
9/18/93	1.1	0.11			160	20.0
	1.6	0.73				
	2.0	0.51	0.29	285		
	3.6	0.85				
	4.1	1.7	0.63	443		
10/4/93	0.51	≥ 0.65	≥ 0.20	415	129	18.9
	0.53	0.65	0.26	320		
3/1/94	0.82	0.89			42	17.5
	0.84	1.2				
	0.87	1.1				
5/18/94	0.73	1.2	0.18 ± 0.079	643[a]	84	18.7
	0.75	2.0				
	0.75	2.3				
6/27/94	0.76	29	0.071	2448	6.0	21.1
	0.77	31				
	0.78	30	0.065 ± 0.0020	2854[b]		
7/5/95	5.0	13	0.36 ± 0.30	3247[a]	60	18.6
	5.3	17				
	5.3	5.7				
	5.4	42				
7/5/95	9.9	73	0.86 ± 0.42	3247[a]	60	18.6
	10.3	31				
	10.4	36		810[c]		

[a] Sample taken for protein assay immediately after seawater concentration step; given rate is average of three values.

[b] Two bottles combined for protein assay.

[c] Protein measured after 39 days of incubation at end of $CHBr_3$ experiment.

Table 4.7. CH_2Br_2 microbial degradation rates in kelp-bed seawater samples with extrapolation to relevant environmental concentrations. Minimum and maximum rates observed in laboratory seawater incubations from June 1993 to June 1995 are shown. Degradation rates were measured at the initial water phase concentration, C_w. These rates were extrapolated to a typical kelp-bed seawater concentration ($1.8x10^{-5}$ μM; 3.2 ng/L). Microbial degradation in the kelp-bed water column is given as a percentage of CH_2Br_2 macroalgal production in the kelp bed (see text). See Table 4.1 for description of rate calculations.

		nmoles CH_2Br_2/day·L seawater		
date	initial C_w (μM)	at initial C_w	at $1.8x10^{-5}$ μM	% of kelp production
9/18/93	1.1	0.11	$1.8x10^{-6}$	0.002
7/5/95	9.9	73	$1.4x10^{-4}$	0.1

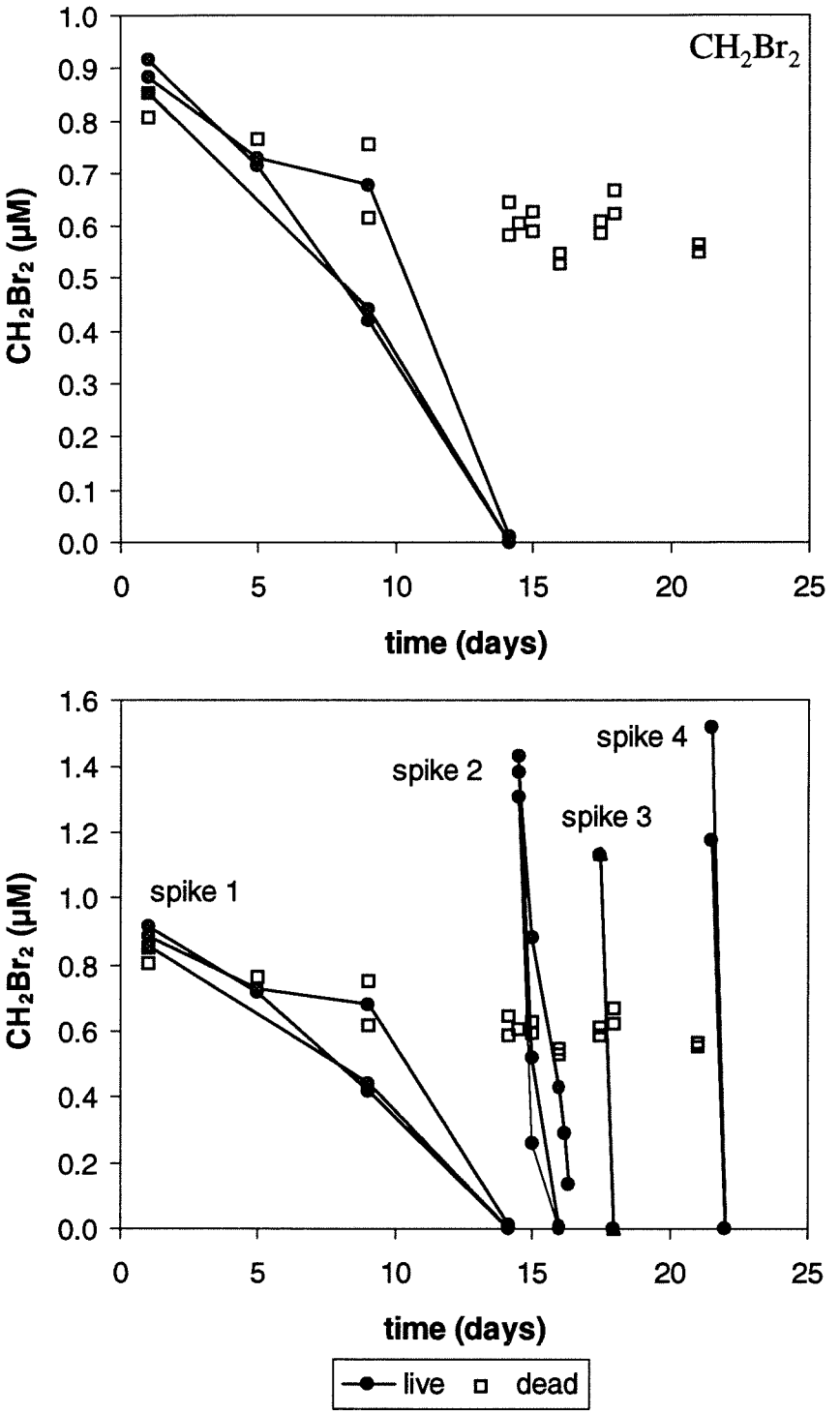

Figure 4.1. Marine microbial CH_2Br_2 degradation for seawater collected 3/1/94 and concentrated by transverse filtration. CH_2Br_2 was degraded in replicate seawater samples ("live") after a several day lag period. CH_2Br_2 was then quickly degraded when added to acclimated samples (lower figure; "spike 1" also shown in upper figure). Concentrations (µM) are in water phase. "Dead" are formaldehyde killed controls.

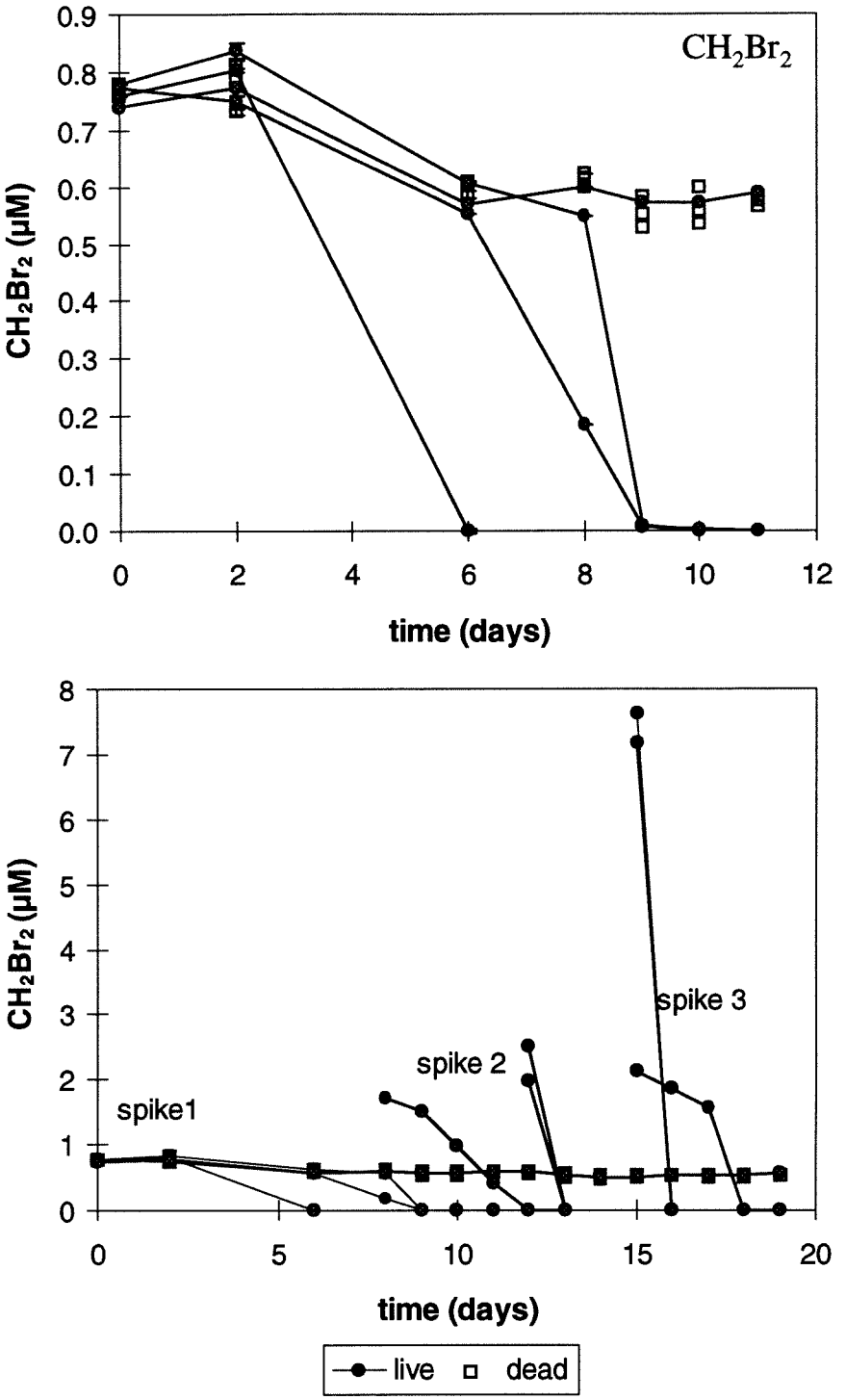

Figure 4.2. Marine microbial CH_2Br_2 degradation for seawater collected 6/27/94 and concentrated by transverse filtration. Seawater was unusually turbid. Degradation was not detected in one of the live replicate samples. See Figure 4.1 for further description.

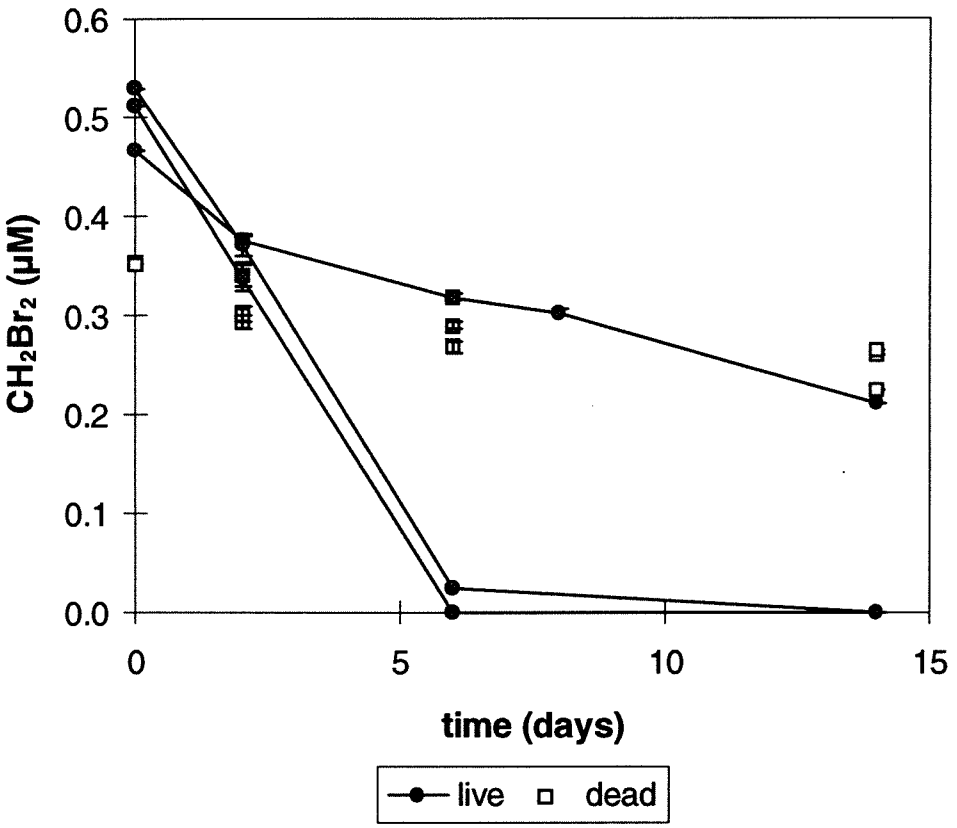

Figure 4.3. Marine microbial CH_2Br_2 degradation for seawater collected 10/4/93 and concentrated by resuspending cells captured on 10 and 0.2 µm filters. Degradation was not detected in one of the live replicate samples. Error bars are range of two headspace injections per sample vial. Concentrations (µM) are water phase. "Dead" are formaldehyde killed controls.

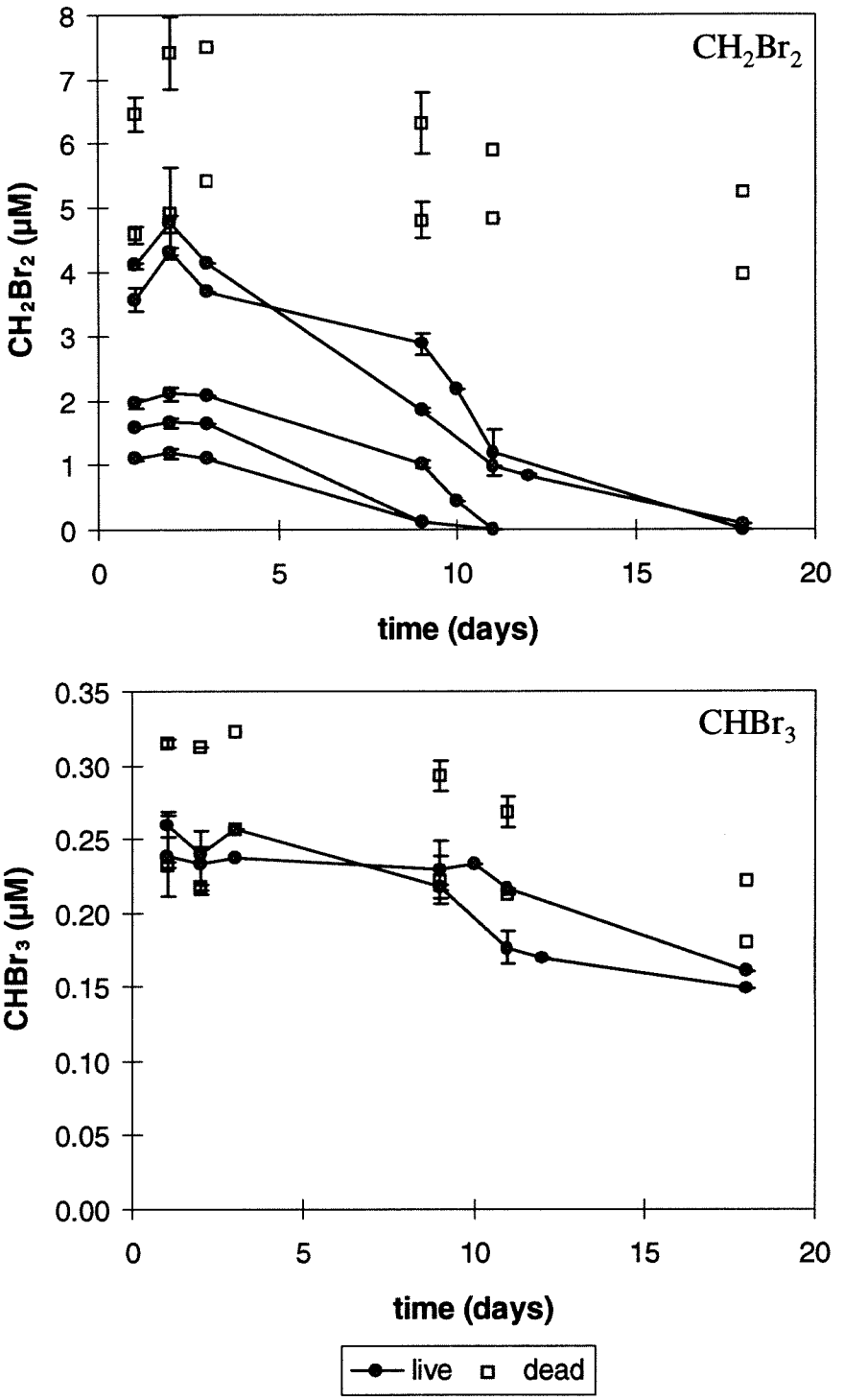

Figure 4.4. Marine microbial CH_2Br_2 degradation for seawater samples spiked with different amounts of CH_2Br_2 (upper figure). Seawater was collected 9/18/93 and concentrated by resuspending cells captured on 10, 1, and 0.2 µm filters. A small amount of $CHBr_3$ was added to two bottles (4 µM CH_2Br_2) but it was not degraded (lower figure). See Fig. 4.3 for further description.

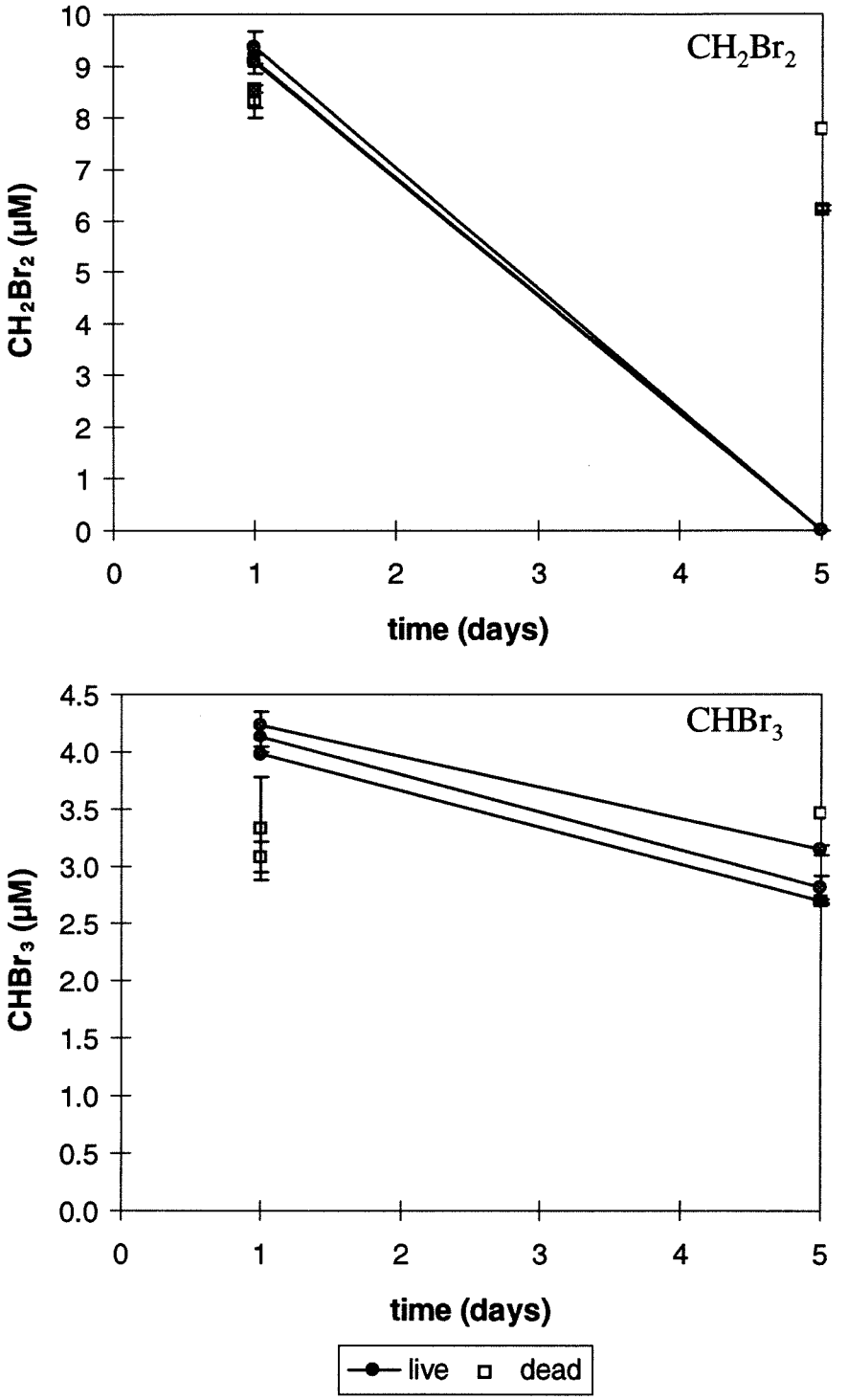

Figure 4.5. Marine microbial CH_2Br_2 degradation for seawater samples collected 8/18/93 and spiked with both CH_2Br_2 and $CHBr_3$. Microbial degradation is apparent for CH_2Br_2 (upper figure), but not $CHBr_3$ (lower figure). See Fig. 4.3 for further description.

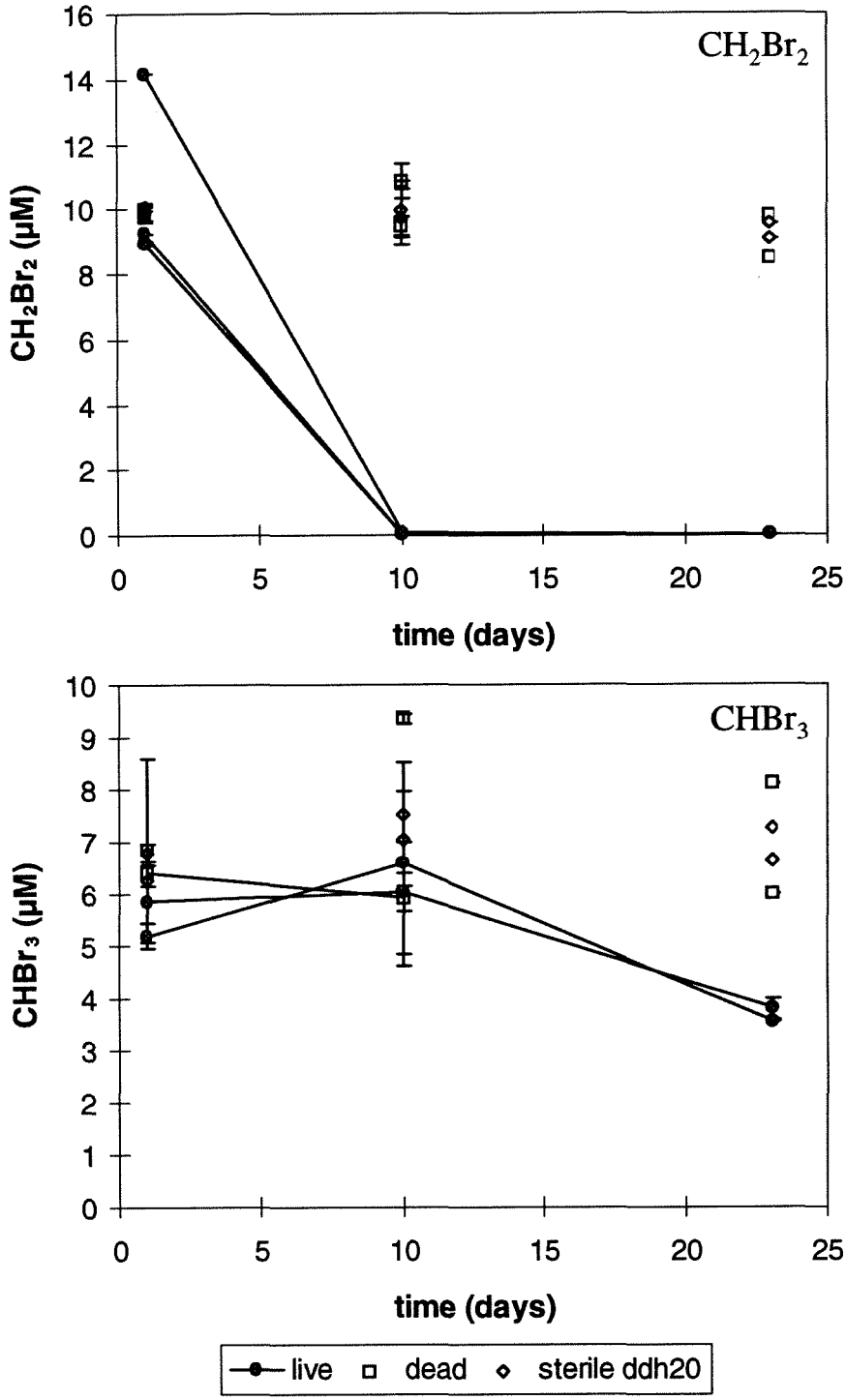

Figure 4.6. Marine microbial CH_2Br_2 degradation for seawater samples collected 7/27/93 and spiked with both CH_2Br_2 and $CHBr_3$. Microbial degradation is apparent for CH_2Br_2 (upper figure), but not $CHBr_3$ (lower figure). Formaldehyde killed samples ("dead") and sterile, double-distilled water were used as controls. See Fig. 4.3 for further description.

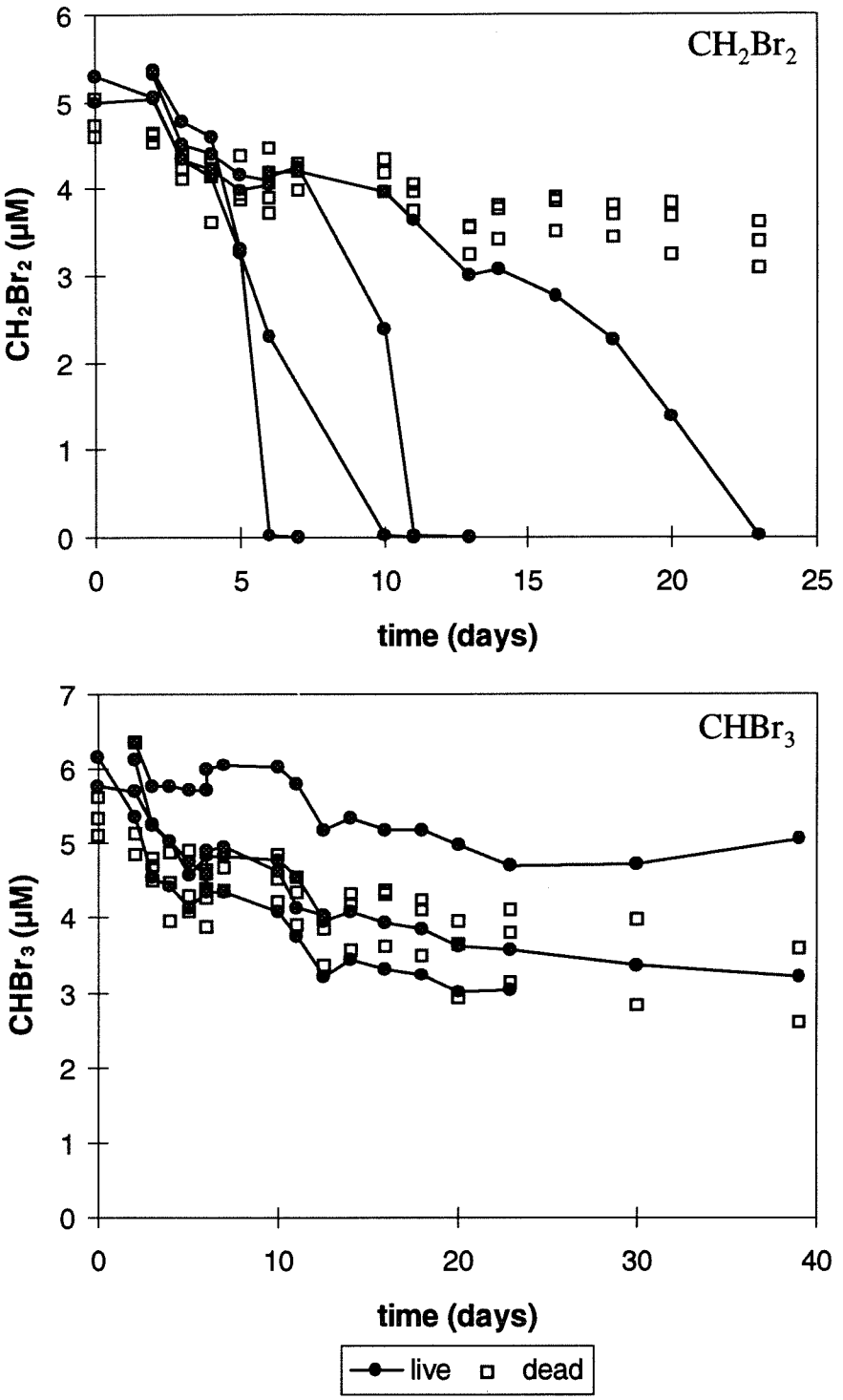

Figure 4.7. Marine microbial CH_2Br_2 degradation for seawater samples collected 7/5/95 and spiked with both CH_2Br_2 and $CHBr_3$. Microbial degradation is apparent for CH_2Br_2 (upper figure), but not $CHBr_3$ (lower figure) even after 39 days of incubation and up to one month after the CH_2Br_2 disappearance. Seawater was concentrated as in Fig. 4.1. Concentrations (μM) are water phase.

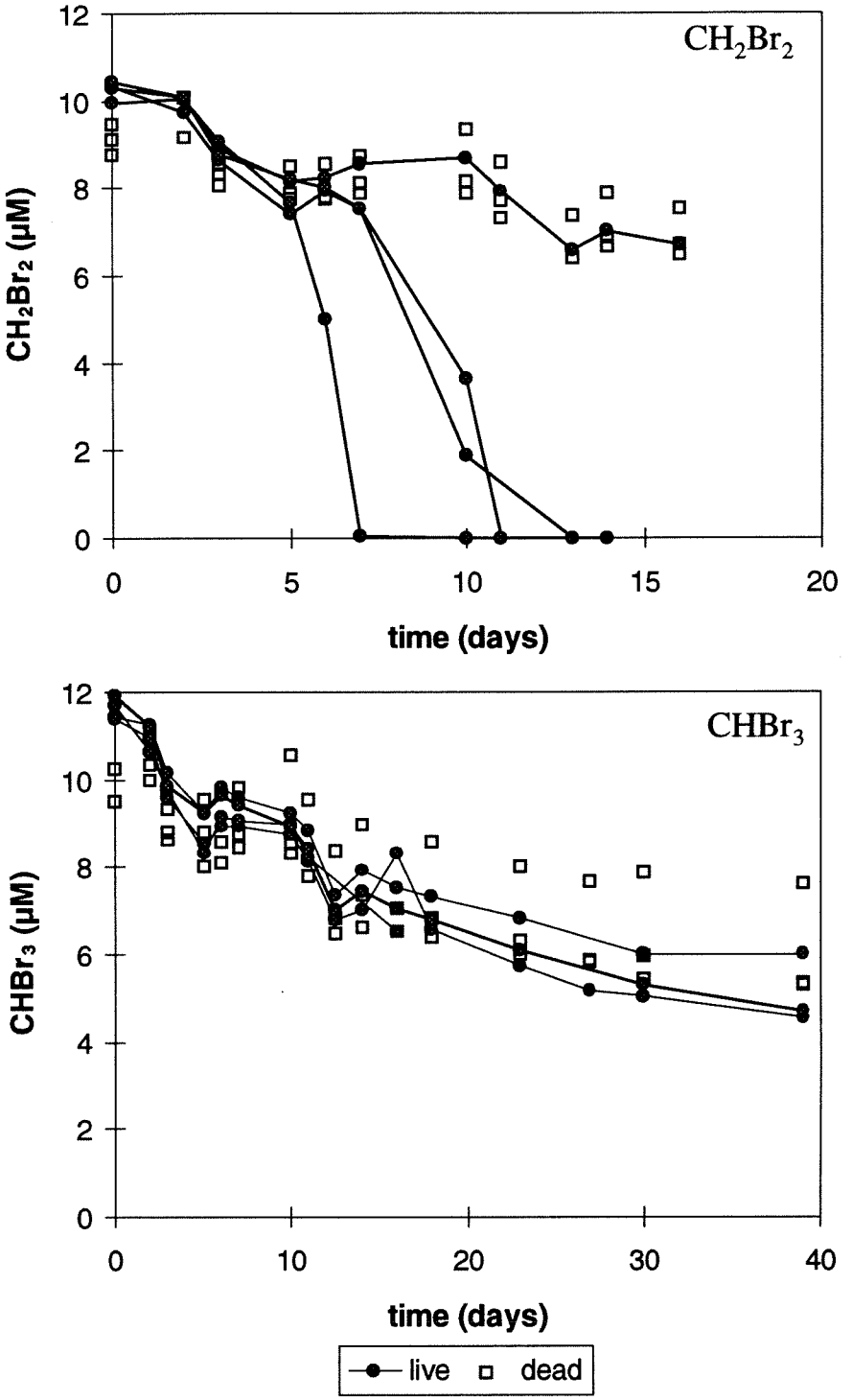

Figure 4.8. Marine microbial CH_2Br_2 degradation for seawater samples collected 7/5/95 and spiked with both CH_2Br_2 and $CHBr_3$, as Figure 4.7, except higher initial concentrations.

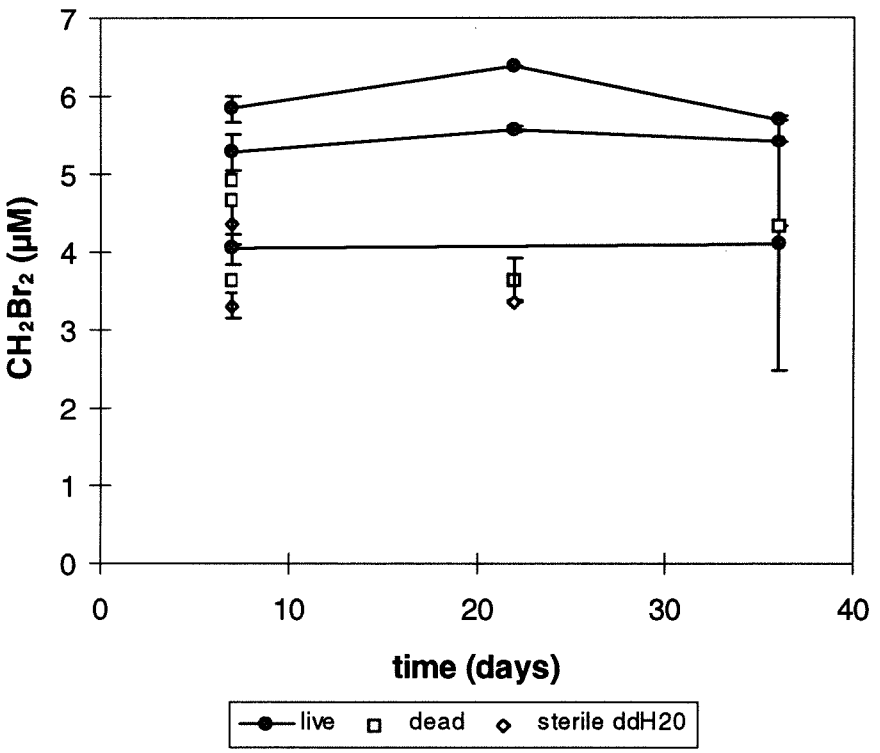

Figure 4.9. Incubation of kelp-bed seawater collected 7/12/93 and spiked with $CHBr_3$ only. Microbial degradation was not observed in replicate seawater samples even after 36 days of incubation. Error bars are range of two headspace injections per sample vial. See Fig. 4.6 for further description.

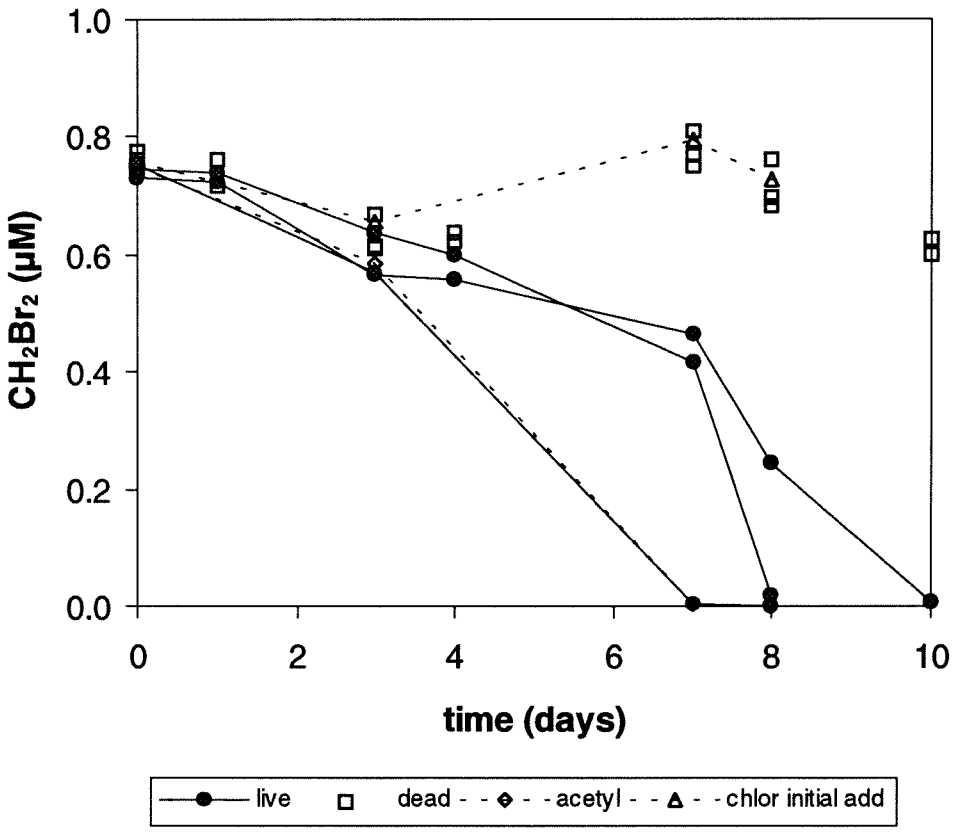

Figure 4.10. Marine microbial CH_2Br_2 degradation for seawater samples collected 5/18/94 and concentrated by reverse filtration. Acetylene ("acetyl"), an inhibitor of monooxygenase enzymes, and chloramphenicol ("chlor"), a prokaryotic protein synthesis inhibitor, were added to certain samples at the start of the incubation. Microbial CH_2Br_2 degradation occurred in the presence of acetylene but not chloramphenicol (see text). "Dead" are formaldehyde killed controls. Concentrations (µM) are water phase.

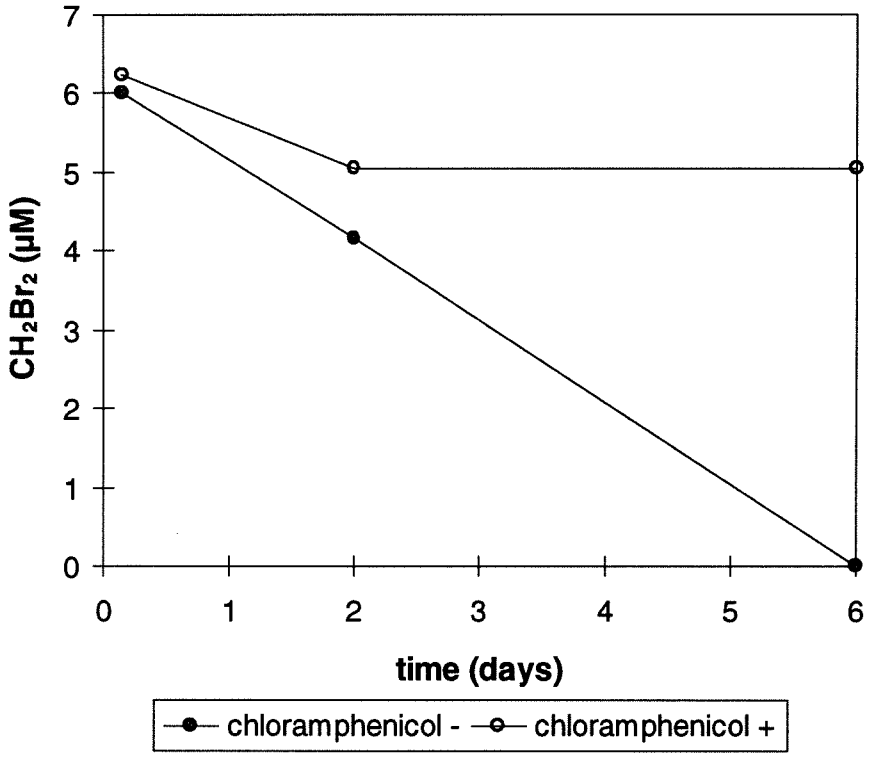

Figure 4.11. Microbial CH_2Br_2 degradation with (+) and without (-) chloramphenicol, a prokaryotic protein synthesis inhibitor. Degradation was not sustained in the chloramphenicol treated sample. Culture was incubated 16 hr with or without chloramphenicol before adding CH_2Br_2. Sample had previously depleted CH_2Br_2 and was incubated an additional eight days without CH_2Br_2 prior to treatment (see text). Kelp-bed seawater originally collected and concentrated by reverse filtration on 5/18/94. Concentrations (µM) are water phase.

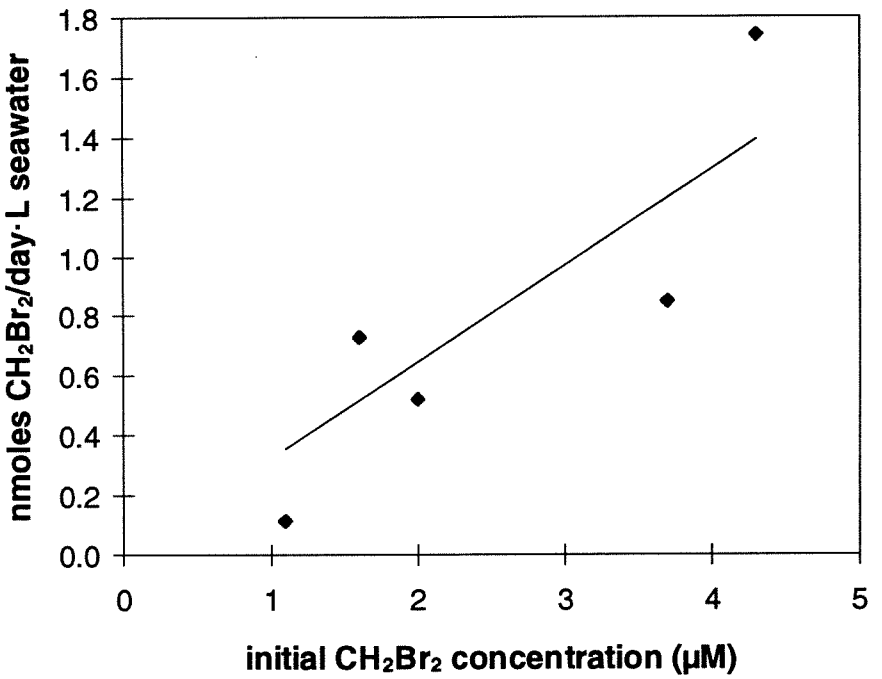

Figure 4.12. Increased microbial CH_2Br_2 degradation rates with increased initial concentration for seawater collected 9/18/93 (Fig. 4.4). The approximately linear rate increase suggests that these CH_2Br_2 concentrations were not saturating. Rates were calculated as described in Table 4.1.

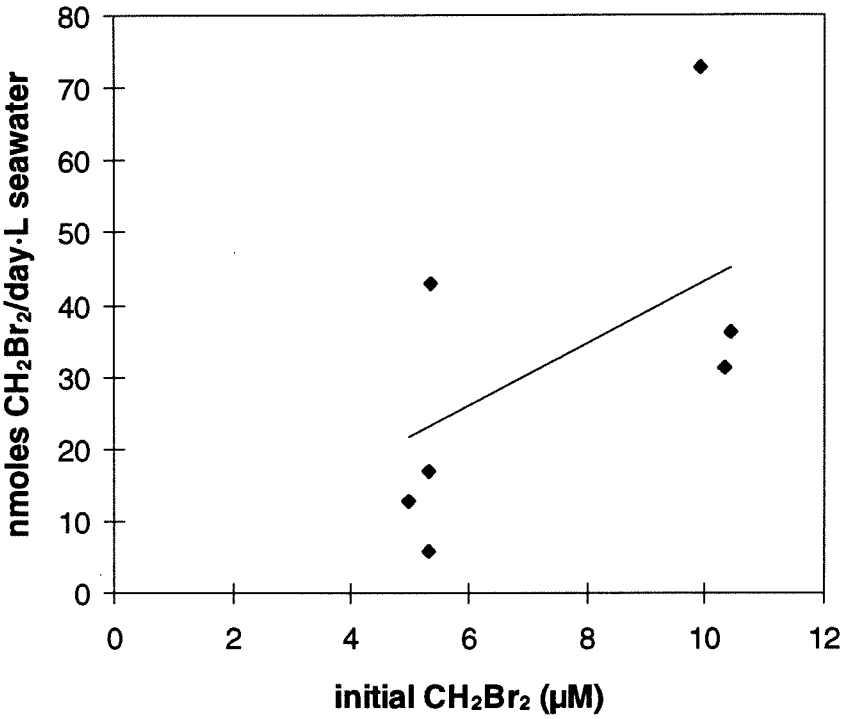

Figure 4.13. Microbial CH_2Br_2 degradation rates versus initial concentration for seawater collected 7/5/95 (Figs. 4.7 - 4.8). Rates tended to increase with initial concentration. Rates calculated as described in Table 4.1.

References

Bailey, J.E. & Ollis, D.F. (1986). *Biochemical Engineering Fundamentals 2nd Ed.* McGraw-Hill, San Francisco.

Bartnicki, E.W. & Castro, C.E. (1994). Biodehalogenation: Rapid Oxidative Metabolism of Mono- and Polyhalomethanes by *Methylosinus trichosporium* OB-3b. *Environ. Toxicol. Chem.* **13**, 241-245.

Bouwer, E.J., Rittmann, B.E. & McCarty, P.L. (1981). Anaerobic Degradation of Halogenated 1- and 2-Carbon Organic Compounds. *Environ. Sci. Technol.* **15**, 596-599.

Braus-Stromeyer, S.A., Hermann, R., Cook, A.M. & Leisinger, T. (1993). Dichloromethane as the Sole Carbon Source for an Acetogenic Mixed Culture and Isolation of a Fermentative, Dichloromethane-Degrading Bacterium. *Appl. Environ. Micro.* **59**, 3790-3797.

Brock, T.D. & Madigan, M.T. (1991). *Biology of Microorganisms 6th Ed.* Prentice Hall, Englewood Cliffs.

Brunner, W., Staub, D. & Leisinger, T. (1980). Bacterial Degradation of Dichloromethane. *Appl. Environ. Micro.* **40**, 950-958.

Chan, E.C.S. & McManus, E.A. (1969). Distribution, Characterization, and Nutrition of Marine Microorganisms from the Algae *Polysiphonia Lanosa* and *Ascophyllum Nodosum. Can. J. Microbiol.* **15**, 409-420.

Chistoserdov, A.Y., Goodwin, K.D. & Lidstrom, M.E. (1995). Isolation and Preliminary Characteristics of Marine Methylotrophic Bacteria. *8th International Symposium on Microbial Growth on C-1 Compounds* (Abstract).

Cundell, A.M., Sleeter, T.D. & Mitchell, R. (1977). Microbial Populations Associated with the Surface of the Brown Alga *Ascophyllum nodosum. Microbial Ecology* **4**, 81-91.

De Vooys, C.G.N. (1979). Primary Production in Aquatic Environments. In *The Global Carbon Cycle* (Bolin, B., Degens, E.T., Kempe, S. and Ketner, P. eds.), John Wiley & Sons, NY, pp. 259-292.

Doronina, N.V. & Trotsenko, Y.A. (1994). *Methylophilus leisingerii* sp. nov., a New Species of Restricted Facultatively Methylotrophic Bacteria. *Microbiol.* **63**, 298-302.

Fenical, W. (1981). Natural Halogenated Organics. In *Marine Organic Chemistry* (Duursma, E.K. and Dawson, R. eds.), Elsevier Scientific, Amsterdam, pp. 375-392.

Geen, C.E. (1992). Selected Marine Sources and Sinks of Bromoform and Other Low Molecular Weight Organobromines. M.S. Thesis, Dalhousie University Halifax, Nova Scotia.

Gossett, J.M. (1987). Measurement of Henry's Law Constants for C_1 and C_2 Chlorinated Hydrocarbons. *Environ. Sci. Technol.* **21**, 202-208.

Gribble, G.W. (1992). Naturally Occurring Organohalogen Compounds - A Survey. *Journal of Natural Products* **55**, 1353-1395.

Harder, W., Attwood, M. & Quayle, J.R. (1973). Methanol Assimilation by Hyphomicrobium spp. *J. Gen. Microbiol.* **78**, 155-163.

Hartmans, S., Schmuckle, A., Cook, A. & Leisinger, T. (1986). Methyl Chloride: Naturally Occurring Toxicant and C-1 Growth Substrate. *J. Gen. Microbiol.* **132**, 1139-1142.

Jackson, G.A. & Winant, C.D. (1983). Effect of a Kelp Forest on Coastal Currents. *Cont. Shelf Res.* **2**, 75-80.

Kaska, D.D., Polne-Fuller, M. & Gibor, A. (1991). Biotransformation of Alkanes and Haloalkanes by a Marine Amoeba. *Appl Microbiol. Biotechnol.* **34**, 814-817.

Kirchman, D.L. (1993). Particulate Detritus and Bacteria in Marine Environments. In *Aquatic Microbiology An Ecological Approach* (Ford, T.E. ed.), Blackwell Scientific Publications Inc., Boston, pp. 321-341.

Kohler-Staub, D. & Leisinger, T. (1985). Dichloromethane Dehalogenase of *Hyphomicrobium* sp. Strain DM2. *J. Bacteriol.* **162**, 676-681.

Koop, K., Carter, R.A. & Newell, R.C. (1982). Mannitol-Fermenting Bacteria as Evidence for Export from Kelp Beds. *Limnol. Oceanogr.* **27**, 950-954.

LaPat-Polasko, L.T., McCarty, P.L. & Zehnder, A.J.B. (1984). Secondary Substrate Utilization of Methylene Chloride by an Isolated Strain of *Pseudomonas* sp. *Appl. Environ. Micro.* **47**, 825-830.

Leisinger, T. & Bader, R. (1993). Microbial Dehalogenation of Synthetic Organohalogen Compounds: Hydrolytic Dehalogenases. *Chimia* **47**, 116-121.

Leisinger, T., La Roche, S., Bader, R., Schmid-Appert, M., Braus-Stromeyer, S. & Cook, A.M. (1993). Chlorinated Methanes as Carbon Sources for Aerobic and Anaerobic Bacteria. In *Microbial Growth on C_1 Compounds* (Murrell, J.C. and Kelly, D.P. eds.), Intercept Ltd., Andover, pp. 351-363.

Linley, E.A.S., Newell, R.C. & Bosma, S.A. (1981). Heterotrophic Utilisation of Mucilage Released During Fragmentaion of Kelp (*Ecklonia maxima and Laminaria pallida*). I. Development of Microbial Communities Associated with the Degradation of Kelp Mucilage. *Mar. Ecol. Prog. Ser.* **4**, 31-41.

Lucas, M.I., Newell, R.C. & Velimirov, B. (1981). Heterotrophic Utilisation of Mucilage Released During Fragmentation of Kelp (*Ecklonia maxima* and *Laminaria pallida*). II. Differential Utilisation of Dissolved Organic Components from Kelp Mucilage. *Mar. Ecol. Prog. Ser.* **4**, 43-55.

Mabey, W. & Mill, T. (1978). Critical Review of Hydrolysis of Organic Compounds in Water Under Environmental Conditions. *J. Phys. Chem. Ref. Data* **7**, 383-409.

Manley, S.L., Goodwin, K. & North, W.J. (1992). Laboratory Production of Bromoform, Methylene Bromide, and Methyl Iodide by Macroalgae and Distribution in Nearshore Southern California Waters. *Limnol. Oceanogr.* **37**, 1652-1659.

Mazure, H.G.F. & Field, J.G. (1980). Density and Ecological Importance of Bacteria on Kelp Fronds in an Upwelling Region. *J Exp. Mar. Biol. Ecol.* **43**, 173-182.

Moore, R.M. & Tokarczyk, R. (1993). Volatile Biogenic Halocarbons in the Northwest Atlantic. *Glob. Biogeochem. Cycles* **7**, 195-210.

North, W.J. (1971). Introduction and Background. In *The Biology of Giant Kelp Beds (Macrocystis) in California.* Beihefte Zur Nova Hedwigia 32 (North, W.J. ed.), Verlag Von J. Cramer, Lehre, Germany, pp. 1-97.

North, W.J. (1994). Review of *Macrocystis* Biology. In *Biology of Economic Algae* (Akatsuka, I. ed.), SPB Academic Publishing, Hague, Netherlands, pp. 447-527.

Oppenheimer, C.H. (1961). *Symposium on Marine Microbiology.* Charles C. Thomas Publ., Springfield.

Oremland, R.S., Miller, L.G., Culbertson, C.W., Connell, T.L. & Jahnke, L. (1994a). Degradation of Methyl Bromide by Methanotrophic Bacteria in Cell Suspensions and Soils. *Appl. Environ. Micro.* **60**, 3640-3646.

Oremland, R.S., Miller, L.G. & Strohmaier, F.E. (1994b). Degradation of Methyl Bromide in Anaerobic Sediments. *Environ. Sci. Technol.* **28**, 514-520.

Oremland, R.S. & Capone, D.G. (1988). Use of "Specific Inhibitors" in Biogeochemistry and Microbial Ecology. In *Adv. Microbial Ecology 10* (Marshall, K.C. ed.), Plenum Publish. Co., NY, pp. 285-383.

Poindexter, J.S. (1992). Dimorphic Prosthecate Bacteria: The Genera *Caulobacter, Asticcacaulis, Hyphomicrobium, Pedomicrobium, Hyphomonas,* and *Thiodendron.* In *The Prokaryotes. A Handbook on the Biology of Bacteria: Ecophysiology, Isolation, Identification, Applications. Vol. III.* (Balons, A., Truper, H.G., Dworkin, M., Harder, W. and Schlerfer, K. eds.), Springer-Verlag, New York, pp. 2177-2196.

Ramanathan, V., Cicerone, R.J., Singh, H.B. & Kiehl, J.T. (1985). Trace Gas Trends and Their Potential Role in Climate Change. *J. Geophys. Res.* **90**, 5547-5566.

Rasche, M.E., Hyman, M.R. & Arp, D.J. (1990). Biodegradation of Halogenated Hydrocarbon Fumigants by Nitrifying Bacteria. *Appl. Environ. Micro.* **56**, 2568-2571.

Schlegel, H.G. (1993). *General Microbiology.* Cambridge University Press, Cambridge, UK.

Scholtz, R., Wackett, L.P., Egli, C., Cook, A.M. & Leisinger, T. (1988). Dichloromethane Dehalogenase with Improved Catalytic Activity Isolated from a Fast-Growing Dichloromethane-Utilizing Bacterium. *J. Bacteriol.* **170**, 5698-5704.

Scotten, H.L. (1971). Microbiological Aspects of the Kelp Bed Environment. In *The Biology of Giant Kelp Beds (Macrocystis)* in California. Beihefte Zur Nova Hedwigia 32 (North, W.J. ed.), J. Cramer, Lehre, Germany, pp. 315-318.

Sheridan, P.J., Schnell, R.C., Zoller, W.H., Carlson, N.D., Rasmussen, R.A., Harris, J.M. & Sievering, H. (1993). Composition of Br-Containing Aerosols and Gases Related to Boundary Layer Ozone Destruction in the Arctic. *Atmospheric Environment* **27A**, 2839-2849.

Sieburth, J.M. (1988). The Trophic Roles of Bacteria in Marine Ecosystems are Complicated by Synergistic-Consortia and Mixotrophic-Cometabolism. *Prog. Oceanog.* **21**, 117-128.

Singh, H.B., Salas, L.J. & Stiles, R.E. (1983). Methyl Halides In and Over the Eastern Pacific (40 N - 32 S). *J Geophys. Res.* **88**, 3684-3690.

Staley, J.T. (1968). *Prosthecomicrobium* and *Ancalomicrobium:* New Prosthecate Freshwater Bacteria. *J. Bacteriol.* **95**, 1921-1942.

Stirling, D.I. & Dalton, H. (1979). The Fortuitous Oxidation and Cometabolism of Various Carbon Compounds by Whole-Cell Suspensions of *Methylococcus Capsulatus* (Bath). *FEMS Micro. Biol. Lett.* **5**, 315-318.

Stucki, G., Gälli, R., Ebersold, H-R. & Leisinger, T. (1981). Dehalogenation of Dichloromethane by Cell Extracts of *Hyphomicrobium* DM2. *Arch. Microbiol.* **130**, 366-371.

Sturges, W.T., Cota, G.F. & Buckley, P.T. (1992). Bromoform Emission from Arctic Ice Algae. *Nature* **358**, 660-662.

Tse, G., Orbey, H. & Sandler, S.I. (1992). Infinite Dilution Activity Coefficients and Henry's Law Coefficients of Some Priority Water Pollutants Determined by a Relative Gas Chromatographic Method. *Environ. Sci. Technol.* **26**, 2017-2022.

van der Leeden, F., Troisc, F.L. & Todd, D.K. (1990). *Water Encyclopedia 2nd Ed.*. Lewis Publishers, Chelesa, MI.

Whittenbury, R.K., Philips, K.D. & Wilkinson, J.F. (1970). Enrichment, Isolation and Some Properties of Methane-Utilizing Bacteria. *J Gen. Microbiol.* **61**, 205-218.

Yanagita, T. (1990). *Natural Microbial Communities: Ecological and Physiological Features*. Springer-Verlag, Berlin.

Chapter Five

Macrocystis Pyrifera Biomass and Production of Brominated Methanes *In Situ*

Introduction

Macrocystis Biology and Ecology

Macrocystis (or Giant Kelp) occurs in both hemispheres along temperate-water coasts. All major land masses in the southern hemisphere except Antarctica have *Macrocystis* stands (Australia, New Zealand, South Africa, and both coasts of South America) (De Vooys 1979). The overview of *Macrocystis* biology and ecology given here is based on detailed descriptions provided by North (1971, 1982, 1994). The genus *Macrocystis* belongs to Phylum Phaeophyta, Class Heterogeneratae, Order Laminariales, and Family Lessoniaceae with four species generally recognized, *M. integrifolia*, *M. angustifolia*, *M. pyrifera*, and *M. laevis*. *Macrocystis* in the northern hemisphere extends only along the northeast Pacific coast. *M. integrifolia* in North America occurs from Sitka, Alaska to Point Conception, California (CA). *M. angustifolia* overlaps the *M. integrifolia* range near Santa Cruz and formerly occurred as far south as Camp Pendleton, CA. *M. pyrifera* occurs at least as far north as Monterey Bay, and presently is the only *Macrocystis* species from Palos Verdes to Punta San Hipolito in Baja California. *Macrocystis* is the dominant alga in its depth range south of Point Conception. It shares dominance north of Point Conception with another canopy forming alga, *Nereocystis luetkeana* (Bull Kelp). *M. laevis* occurs only at Marion Island in the Indian Ocean (North 1994).

Kelp beds are a valuable economic and ecological resource. *Macrocystis* is harvested in the U.S. primarily to produce alginic acid or alginate. Alginate serves as a thickening, stabilizing, or emulsifying agent in a variety of products, including foods and beverages. Kelp beds also support rich marine communities providing food, shelter, and substrate for resident organisms. Commercial and recreational fishing and scuba diving industries capitalize on these resources. Drift kelp provide organic material to deep oceanic regions. The economic value of kelp beds has motivated several past studies of *Macrocystis* biology and ecology in order to understand and manage this resource.

Macrocystis species are distinguished primarily by holdfast and blade characteristics. An adult *Macrocystis* plant is comprised of numerous fronds of various lengths and ages. Fronds can grow to lengths of 60 m (200 ft). A plant may live several years while individual fronds have life-spans of about six months. Plants typically occur in depths of 8-20 m but may grow at 30 m depths in water of exceptional clarity. Plants are anchored by a basal holdfast, usually attached to rocky substrates. Holdfasts can attach to sedimentary bottoms in well-protected locations.

A frond is composed of laminae, pedicels, pneumatocysts (bulbs), and a vine-like stipe (Figure 5.1). Laminae are leaf-like structures connected to gas-filled pneumatocysts; a blade is a lamina plus pneumatocyst and pedicel. Pneumatocysts provide buoyancy to the frond and are attached by pedicels to the approximately ½ cm diameter stipe. Blades specializing in spore production (sporophylls) occur at the frond base just above the holdfast. The apical meristem located at the frond tip forms new blades and stipe tissue. Stipe elongation continues throughout the frond lifespan pushing the apical meristem upward. A terminal blade forms if the frond eventually ceases growth. *Macrocystis*

fronds can elongate up to 24 inches per day (W.J. North, personal communication) making it one of the fastest growing plants in the world (Clendenning 1971). Vigorous tissue formation occurs in the distal 2-3 m of a frond while remaining mature tissues grow slowly or not at all.

Fronds grow upward to the water surface, thence horizontally along the surface forming the canopy of the kelp "forest." Continuous canopies normally form after frond densities reach two or more fronds per square meter of substratum. Usually more than half the blades of a mature frond occur in the canopy region (North 1982), and 47-60% of plant biomass, excluding the holdfast, occurs there (McFarland and Prescott 1959). Kelp canopy shading severely limits growth of underlying bottom vegetation. Canopy fronds also shade their own plant tissues. Translocated photosynthetic products overcome the self-shading problem. Kelp blades are the primary photosynthetic tissues, although all tissues can photosynthesize (Clendenning 1971) and accumulate nutrients (North 1982).

Macrocystis Biomass Estimates

Algal biomass estimates can be used to monitor changes in kelp bed density caused by climate, pollution, and harvesting practices. Biomass estimates were needed in this work to extrapolate laboratory measurements of macroalgal brominated methane release to a regional scale (Chapter 3) and to compare macroalgal production and microbial degradation of brominated methanes in the kelp-bed ecosystem (Chapter 4).

Algal biomass estimates fall into two categories, standing crop (i.e., plant cover) and numerical counts (i.e., plant population) (Schiel and Foster 1986). North *et al.* (1993), for example, present a 25-year record of *Macrocystis* standing crop. This record is based on aerial photographs taken from 1967 to 1991 in Orange and San Diego

Counties. Plant and frond density measurements have also been used to characterize *Macrocystis* populations (North 1971, pp. 124-168; Gerard 1984). Plant counts alone do not estimate biomass density adequately because adult plants vary greatly in size and plant distributions may be aggregated. More accurate estimates assess mean numbers of fronds per substratum (fronds/m^2) and average mass of a frond (kg/frond). These parameters together give the biomass density (kg/m^2). We determined frond size distributions by randomly collecting and measuring masses and lengths of many fronds. The mean frond mass varies with depth and season but is about 1 kg/frond for common bed depths (10-20 m). Biomass densities of kelp stands situated at 10-20 m depths can thus be estimated roughly by multiplying the number of fronds/m^2 by one kg mass per frond (North 1994).

In Situ Algal Measurements

Monitoring a biological system risks changing its behavior. This problem is particularly acute for an immense marine organism such as *Macrocystis*. The plant must be enclosed to monitor its physiology, whether that be carbon fixation, respiration, or brominated methane production. Care was taken to minimize stress and damage to whole blades of *M. pyrifera* used in laboratory incubations described in Chapter 3. Additional incubations were conducted *in situ* to evaluate feasibility of field experiments and compare *in situ* and laboratory results. We incubated frond portions *in situ* to identify scale-up problems before conducting intensive laboratory incubations. This preliminary work enabled design of laboratory whole blade incubations to ensure consistency with future *in situ* frond incubations and improve result comparisons. Advantages of *in situ* experiments include natural light and temperature and avoidance of transport or tissue cutting. *In situ*

marine incubations, however, are difficult because they require substantial boat time, conducting incubations in ocean swell, and planning around favorable weather conditions.

Other researchers have enclosed *M. pyrifera* tissue in plastic bags for various *in situ* measurements. Towle and Pearse (1973) estimated primary production by measuring *in situ* ^{14}C incorporation into blades enclosed for 3 hr in polyethylene bags. Gerard (1982) measured *in situ* nitrate uptake rates by enclosing *M. pyrifera* blades in polyethylene bags for up to 2.2 hr. She found no difference in nitrate uptakes rates for bags shaken only by water motion versus those continuously shaken by divers.

Materials and Methods

Biomass Estimates

Biomass estimates were derived from field and laboratory information. The *M. pyrifera* kelp bed adjacent to Laguna Beach, CA was sampled during summers of 1990 to 1991. Laboratory work was performed during summers of 1990 to 1992. Frond density (number of fronds/m^2) was determined in July and August 1990 from six circular quadrats (6 m diam, 28.27 m^2) randomly placed near the inshore edge of the Laguna kelp bed. A permanent nylon rope transect was placed in the kelp bed approximately along a bottom contour to guide SCUBA divers to experimental plants. Plants lying within 2-3 m of the transect line were marked with numbered tags tied to holdfasts. A transect was laid in 9-10 m of water during 1990. The canopy in that location disappeared, thus a new line was laid at about 14-m depth during 1991.

One hundred plants were tagged along the 61 m of the 1991 transect line. The position of each plant relative to the transect line was mapped by Dr. W.J. North; from

this the area of the experimental plot was estimated (362 m^2). Frond density (as fronds/m^2) was determined by counting numbers of stipes per plant in the experimental area. Multiple visits were necessary to determine stipe numbers on all tagged plants. Total stipe numbers were determined during July to August 1991 (7/15, 8/12, 8/13, 8/20) and again during October 1991 (10/2, 10/16).

Frond lengths were measured underwater after disentangling fronds from one another. Numbers of fronds of a particular length were estimated by measuring lengths in 2-m increments for all fronds (n=264) on ten tagged plants (11/2/91, 11/20/91). The frond length distribution was obtained by dividing the number of fronds for each length by the total number of fronds.

Fronds with an apical meristem were removed from untagged plants at the holdfast and returned to the laboratory for weight, length, and area measurements. Fronds free of visible epiphytes were chosen whenever possible. Bryozoans, when present, were scraped off before laminae were weighed. Excessive evaporation was minimized by keeping fronds covered and wet during transport to the laboratory and thereafter by keeping fronds in flowing seawater until used. Laminae were pinched from the bulb and gently patted (not wiped) to remove excess water droplets before weighing. Frond length, lamina mass and area, stipe and bulb mass, bulb number, and number of bulbs per meter were measured. Each lamina was weighed and then area was determined by a LI-COR area meter. Frond laminae were analyzed in order from proximal to distal end, noting any missing blades. Biomass estimates did not include approximations of missing blade mass.

The average frond mass (or expected frond mass) was calculated as the product of the frond length distribution and the average frond mass in a length class according to the following:

$$\overline{m} = \sum_i m_i \cdot \Pr(x = x_i) \tag{5.1}$$

where x_i is frond length (m), m_i is average mass of a frond of length x_i (kg), $\Pr(x = x_i)$ is the probability that a frond is of length x_i, and $\overline{m}$ is the average frond mass (kg). The frond length distribution ($\Pr(x = x_i)$) was determined from field measurements and the average frond mass in a length class (m_i) came from laboratory measurements. The proportion of mass in the kelp bed corresponding to fronds of a particular length was determined from the following:

$$f(x_i) = \frac{m_i \cdot \Pr(x = x_i)}{\overline{m}} \tag{5.2}$$

where $f(x_i)$ is the proportion of mass corresponding to fronds of length x_i.

Biomass area density (kg/m^2) was estimated by multiplying the average frond mass (kg/frond) by frond density (fronds/m^2). Biomass volume density (kg/m^3) averaged over the water column was calculated by dividing biomass density by the average water-column depth. Biomass volume density (kg/m^3) was also determined for different vertical sections of the kelp bed by accounting for the vertical distribution in biomass. The vertical biomass distribution was derived from bulb numbers per meter of frond and corresponding blade weights. The relationship between stipe length and stipe weight was linear (data not shown); stipe weight was proportioned accordingly. The proportion of kelp biomass above and below 4 m depth was calculated in the same manner as for average frond mass. For example, to calculate the proportion of biomass found above 4 m depth, replace m_i in

equation 5.2 above (the average mass of a frond of length x_i) with the average mass found above 4 m depth for fronds of each length.

In Situ Production Measurements

The upper 2-4 ft of *M. pyrifera* fronds were enclosed while still attached to the plant in either mylar or polyethylene bags. Fronds from five plants were incubated for 2 hr *in situ* in Laguna Beach or Dana Point kelp beds (7/12, 7/30, 8/3, and 8/10/93). Bags were sealed around stipes with large rubber bands or cable ties and tied to buoys to prevent sinking. Control bags were treated similarly except they contained no kelp. Fronds were severed from plants at the end of the experiment. Bags were sealed and returned to the laboratory where water volumes and kelp mass were measured. Surface seawater temperatures for all experiments were between 20-20.5 °C (68-69 °F).

Each bag was equipped with a septum port for sampling seawater *via* syringe at specified times. Samples were transferred immediately into amber-colored glass, screw-top bottles (240 or 125 ml) with Teflon-faced silicone septa. Bottles were filled without headspace and transported on ice to the laboratory where they were stored upside down at 4 °C. Within 48 hr, N_2 headspace was introduced into the bottles while simultaneously removing seawater. Seawater to headspace ratio was 6:1. Bottles were shaken upside down for at least 2 hr at 28 °C prior to headspace sampling. Headspace samples (100 µl) were injected into an electron-capture gas chromatograph (Shimadzu 14A ECD-GC; column: Restek Rtx-502.2, 60 m x 0.32 mm x 1.8 µm film thickness; typical temperature program: 90 °C for 3 min, ramp 20 °C/min to 190 °C for 10 min; 0.3 min splitless). CH_2Br_2 and $CHBr_3$ standards were made from neat compound (Alltech) diluted into

hexane (Burdick and Jackson). Halomethane production rates were calculated as described in Chapter 3 for a manual injection system.

Mylar bags were made from rolled sheet plastic heat-sealed to desired dimensions. Bag design was relatively long and narrow. A typical size was 4 ft x 1 ft. Bags of up to 6 ft long were tested, but they were too cumbersome in the swell. Manufactured polyethylene bags had dimensions of 1.4 ft x 1 ft.

Plastic and glass syringes were compared to see whether plastic was adequate with respect to leakage and contamination. Syringes were rinsed with ddH_20 and baked at 80 °C overnight prior to use. Kelp was incubated for 2 h prior to seawater removal by both glass (Baxter, 50 ml) and plastic syringes with rubber-tipped plungers (B-D sterile syringes, 60 ml).

Results and Discussion

Macrocystis Biomass

The mean frond density (± SD) determined by random quadrat sampling in 1990 was 11.6 ± 4.5 fronds/m^2. The mean 1991 frond density determined by counting stipes within the experimental area was 4.67 ± 0.55 (Table 5.1). These frond densities are within the range observed for *Macrocystis* beds in CA. North (1971, p. 46) measured frond densities ranging from 1.9 to 15 fronds/m^2 for sample areas of at least 100 m^2. The high *Macrocystis* frond density in 1990 reflected a particularly productive year. Recorded canopy coverage determined by aerial photography was higher in 1990 than in any previous year between 1967 and 1991 in Orange and San Diego Counties (North *et al.*

1993). The maximum yearly canopy reported for Laguna Beach was 0.277 km^2 in 1990. The canopy coverage fell to 0.121 km^2 in 1991 (North *et al.* 1993).

The average mass of a frond was calculated from the frond length distribution (Figure 5.2) and the relationship of frond length to frond mass (Figure 5.3). The frond length distribution was derived from field measurements of 264 fronds from ten plants. The relationship of frond length to frond mass was derived from laboratory measurements of 42 fronds. Combining these field and laboratory measurements, the estimated average fresh mass of a frond was 1.1 kg/frond (Table 5.2). This value is in close agreement with results from other researchers. North (1971, p. 45) computed an average frond mass of 1-1.5 kg/frond for samples in the vicinity of San Diego in the late 1950's, and Towle and Pearse (1973) computed 1.16 kg/frond for fronds in Monterey Bay. Gerard (1976) calculated 1-1.3 kg/frond, finding greater average frond mass during the spring and summer due to seasonal changes in frond length distribution. The frond length distribution may also change with depth, but 1 kg/frond remains a good estimate for kelp stands situated at about 10-20 m depths (North 1994).

Biomass density for Laguna Beach *Macrocystis* was 5.1 kg/m^2 in 1991 calculated as the product of the average frond density (kg/m^2) and the average frond mass (Table 5.2). This number closely agrees with results of several researchers for other locations. North (1982) listed a biomass density range of 3-22 kg/m^2 with a mean of about 6 kg/m^2 for *Macrocystis* in CA and Baja California in the late 1950's. Aleem (1956) reported a biomass range of 5-9 kg/m^2 for La Jolla, and McFarland and Prescott (1959) reported 5.78 kg/m^2 for Paradise Cove. Towle and Pearse (1973) reported a biomass range of 5.9

kg/m^2 for Monterey Bay (5.1 fronds/m^2·1.16 kg/frond). It seems that 6 kg/m^2 is good estimate of typical biomass density for *Macrocystis*.

Macrocystis biomass is not uniformly distributed within the water column; it grows so that the majority of photosynthetic tissues lie in the region of maximum illumination. Internode lengths (distance between adjacent pneumatocysts) are longer at the frond base than at apex. Although there is considerable variability, there are more blades near the distal end of a frond (North 1971, p. 29). Longer fronds were found to have proportionally more biomass, particularly laminal biomass, in the upper part of the water column compared to shorter fronds (Figure 5.4). The relationship between laminal mass and laminal area was essentially linear (Figure 5.5; $r^2 = 0.91$, n = 1956 laminae from 24 fronds). Jackson *et al.* (1985) found a similar relationship. They concluded that area and mass are nearly equivalent measures of laminal tissue, given the small deviation from linearity. Laminae reach their maximum size near the middle of a frond (Jackson *et al.* 1985), thus middle frond portions will be heaviest.

The frond length distribution reflects initiation and growth rates (Jackson *et al.* 1985) and is thus expected to be influenced by a variety of environmental factors. Jackson *et al.* (1985), however, found that the simple relationship of water depth to maximum frond length accounted for 87% of their sample variance. We observed a similar trend. The frond length distribution (Figure 5.2) showed frequent occurrences of small, young fronds (< 2 m) and fronds that were about as long as the water was deep (12-14 m). However, the proportion of biomass in each frond class (Figure 5.6) clearly shows that most of the biomass is in fronds with lengths near the water depth (14 m). This occurred because smaller fronds, although frequent (Figure 5.2), contain less mass. Such a

distribution suggested that fronds reach the water surface and perhaps then cease growth in response to environmental cues. Fronds in summer might cease growth because of warm surface temperatures; 30-40 ft long frond portions are often encountered during winter and early spring (W.J. North personal communication).

Biomass volume density averaged over the entire water column was determined by dividing biomass area density (kg/m^2) by average water depth. Average biomass volume density was 0.37 kg/m^3 (5.1 kg/m^2 over a 14 m depth) for Laguna Beach *Macrocystis* in 1991. The estimated biomass density using "typical" values of 6.0 kg/m^2 and a 15 m water depth (average beds are 10-20 m) was 0.40 kg/m^3 (Table 5.2). Average biomass volume density was used to convert halomethane production on a per weight kelp basis roughly to production on a per volume seawater basis (ng/gfwt·day to ng/(m^3 kelp-bed seawater)·day) (Chapter 4). Such a conversion is most useful if the water column is fully mixed because kelp densities averaged over the whole water column do not reflect the actual vertical distribution of biomass. Full vertical mixing is most likely to occur during upwelling events or large storms. Upwelling is strongest during periods of dominant north and northwest winds which normally occur in May and June for southern and central California and in June and July for northern California (Newberger 1982).

Kelp bed waters are usually not fully mixed over the water column. Stratification is evident by thermocline existence. Thermoclines in kelp beds often occur at 4-6 m depth (W.J. North, personal communication). Dye dispersal studies conducted in the Laguna Beach kelp bed during November and December 1980 addressed vertical mixing in kelp beds (W.J. North, unpublished data). The dye cloud stabilized between 5-6.5 m depth within the bed and at about 3 m outside the bed. Vertical circulation within the bed

appeared to be complicated by presence of large plants. The dye cloud mixed to the bed bottom (12.5 m) when stalled against dense clusters of kelp fronds.

The vertical biomass distribution for fronds collected in 1991 was analyzed to determine biomass density above and below a given stratification level. The upper 4 m of bed was assumed vertically well-mixed. This assumption is presumably conservative based on the information presented above. Biomass in the upper 4 m was compared to the underlying 10 m of the water column, excluding holdfast. Not all fronds reach the upper 4 m, and fronds extending to the upper 4 m have a proportion of biomass within that region and a proportion below. The upper 4 m accounted for 40% of total frond biomass with 60% in the lower 10 m. Comparing laminal tissues only, 51% of the laminal biomass occurred in the upper 4 m of the bed. Although the majority of biomass occurred in fronds nearly as long as the water depth (12-14 m; Figure 5.6), biomass in those fronds was fairly evenly distributed above and below 4-m depth (Figure 5.4). Fronds longer than 14 m had proportionally more biomass in the region above 4 m (Figure 5.4), but their frequency was less than that of the 12-14 m class (Figure 5.2).

Biomass volume density was proportioned into densities above and below 4 m depth. The density in the upper 4 m was 0.51 kg/m^3 (40% of 5.1 kg/m^2 in 4 m). Biomass density in the lower 10 m was 0.31 kg/m^3 (60% of 5.1 kg/m^2 in 10 m). Using this vertical distribution of biomass with the "typical" biomass density of 6 kg/m^2 in the "typical" 15 m kelp bed, biomass density was 0.60 kg/m^3 in the upper 4m and 0.33 kg/m^3 in the lower 11 m. McFarland and Prescott (1959) found 47-60% of plant biomass, excluding the holdfast, to occur in the canopy region. Only 40% of the biomass was located in the upper 4 m of the Laguna Beach bed in this study which probably reflects a decline in

canopy biomass associated with southern California summer-time temperature and nutrient conditions (W.J. North, personal communication).

In Situ Brominated Methane Production

M. pyrifera production of $CHBr_3$ and CH_2Br_2 was measured *in situ* (Figures 5.7-5.9; Table 5.3). Detection limits were approximately 160 ng/L $CHBr_3$ and 50 ng/L CH_2Br_2 in seawater using a standard ECD-GC without cryogenic or vacuum concentration. The mean $CHBr_3$ concentration measured in control bags was 254 ± 82 ng/L (± SD, n=3). Dibromomethane concentrations in control bags were below detection. Brominated methane production in controls was not observed.

In situ production rates of $CHBr_3$ and CH_2Br_2 was similar to laboratory production by whole blades (Table 5.4; see Chapter 3 for full discussion of laboratory production results). Median production rates from *in situ* incubations were 256 ng $CHBr_3$/gfwt·day and 41 ng CH_2Br_2/gfwt·day for four incubations performed within a one-month period (12 hr photoperiod; gfwt = g fresh weight). Rates were calculated by linear regression, but samples were removed at only two times for the 7/12/93 incubation (Figure 5.7). Mean production rates were 238 ± 75 ng $CHBr_3$/gfwt·day and 46 ± 35 ng CH_2Br_2/gfwt·day (± SD). The median is a better estimate of the central value for small sample sets (Kennedy 1984). Median production rates for laboratory incubations of whole blades were 171 ng $CHBr_3$/gfwt·day and 48 ng CH_2Br_2/gfwt·day for 19 incubations conducted over a nine-month period. The similar results from the two methods is encouraging and supports the validity of laboratory measurements for estimating brominated methane release from macroalgae.

In situ incubations contained portions of entire fronds (blades and stipes) with fronds still attached to the plant. Laboratory incubations utilized whole blades only. Laminae comprised the bulk of *M. pyrifera* biomass (Figure 5.3) with bulbs about ½ the combined weight of stipes and bulbs (W.J. North, personal communication). Blades thus presumably comprised most of the biomass and tissue surface in *in situ* incubations. *M. pyrifera* stipes were not separately tested for brominated methane production; however, other macroalgal species produced brominated methanes from various morphological structures (Laturnus *et al.*, submitted for publication). Rates varied for the different structures and differed among algal species, thus it would be difficult to generalize those results to *Macrocystis*.

These preliminary *in situ* production studies were undertaken to assess the feasibility of field experiments. Glass syringes were used previously in field work (Chapter 2), but plastic syringes are more convenient. The feasibility of using plastic was therefore tested. Seawater contacted syringes for only a few minutes before transfer to septa vials. Seawater CH_2Br_2 concentrations were similar for both plastic and glass syringes. Bromoform concentrations were slightly lower in seawater removed by glass syringes than by plastic (Table 5.5). Seawater removed from control bags by plastic syringes did not exhibit interfering chromatographic peaks. Plastic syringes where easier to use and they appeared to provide a better air-tight seal. Overall, plastic syringes were more convenient and performed adequately, thus they were used instead of glass in subsequent laboratory experiments.

Frond incubations *in situ* appeared to adequately estimate macroalgal halomethane production, in spite of certain pitfalls. Bag strength was the greatest problem. Mylar

proved inadequate because it tended to split lengthwise. The heat-sealed seams were typically stronger than the material itself. Polyethylene performed better than mylar. Although polyethylene did fail while hoisting onto the boat, failures were small punctures instead of catastrophic lengthwise splits. A thick polyethylene (e.g., 6 mil) should withstand moderate swell and wind chop and probably could withstand transfer to the boat. A platform designed to hoist bags would be advisable. The ideal structure would keep the entire bag flat while draining excess seawater during lift. Broken bags were repaired upon arrival at the marine lab without removing kelp. Bags were then refilled with seawater and volumes measured to estimate experimental volumes.

Water exchange was another problem encountered in the field experiments. Bags were sealed as tightly as possible around stipe bundles, but a complete seal may not have been achieved. Previous *in situ* experiments (e.g., Gerard 1982) only enclosed a single blade thus bags were sealed around a single stipe. Our experiments employed several fronds to ensure that production rates represented averages of several fronds, but sealing around more than one stipe was difficult. Future experiments might benefit from using a single frond per incubation. Large syringe needles (16 gauge) tended to core septa which might have allowed limited water exchange. Smaller gauge needles, however, would increase sampling time. One must minimize septa coring yet sample in a timely manner because samples are collected while treading water.

Conclusions

A variety of biomass parameters were determined from field and laboratory work. *Macrocystis* mean frond density in the Laguna Beach kelp bed was 11.6 ± 4.5 fronds/m^2

(± SD) in 1990, determined by random quadrat sampling. Mean frond density in 1991 was 4.67 ± 0.55, determined by counting stipes in a defined experimental area. The estimated average mass of a frond was 1.1 kg/frond. This value closely agrees with the "typical" value of 1 kg/frond often used to represent fronds in 10-20 m depths. Estimated biomass density was 5.1 kg/m^2 for Laguna Beach *Macrocystis* based on the 1991 frond density. This closely agrees with the "typical" value of 6 kg/m^2 based on this and several other published survey results conducted in kelp beds throughout California.

Estimates of biomass density averaged over the entire water column are most meaningful for conditions of full vertical mixing (e.g., upwelling events). Biomass volume density was an estimated 0.37 kg/m^3 based on the 1991 frond density and averaged over the entire water column (14 m). This result compares well with an average density of 0.40 kg/m^3 estimated from "typical" values of 6 kg/m^2 and a 15 m water depth (average bed depths are 10-20 m). Biomass may also be estimated within and below the mixed zone in the absence of full vertical mixing. A mixed zone thickness of 4 m was assumed here. Approximately 40% of *Macrocystis* biomass occurred in the upper 4 m of the Laguna Beach bed with 60% in the underlying 10 m. Biomass volume density estimates were 0.51 kg/m^3 in the upper 4 m and 0.31 kg/m^3 in the lower 10 m using the observed 40/60 distribution. Biomass volume density estimates using "typical" values (6.0 kg/m^2 over 15 m depth) were 0.60 kg/m^3 in the upper 4 m and 0.33 kg/m^3 in the lower 11 m, very similar to our findings.

In situ production of $CHBr_3$ and CH_2Br_2 by portions of *M. pyrifera* fronds was similar to laboratory production by whole blades. Median production rates from four *in situ* incubations were 256 ng $CHBr_3$/gfwt·day and 41 ng CH_2Br_2/gfwt·day. Median

production rates for laboratory incubations were 171 ng $CHBr_3$/gfwt·day and 48 ng CH_2Br_2/gfwt·day for 19 incubations conducted over a nine-month period (Chapter 3). Similar results from both methods indicates the validity of the laboratory incubation procedure.

Table 5.1. Frond density measurements. 1990 values determined by counting numbers of fronds in randomly laid quadrats (28.27 m^2/quadrat). 1991 values determined by counting the number of fronds in a defined experimental plot (362.4 m^2).

date	number of fronds	fronds/m^2
1990:		
7/11	307	10.8
7/11	414	14.6
7/30	160	5.7
7/30	337	11.9
8/8	516	18.3
8/21	230	8.1
mean ± SD:		**11.6 ± 4.5**
1991:		
7/15-8/20	1833	5.1
10/2-10/16	1549	4.3
mean ± SD:		**4.67 ± 0.55**

Table 5.2. Biomass parameters are based on 1991 *M. pyrifera* field and laboratory measurements or "typical" values from a combination of studies (see text). Biomass area density is the product of frond density and frond weight. Average biomass volume density (kg/m^3) is the biomass density (kg/m^2) divided by the average water depth. Biomass volume densities above and below 4 m depths are based on the vertical biomass distribution (see text).

source	frond density (fronds $/m^2$)	average frond weight (kg)	biomass area density (kg/m^2)	water depth (m)	average biomass volume density (kg/m^3)	biomass volume density above 4m (kg/m^3)	biomass volume density below 4m (kg/m^3)
1991 values	4.7	1.1	5.1	14	0.37	0.51	0.31
"typical" values	6.0	1	6.0	15	0.40	0.60	0.33

Table 5.3. *M. pyrifera* production of $CHBr_3$ and CH_2Br_2 (± std error) estimated by *in situ* frond incubation. See Figs. 5.7-5.9.

date	$CHBr_3$ ng/gfwt·day	CH_2Br_2 ng/gfwt·day
7/12/93	283 ± 10	88 ± 0.24
7/19/93	228 ± 34	14 ± 3.4
7/19/93	304 ± 48	20 ± 2.2
8/10/93	136 ± 16	61 ± 2.5

Table 5.4. Comparison of *M. pyrifera* $CHBr_3$ and CH_2Br_2 production rates estimated by *in situ* frond incubation and laboratory whole blade incubation (Chapter 3). Bags for *in situ* incubations were mylar and those for laboratory incubations were polyethylene.

	$CHBr_3$ ng/gfwt·day	CH_2Br_2 ng/gfwt·day
***in situ* production**		
date:	7/12/93 - 8/10/93	
median:	256	41
range (n = 4):	136 - 304	14 - 88
laboratory production		
date:	5/18/94 - 2/22/95	
median:	171	48
range (n = 19):	25 - 1,126	21 - 173

Table 5.5. Concentrations (ng/L) of $CHBr_3$ and CH_2Br_2 taken by plastic or glass syringe after 2 hr of *M. pyrifera* incubation, *in situ*. Values are mean ± range for two replicate samples. Incubation was conducted on 8/3/93 using a polyethylene bag.

date	[$CHBr_3$]	[CH_2Br_2]
plastic	1682 ± 189	785 ± 76
glass	1167 ± 74	803 ± 58

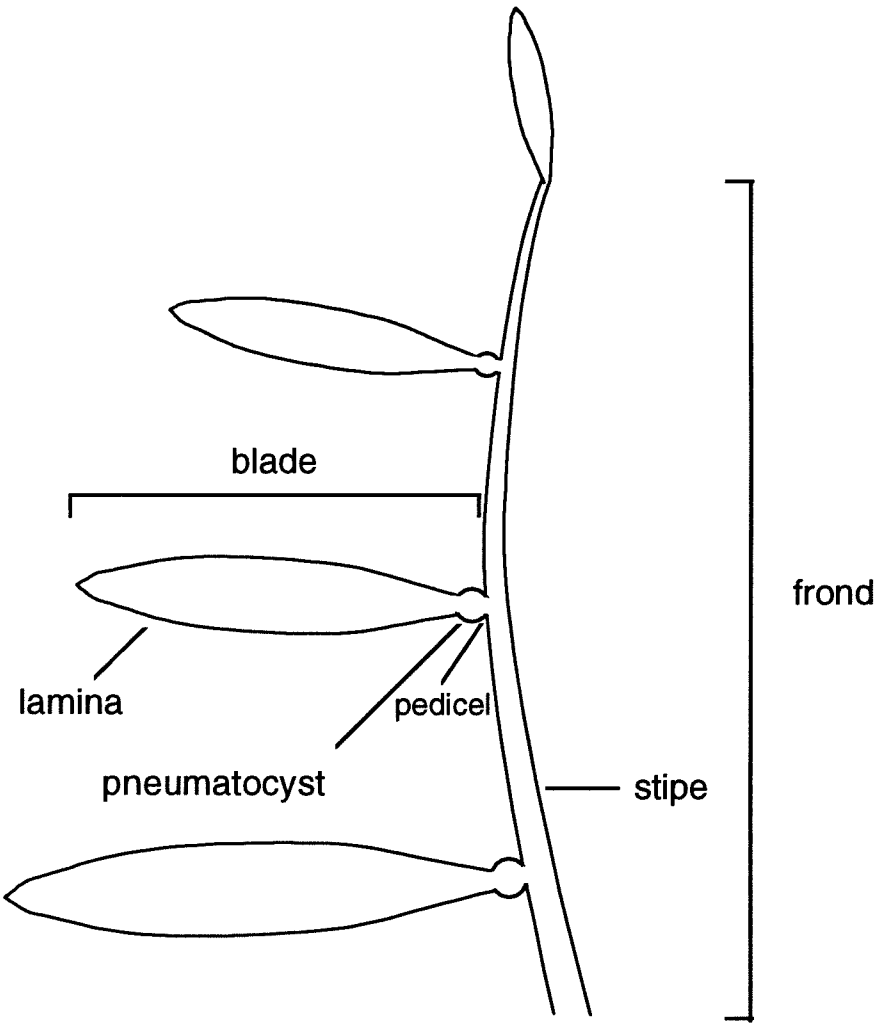

Figure 5.1. Diagram of a *M. pyrifera* frond identifying various blade parts including leaf-like lamina, gas-filled pneumatocyst, and pedicel which connects the blade to a vine-like stipe.

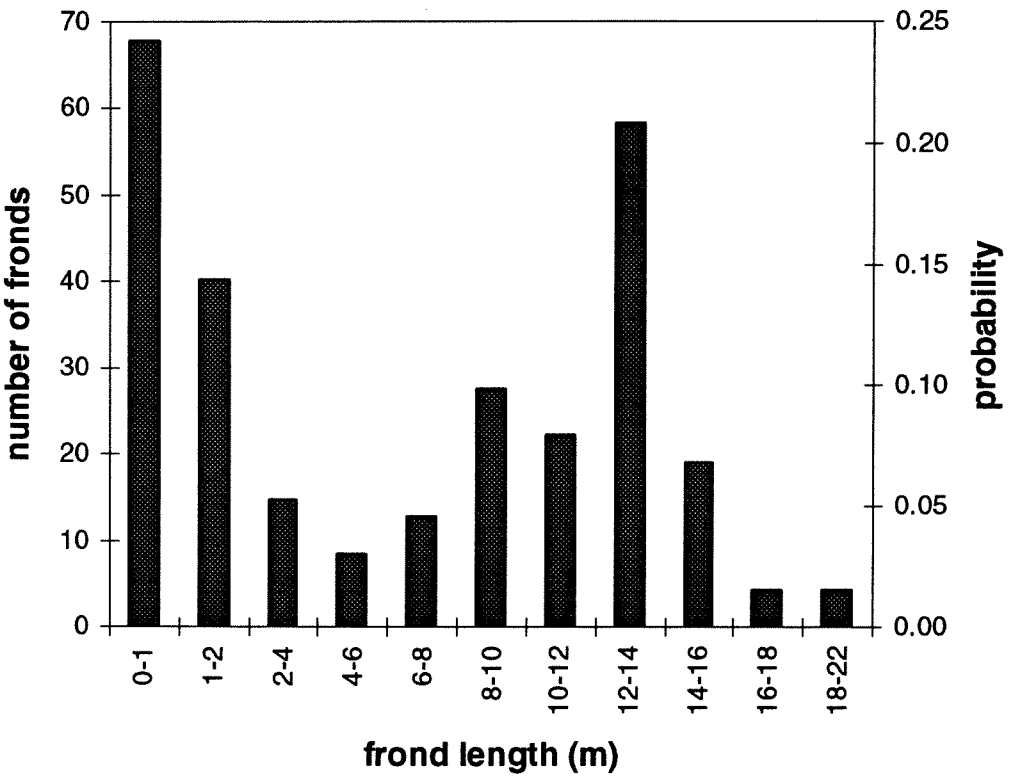

Figure 5.2. *M. pyrifera* frond length distribution obtained from field measurements of all fronds on ten plants. Water depth was about 14 m. The frond length distribution was obtained by dividing the number of fronds occurring in each length class (right axis) by the total number of fronds measured (n=264).

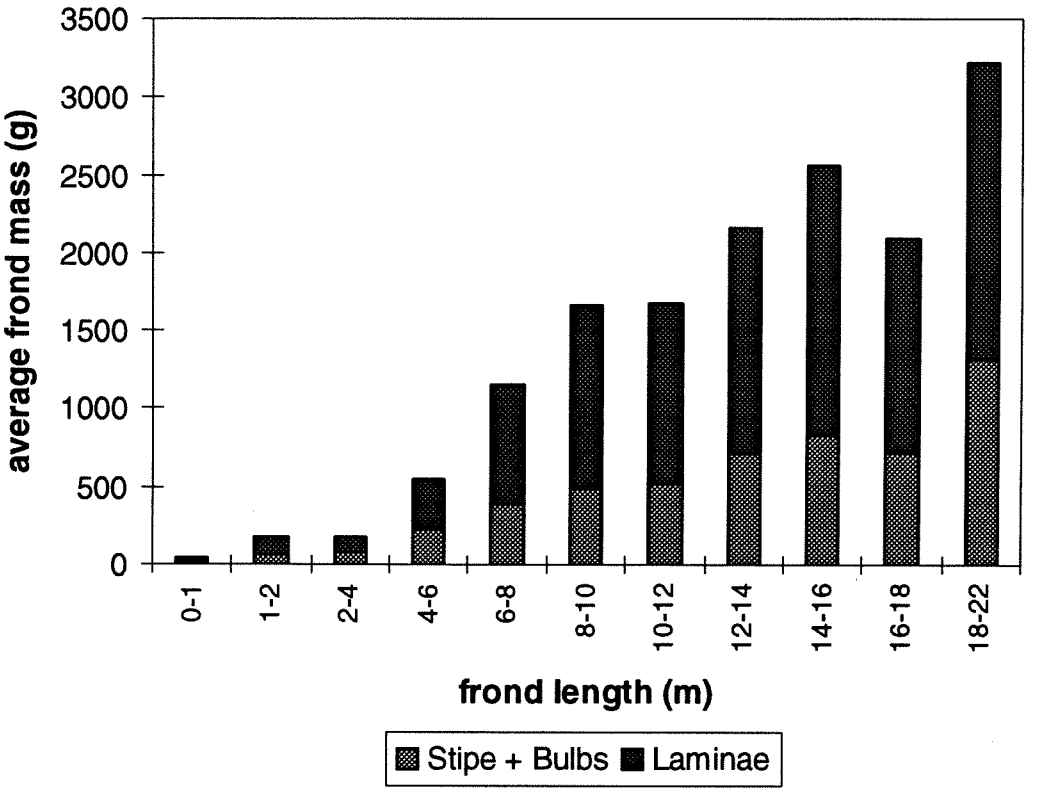

Figure 5.3. *M. pyrifera* frond mass as a function of frond length obtained from laboratory measurements of 42 fronds. Shading differentiates the proportion of total weight comprised by laminae from that comprised by stipe and bulbs.

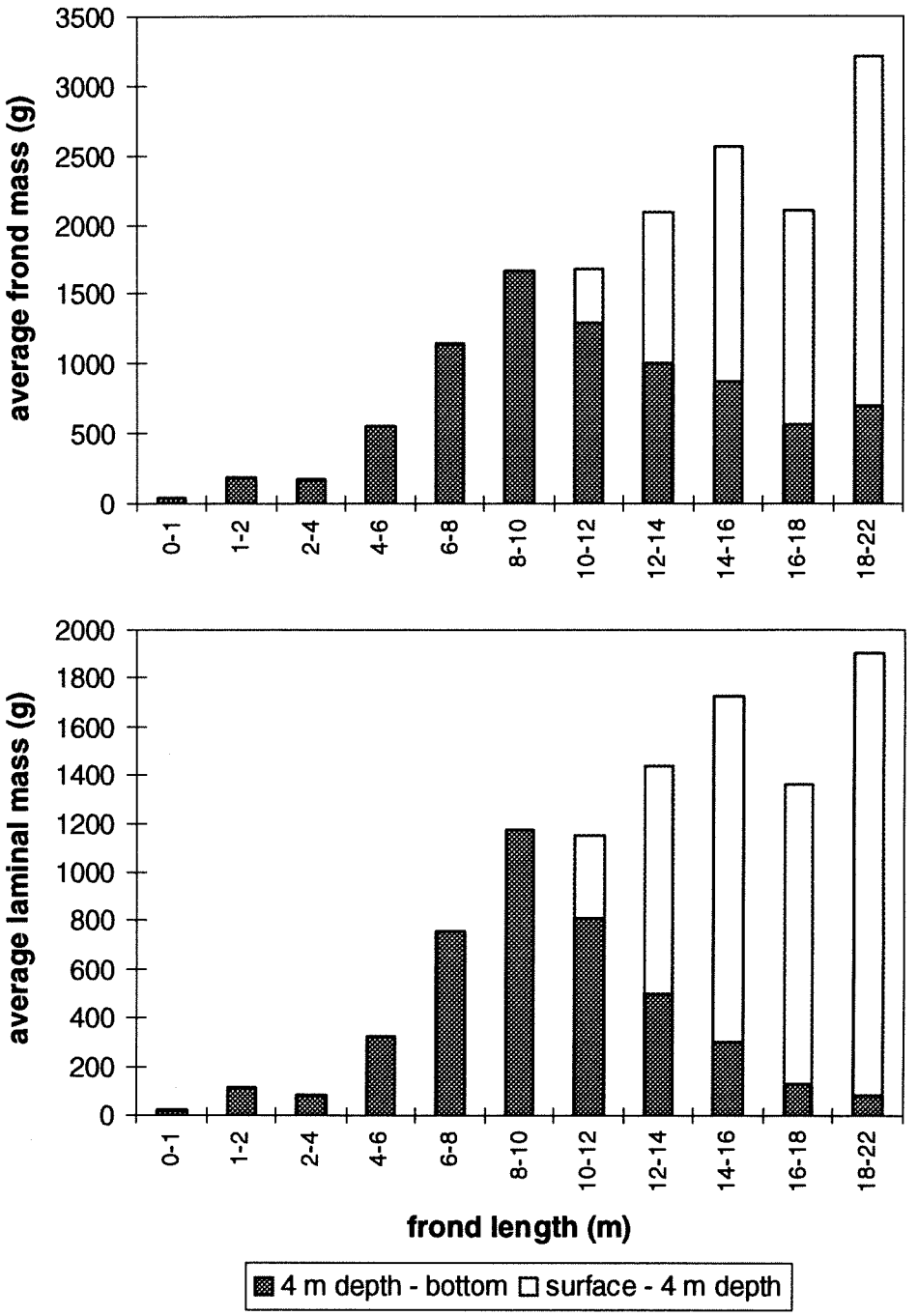

Figure 5.4. Average frond mass (upper figure) and laminal mass (lower figure) as a function of frond length. Shading differentiates the proportion of weight found in the upper 4 m from that in the underlying 10 m of the water column for different sized fronds (water depth was about 14 m).

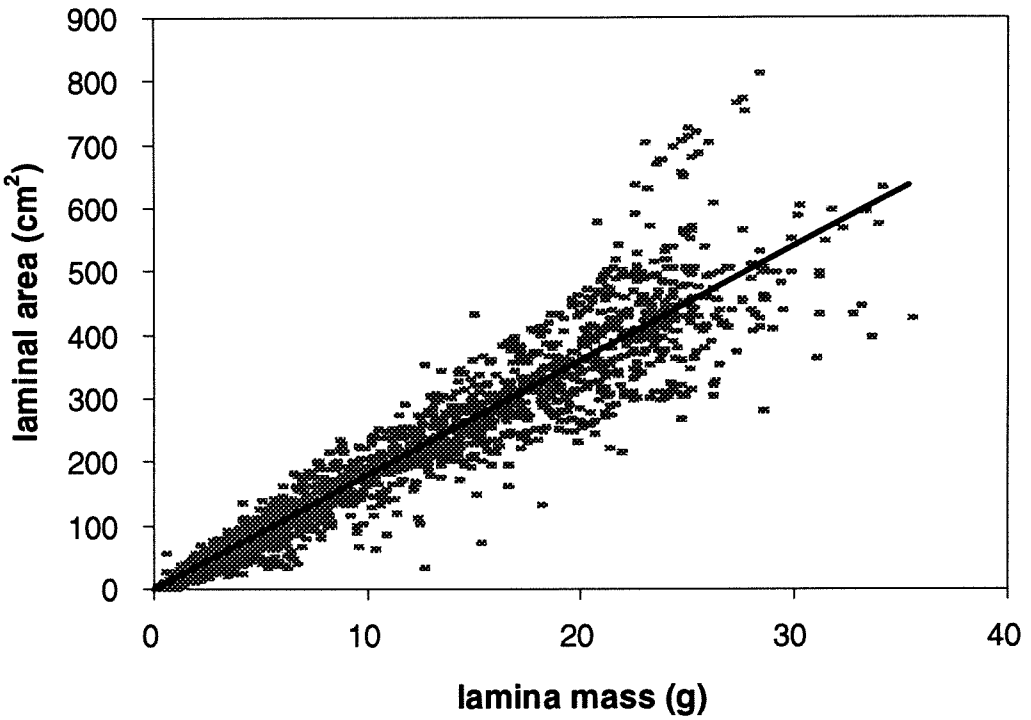

Figure 5.5. *M. pyrifera* laminal area as a function of laminal mass obtained from laboratory measurements of 1,956 laminae from 24 fronds. Linear regression line is shown ($y = 18.04$, $r^2 = 0.91$).

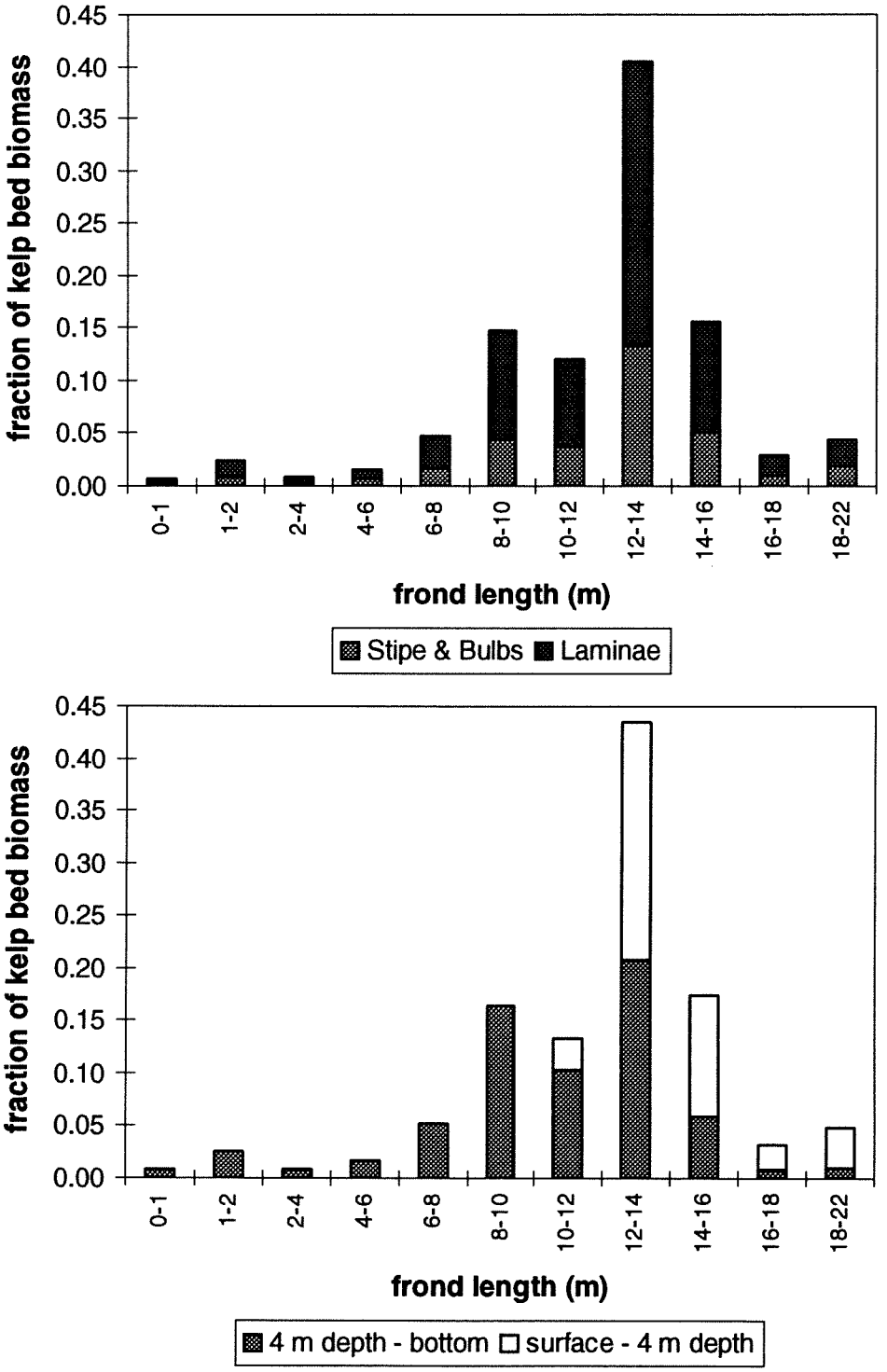

Figure 5.6. *M. pyrifera* proportion of biomass in each frond length class. Values obtained by multiplying the frond length distribution (Figure 5.2) by the average mass of a frond in each length class (Figure 5.3). Kelp biomass is subdivided by morphology (upper figure) or location above or below 4 m depth (lower figure).

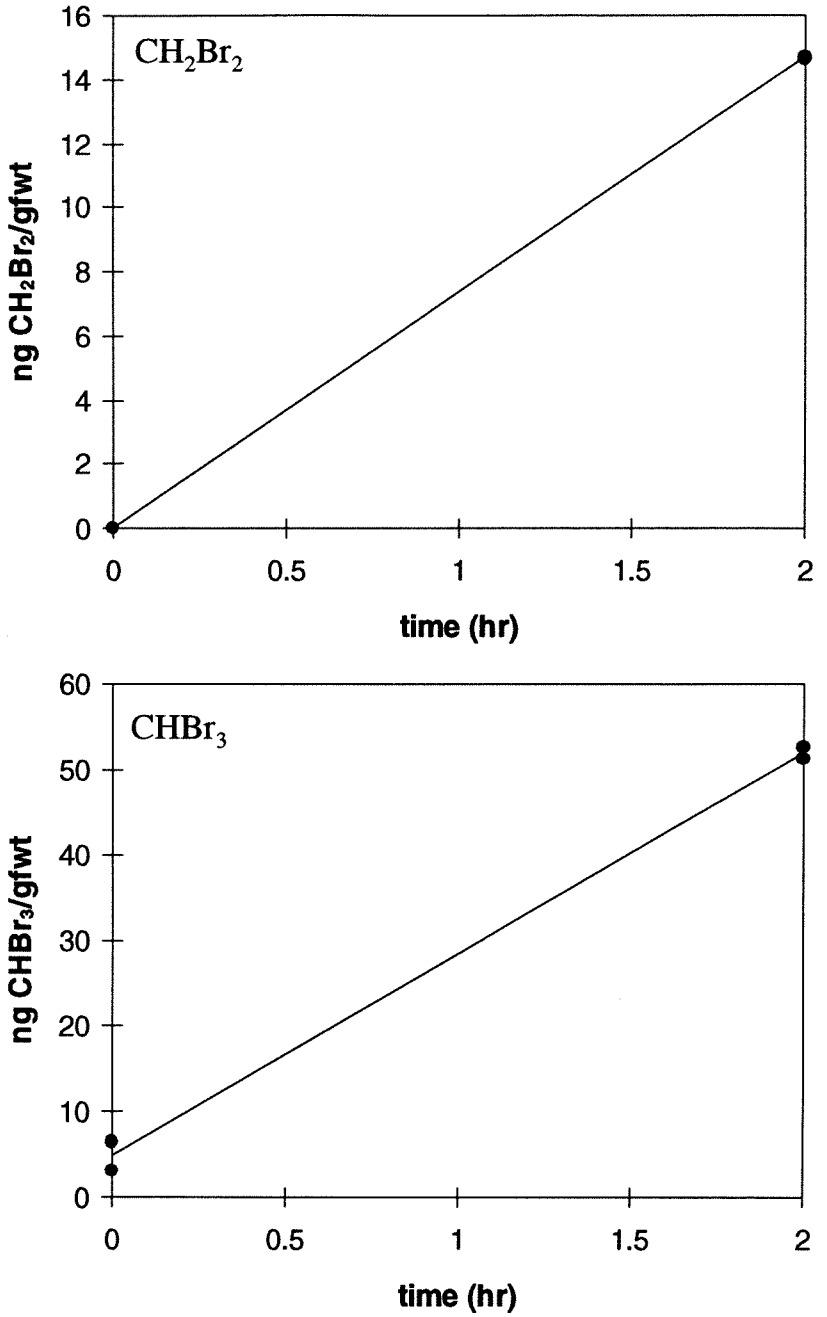

Figure 5.7. *M. pyrifera* CH_2Br_2 and $CHBr_3$ production *in situ* for fronds incubated 7/12/93. Two symbols at a single time point are replicate seawater samples.

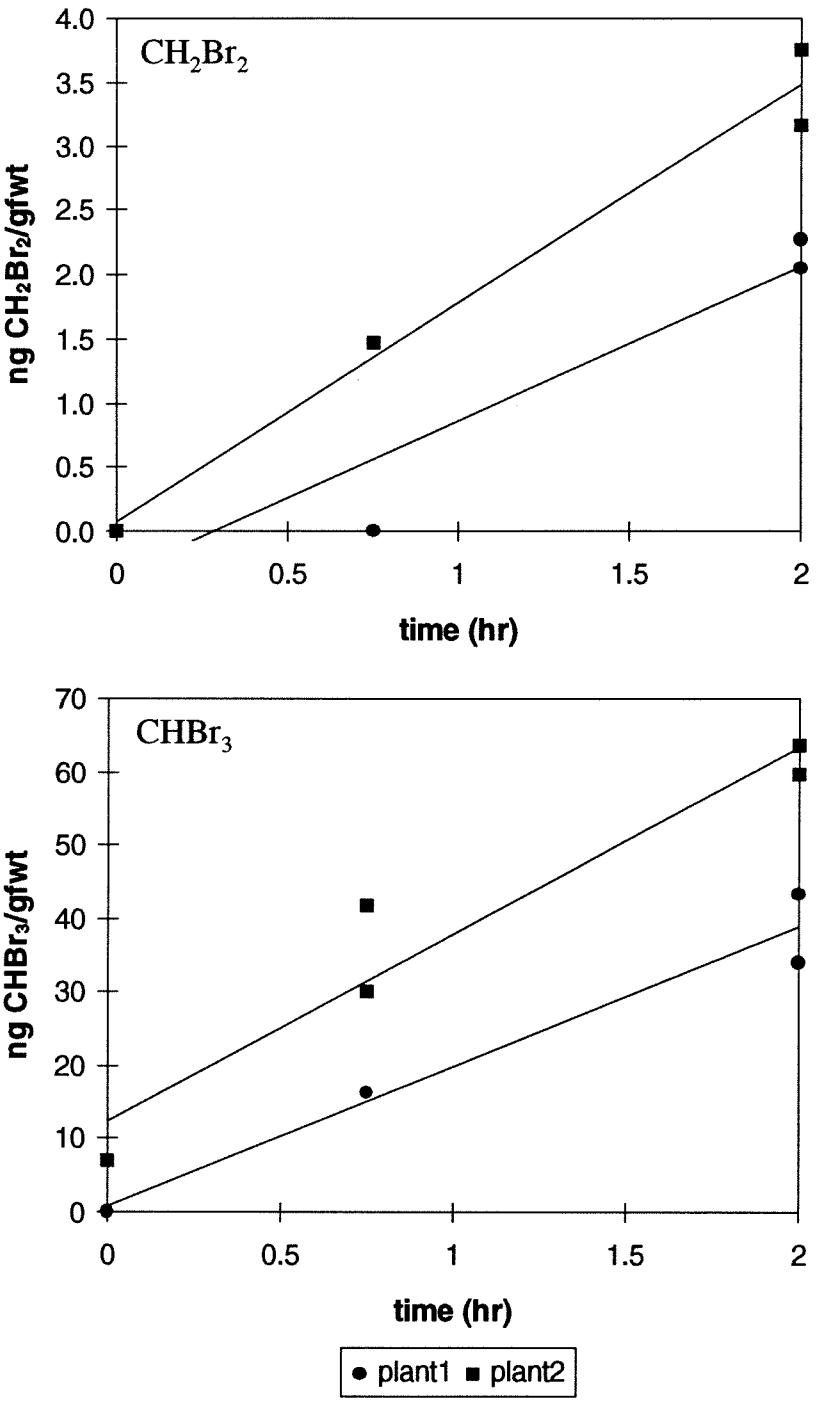

Figure 5.8. *M. pyrifera* CH_2Br_2 and $CHBr_3$ production *in situ* for fronds incubated 7/19/93 from two separate plants. CH_2Br_2 was below detection at 0.75 hr for the "plant1" incubation. Two symbols at a single time point are replicate seawater samples.

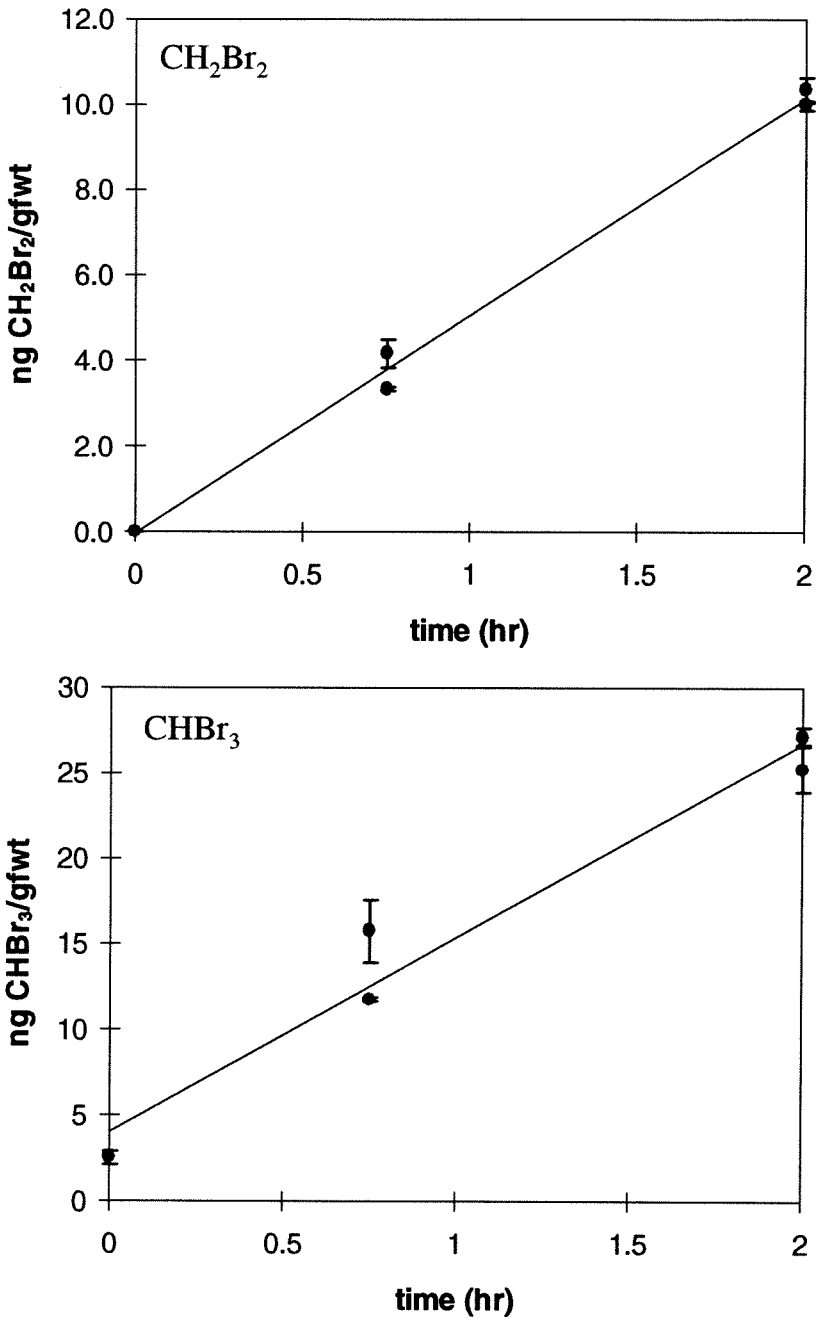

Figure 5.9. *M. pyrifera* CH_2Br_2 and $CHBr_3$ production *in situ* by fronds incubated 8/10/93. Two symbols at a single time point are replicate seawater samples. Error bars show range of two replicate injections of the same sample.

References

Aleem, A.A. (1956). Quantitative Underwater Study of Benthic Communities Inhabiting Kelp Beds off California. *Science* **123**, 183-183.

Clendenning, K.A. (1971). Photosynthesis and General Development in *Macrocystis*. In *The Biology of Giant Kelp Beds (Macrocystis)* in California (North, W.J. ed.), Beihefte Zur Nova Hedwigia 32. J. Cramer, Lehre, Germany, pp. 169-190.

De Vooys, C.G.N. (1979). Primary Production in Aquatic Environments. In *The Global Carbon Cycle* (Bolin, B., Degens, E.T., Kempe, S. and Ketner, P. eds.), John Wiley & Sons, NY, pp. 259-292.

Gerard, V.A. (1982). *In Situ* Rates of Nitrate Uptake by Giant Kelp, *Macrocystis Pyrifera* (L.) C. Agardh: Tissue Differences, Environmental Effects, and Prediction of Nitrogen-Limited Growth. *J. Exp. Mar. Biol. Ecol.* **62**, 211-224.

Gerard, V.A. (1984). Physiological Effects of El Niño On Giant Kelp in Southern California. *Mar. Biol. Lett.* **5**, 317-322.

Gossett, J.M. (1987). Measurement of Henry's Law Constants for C_1 and C_2 Chlorinated Hydrocarbons. *Environ. Sci. Technol.* **21**, 202-208.

Jackson, G.A., James, D.E. & North, W.J. (1985). Morphological Relationships Among Fronds of Giant Kelp, *Macrocystis Pyrifera*, off La Jolla, California. *Mar. Ecol. Prog. Ser.* **26**, 261-270.

Kennedy, J.H. (1984). *Analytical Chemistry*. Harcourt Brace Jovanovich San Diego, pp. 17.

Laturnus, F., Wiencke, C. & Klöser, H. (submitted for publication). Antarctic Macroalgae -Sources of Volatile Halogenated Organic Compounds. *Mar. Environ. Res.*

McFarland, W.N. & Prescott, J. (1959). Standing Crop, Chlorophyll Content, and *in Situ* Metabolism of a Giant Kelp Community in Southern California. *Inst. Mar. Sci., Univ. Texas* **6**, 109-132.

Newberger, P. (1982). Physical Oceanography and Meteorology of the California Outer Continental Shelf. *U.S. Dept. of Interior POCS Tech. Paper No. 82-2* T-82-002-1792.

North, W.J. (1971). *The Biology of Giant Kelp Beds (Macrocystis) in California.* Beihefte Zur Nova Hedwigia 32. J. Cramer, Lehre, Germany.

North, W.J. (1982). A General Description of *Macrocystis*. In *CRC Handbook of Biosolar Resources* (Mitsui, A. and Black, C.C., eds.), CRC Press Inc., Boca Raton, FL.

North, W.J. (1994). Review of *Macrocystis* Biology. In *Biology of Economic Algae* (Akatsuka, I., ed.), SPB Academic Publishing, Hague, Netherlands, pp. 447-527.

North, W.J., James, D.E. & Jones, L.G. (1993). History of Kelp Beds (*Macrocystis*) in Orange and San Diego Counties, California. *Hydrobiologia* **260/261**, 277-283.

Schiel, D. & Foster, M.S. (1986). The Structure of Subtidal Algal Stands in Temperate Waters. *Oceanogr. Mar. Biol. Ann. Rev.* **24**, 265-307.

Towle, D.W. & Pearse, J.S. (1973). Production of the Giant Kelp, *Macrocystis,* Estimated by *in situ* Incorporation of ^{14}C in Polyethylene Bags. *Limnol. Oceanogr.* **18**, 155-159.

Tse, G., Orbey, H. & Sandler, S.I. (1992). Infinite Dilution Activity Coefficients and Henry's Law Coefficients of Some Priority Water Pollutants Determined by a Relative Gas Chromatographic Method. *Environ. Sci. Technol.* **26**, 2017-2022.

Chapter Six

Summary: Macroalgal Production and Marine Microbial Degradation of Bromoform and Dibromomethane

This project evaluated macroalgal production and marine microbial degradation of the brominated methanes bromoform ($CHBr_3$) and dibromomethane (CH_2Br_2). Natural production and degradation of brominated methanes are two pieces in a large and dynamic puzzle – the bromine biogeochemical cycle. Bromoform and CH_2Br_2 are volatile halomethanes with oceanic sources. These compounds are destroyed by releasing free bromine to the atmosphere (Figure 6.1). Bromine may then become involved in catalytic reactions that destroy ozone (Yung *et al.* 1980). Ozone is a critical component of the atmosphere because it absorbs both solar and infrared radiation. Ozone is thus important to the energy balance of the atmosphere, and it screens the earth from harmful ultraviolet radiation (see Chapter 1).

Seawater concentrations of $CHBr_3$ and CH_2Br_2, as well as methyl iodide, were measured from a variety of southern California coastal sites to identify areas with enhanced halomethane concentrations. Elevated halomethane concentrations were associated with the Giant Kelp, *Macrocystis pyrifera* (Chapter 2). A cross-shore gradient was observed with highest halomethane concentrations in and near the kelp canopy relative to surface waters 5 km offshore. Water exiting a productive estuary was also enriched with CH_2Br_2. Seawater adjacent to decaying macroalgae on the bottom of a submarine canyon was not enriched in these halomethanes relative to surface water,

indicating that bacterial degradation of drift kelp was not a significant source of halomethanes in this environment.

M. pyrifera produced $CHBr_3$ and CH_2Br_2 during laboratory incubations of tissue disks (Chapter 2) and whole blades (Chapter 3). Production from whole blades ranged from 25-1126 ng $CHBr_3$/gfwt·day and 21-173 ng CH_2Br_2/gfwt·day for kelp collected on different days between May 1994 and February 1995. The ranges in production rates indicate that short-term sampling may not accurately reflect the overall release behavior of halogenated methanes. Median production rates measured from whole blade incubations were 171 ng $CHBr_3$/gfwt·day (0.68 nmoles $CHBr_3$/gfwt·day) and 48 ng CH_2Br_2/gfwt·day (0.27 nmoles CH_2Br_2/gfwt·day), based on a 12 hr photoperiod (19 experiments; 190 kelp blades). Comparable $CHBr_3$ and CH_2Br_2 production rates were measured from preliminary *in situ* incubations of *M. pyrifera* fronds (Chapter 5). Median production rates from four *in situ* incubations were 256 ng $CHBr_3$/gfwt·day and 41 ng CH_2Br_2/gfwt·day. Similar results from both laboratory and *in situ* methods support the validity of the laboratory incubation procedure.

Light and algal photosynthetic activity affected $CHBr_3$ and CH_2Br_2 release by *M. pyrifera* (Chapter 3). These results suggest that environmental factors influencing kelp physiology (e.g., health, light, season, climate, etc.) may ultimately affect release of halomethanes into the atmosphere. Brominated methane production rates were significantly lower from kelp incubations in darkness relative to simultaneous incubations in light. Production was inhibited in light by the addition of the photosynthetic inhibitor, DCMU. DCMU probably affected brominated methane production by halting

photosynthetic production of hydrogen peroxide (H_2O_2). Hydrogen peroxide is a substrate of the vanadium bromoperoxidase enzyme *in vitro* (Soedjak and Butler 1990), and H_2O_2 is produced in photosynthesis during pseudocyclic photophosphorylation (the "Mehler reaction") (Elstner 1987). External H_2O_2 concentrations and the effect of adding additional H_2O_2 to different kelp treatments (i.e., light, dark, light/DCMU, light/aniline) suggested that internal H_2O_2 is available to vanadium bromoperoxidase (Chapter 3).

Anthropogenic bromine emissions appear to dominate algal emissions in southern California. *M. pyrifera*, the dominant macroalga in southern California, produces an estimated $3x10^6$ g Br/yr from $CHBr_3$, CH_2Br_2, and methyl bromide (MeBr) in Orange and San Diego Counties. Bromoform contributes 77% of this regional bromine source. The production estimate was based on the following: *M. pyrifera* $CHBr_3$ and CH_2Br_2 production rates measured in this study, *M. pyrifera* MeBr production rates measured by Manley and Dastoor (1987), the average *M. pyrifera* standing crop recorded for 1963 to 1991 (North *et al.* 1993), and a kelp bed density of 6 kg/m^2 (Chapter 5). In comparison, anthropogenic bromine emissions in this region are approximately 10^8 g Br/yr from MeBr fumigation alone (State of California 1995). California accounts for approximately 10% of global MeBr use, thus this pattern of MeBr domination is not expected for all coastal regions, but it may be representative of other areas with dense urban and agricultural development.

Global bromine emissions from kelp are roughly estimated as $3.0x10^9$g Br/yr from $CHBr_3$ and CH_2Br_2, assuming a value of 40 Tg for global kelp biomass (De Vooys 1979) and that median *M. pyrifera* brominated methane production rates are representative of

other kelp species. Bromoform contributes about 80% of the estimated total bromine produced by kelp worldwide. Estimates of bromine emissions from macroalgae (kelp and non-kelp) and ice algae communities are on the order of 10^{10} to 10^{11} g Br/yr (this study; Nightingale *et al.* 1995; Manley *et al.* 1992; Sturges *et al.* 1992). Anthropogenic bromine emissions were estimated at ~$7x10^{10}$ g Br/yr (Chapter 3). Marine algae thus appear to be an important part of the global bromine cycle based on their combined bromine emissions. The estimated global input of $CHBr_3$ to the atmosphere based on atmospheric measurements is on the order of 10^{12} g $CHBr_3$/yr, which greatly exceeds anthropogenic inputs (Penkett *et al.* 1985; Krysell 1991) (Table 6.1). Presuming this estimate to be approximately correct, $CHBr_3$ sources are not yet fully budgeted. Phytoplankton may be an additional bromine source, but more information is required before an adequate assessment can be made (Tokarczyk and Moore 1994).

Although both $CHBr_3$ and CH_2Br_2 are released by macroalgae, only CH_2Br_2 was degraded by kelp-associated bacteria in seawater enrichments (Chapter 4). Dibromomethane degradation typically began after a few days lag period and was rapid thereafter. Microbial degradation was observed only for dihalomethanes; CH_2Br_2 and dichloromethane (CH_2Cl_2) were degraded, but not $CHBr_3$ or MeBr. Inhibitor studies indicated that eukaryotic organisms and a number of microbial processes, including nitrification and methanotrophy, did not contribute to CH_2Br_2 degradation. Protein synthesis was required for development of detectable CH_2Br_2 degradation as indicated by chloramphenicol studies. Chloramphenicol did not impede degradation once protein synthesis and/or growth had occurred. Chloramphenicol did inhibit development of

CH_2Br_2 degradation when added initially to cultures, and it blocked sustained degradation after cultures had been depleted of CH_2Br_2 for several days. Therefore, either enzyme synthesis (induction) and/or bacterial growth was required for CH_2Br_2 degradation.

Dibromomethane degradation rates in laboratory seawater enrichments ranged from 0.11 to 73 nmoles CH_2Br_2/day·L seawater, depending in part on the initial CH_2Br_2 concentration. Laboratory degradation rates were extrapolated linearly to environmental conditions based on seawater CH_2Br_2 concentrations measured in a *M. pyrifera* canopy (3.2 ng/L, 0.018 nM; Chapter 2). Estimated microbial degradation at this CH_2Br_2 concentration was 0.023 ng CH_2Br_2/day·L seawater ($1.35x10^{-4}$ nmoles/day·L), based on the maximum laboratory rate of 73 nmoles CH_2Br_2/day·L seawater occurring at an initial concentration of 9.9 μM CH_2Br_2. Macroalgal production was estimated to be 19 ng CH_2Br_2/day·L seawater based on *M. pyrifera* whole blade incubations (Chapter 3) and a *M. pyrifera* biomass density of 0.4 kg/m^3 (averaged over the water column; Chapter 5). Microbial CH_2Br_2 degradation thus represents only 0.1% of CH_2Br_2 production by *M. pyrifera*, well within the error of the production estimate itself.

Microbial degradation of 0.018 nM CH_2Br_2 would take 136 days at the estimated degradation rate of $1.35x10^{-4}$ nmoles CH_2Br_2/ day·L seawater, based on the extrapolated maximum laboratory degradation rate of 73 nmoles CH_2Br_2/day·L seawater. This estimate suggests that microbial degradation might be faster than hydrolysis or halide substitution but slower than volatilization (see Table 6.1). It is noteworthy that Moore and Tokarczyk (1993) observed CH_2Br_2 distributions in the northwest Atlantic Ocean that indicated more pronounced consumption of CH_2Br_2 in deep waters relative to $CHBr_3$. Investigations of

microbial CH_2Br_2 degradation in open-ocean environments may assess whether microbial CH_2Br_2 degradation of contributes significantly to oceanic CH_2Br_2 profiles.

Although microbial degradation of CH_2Br_2 occurs, it appears to be an insignificant water column sink in the kelp bed relative to algal production and volatilization. Dibromomethane degradation was associated with particles >1.2 μm, supporting the hypothesis that CH_2Br_2-degrading bacteria may be attached to kelp surfaces in the environment. Microbes attached to kelp surfaces may encounter elevated CH_2Br_2 concentrations, and significant degradation thus might occur at the kelp surface. If this were the case, $CHBr_3$ and CH_2Br_2 concentrations observed in kelp beds and surrounding waters may reflect not only enhanced macroalgal production of $CHBr_3$, but also microbial degradation of CH_2Br_2 as it occurs on blade surfaces. Macroalgal production measurements would thus reflect net production from kelp and associated CH_2Br_2-degrading microbes, but production estimates themselves would remain unchanged.

Table 6.1. A variety of parameters for bromine, MeBr, CH_2Br_2 and $CHBr_3$. ND = not detected; NF = literature value not found.

	bromine	**MeBr**	**CH_2Br_2**	**$CHBr_3$**
MW (g/mol)[a]	80	95	174	253
boiling point (°C)[a]		3.6	97	150
specific density (20 °C /4 °C)[a]		1.7	2.5	2.9
partition coeff., C_g/C_w 25°C seawater		0.31[b]	0.043[c]	0.026[c]
atmospheric conc.		10-11 pptv[defgh] 0.04-0.05 ng/L	0.72-50 pptv[eij] 0.0056-0.39 ng/L	~2[d] (2-460) pptv[defgij] 0.023-5.2 ng/L
seawater conc.	67 mg/L[k] 0.84 mM	0.5-3.7 ng/L[b] 5.3-39 pM	0.3-80 ng/L[lmn] 1.7 pM-0.46 nM	0.6-516 ng/L[lmnopqr] 2.4 pM-2.0 nM
source (g/yr)		$8.4x10^{10}$-$1.2x10^{11}$[s]	NF	10^{12}[e]
atmos. burden (g)		$2.3x10^{11}$[e]	NF	NF
atmos. lifetime		1.2 years[s]	~5 months[i]	~ 2 weeks[e]
half-life hydrolysis[t]		20 days	183 yr	686 yr
half-life halide subst.		3 weeks[u]	NF	1.3-18.5 yrs[v]
aquatic photolysis		NF	NF	NF
microbial degradation			136 days[w]	ND[w]
half-life volatilization[x] (L = 5m to 75m)		≈3.5 to 53 days	≈3.5 to 53 days	3.5 to 53 days

[a] CRC Handbook of Chemistry and Physics 1987.
[b] Singh *et al.* 1983.
[c] value interpolated from Tse *et al.* 1992 and multiplied by 1.2 salting-out coefficient. Salting-out coefficient was empirically determined by the method of Gossett 1987, see Chapter 3 Material and Methods.

[d] Cicerone *et al.* 1988
[e] Penkett *et al.* 1985.
[f] Khalil *et al.* 1993
[g] Sturges *et al.* 1993.
[h] Butler 1994.
[i] Mellouki *et al.* 1992.
[j] Class and Ballschmiter 1988.
[k] North 1994.
[l] Manley *et al.* 1992.
[m] Klick 1992.
[n] Moore and Tokarczyk 1993 (above 100 m depth).
[o] Fogelqvist 1985.
[p] Fogelqvist 1991.
[q] Klick and Abrahamsson 1992.
[r] Heumann 1993.
[s] Lobert *et al.* 1995
[t] Mabey and Mill 1978.
[u] Elliott and Rowland 1993.
[v] Geen 1992.
[w] Time required for bacterial degradation of CH_2Br_2 at initial concentration of 0.018 nM with degradation rate of 1.35×10^{-4} nmoles CH_2Br_2/ day·L seawater. Degradation rate based on the maximum measured laboratory degradation rate (73 nmoles CH_2Br_2/day·L seawater at 9.9 μM initial CH_2Br_2) extrapolated to a kelp bed concentration of 0.018 nM CH_2Br_2. No microbial degradation of $CHBr_3$ was observed. See Chapter 4.
[x] Helz and Hsu 1978: half-life = $0.69LK^{-1}$; L= mixed-layer depth, K = piston velocity = 4.1 cm/hr for $CHBr_3$. K should be similar for CH_2Br_2 and MeBr because of similar diffusivities (see Hayduk and Laudie 1974).

Brominated Methanes in the Bromine Cycle

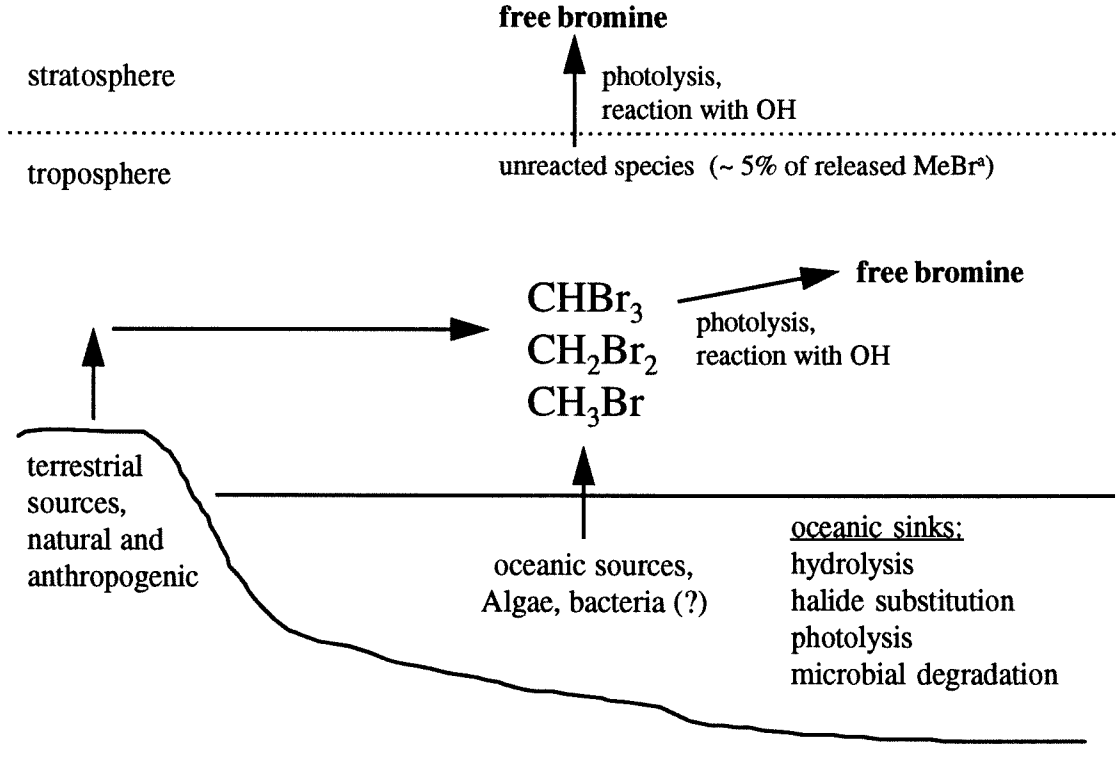

Figure 6.1. Simple schematic of the bromine biogeochemical cycle with emphasis on brominated methanes. Diagram notes terrestrial and oceanic sources as well as oceanic and atmospheric sinks. Transport from troposphere to stratosphere of relatively long-lived compounds such as CH_3Br is shown ([a] R.J. Cicerone, personal communication). Free bromine released from brominated methanes in the atmosphere is available for catalytic destruction of ozone (see text).

References

Butler, J.H. (1994). The Potential Role of the Ocean in Regulating Atmospheric CH_3Br. *Geophys. Res. Lett.* **21**, 185-188.

Cicerone, R.J., Heidt, L.E. & Pollock, W.H. (1988). Measurements of Atmospheric Methyl Bromide and Bromoform. *J. Geophys. Res.* **93**, 3745-3749.

Class, T. & Ballschmiter, K. (1988). Chemistry of Organic Traces in Air VIII: Sources and Distribution of Bromo- and Bromochloromethanes in Marine Air and Surfacewater of the Atlantic Ocean. *J. Atmos. Chem.* **6**, 35-46.

CRC Handbook of Chemistry and Physics. (1987). (Weast, R.C., ed.), CRC Press, Inc., Boca Raton, FL.

De Vooys, C.G.N. (1979). Primary Production in Aquatic Environments. In: *The Global Carbon Cycle* (Bolin, B., Degens, E.T., Kempe, S., and Ketner, P. eds.), John Wiley & Sons, NY, pp. 259-292.

Elliott, S. & Rowland, S. (1993). Nucleophilic Substitution Rates and Solubilities for Methyl Halides in Seawater. *Geophys. Res. Lett.* **20**, 1043-1046.

Elstner, E.F. (1987). Metabolism of Activated Oxygen Species. In *The Biochemistry of Plants A Comprehensive Treatise, Vol. 11, Biochemistry of Metabolism* (Stumpf, P.K. and Conn, E.E. eds.), Academic Press, NY, pp. 253-315.

Fogelqvist, E. & Krysell, M. (1991). Naturally and Anthropogenically Produced Bromoform in the Kattegatt, a Semi-Enclosed Oceanic Basin. *J. Atmos. Chem.* **13**, 315-324.

Fogelqvist, E. (1985). Carbon Tetrachloride, Tetrachloroethylene, 1,1,1-Trichloroethane and Bromoform in Arctic Seawater. *J. Geophys. Res.* **90**, 9181-9193.

Geen, C.E. (1992). Selected Marine Sources and Sinks of Bromoform and Other Low Molecular Weight Organobromines. M.Sc. Thesis, Dalhousie University, Halifax, Nova Scotia.

Gossett, J.M. (1987). Measurement of Henry's Law Constants for C_1 and C_2 Chlorinated Hydrocarbons. *Environ. Sci. Technol.* **21**, 202-208.

Hayduk, W. & Laudie, H. (1974). Prediction of Diffusion Coefficients for Nonelectrolytes in Dilute Aqueous Solutions. *AIChE Journal* **20**, 611-615.

Helz, G.R. & Hsu, R.Y. (1978). Volatile Chloro- and Bromocarbons in Coastal Waters. *Limnol. Oceanogr.* **23**, 858-869.

Heumann, K.G. (1993). Determination of Inorganic and Organic Traces in the Clean Room Compartment of Antarctica. *Analytica Chemica Acta* **283**, 230-245.

Khalil, M.A.K., Rasmussen, R.A. & Gunawardena, R. (1993). Atmospheric Methyl Bromide: Trends and Global Mass Balance. *J. Geophys. Res.* **98**, 2887-2896.

Klick, S. (1992). Seasonal Variations of Biogenic and Anthropogenic Halocarbons in Seawater from a Coastal Site. *Limnol. Oceanogr.* **37**, 1579-1585.

Klick, S. & Abrahamsson, K. (1992). Biogenic Volatile Iodated Hydrocarbons in the Ocean. *J. Geophys. Res.* **97**, 12683-12687.

Krysell, M. (1991). Bromoform in the Nansen Basin in the Arctic Ocean. *Mar. Chem.* **33**, 187-197.

Lobert, J.M., Butler, J.H., Montzka, S.A., Geller, L.S., Myers, R.C. & Elkins, J.W. (1995). A Net Sink For Atmospheric CH_3Br in the East Pacific Ocean. *Science* **267**, 1002-1005.

Mabey, W. & Mill, T. (1978). Critical Review of Hydrolysis of Organic Compounds in Water Under Environmental Conditions. *J. Phys. Chem. Ref. Data* **7**, 383-409.

Manley, S.L., Goodwin, K. & North, W.J. (1992). Laboratory Production of Bromoform, Methylene Bromide and Methyl Iodide by Macroalgae and Distribution in Nearshore Southern California Waters. *Limnol. Oceanogr.* **37**, 1652-1659.

Manley, S.L. & Dastoor, M.N. (1987). Methyl Halide (CH_3X) Production from the Giant Kelp, *Macrocystis* and Estimates of Global CH_3X Production by Kelp. *Limnol. Oceanogr.* **32**, 709-715.

Mellouki, A., Talukdar, R.K., Schmoltner, A., Gierczak, T., Mills, M.J., Solomon, S. & Ravishankara, A.R. (1994). Atmospheric Lifetimes and Ozone Depletion Potentials of Methyl Bromide (CH_3Br) and Dibromomethane (CH_2Br_2). *Geophys. Res. Lett.* **19**, 2059-2062.

Moore, R.M. & Tokarczyk, R. (1993). Volatile Biogenic Halocarbons in the Northwest Atlantic. *Global Biogeochem. Cycles* **7**, 195-210.

Nightingale, P.D., Malin, G. & Liss, P.S. (1995). Production of Chloroform and Other Low Molecular Weight Halocarbons by Some Species of Macroalgae. *Limnol. Oceanogr.*, **40**, 680-689.

North, W.J., James, D.E. & Jones, L.G. (1993). History of Kelp Beds (*Macrocystis*) in Orange and San Diego Counties, California. *Hydrobiologia* **260/261**, 277-283.

North, W.J. (1994). Review of *Macrocystis* Biology. In: *Biology of Economic Algae* (Akatsuka, I., ed.), SPB Academic Publishing, Hague, Netherlands, pp. 447-527.

Penkett, S.A., Jones, B.M.R., Rycroft, M.J. & Simmons, D.A. (1985). An Interhemispheric Comparison of the Concentrations of Bromine Compounds in the Atmosphere. *Nature* **318**, 550-553.

Ramanathan, V., Cicerone, R.J., Singh, H.B. & Kiehl, J.T. (1985). Trace Gas Trends and Their Potential Role in Climate Change. *J. Geophys. Res.* **90**, 5547-5566.

Singh, H.B., Salas, L.J. & R.E. Stiles. (1983). Methyl Halides in and Over the Eastern Pacific (40°N-32°S). *J. Geophys. Res.* **88**, 3684-3690.

Soedjak, H.S. & Butler, A. (1990). Characterization of Vanadium Bromoperoxidase from *Macrocystis* and *Fucus*: Reactivity of Vanadium Bromoperoxidase Toward Acyl and Alkyl Peroxides and Bromination of Amines. *Biochemistry* **29**, 7974-7981.

State of California Department of Pesticide Regulation (1995). Annual Pesticide Use Report by County, January to December 1993 (Draft).

Sturges, W.T., Sullivan, C.W., Schnell, R.C., Heidt, L.E. & Pollock, W.H. (1993). Bromoalkane Production by Antarctic Ice Algae. *Tellus* **45B**, 120-126.

Sturges, W.T., Cota, G.F. & Buckley, P.T. (1992). Bromoform Emission from Arctic Ice Algae. *Nature* **358**, 660-662.

Tokarczyk, R. & Moore, R.M. (1994). Production of Volatile Organohalogens by Phytoplankton Cultures. *Geophys. Res. Lett.* **21**, 285-288.

Tse, G., Orbey, H. & Sandler, S.I. (1992). Infinite Dilution Activity Coefficients and Henry's Law Coefficients of Some Priority Water Pollutants Determined by a Relative Gas Chromatographic Method. *Environ. Sci. Technol.* **26**, 2017-2022.

Yung, Y.L., Pinto, J.P., Watson, R.T. & Sander, S.P. (1980). Atmospheric Bromine and Ozone Perturbations in the Lower Stratosphere. *J. Atmos. Sci.* **37**, 339-353.